The Design, Synthesis and Protease Inhibitor Properties of Latent Reactive Amino Acid Analogues

---

A Thesis

presented for the Degree

of

Doctor of Philosophy in Chemistry

in the

University of Canterbury

by

J. CHRISTOPHER LITTEN

University of Canterbury

Christchurch

New Zealand

1992

Table of Contents

Appendices

Acknowledgements

I extend my most sincere thanks to my Ph.D supervisor, Dr. Andrew Abell. His help, guidance and friendship during this period were unparalleled, as was his patience and humour.

Dr. Alan Happer and the "A-Team", especially John Trent and Jane Taylor, were of incredible value with their plethora of wisdom, knowledge and companionship.

The assistance of the all the staff of the Chemistry Department was most appreciated, especially Wendy Marsh.

I also thank my family, Mum and Dad, and Jeremy and Gregory, for their continued love and support, without this I would not have succeeded this far.

Finally to my best friend, Sheri, thank-you for everything.

Abstract

This thesis examines the synthesis and proteolytic properties of a new class of latent reactive amino acid analogue, eg: **1-(*N*-Phthaloyl-L-phenylalanyl)-2-hydroxymethylpyrrole 2.52**, designed to inhibit serine proteases and the HIV protease.

Chapter One discusses the possible mode of protease inhibition by these derivatives. The substrate specificity of chymotrypsin, and HIV-1 protease suggests that the pyrrole occupies the P_1' subsite, and the *N*-acyl group the P_1 subsite. Acceptance into the active site, and subsequent cleavage of the amide bond releases the highly reactive 1-azafulvene **1.3** that can alkylate an active site nucleophilic residue.

Chapter Two presents procedures for the *N*-acylation of pyrrole derivatives. Pyrrole-2-carboxaldehyde was successfully *N*-acylated with non-amino acid acylating agents using either, NaH, MeLi, or BuLi. A new mild procedure was developed for the *N*-acylation of pyrroles using a DMAP/organic base combination. The DMAP/organic base (TEA or Hünigs base) methodology was extended to the *N*-acylation of pyrrole-2-carboxaldehyde with *N*-Pth protected amino acid acid chlorides. The subsequent reduction of the *N*-acylated formyl pyrrole, **1-(*N*-Phthaloyl-L-phenylalanyl)-2-formylpyrrole 2.37**, with $Zn(BH_4)_2$ produced high yields of the *N*-acylated hydroxymethyl pyrrole **2.52**. A ^1H NMR analysis of the camphanate prepared from **2.37** demonstrated that racemisation had not occurred. A detailed ^1H and ^{13}C NMR spectral analysis of the formyl and hydroxymethyl pyrroles is discussed in this chapter.

Chapter Three extends the synthesis to incorporate potential hydrogen bonding sites in the P_x' subsite direction. The imine ***N*-(2-Pyrrolylmethylene)-L-alanine Ethyl Ester 3.12** was prepared from pyrrole-2-carboxaldehyde, by reaction with H_2N-Ala-OEt and pyrrole-2-carboxaldehyde with removal of water. The analogous imine formation using the *N*-acylated formyl pyrrole **1-(3-Phenylpropionyl)-2-formylpyrrole 2.31** produced high yields of the non-acylated imine **3.12**. The *N*-acylation of **3.12** under the DMAP/Hünigs base conditions using hydrocinnamoyl chloride did not proceed.

Esterification of the hydroxymethyl pyrrole **2.52** under Mitsunobu conditions with the dipeptide *N*-Cbz-Val-Val-OH produced the tetrapeptide, ***N*-benzyloxycarbonyl-L-valinyl-L-valine-1-(*N*-phthaloyl-L-phenylalanyl)pyrrol-2-ylmethyl Ester 3.39**.

Chapter Four presents a hydrolysis and mechanistic study on the

deacylation of **1-(3-Phenylpropionyl)-2-hydroxymethylpyrrole 2.32** with HO^-. The deacylation of **2.32** in CD_3CN, containing one equivalent of KOH, produced **2-(3-Phenylpropionyl)-2-methylpyrrole Ester 4.5**. This species was shown to form via an intramolecular mechanism. Chiral, deuterium labelling of the methylene position showed that racemisation at this position had not occurred in the formation of **4.5**. An azafulvene intermediate is therefore precluded. A kinetic analysis of the subsequent conversion of **4.5** to **2-Butylaminomethylpyrrole 4.6**, in the presence of n-butylamine, showed the reaction to be first order with respect to HO^-.

The hydrolysis of deuterium labelled **[6-d_1]-(6S)-1-(*N*-Phthaloyl-L-leucyl)-2-hydroxymethylpyrrole 4.14** with HO^- in CD_3CN, gave the corresponding *O*-acetylated pyrrole **4.9** without racemisation. The addition of (S)-(+)-*sec*-butylamine to the reaction, trapped the azafulvene as **[6-d_1]-(8S)-(+)-2-(1-methylpropionylamino)methylpyrrole 4.36**. *N*-acylation was also shown to suppress azafulvene chemistry and therefore increase the stability of the hydroxymethyl pyrrole system. The camphanate from **[6-d_1]-(6S)-1-(3-Phenylpropionyl)-2-hydroxy methylpyrrole 4.10** formed under the Mitsunobu conditions proceeded with 62% inversion of configuration of the methylene position.

Chapter Five deals with the α-chymotrypsin and HIV-1 protease inhibitor properties of the pyrrole derivatives **2.32**, **2.52**, **1-(*N*-Phthaloyl-D-phenylalanyl)-2-hydroxymethylpyrrole 2.55**, **3.39**, **1-(Undecyl)-2-hydroxymethylpyrrole 3.53** and **1-((5-Methoxycarbonyl) hexanyl)-2-hydroxymethylpyrrole 3.55**. These compounds were found to be modest inhibitors of α-chymotrypsin, but poor inhibitors of HIV-1 protease. The stability of the hydroxymethyl pyrrole **2.52** was shown to be low under the HIV protease assay conditions. A discussion on molecular modelling and docking the proposed inhibitors into the active site of HIV-1 protease is presented.

Chapter One

Introduction

HIV protease and chymotrypsin are two examples of proteases that cleave peptide substrates on the carboxyl side of aromatic amino acids. The work described in this thesis outlines the design, synthesis and protease inhibitor properties of a new class of potential mechanism based enzyme inhibitors. The inhibitors target those enzymes that cleave on the carboxyl side of aromatic amino acids.

Additionally, there are several enzymes that have the unusual characteristic of cleaving a peptide on the *N*-terminal side of proline (Pro). Among these enzymes are the HIV-1 and HIV-2 proteases[1] and Kidney Prolidases[2]. Cleavage next to Pro is unusual in mammalian systems, and as such to develop an inhibitor that acts specifically on this system must be of pharmaceutical importance.

The inhibitors discussed in this thesis have been designed so that phenylalanine (Phe), or indeed any amino acid, is joined to a group X that possess latent reactivity, see **1.1** in Figure 1.1. A hydroxymethyl pyrrole, **1.2**, has been chosen for the latent reactive group X.

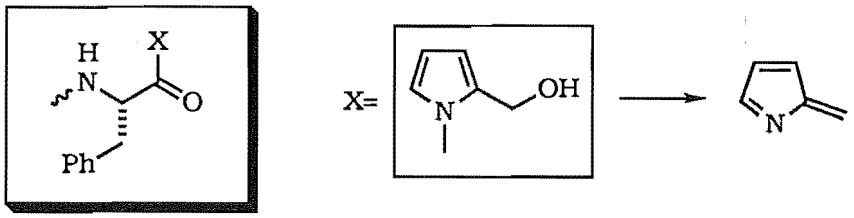

1.1 **1.2** **1.3**

Figure 1.1

Enzyme catalysed hydrolysis of the Phe-X amide bond releases a highly reactive azafulvene **1.3**, that is postulated to react with a nucleophilic residue in the protease active site, to give covalent inhibition. Since the latent reactivity is released on enzyme hydrolysis, and since the reactive group is not directly bound to the enzyme, the process is classed as metabolically activated inhibition. This is an important subset of true mechanism based inhibition. A general discussion of *latent reactive inhibitors* is discussed in Section 1.1.1.

If the hydroxymethyl pyrrole is thought of as a proline analogue, then the potential inhibitor **1.1** represents a *dipeptide analogue, containing latent reactivity*. The system then represents an analogue of the dipeptide Phe-Pro, suitable to target the HIV protease and Kidney Prolidase.

1.1 Mechanism Based Inhibition

Mechanism based inhibitors were first conceptualised in the early 1940s, but were not given a name until 1970 when Bloch and co-workers described the inhibition of β-hydroxydecanoylthioester dehydrase by 3-decyanoylthioesters[3]. A mechanism based enzyme inhibitor is formally described as "a relatively unreactive compound, having a structural similarity to the substrate or product for a particular enzyme that, via its normal catalytic mechanism of action, converts the inhibitor molecule into a species which, without prior release from the active site, binds, most often covalently, to that enzyme."[4]

Mechanism based inhibitors are designed as non-reactive, latent reactive compounds, which are delivered to the targeted enzyme in such a way as not to disturb other enzymic processes in the body. The latent inhibitor must be sufficiently similar to the natural substrate to be accepted into the active site of the enzyme where hydrolysis of the scissile bond occurs, to produce a highly reactive species. This reactive species alkylates or acylates a nucleophilic residue on the enzyme.

Le Chatelier principle dictates that the position of the equilibrium to form the enzyme-inhibitor complex, E•I, over the enzyme-substrate complex, E•S, is governed by the concentration of the enzyme, the inhibitor and the substrate.

$$E + I \rightleftharpoons E{\bullet}I \longrightarrow E\text{-}I$$

$$E + S \rightleftharpoons E{\bullet}S \longrightarrow E{\bullet}P \rightleftharpoons E + P$$

Figure 1.2

The concentration of a drug must be maintained at a saturation level at the site of action for a drug to have maximum pharmacological effect. Mechanism based inhibitors are designed so that nonspecific alkylations and acylations do not occur at other proteins. Therefore, undesired side effects do not occur, and hence the toxicity of the specific inhibitor is low. Table 1.1 shows a selection of enzymes that have been targeted for mechanism based inhibition.

Enzymes Targeted by Mechanism Based Inhibitors and Their Therapeutic Goal

Enzyme	Therapeutic goal
Monoamine oxidase	Antidepressant agent
	Antiparkinsonian agent
Thymidylate synthetase	Anticancer agent
β-Lactamase	Synergistic with antibiotics
Serine Proteases	Anticoagulant agent
	Antiviral agent
	Treatment of emphysema
	Arthritis
	Pancreatitis
	Inflammation
DNA Polymerase I	Antiviral agent
Dihydrofolate reductase	Anticancer agent
	Antibacterial agent
	Antiprotozoal agent

Table 1.1

1.1.1 The Design of the Latent Reactive Enzyme Inhibitor

The *N*-acylated pyrrole **1.4**, Figure 1.3, is designed to mimic the enzyme's natural substrate, hence the "pseudo" amino acid Pyr is placed at P_1' subsite and Phe at P_1, where P_1 and P_1' define the cleavage site. Shecter and Berger[5] developed a notation to describe the amino acid sequence of the substrate residues flanking the scissile bond, Figure 1.4. The letter 'S' is used for subsites on the enzyme and 'P' for the inhibitor or substrate. The scissile bond is placed between P_1 and P_1' with subsequent amino acids being numbered sequentially from the scissile bond and denoted with a prime (') if on the *C*-terminal side of the scissile bond, and without the prime if on the *N*-terminal side.

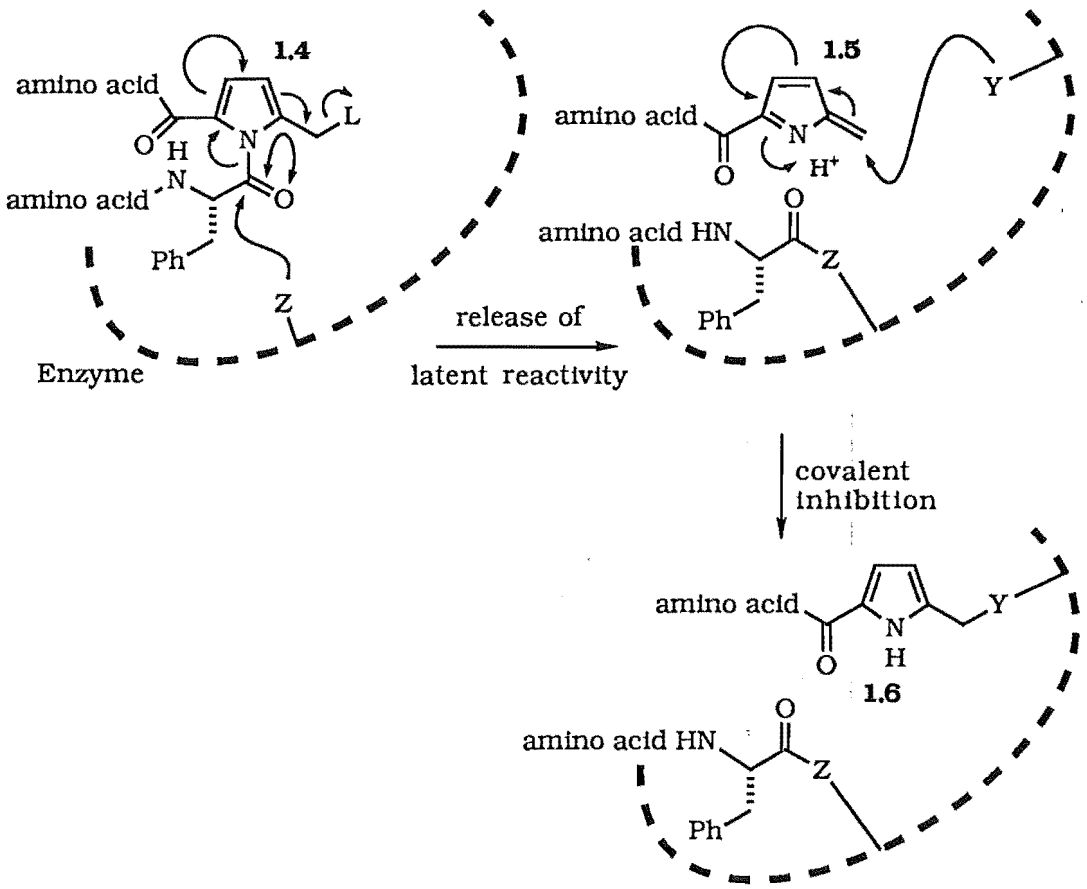

Figure 1.3

Catalytic hydrolysis of the amino acid-Pyr **1.4** scissile bond, with subsequent loss of the leaving group L, would produce an electrophilic azafulvene **1.5** in Figure 1.3.

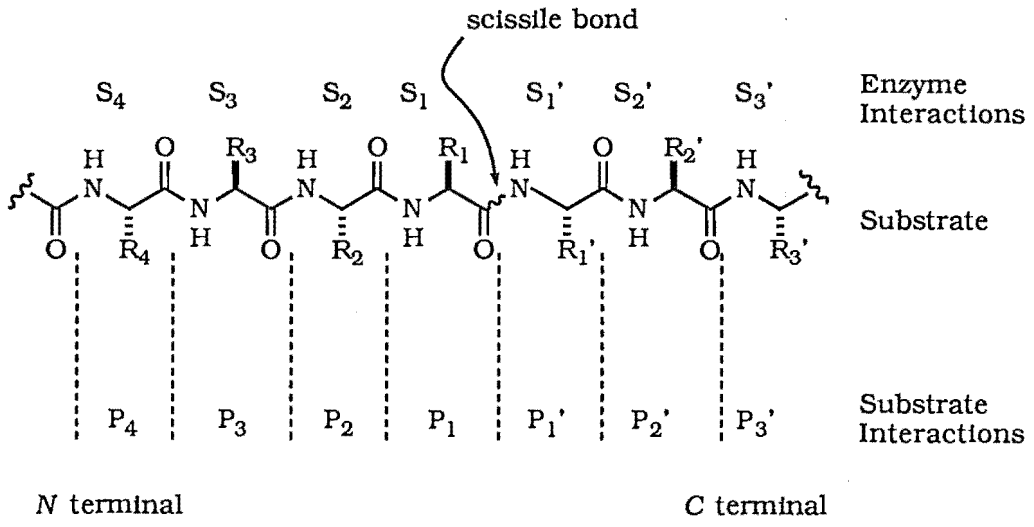

Figure 1.4

The azafulvene, produced at the active site, would then alkylate a nucleophilic or charged residue, to give the bound pyrrole derivative **1.6.**

Serine proteases, eg: chymotrypsin, would be expected to be particularly susceptible to this type of inhibition, as they have several suitable nucleophilic residues in the active site.

Aspartic acid proteases, eg: the HIV protease, lack obvious nucleophilic residues although some covalent inhibitors of HIV protease are known[6]. The catalytic aspartic acids may themselves act as the nucleophilic residue. Other possible nucleophilic species included Thr26 or an active site water molecule that has been identified by X-ray crystallography[7]. There is a possibility that this tightly bound water molecule could act as the nucleophilic residue, see the discussion on HIV proteases.

1.1.2 Azafulvene Chemistry - The Mode of Inhibition

A pyrrole substituted with a leaving group at the 2-position as in **1.7** Figure 1.5, is known to undergo loss of this leaving group to form an azafulvene **1.3**[8,9,10,11]. This process occurs readily when the pyrrole nitrogen is not acylated.

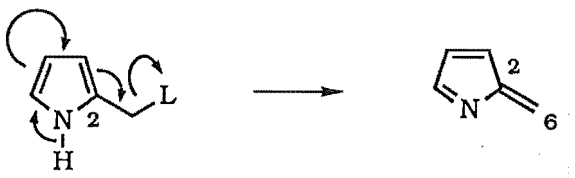

1.7
A 2-substituted pyrrole

1.3
Azafulvene

Figure 1.5

The reaction of **1.8** with $LiAlH_4$ does not give **1.9** as in Figure 1.6, this suggests that *N*-acylation of a pyrrole, as in **1.10**, suppresses azafulvene **1.3** formation[11], see Section 2.1.2 and Section 4.7.1 for further details. When pyrrole-2-carboxaldehyde is subjected to the same $LiAlH_4$ conditions the product is 2-methyl pyrrole.

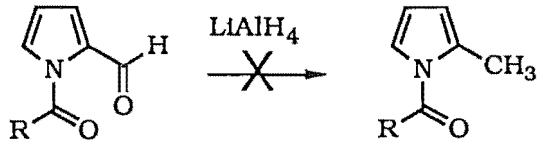

1.8 **1.9**

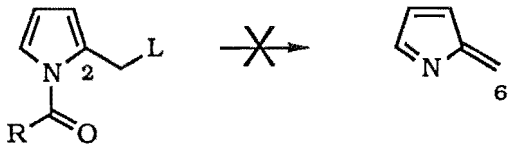

1.10 **1.3**

An *N*- substituted, 2 substituted pyrrole

Azafulvene

Figure 1.6

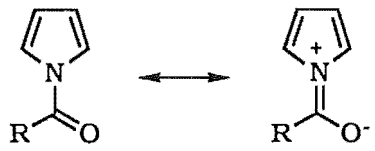

1.11 **1.12**

Figure 1.7

Pyrrole *N*-acylation, as in **1.11** removes electron density from the nitrogen, see Figure 1.7, and thus suppresses azafulvene formation. The more electron withdrawing the substituent, the more suppressed the pyrrole is to azafulvene formation.

Spectroscopic data suggest that azafulvenes, eg: **1.13**, are best represented by the resonance forms as depicted in Figure 1.8[12].

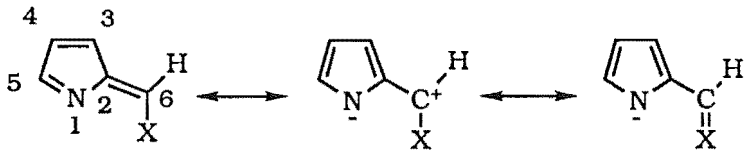

$X=NMe_2, O^-$ $X=NMe_2, O^-$ $X=NMe_2^+, O$

1.13 **1.14** **1.15**

Figure 1.8

The resonance contributing structure, **1.14** shown in Figure 1.8, has a positive charge at the 6-position and as such, an azafulvene is extremely susceptible to nucleophilic attack at this position.

1.2 Target Proteases

CHYMOTRYPSIN

Serine proteases are ideal for mechanism based inhibition. The nucleophilic residues Ser and His are both contained within the active site. Serine proteases comprise the largest and most thoroughly understood group of proteolytic enzymes[13]. Many serine proteases are known with a diversity of function. They include chymotrypsin (digestion), trypsin (digestion), thrombin (blood coagulation), plasmin (lysis of blood clots), acrosin (sperm penetration) and subtilisin (digestion) as well as elastase (emphysema).

Chymotrypsin is biosynthesised in the pancreas as non-active pre-chymotrypsin. The proteolitic enzyme trypsin cleaves the pre-chymotrypsin in the intestine to produce π-chymotrypsin. Several further modifications to π-chymotrypsin, by π-chymotrypsin itself, produce the fully active form, α–chymotrypsin[14]. This contains a total of 245 amino acid residues that make up three polypeptide chains linked by disulfide bridges. Chymotrypsin is therefore not strictly a monomeric enzyme. X-Ray crystallography confirmed that chymotrypsin possesses two active sites and is a roughly symmetrical globular enzyme[17].

The X-ray crystal structure also reveals the position of the polypeptide backbone with three amino acid residues of the active site clearly set up to act in a charge relay system, Section 1.2.1, the aspartyl residue at position 102, the imidazole ring of histidine at position 57 and the serine residue at position 195. The catalytic triad described here is characteristic of all serine proteases.

The ingested proteins and polyproteins found in the intestine are the natural substrates for chymotrypsin[15]. On contact with the substrate, the enzyme acts as an endopeptidase cleaving the polypeptides in a broad but clearly defined region. Chymotrypsin cleaves at aromatic residues, and less readily at hydrophobic aliphatic residues. Cleavage at Phe, Tyr and Trp residues positioned at P_1 occur readily, while Ile, Leu and Val represent less favoured cleavage sites. The enzyme-substrate recognition of serine proteases relies on the recognition of the primary binding substituent S_1. The amino acid side chain of the cleaved peptide, positioned at P_1', has been found to be important in the stability of the new peptide before it leaves the active site[16]. Hydrogen bonding interactions between active site amino acids and the peptide substrate up to three peptides removed from the primary binding amino acid are also important. The subsites S_4, S_2, S_2' and S_3' have been found to be particularly sensitive to replacement with amino acid residues

with different properties, ie: acidic groups for basic groups.

1.2.1 Mechanism of Serine Protease Hydrolysis of a Peptide Bond

The driving force for the hydrolysis of the peptide bond in serine proteases is the catalytic triad, comprising Asp102, His57 and Ser195 in chymotrypsin **1.16**, Figure 1.9. The Asp and His residues act as an electron sink and source in a charge relay system that enhances the nucleophilicity of the Ser-OH residue[17].

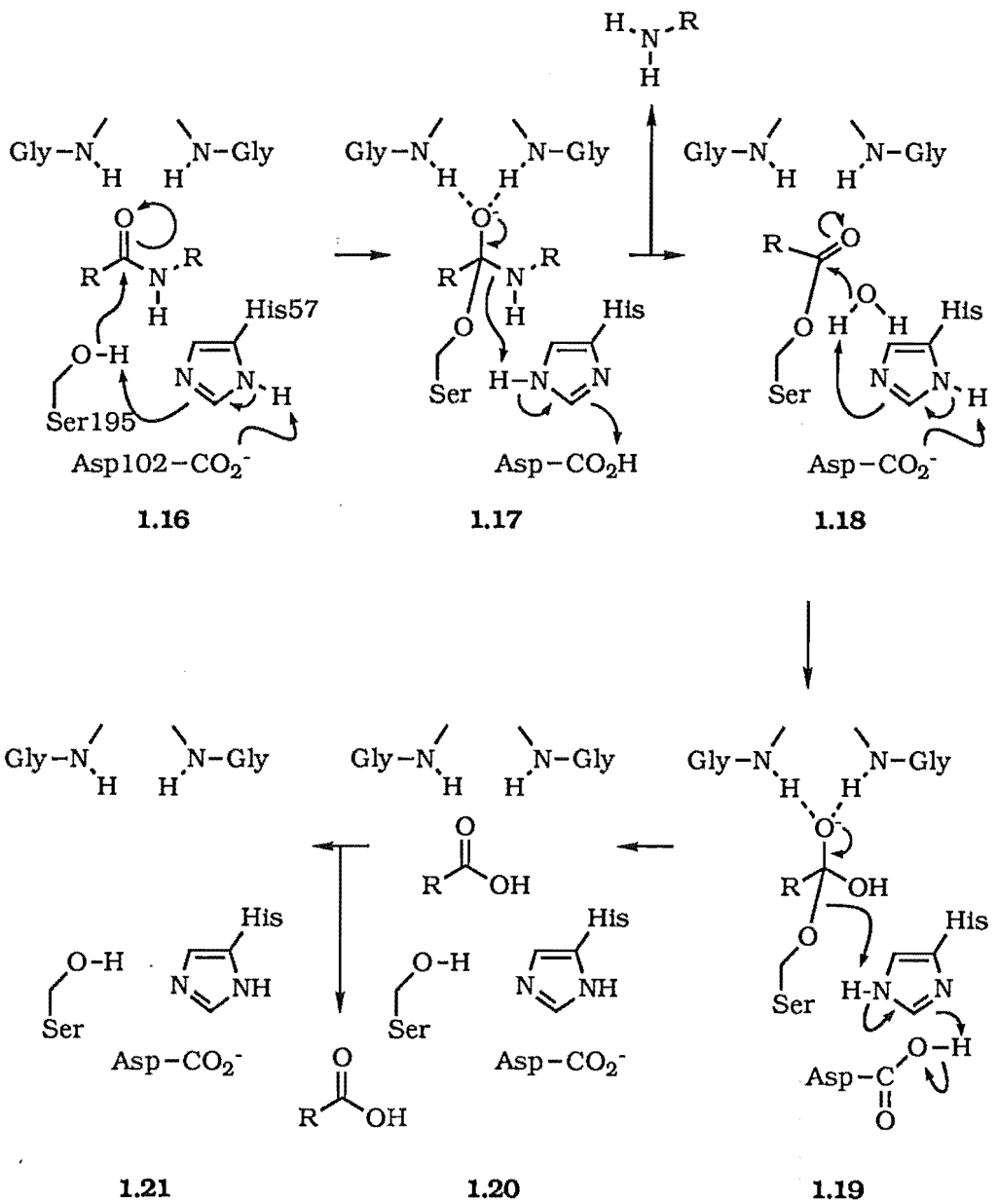

Figure 1.9

The Ser-OH is acylated by the substrate to give the acyl enzyme

intermediate with the release of a new *N*-terminal peptide **1.18**. The reaction proceeds via a tetrahedral intermediate that is stabilised by an oxyanion hole of the enzyme backbone **1.17**. The acyl enzyme is finally hydrolysed to yield the *C*-terminal peptide with the regeneration of the catalytic triad **1.19-1.21**.

1.2.2 Inhibition of Chymotrypsin

Inhibitors of serine proteases provide anticoagulant agents, antiviral agents, and potential treatments of emphysema, inflamation, arthritis, adult respiratory distress syndrome, pancreatitis, some degenerative skin disorders and digestive disorders. Chymotrypsin is responsible for a variety of digestive disorders. The inhibition of these enzymes must lead to a potential pharmocalogical agent.

A brief description of several classes of chymotrypsin and serine protease inhibitors is described below. There are several books and reviews on the inhibition of serine proteases[4,15,17,18].

1.2.2.1 *Mechanism Based Inhibition of Serine Protease*

Chymotrypsin has been shown to be inhibited by the succinimide **1.22**, Figure 1.10[18].

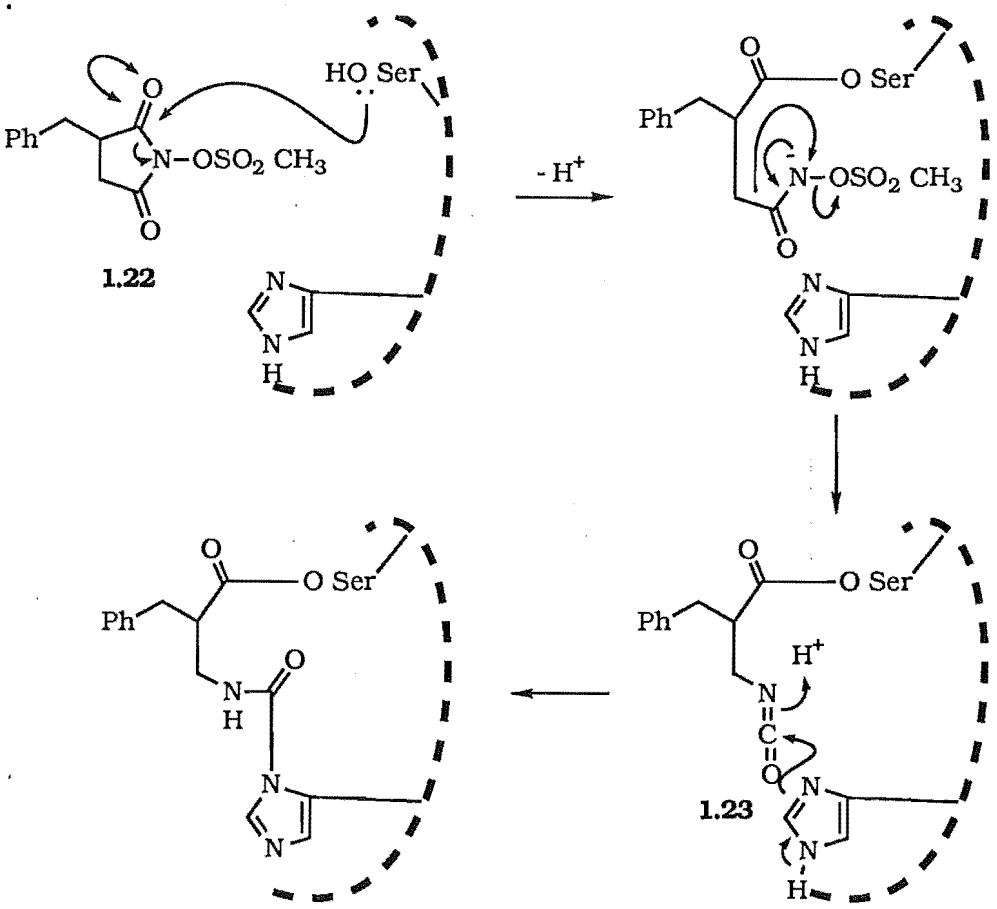

Figure 1.10

Enzyme hydrolysis of the succinimide amide bond, generates an electrophilic isocyanate **1.23** via a "Lossen Rearrangement". Figure 1.10 summarises the mechanism of a typical mechanism based inhibitor in the active site of chymotrypsin.

The isocyanate **1.23** rapidly reacts with the active site His residue, to inactivate the enzyme. This reaction gives credence to the postulate that serine proteases may well be inactivated by the amino acid-Pyr type inhibitors that have been designed in the present work.

The synthesis of α-amino halo enol lactones has been developed in order to achieve more selective protease inhibitors[19]. This allows for the inclusion of the halo enol lactone into an oligopeptide.

Halo enol lactones, as in **1.24** in Figure 1.11, contain a latent reactive halogen within the inhibitor[20]. On enzyme action, Figure 1.11, the reactivity is released as an electrophilic α-halo ketone **1.25**. This species is attacked by a nucleophilic residue, again most likely His, to give the bound compound **1.26**.

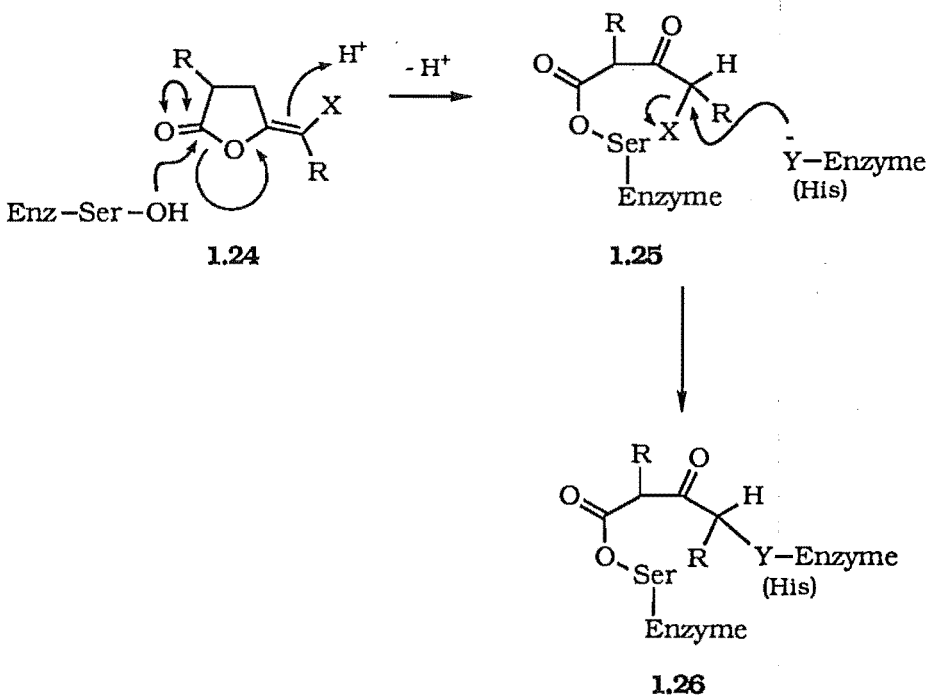

Figure 1.11

The 4-chloroisocoumarin system **1.27** forms the basis of a number of mechanism based inhibitors of serine proteases[21]. The nature of the substituents R and R' determine the inactivator specificity. The dichloroisocoumarin, R=Cl, R'=H, is a general inhibitor of all chymotrypsin like enzymes. A proposed mechanism based inhibition mechanism is summarised in Figure 1.12.

Ser195 catalyses lactone ring opening to give **1.28**. Tautomerisation releases the latent reactivity in the form of an acid chloride **1.29**, R=Cl. Irreversible covalent inhibition occurs when a nucleophilic residue, either Ser195 or His57, reacts with the acid chloride to give **1.30** .

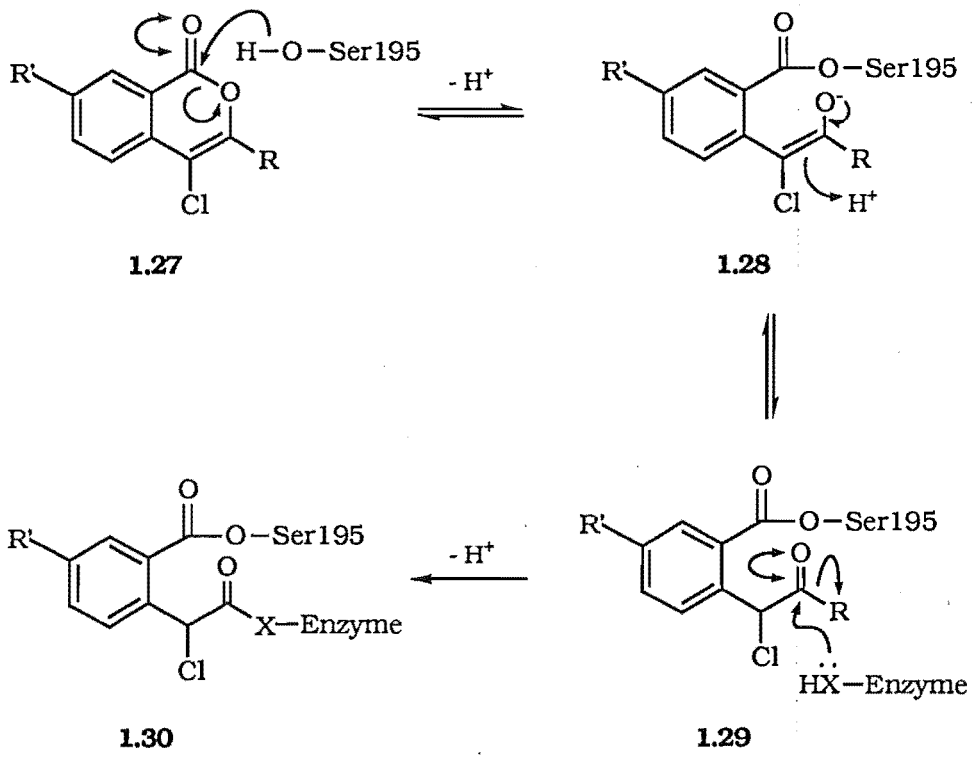

Figure 1.12

1.2.2.2 *Affinity Labelled Inhibitors*

This class of inhibitors is comprised exclusively of covalent inhibitors. They contain a reactive functional group that generally inhibits via S_N2 alkylation or acylation. Often, more than one enzyme or protein undergoes the alkylation or acylation and therefore, this is not a selective inhibition approach.

An affinity labelling reagent gains specificity if it binds initially to the enzymes active site, rather than simply undergoing degradation in solution[22]. On attack at the reactive centre and covalent bond formation, the enzyme becomes irreversibly alkylated. Figure 1.13 shows an affinity labelling reagent based on the α-chloro ketone system, and a reactive azapeptide.

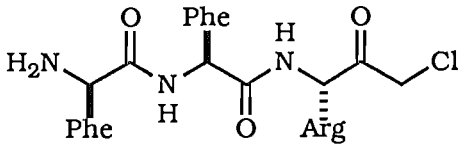

D-Phe-Phe-Arg-CH_2-Cl
chloromethyl ketone

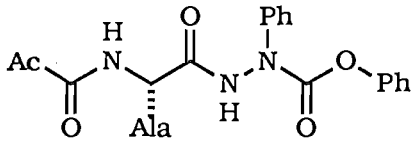

Ac-Ala-Aphe-OPh
azapeptide

Figure 1.13

This method has been useful in the identification of nucleophilic residues active site residues[23].

1.2.2.3 *Transition State Analogues*

This approach to protease inhibition is discussed in detail in Section 1.2.4.1. The carbonyl of the scissile bond is replaced with a non-hydrolysable group to block the active site. These inhibitors often employ aldehydes or boronic acids[24]. The trigonal arrangement of the boron in boronic acids appears similar to a transition state in the normal hydrolysis pathway, discussed earlier in Section 1.2.2.1.

1.2.2.4 *Peptides*

Simple peptides have frequently been found to possess some inhibitory action. Cyclic peptides have been designed to mimic the reactive site structures of naturally occurring protease inhibitors. These simple cyclic peptides inhibit chymotrypsin more efficiently than linear peptides[24].

Serine proteases, such as chymotrypsin, are ideally suited to mechanism based inhibition by virtue of the nucleophilic residues in the active site. Several mechanism based inhibitors have been developed to target this important class of enzyme, but none as yet, have reached the human drug market. Many other classes of inhibitor are known, but only a selection is described in the text above.

HIV-1 PROTEASE

Barre-Sinoussi's group[25] in 1983 described a virus which was to become one of the most feared diseases of the latter portion of the 20th century. Almost without precedence it promoted a huge scientific and clinical effort to understand and to find a cure for the deadly virus. The Human Immunodefieciency Virus (HIV) is the causative agent of the Acquired

Immunodeficiency Syndrome - AIDS[1].

The virus targets the immune system, over time leading to a severe depletion of the $CD4^+$ T-lymphocytes. $CD4^+$ T-lymphocytes are responsible for the detection and destruction of foreign material entering the body. A depletion of the lymphocytes results in opportunistic infections, and also in many neurologic disorders. Ultimately, death is caused by these complications.

Much of the initial research on HIV lead to an understanding of the virus action at a molecular level. This, in turn, produced several potential molecular targets for AIDS therapy, Figure 1.14[26].

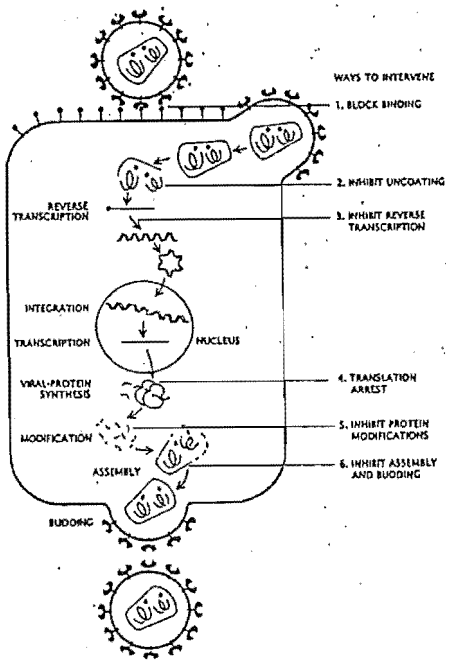

Figure 1.14

One of these targets was identified as a viral protease, HIV-1 protease. This proteolytic enzyme is responsible for viral component maturation by cleavage of the large polyproteins. The amino acid sequence of the protease shows that a highly conserved triad, Asp-Thr(Ser)-Gly, was homologous to other proteases in the aspartic acid family. Classical aspartic acid proteases such as pepsin and renin have approximately 200 amino acid residues and two catalytic triads.

An initial X-ray crystal structure of the HIV protease[27] firmly established the homodimeric nature of the enzyme and showed that each monomer of 100 residues was related to the other by a crystallographic C_2 axis of symmetry. The catalytic triad of Asp25-Thr26-Gly27 occurs in a loop which is hydrogen bonded to the corresponding loop in the other monomer. This characteristic is called the "fireman's grip" and is typical of aspartic acid proteases such as Rocus Sarcoma Virus (RSV)[28], and Simian Immunodeficiency Virus (SIV)[29] proteases. A distinct β-hairpin loop extends from each monomer over the active site to enclose a cleft in which the substrate is bound. This "flap" allows the protease to bind six to seven residues in a hydrophobic environment.

Site directed mutagenesis of the HIV protease established that without the functioning protease enzyme, a non-infectious virus was formed[30]. These experiments also showed that the mammalian host cell is unable to process the HIV genome. Hence with the HIV-1 protease inactivated, only immature and non-infectious virons would be produced.

The HIV protease is required to make several highly specific cleavages on large polyprotein substrates. The cleavage sites span amino acid sequences which are not homogeneous. The conformation of the amino acid sequence is also important for substrate recognition.

The commonly observed cleavage at an aromatic amino acid-Pro site, is of particular interest. *N*-Terminal hydrolysis next to Pro is most uncommon in mammalian systems and leads to the possability of a target for inhibition. Remarkable diversity of amino acids is observed about the scissile bond (P_1-P_1'): Leu-Ala, Phe-Leu, Met-Met, Leu-Phe are found at the cleavage site.

Crystallographic data was in agreement with the postulate that multiple hydrogen bonding occurs between the enzyme and inhibitor[1,7]. These were found to span the P_4-P_3' subsites of the enzyme. Close van der Waals contact for P_3-P_3' side chains are also evident.

1.2.3 Mechanism of Aspartic Acid Protease Hydrolysis of Peptide Bonds

Aspartic acid proteases are fewer in number than the serine proteases and are less well understood. Examples include pepsin and renin (both digestive enzymes) and HIV protease (viral maturation). Unlike the serine proteases, the aspartic acid proteases do not appear to utilise covalent interactions in their catalytic mechanism. Water is instead directly added to the substrate bond. Aspartic proteases appear to utilise the β-carboxyl groups located on two active site aspartic acids to catalyse the hydrolysis. The mechanism is thought to proceed as shown in Figure 1.15.

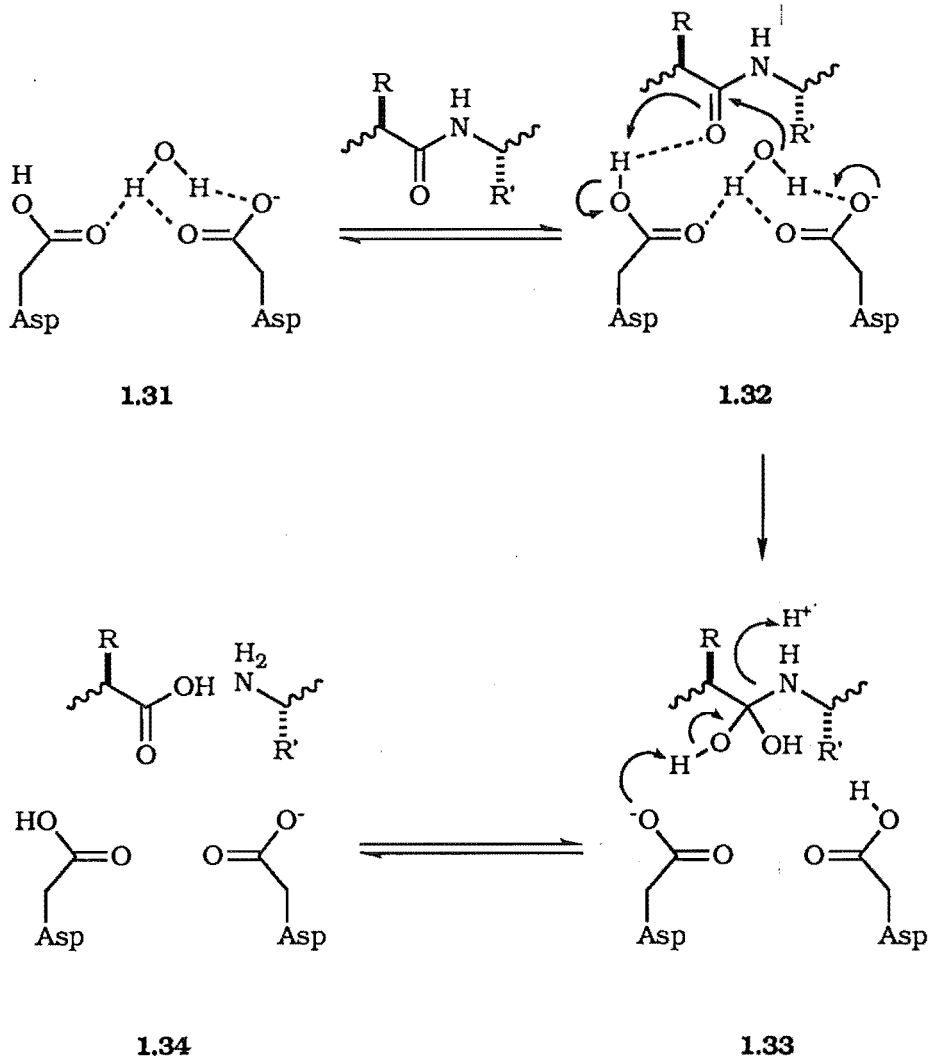

1.31 **1.32**

1.34 **1.33**

Figure 1.15

1.2.4 Inhibition of HIV Protease

The close similarity of the inhibited protease crystal structures is remarkable. Figure 1.16 shows a number of HIV protease inhibitors.

A slight reorganisation of the enzyme's core with respect to the native enzyme is observed in each of the enzyme-inhibitor complexes. The enzyme-inhibitor structure for acetyl-pepstatin[31,32,33], **1.35** Figure 1.16, revealed that the 44 Cα core atoms of each monomer in the enzyme move with a root mean square deviation of 0.4Å relative to the native enzyme. In **1.36** and **1.37** the corresponding movement is only 0.65Å, despite the very different structures.

The flap region of the enzyme has the largest conformational change for the unbound relative to the inhibitor bound protease. The tips of each loop move up to 7Å on binding with the inhibitor. "Closing" the flaps forms a hydrophobic tube which shields approximately 80% of a bound inhibitor from solvent.

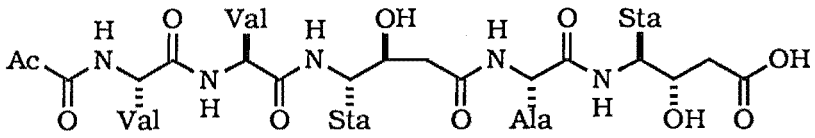

1.35 Acetyl pepstatine

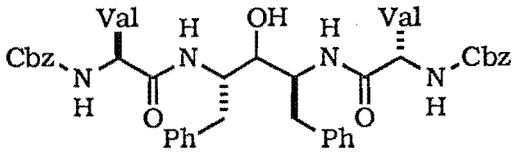

1.36 C_2 Inhibitor

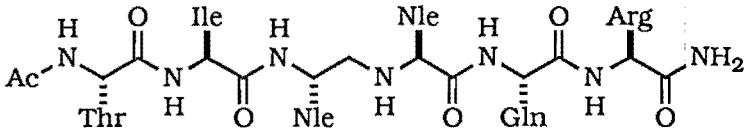

1.37

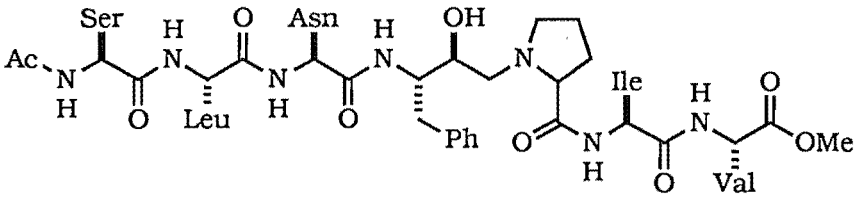

1.38 JG-365

Figure 1.16

All of the enzyme-inhibitor complexes studied by X-ray crystallography have a tightly bound water molecule that bridges the two enzyme flaps positioned by hydrogen bonds to Ile50 and Ile250 and amide hydrogens of the P_2 and P_1' carbonyl oxygens of the inhibitor. Each of the four inhibitors is bound in an extended conformation spanning the P_4-P_3' sites of the enzyme. A complex network of hydrogen bonds exists between the enzyme and polar atoms in the inhibitor.

1.2.4.1 *Transition State Mimic Inhibitors*

A classical approach for designing an enzyme inhibitor is to replace the scissile amide bond, as in **1.39** with a transition state mimic. This technique has had good results in the production of potent renin inhibitors[34]. Dreyer and co-workers[35] attempted a similar ploy with the HIV protease by replacing the scissile amide bond with non-hydrolysable dipeptide isosteres, **1.40**, **1.41**, **1.42**, **1.43**, **1.44**, **1.45**, Figure 1.17. They found that

hydroxyethylene isostere **1.41** containing peptides, had the greatest affinity for the HIV protease. The statine based inhibitors **1.40** had moderate to low potency, while the phosphinate isostere inhibitors **1.44** had modest affinity. The reduced-peptide **1.45** analogues were also weak inhibitors.

Many other hydroxyethylene isostere based inhibitors have been synthesised and tested[36].

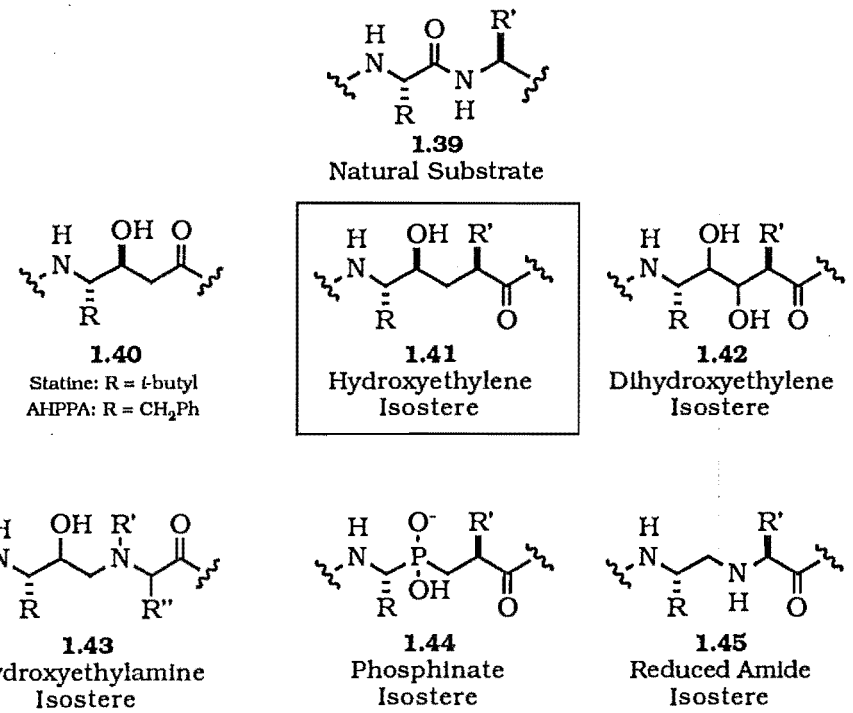

Figure 1.17

The observation that the HIV protease cleaves at the unusual position of the *N*-terminal side of proline, caused Roberts[37] and co-workers to develop a series of modified hydroxyethylamine dipeptide isosteres to mimic Phe-Pro, Figure 1.18.

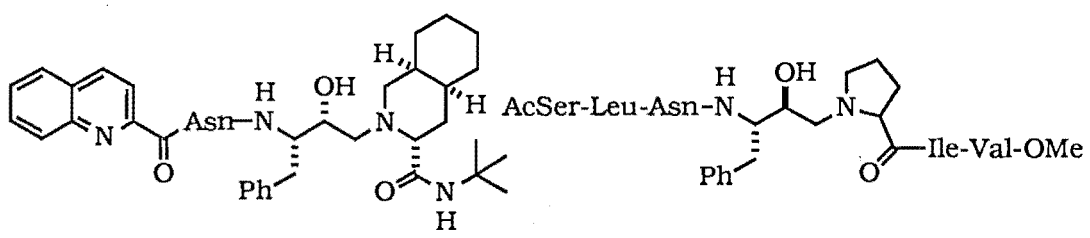

Figure 1.18

These compounds were shown to be are respectable inhibitors of HIV-1 protease.

Other selective inhibitors of HIV-1 protease have been developed by

replacing Pro with the six membered analogue, pipecolic acid[38].

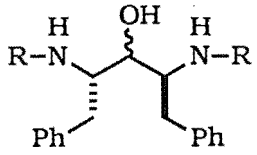

1.46

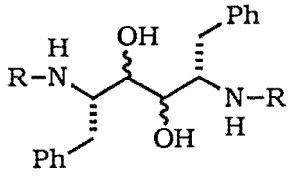

1.47

Figure 1.20

A novel series of transition state mimics have been developed by Sham and co-workers[39]. In these inhibitors the hydrolysable Phe-Pro bond was replaced with a non-hydrolysable difluoroketone transition state mimic, Figure 1.19.

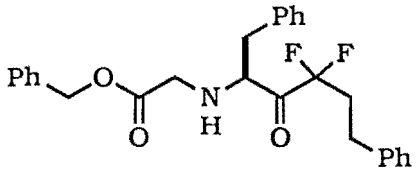

Figure 1.19

1.2.4.2 *Symmetry Based HIV Protease Inhibitors*

The crystallographic observation that the HIV protease is a homodimer with each monomer related by a C_2 axis of symmetry prompted Kempf[40] to synthesise C_2 symmetry based inhibitors, eg: **1.46** and **1.47**, Figure 1.20. These inhibitors have several advantages over the classical transition state mimic inhibitor. The first is that the less peptide like structure may overcome stability problems *in vivo*, where genuine peptides tend to degrade. The second is that the symmetry imparts a high degree of enzyme specificity for the targeted enzyme.

The amino acid sequence was extended in the *N*-direction. Compounds with only P_1 and P_1' residues produced little inhibitory action, eg: R=Ac. Introduction of the P_2 and P_2' residues, eg: R=Val-Cbz, resulted in nanomolar inhibitors. Replacement of the hydroxyl group of **1.46** with a carbonyl group, caused a one thousand fold decrease in potency, thus indicating that tetrahedral geometry is important.

1.2.4.3 *Non-Peptide Based Inhibitors of HIV Protease*

Peptide based transition state inhibitors are plagued with a lack of oral activity, short duration of action, a lack of specific target ability and the inability to cross the blood-brain barrier. The following are non-peptide based inhibitors which are expected to be more robust in the body.

The epoxide containing antifungal antibiotic cerulenin, Figure 1.21,

was identified by both Blumenstein[7] and Pearl[41] as a potent HIV protease inhibitor.

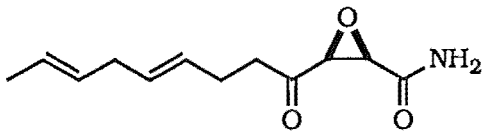

cerulenin, IC_{50} 2 500

Figure 1.21

The epoxides are thought to inhibit the protease by electrophilic ring opening and subsequent alkylation. The carbon chain appears to position the epoxide at the active site.

The electrophilic inhibition postulated for the epoxides, is similar to the mode of action that is postulated for the azafulvenes, eg: **1.3** produced in our inhibitors.

A series of long chain dicarboxylates, eg: $HOOC(CH_2)_{20}COOH$, were tested against the HIV protease[42]. Crystal structures of other HIV protease inhibitor complexes reveal a hydrophobic substrate binding groove. This groove, approximately 24Å long, has several charged hydrophilic residues (Asp29 & 30 and Arg8) at either end of the hydrophobic tube. The long chain dicarboxylates are thought to interact with these charged residues.

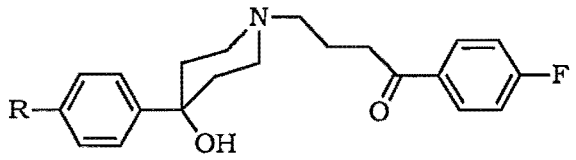

Haloperidol R = Cl
Bromoperidol R = Br

Figure 1.22

DesJarlais[43] identified Haloperidol, Figure 1.22 (R=Cl), as an HIV protease inhibitor by a comparison of the active site of the enzyme and the crystal structures of small molecules contained in the Cambridge Database.

This represents the first attempt to solely use receptor structure to search for an innovative new inhibitor lead. The search produced a small set of molecules which fitted the profile; bromoperidol was one such compound (Figure 1.22, R=Br).

Haloperidol was used for the inhibitory studies, but was found to be highly toxic at the levels required to inhibit HIV-1 and HIV-2 protease and as such is not useful as an anti-AIDS pharmaceutical. The drug Haloperidol points the way to a new generation of protease inhibitors.

A recent report by Karlström and Levine[44] has indicated that Cu^{2+} also inhibits the HIV protease. On recovery, denaturation and refolding of the enzyme, full activity was restored. This evidence strongly suggests that cysteine is binding the copper.

A remarkable amount of progress has been made towards establishing potent inhibitors of the HIV protease. A casual observation of the previously described inhibitors indicates that there is not a great deal of structural consistency. Hydrophobic interactions dominate the crystal structures of the enzyme-inhibitor complexes and this trend appears to follow through into the other non-crystalline enzyme-inhibitor complexes. Optimum residues for an inhibitor need not resemble substrate sequences as these appear less crucial to recognition than in other enzyme systems.

KIDNEY PROLIDASE

The manganese dependent dipeptidase, Prolidase (or Prolinedipeptidase) is another of the few enzymes known to catalyse the hydrolysis of peptide bonds on the *N*-terminal side of Proline[2]. The enzyme is cytosolic and therefore an inhibitor would be required to pass through the cell membrane. Humans lacking this enzyme suffer from skin lesions and limb abnormalities. Prolidases are found in most mammalian tissues and microorganisms where they degrade exogenous and endogenous polypeptides, allowing for recycling or renal excretion of proline and hydroxyproline[45].

1.2.5 Inhibitors of Prolidase

A model of the active site of the kidney prolidase has been proposed. There are three distinct subsites in the active site region, acidic, basic and hydrophobic. Using this information Wolfenden[2] proposed that the cyclopentane-1,2-dicarboxylic acid **1.49**, Figure 1.23, would be an inhibitor of the enzyme, since it resembles the product of hydrolysis (Pro).

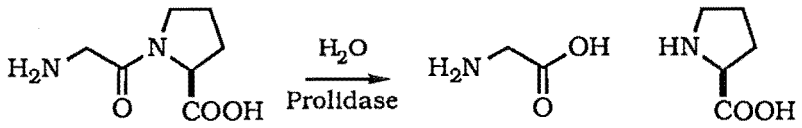

1.48
Glycyl-L-Proline
K_m=1.2μM

Glycine
K_i>10^{-2}M

Proline
K_i=0.51μM

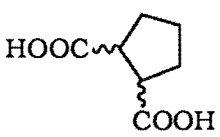

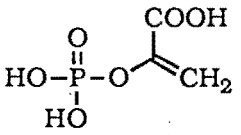

1.49
Cyclopentane-1,2-dicarboxylate acid
K_i=0.51μM

1.50
Phosphenolpyruvate
K_i=8.5nM

Figure 1.23

The dicarboxylate **1.49** also has the same spatial arrangement as the natural substrate Gly-Pro **1.48.**

It was found that although the "substrate shaped" inhibitor provided adequate inhibition of the prolidase, the transition state analogues of phosphyl and phosphonyl based inhibitors, were superior. The discovery that the phosphonic compounds and phosphoenol pyruvate **1.50**, a well known glycolytic intermediate, were respectable inhibitors[46] lead to much work optimising the type of phosphonic compounds that inhibit the enzyme.

1.3 The Aim of the Research

The synthesis of amino acid-pyrrole compounds, eg: **1.4** requires a new methodology to be developed for the *N*-acylation of pyrrole. The few existing methods for the acylation reaction tend to be harsh and low yielding. A mild general reaction suitable for use with an amino acid sequence was the aim of the synthesis.

The initial aim was to produce simple *N*-acylated pyrrole derivatives, with the aim of extension to amino acids on the pyrrole nitrogen to utilise the important P region recognition. This is described in Chapter Two.

The next step was to extend the P' recognition aspects of simple derivatives to larger analogues, this work is described in Chapter Three.

An understanding of the postulated mode of inhibitor action, azafulvene chemistry, was also proposed via hydrolysis studies, Chapter Four and enzyme assays, Chapter Five.

The results are presented in this thesis, and although not complete, pave the way for future developments.

1.4 References to Chapter One

[1] Huff, J. R. *J. Med. Chem.* **1991**, *34*, 2305-2314.

[2] Radzicka, A.; Wolfenden, R. *J. Am. Chem. Soc.* **1990**, *112*, 1248-1249.

[3] Endo, K.; Helmkamp Jn, G. M.; Bloch, K. *J. Biol. Chem.* **1970**, *245*, 4293.

[4] Silverman, R. B. *Mechanism-Based Enzyme Inactivation: Chemistry and Enzymology*; CRC Press Inc.: Florida, 1988.

[5] Schechter, T.; Berger, A. *Biochem. Biophys. Res. Commun.* **1967**, *27*, 157-162.

[6] Blumenstein J. J.; Copeland, T. D.; Oroszlan, S.; Michejda, C. J. *Biochem. & Biophys. Res. Comm.* **1989**, *163*, 980-987.

[7] Swain, A. L.; Miller, M. M.; Green, J.; Rich, D. H.; Schneider, J.; Kent, S. B. H.; Wlodawer, A. *Proc. Natl. Acad. Sci. USA* **1990**, *87*, 8805-8809.

[8] Schauder, J-R.; Jendrezejewski, S.; Abell, A. ; Hart, G. J.; Battersby, A. R. *J. Chem. Soc., Chem. Commun.* **1987**, 436-438.

[9] Miller, A. D.; Leeper, F. J.; Battersby, A. R. *J. Chem. Soc. Perkin Trans. 1* **1989**, 1943-1956.

[10] Jones, A. R.; Bean, G. P. *The Chemistry of Pyrroles*; Academic Press Inc.: London, 1977.

[11] Bray, B. L.; Muchowski, J. M. *J. Org. Chem.* **1988**, *53*, 6115-6118.

[12] Meyers, F.; Adant, C.; Brédas, J. L. *J. Am. Chem. Soc.* **1991**, *113*, 3715-3719.

[13] Powers, J. C.; Harper, J. W. *Proteinase Inhibitors*; Elsevier Science: England, 1986.

[14] Birktoft, J. J.; Blow, D. M. *J. Med. Biol.* **1972**, *68*, 187.

[15] Walsh, C. *Enzymic Reaction Mechanisms*; W. H. Freeman: San Francisco, 1979.

[16] Laskowski, M.; Tashiro, M.; Empie, M. W.; Park, S. J.; Kato, I.; Ardelt, W.; Wieczork, M. *Proteinase Inhibitors: Medical and Biological Aspects*; Springer-Verlag: Tokyo, 1983.

[17] Rich, D. H. *Comprehensive Medicinal Chemistry: The Rational Design, Mechanistic Study and Therapeutic Application of Chemical Compounds*, Vol. 2; Pergamon Press: Great Britain, 1990; pp391-441.

[18] Groutas, W. C.; Stanga, M. A.; Brubaker, M. J. *J. Am. Chem. Soc.* **1989**, *111*, 1931-1932.

[19] Sofia, M. J.; Chakravarty, P. K.; Katzenellenbogen, J. A. *J. Org. Chem.* **1983**, *48*, 3318-3325.

[20] Rando, R. *Science* **1974**, *185*, 320.

[21] Powers, J. C.; Kam, C.-M.; Narasimhan, L.; Oleksyszyn, J.; Hernandez, M. A.; Ueda, T. *J. Cellular Biochem.* **1989**, *39*, 33.

[22] Walsh, C. *Enzymic Reaction Mechanisms*; W. H. Freeman: San Francisco, 1979; p86.

[23] Walsh, C. *Enzymic Reaction Mechanisms*; W. H. Freeman: San Francisco, 1979; p61.

[24] Ferdinand, W. *The Enzyme Molecule*; John Wiley and Sons: London, 1976; p101.

[25] Barré-Sinoussi, F.; Chermann, J. C.; Rey, F.; Nugeyre, M. T.; Chamaret, S.; Gruest, J.; Dauguet, C.; Axler-Blin, C.; Vézinet-Brun, F.; Rouzioux, C.; Rozenbaum, W.; Montagnier, L. *Science* **1983**, *220*, 868-871.

[26] Yarchoan, R.; Mitsuya, H.; Broder, S. *Sci. Am.* **1988**, 88-97.

[27] Navia, M. A.; Fitzgerald, P. M. D.; McKeever, B. M.; Leu, C.-T.; Heimbach, J. C.; Herber, W. K.; Sigal, I. S.; Drake, P. L.; Springer, J. P. *Nature* **1989**, *337*, 615-620.

[28] Weber, I. T. *J. Biol. Chem.* **1990**, *265*, 10492-10496.

[29] Henderson, L. E.; Benveniste, R. E.; Sowder, R.; Copeland, T. D.; Schultz, A. M.; Oroszlan, S. *J. Virology* **1988**, *62*, 2587-2595.

[30] Le Grice, S. F. J.; Mills, J.; Mous, J. *EMBO J.* **1988**, *7*, 2547-2553.

[31] Kay, J.; Dunn, B. M. *Biochem. Biophys. Acta* **1990**, *1048*, 1-18.

[32] Rich, D. H.; Salituro, F. G.; Holladay, M. W.; Schmidt, P. G. *Conformationally Directed Drug Design*, American Chemical Society: New York, 1984; pp211-237.

[33] Salituro, F. G.; Agarwal, N.; Hofmann, T.; Rich, D. H. *J. Med. Chem.* **1987**, *30*, 286-295.

[34] Greenlee, W. J. *Med. Res. Rev.* **1990**, *10*, 173-236.

[35] Dreyer, G. B.; Metcalf, B. W.; Tomaszek Jn, T. A.; Carr, T. J.; Chandler III, A. C.; Hyland, L.; Fakhoury, S. A.; Magaard, V. W.; Moore, M. L.; Strickler, J. E.; Debouck, C.; Meek, T. D. *Proc. Natl. Acad. Sci. USA* **1989**, *86*, 9752-9756.

[36] Vacca, J. P.; Guare, J. P.; deSolms, S. J.; Sanders, W. M.; Giuliani, E. A.; Young, S. D.; Darke, P. L.; Zugay, J.; Sigal, I. S.; Schleif, W. A.; Quintero, J. C.; Emini, E. A.; Anderson, P. S.; Huff, J. R. *J. Med. Chem.* **1991**, *34*, 1225-1228.

[37] Roberts, N. A.; Martin, J. A.; Kinchington, D.; Broadhurst, A. V.; Craig, J. C.; Duncan, I. B.; Galpin, S. A.; Handa, B. K.; Kay, J.; Kröhn, A.; Lambert, R. W.; Merrett, J. H.; Mills, J. S.; Parkes, K. E. B.; Redshaw, S.; Ritchie, A. J.; Taylor, D. L.; Thomas, G. J.; Machin, P. J. *Science* **1990**, *247*, 358-361.

[38] Copeland, T. D.; Wondrak, E. M.; Tozser, J.; Roberts, M. M.; Oroszlan, S. *Biochem. Biophys. Res. Commun.* **1990**, *169*, 310-314.

[39] Sham, H. L.; Betebenner, D. A.; Wideburg, N. E.; Saldivar, A. C.;

Kohlbrenner, W. E.; Vasavanonda, S.; Kempf, D. J.; Norbeck, D. W.; Zhao, C.; Clement, J. J.; Erickson, J. E.; Plattner, J. J. *Biochem. Biophys. Res. Commun.* **1991**, *175*, 914-919.

[40] Kempf, D. J.; Norbeck, D. W.; Codacovi, L-M.; Wang, X. C.; Kohlbrenner, W. E.; Wideburg, N. E.; Paul, D. A.; Knigge, M. F.; Vasavanonda, S.; Craig-Kennard, A.; Saldivar, A.; Rosenbrook Jn, W.; Clement, J. J.; Plattner, J. J.; Erickson, J. *J. Med. Chem.* **1990**, *33*, 2687-2689.

[41] Moelling, K.; Schulze, T.; Knoop, M-T; Kay, J.; Jupp, R.; Nicolaou, G.; Pearl, L. H. *F.E.B.S.* **1990**, *261*, 373-377.

[42] Brinkworth, R. I.; Woon, T. C.; Fairlie, D. P. *Biochem. Biophys. Res. Commun.* **1991**, *176*, 241-246.

[43] DesJarlais, R. L.; Seibel, G. L.; Kuntz, I. D.; Furth, P. S.; Alvarez, J. C.; de Montellano, P. R. O.; DeCamp, D. L.; Babé, L. M.; Craik, C. S. *Proc. Natl. Acad. Sci. USA* **1990**, *87*, 6644-6648.

[44] Karlstrom, A. R.; Levine, R. L. *FASEB J.* **1991**, *5*, A452.

[45] Radzicka, A.; Wolfenden, R. *Biochemistry* **1991**, *30*, 4160-4164.

[46] Lacoste, A-M.; Neuzil, E. *Biochem. Soc. Trans.* **1989**, *17*, 782-783.

Chapter Two

N-Acylation of Pyrrole Derivatives

2.0 Pyrrole Nomenclature

A descriptive naming system is used throughout this thesis for the ease of reading and understanding. This system is based on the standard procedure of describing peptides in the *N*- to *C*-direction. 2-Substituted pyrrole derivatives are described as p-2-X, where the descriptor X describes the functionality on the 2 position of pyrrole. The main descriptor is 'c' for a carboxaldehyde derivative, (-CHO), eg: p-2-c represents pyrrole-2-carboxaldehyde, **2.A**, Figure 2.0.

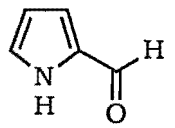

2.A
p-2-c

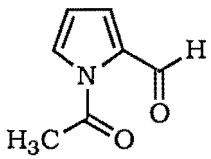

2.B
N-Acetyl-p-2-c

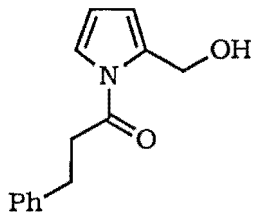

2.C
N-Cinnamoyl-p-2-OH

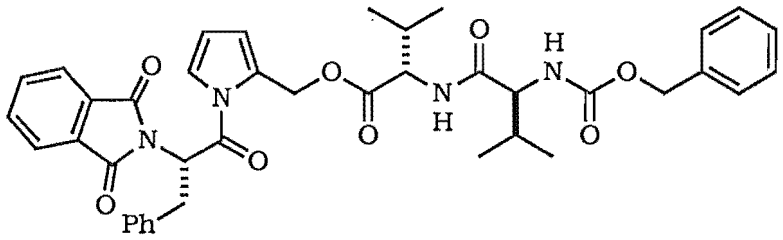

2.D
N-(*N*-Pth-Phe)-p-2-O-Val-Val-Cbz

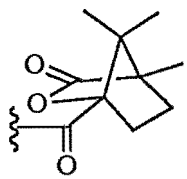

camphanate

pyr

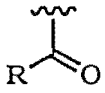

acyl

Figure 2.0

The hydroxymethyl pyrrole derivatives are described as p-2-OH, while further extension in the *C*-direction (Figure 2.9) is described in that direction. The description implies a CH_2 substituent between the pyrrole and the -OR group. This is not, however, the case where the formyl pyrrole (-CHO, c) is described.

The designator *N*- precedes p-2-X for compounds acylated on the pyrrole nitrogen, for examples see Figure 2.0. Hence *N*-acetyl-p-2-c **2.B** describes *N*-acetyl-pyrrole-2-carboxaldehyde, and *N*-cinnamoyl-p-2-OH **2.C** describes the *N*-cinnamoyl hydroxymethyl pyrrole, and *N*-(*N*-Pth-Phe)-p-2-O-Val-Val-Cbz is the pseudo peptide **2.D** drawn, in Figure 2.0. A selection of other partial descriptors used throughout this work are shown in Figure 2.0.

2.1 Introduction

The retrosynthetic analysis presented in Scheme 2.1 indicates the steps required to synthesise the potential hydroxymethyl pyrrole mechanism based inactivators **2.1**.

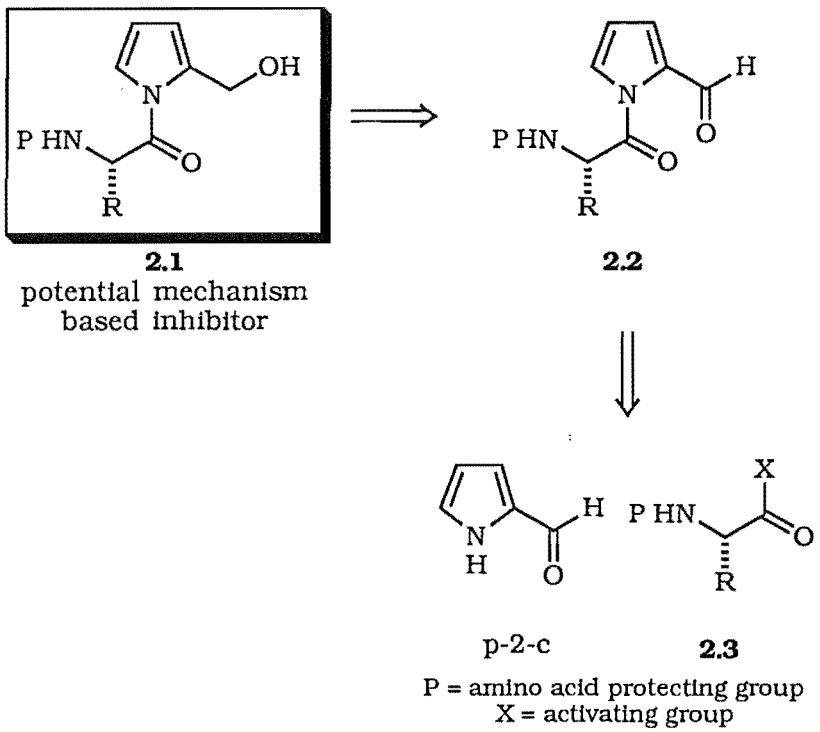

Scheme 2.1

The synthesis necessitates the acylation of pyrrole-2-carboxaldehyde (p-2-c) on nitrogen with an amino acid, eg: **2.3**. A general methodology was required to enable different acyl groups to be used. The reduction of the *N*-acylated formyl pyrrole **2.2** to the *N*-acylated hydroxymethyl pyrrole **2.1**, would then complete the synthesis. This species contains an amino acid for recognition and a leaving group for azafulvene formation, on enzyme hydrolysis of the amino acid-pyrrole amide bond, see Section 1.1.2 for a detailed discussion.

N-Acylated-p-2-c derivatives are commonly prepared via the initial *N*-acylation of pyrrole followed by a Vilsmeier-Haack formylation. Other preparations have been carried out using Thallium(I) ethoxide and acetyl chloride[1], while the reaction of pyrrole derivatives in triethylamine (TEA) and acetic anhydride (Ac_2O) at reflux have also been reported[2]. These preparations suffer from either low yields and/or cumbersome reaction conditions. Only a few isolated reports of mild acylation conditions have been

reported and in these few examples the pyrrole ring is heavily substituted[3,4,5]. The designed hydroxymethyl pyrrole inhibitor requires the acylation of the pyrrole nitrogen with an amino acid. Non-acidic conditions are required in the synthesis to eliminate pyrrole polymer formation, and mildly basic conditions must also be used to ensure that racemisation of the amino acid does not occur. Extensive investigations were carried out to arrive at the final DMAP methodology described in Section 2.4.

2.1.1 The Chemistry of Pyrrole-2-Carboxaldehyde

The pyrrole derivative chosen for the *N*-acylation reaction was 2-formyl pyrrole, p-2-c. The pyrrole nucleus of p-2-c causes the formyl substituent to behave in an atypical manner, with respect to other aldehydes. P-2-c can be represented by three resonance forms[6], Figure 2.2, and as such the aldehyde is deactivated and hence less electrophilic than other aldehydes. The deactivated aldehyde of the p-2-c formyl group is manifested by a low carbonyl IR stretching frequency (1667cm^{-1}, with respect to 1740-1720cm^{-1} of aliphatic aldehydes) and the relative upfield ^{1}H NMR formyl signal at 9.54ppm (a usual aldehyde signals at approximately 10ppm).

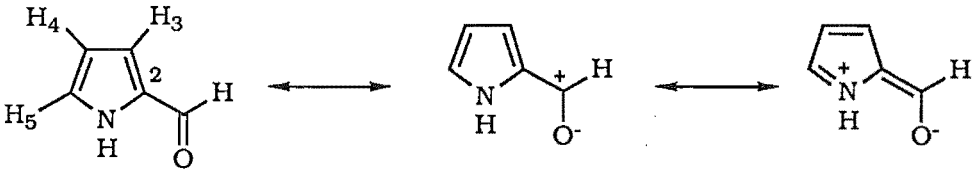

2.4 **2.5** **2.6**

Figure 2.2

The extended conjugation in p-2-c has the overall effect of increasing the acidity of the p-2-c NH and allows electrophilic attack at either *N*- or *O*-. The resonance forms **2.5** and **2.6** account for reaction through *O*; for example, formation of the pyrrylol pyrazine **2.19** in the NaH reaction of p-2-c and *N*-Ts-Leu-Cl, Section 2.2.1.2.

Structure **2.4** also indicates the pyrrole ring numbering system used throughout this thesis when describing the pyrrole derivatives.

Toube[7] performed ^{1}H NMR spectral studies on p-2-c and concluded that the preferred conformation of the aldehyde group is *syn* rather than *anti* based on the five bond coupling ($J_{5\text{-CHO}}$) between the formyl proton and H-5, Figure 2.3. This is in keeping with the well documented "zig-zag" rule[8].

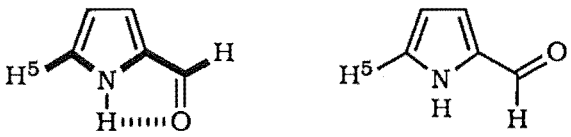

syn *anti*

"zig-zag" coupling

Figure 2.3

The *syn* conformer is also likely to be stabilised by intramolecular hydrogen bonding between the carbonyl group and the pyrrole N*H*.

2.1.1.1 *C- versus O- Acylation and Alkylation of Formyl Pyrroles*

Pyrrole derivatives can be acylated (or alkylated) on carbon-1, Scheme 2.4, with the correct choice of base.

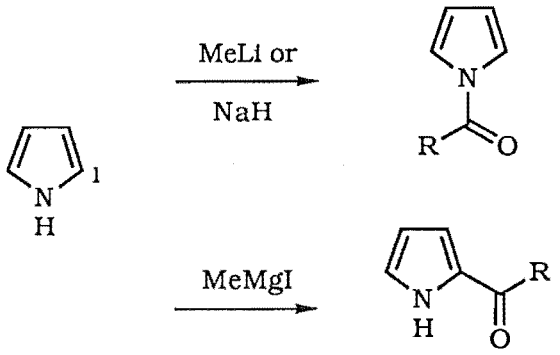

Scheme 2.4

The reaction to form the desired C-methylated derivative **2.10** (a precursor to hydroxymethyl bilane) via the pyrrole aldehyde **2.7** using methyl magnesium iodide, Scheme 2.5, yields the magnesium salt **2.8**, which on reaction with methyl iodide returned starting material, rather than the desired alkylated pyrrole **2.10**. The researchers postulated[9] that the azafulvene like species **2.9**, formed by alkylation on the formyl oxygen rather than carbon, gave starting material on work up.

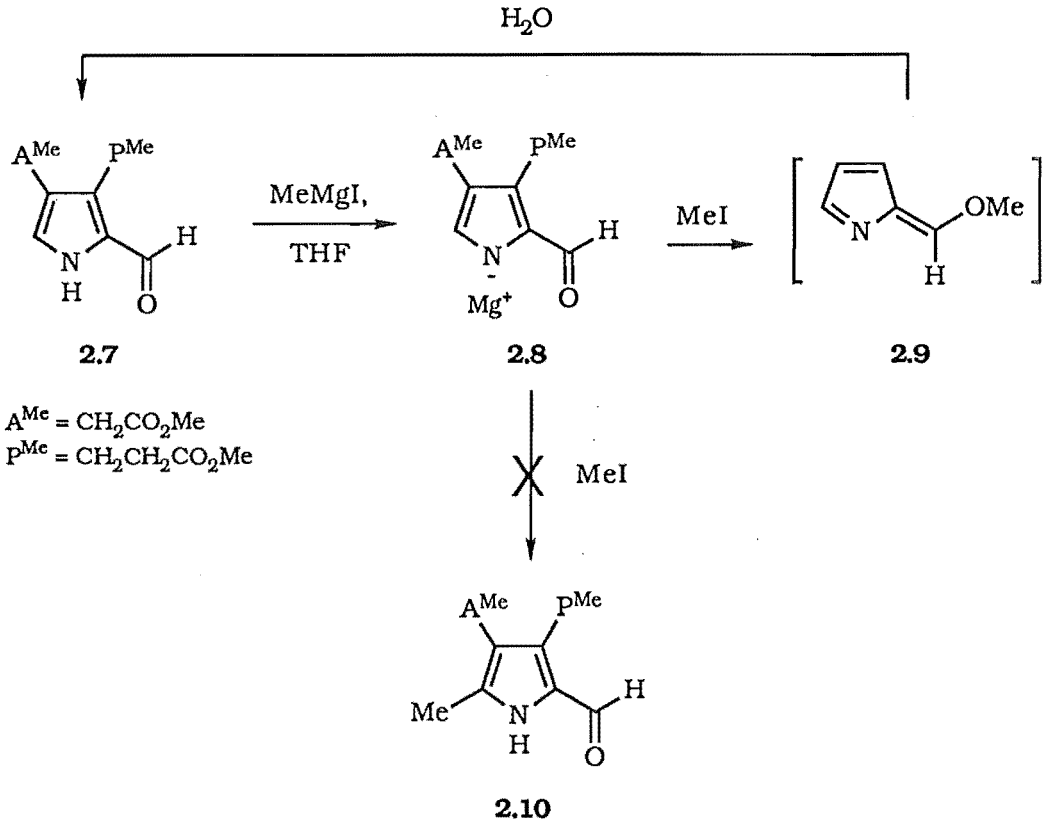

Scheme 2.5

The corresponding acetal protected aldehyde **2.11** gave the desired product on a similar treatment with NaH and methyl iodide, Scheme 2.6.

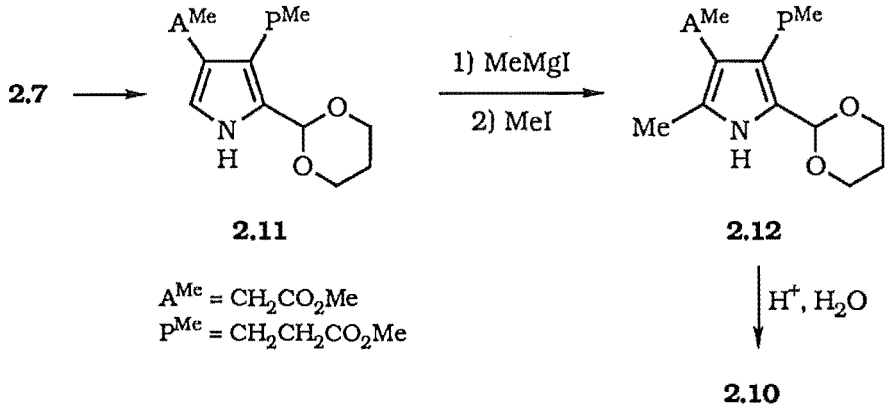

Scheme 2.6

A competition between *O*- and *C*- alkylation therefore exists, work described later supports a similar identified competition as occurring in the reaction of a pyrryl anion and the amino acid acid chloride, *N*-Ts-Leu-Cl, Section 2.2.1.

2.1.2 The Chemistry of *N*-Acylated Pyrrole-2-Carboxaldehyde

N-Acylation of pyrroles results in the deshielding of the pyrrole ring components. The amide bond increases the π electron delocalisation and deactivates the pyrrole ring, Figure 2.7.

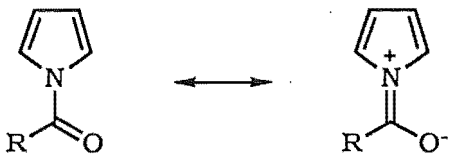

Figure 2.7

^{1}H NMR spectral studies have shown that the change in the NMR spectra peak positions between different *N*-acyl groups is caused by inductive interactions between the substituent and pyrrole ring[10].

N-Acylated-p-2-c also gives similar delocalisation interactions, in addition to the previously described aldehyde delocalisation, Figure 2.2. The overall result is to give the set of resonance contributors shown in Figure 2.8.

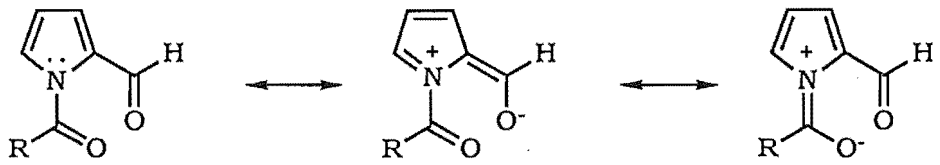

2.13 **2.14** **2.15**

Figure 2.8

The >N$^+$=C< IR stretching vibrations, in **2.15**, confirmed the existence of such canonical forms. A combination of these canonical forms also explains the unusual downfield position of the pyrrole proton resonances. The effect of altering the electron density in the ring is further discussed in Section 2.7. Acylation of formyl pyrroles has been shown to give a more aldehyde like character to the formyl group, see Section 2.7.1 for IR, UV and NMR evidence. This is evidence that the pyrrole nitrogen lone pair of electrons is delocalised into the acyl group rather than into the formyl group. Thus, resonance contributor **2.14** Figure 2.8, becomes less important.

A consequence of this is that azafulvene formation[11], in hydroxymethyl pyrrole derivatives, eg: **2.1**, is suppressed due to the unavailability of the nitrogen lone pair, see Section 4.7.1. This is a crucial factor in the designed

mechanism based inactivators.

P-2-c proved to be a suitable starting material for the synthesis of *N*-acylated p-2-c's. A simple reduction of the aldehyde to give an alcohol, allows for the extension of an amino acid chain in the *C*-direction (see Figure 2.9 for a definition of this term).

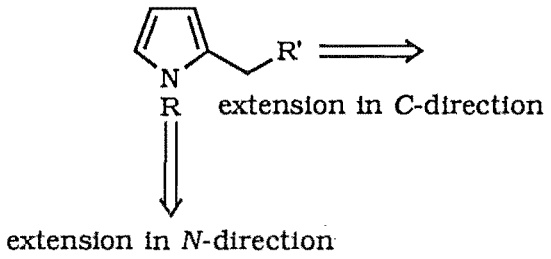

Figure 2.9

2.2 The Sodium Hydride, NaH, reaction

A report by Moon[5] indicated that reaction of *C*-substituted pyrroles with NaH and subsequent reaction with an acid chloride gave the *N*-acylated pyrrole in yields ranging from 75-80% depending on the pyrrole derivative and the acylating agent.

2.2.1 Reaction of Pyrrole-2-Carboxaldehyde Salt with *N*-Ts-Leu-Cl

Moon's methodology was adapted to an acid chloride of an amino acid. NaH (1equiv.) was added to p-2-c dissolved in freshly dried and distiled THF. After fifteen minutes *N*-Ts-Leu-Cl acid chloride **2.17** prepared from *N*-Ts-Leu-OH, using DMF and oxalyl chloride, was added dropwise to the stirred solution of the precipitate of the sodium salt of p-2-c **2.16**, (Scheme 2.10).

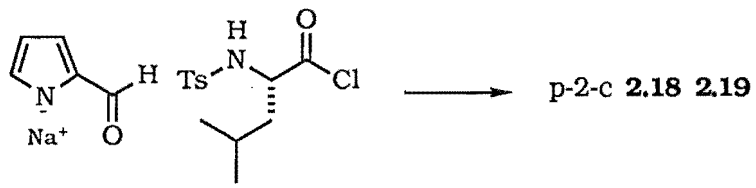

2.16 **2.17**

Scheme 2.10

The addition of the acid chloride to the pyrrole salt caused an immediate discolouration of the solution to produce a deep brown/black solution and a new accompanying precipitate. Work up gave a black oil, that by TLC contained four UV active compounds, three of which were pyrrolic (these gave a positive Ehrlich test, see Section 2.7.3.3 for a full discussion of this test).

The ^{1}H NMR spectrum of the crude products gave further evidence of three different pyrrolic compounds with appropriate signals in the 6.1-7.0ppm range. The crude sample was purified by radial chromatography on silica to give four fractions. The first fraction was identified as the oxazolidinone **2.18** (8.0%), discussed in the following section.

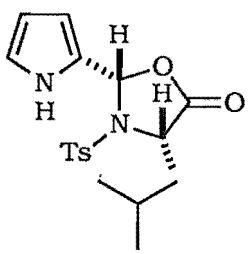

2.18

The second compound was tentatively assigned as the cyclic *N*-substituted pyrrole, a dihydropyrrl piperazine **2.19** (to be discussed in Section 2.2.1.2) as a brown oil (5%). The remaining pyrrolic material was found to be

starting material p-2-c (55%). The low recovery of pyrrolic species was assumed to be due to polymer formation. The final fraction was free *N*-Ts-Leu-OH amino acid. The mode of formation of these compounds is discussed in the mechanism section, Section 2.2.2.

2.2.1.1 *Oxazolidinone from NaH Reaction - Structure Assignment*

The oxazolidinone **2.18** was of particular interest as it existed as a single stereoisomer. NOE difference irradiation of the α-amino acid proton resonance (H-8) at 4.10ppm, Figure 2.11, gave a strong positive enhancement of the resonance at 6.68ppm which was therefore assigned as the pyr-CH (H-6) resonance. An NOE enhancement was observed in the reverse direction on irradiation of H-6 (6.68ppm), enhancements to the amino acid α-proton at 4.10ppm and to pyrrole H-3, 6.24ppm were also observed. The ORD of $[\alpha]^{D}_{26}$=-17° (c1, MeOH) indicated an optically active species.

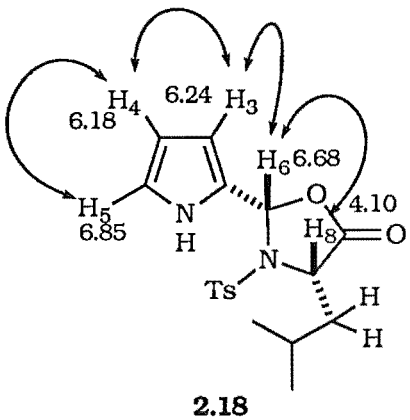

2.18

—— NOE Enhancement

^{1}H NMR (ppm)

Figure 2.11

The NOE data allowed the assignment of the absolute configuration of both stereogenic centres since the stereochemistry of the α-carbon of the amino acid would remain intact. The NOE data and the non-racemisation of the amino acid is consistent with a 6R, 8S *syn* stereochemistry.

One and two dimensional NMR spectral techniques along with comparison with other 2-substituted pyrroles confirmed the structure of the oxazolidinone **2.18**. NOE irradiation of the ^{1}H NMR spectrum signal due to H-5 at 6.85ppm, depicted in Figure 2.11, enhanced the signal at 6.18ppm (H-4). Irradiation of the H-4 signal (6.18ppm) also enhanced the resonances at 6.85ppm (H-5) and 6.24ppm (H-3), thereby assigning the pyrrole ring protons. NOE irradiation at 6.24ppm (H-3) enhanced both the resonances at 6.18ppm (H-4) and 6.68ppm which was assigned as H-6, pyr-CH. Irradiation at 6.68ppm (H-6) enhanced the signal at 4.10ppm (H-8, as described previously) and 6.24ppm (H-3). The amino acid α-proton at 4.10ppm (H-8) on irradiation enhances 6.68ppm (H-6) and also to a lesser extent the protons of the amino acid side chain, $CH_2CH(CH_3)_2$.

The NOE data described above were important in the assignment of the ^{13}C NMR spectra. The ^{13}C NMR spectrum signals for C-3 and C-4 were found to be inverted with respect to other pyrrole C-3 and C-4 signals, as described in Section 2.6.1.3. Generally C-3 is downfield with respect to C-4.

In the oxazolidinone case C-4 is downfield with respect to C-3, as determined by a HETCOR experiment (Figure 2.12).

HETCOR of Oxazolidinone 2.18

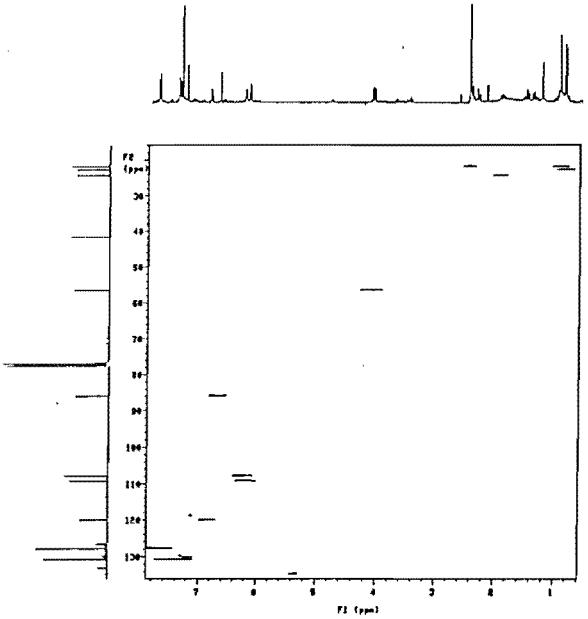

Figure 2.12

A molecular ion at 362mu in the mass spectra of **2.18** is consistent with the structural formulae $C_{17}H_{22}N_2O_3S$. The observed fragmentation pattern is typical of an oxazolidinone with loss of CO[12].

2.2.1.2 *Pyrrylol Pyrazine Formation from the NaH Reaction - Structure Assignment*

The second species isolated from the NaH reaction was assigned as the pyrrylol pyrazine **2.19.**

The ^{1}H NMR spectral data [δ ($CDCl_3$) 0.85 (3H, d, *J*=6.9Hz, Leu-CH_3); 0.93 (3H, d, *J*=6.7Hz, Leu-CH_3); 1.70 (2H, m, Leu-CH_2); 1.89 (1H, sept, *J*=7.0Hz, C*H*(CH_3)$_2$); 2.31 (3H, s, Ts-CH_3); 5.55 (1H, bm, pyr-C*H*(OH)-N); 6.05 (1H, m, H-4); 6.73 (1H, m, H-3); 6.99 (1H, m, H-5); 7.00 (2H, d, *J*=8.2Hz, Ts-CH); 7.35 (2H, *J*=8.3Hz, Ts-CH); 9.09 (1H, s, *N*-pyr-C(O*H*)=)] was consistent with *N*-substitution, ie: each pyrrole proton signal was shifted downfield, this is discussed in Section 2.1.2 and Section 2.7.

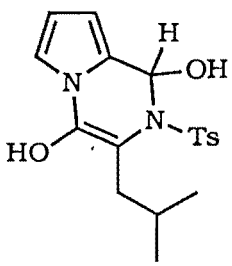

2.19

The ^{1}H NMR spectrum was inconsistent with the desired *N*-(*N*-Ts-Leu)-p-2-c **2.21**, Scheme 2.14, since signals were not observed for the formyl, -C*H*O, group (expected at approximately 10.2ppm) and the α-hydrogen of the amino acid (at approximately 4.5ppm). NOE

experiments, Figure 2.13, showed clearly that the pyrrole H-3, H-4 and H-5 ring system was intact. Irradiation at H-3 (6.73ppm) indicated a very small enhancement at 5.55ppm (pyr-C*H*(OH)-N, H-6). A better correlation was obtained using the HMBC NMR technique to indicate the carbons to which distant protons were attached. The result was positive but not conclusive. The HMBC correlation was found between H-3 (6.73ppm) and the signal at 56.2ppm (pyr-*C*H(OH)-N). These data suggested that a second ring was present in the structure and that the ^{1}H NMR signal at 5.55ppm and ^{13}C NMR spectrum 56.2ppm signal belonged to the moiety at the pyrrole 2-position as in structure **2.19**. The signal at 5.55ppm sharpened on D_2O exchange indicating coupling to the -OH, a signal that was not observed.

A high resolution mass spectrum was also consistent with formulae $C_{18}H_{22}N_2O_4S$ and the cyclic structure. The ^{1}H and ^{13}C NMR signals as well as the NOE and HMBC correlations are summarised in Figure 2.13.

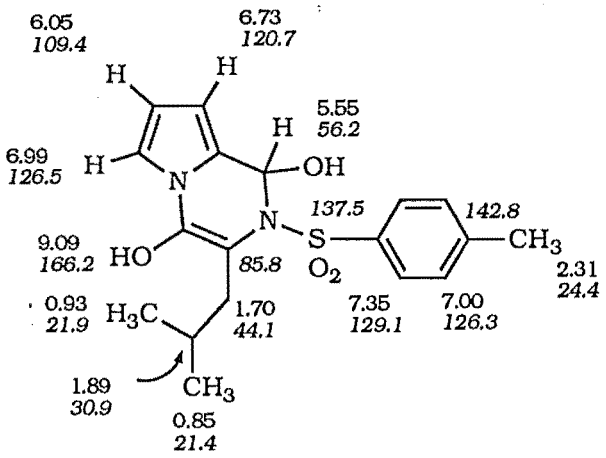

2.19
^{1}H NMR and ^{13}C NMR (ppm)

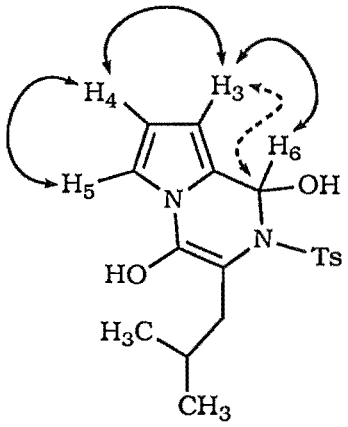

—— NOE enhancement
---- HMBC correlation

Figure 2.13

A possible mechanism for the formation of this cyclic species is summarised in Section 2.2.2.2.

2.2.2 Proposed Mechanisms for the Reaction of Pyrrole-2-Carboxaldehyde with NaH

A possible mechanism for the reaction of *N*-Ts-Leu-Cl and p-2-c anion to give **2.18** and **2.19** is presented in Scheme 2.14 and Scheme 2.17.

2.2.2.1 *Mechanism of Oxazolidinone Formation*

The oxazolidinone is thought to form via the key azafulvene like structure **2.20**, (Scheme 2.14).

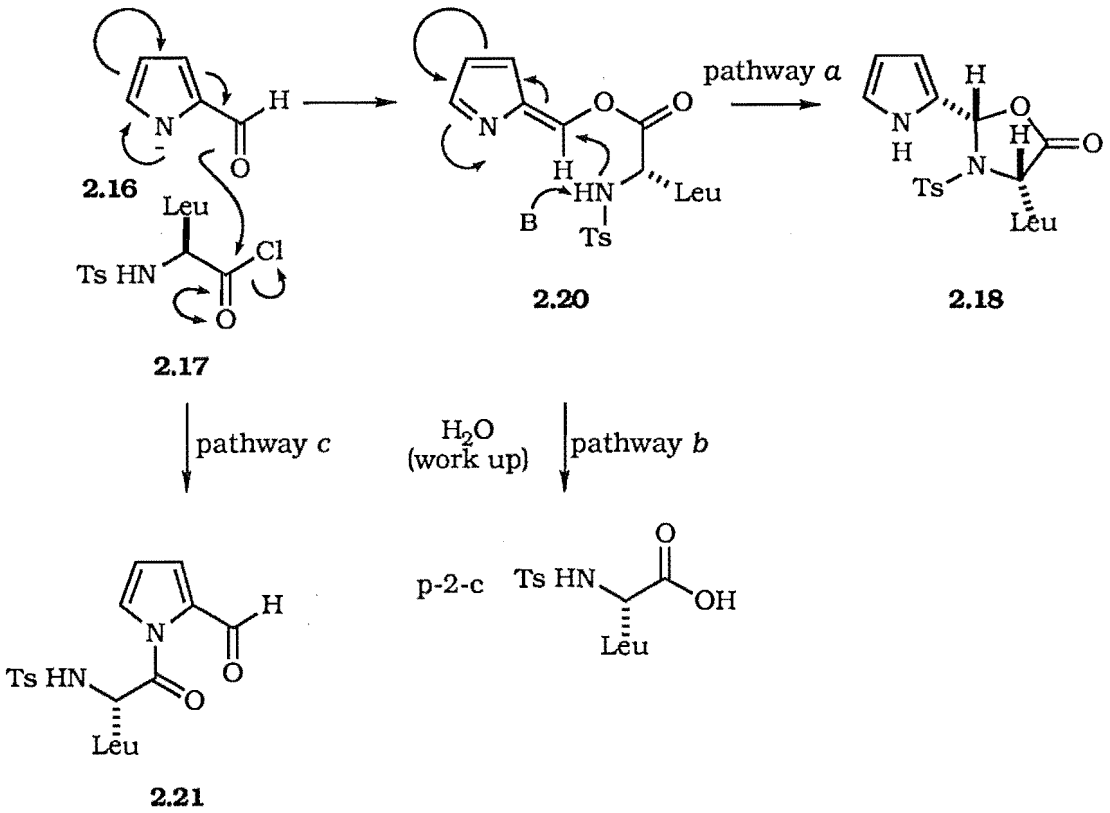

Scheme 2.14

Once the azafulvene has formed, it can either cyclise through nitrogen to give the oxazolidinone **2.18** (pathway *a*), or it can form the starting material (p-2-c) with the release of free amino acid (pathway *b*). The low yields from the NaH reaction appear to be an artefact from the hydrolysis of the azafulvene. Hydrolysis of azafulvene[13] **2.20** to starting materials produces an unreactive amino acid and fully protonated p-2-c. There is therefore no further reaction.

Amino acid nitrogen attack at the electrophilic azafulvene **2.20** centre, before decomposition, produces the oxazolidinone **2.18**. This reaction is analogous to that designed to occur on hydrolysis of the amino acid-pyrrole

bond in an enzyme active site.

The described mechanism explains how polymer formation can occur from the NaH reaction. Details in Section 4.3.3 describe how production of polymer occurs when few nucleophiles are available. The azafulvene reacts indiscriminately with any nucleophile, often other pyrroles. The alkylation of azafulvene by further pyrroles, produces the polymer described in this reaction. Experimental observation of polymer formation via azafulvenes is described in Section 3.2.2 and in Section 4.3.3.

A competition exists between cyclisation of the key intermediate azafulvene **2.20**, Scheme 2.14, to yield the oxazolidinone **2.18**, or a dead end pathway of hydrolysis (pathway *b*) during work up to yield p-2-c and *N*-Ts-Leu-OH. The desired *N*-acylated pyrrole **2.21** (pathway *c*) was not observed. The desired *N*-acylated derivatives were observed for simple non-amino acid examples, using the NaH method, Section 2.2.3.

Precedence for the reaction through *O* of the -CHO group was found in the reaction to synthesize a hydroxymethyl bilane, as described in Section 2.1.1.1.

2.2.2.1.1 Oxazolidinone **2.18** as a Possible Chiral Auxiliary Agent

The oxazolidinone **2.18** is a single *syn* isomer about pyr-CH (H-6) and CH-Leu (H-8) on the basis of the observed NOE. An optical rotation of $[\alpha]^{D}_{26}$ -17° also shows that it is optically active.

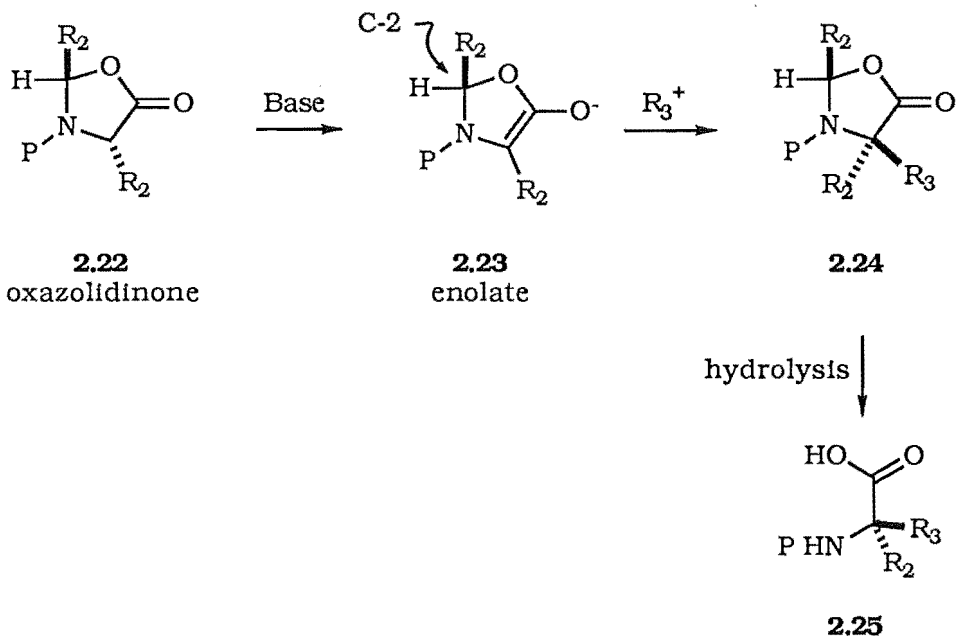

2.22 oxazolidinone

2.23 enolate

2.24

2.25

Scheme 2.15

The high degree of stereoselectivity observed for this reaction suggests that the oxazolidinone may be useful as a chiral auxiliary agent in

amino acid synthesis. The use of oxazolidinones in the asymmetric synthesis of chiral species is well documented[14]. Scheme 2.15 outlines the use of chiral oxazolidinones, eg: **2.22** in the enantioselective alkylation of amino acids, eg: **2.25**.

Bulky R substituents at the C-2 position, **2.23** Scheme 2.15, direct approach of the electrophile to the less hindered face of the planar enolate.

The general protocol for oxazolidinone formation involves reaction of the sodium salt of the free amino acid **2.26** with pivaldehyde to furnish the corresponding imine. The imine is then cyclised in the presence of the acylating reagent benzoyl chloride, PhCOCl, Scheme 2.16, to give a mixture of the *syn* and *anti* oxazolidinones **2.27**[14].

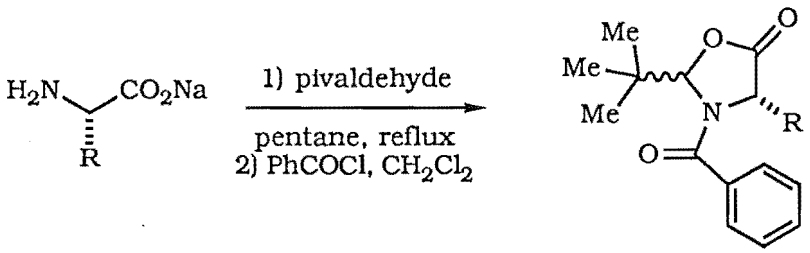

2.26 **2.27**
syn and *anti* oxazolidinone

Scheme 2.16

This is in contrast to the present study where oxazolidinone formation occurs directly via an amino acid acid chloride. The synthesis of the oxazolidinone **2.18** described in this work produces the *syn* isomer optically pure and in a one pot synthesis. Using the oxazolidinone **2.18** for enantioselective alkylations of amino acids, the enolate **2.28** was modelled on proposed enolates derived for existing chiral alkylation reactions[15]. The *Re* face, as drawn, is less hindered to electrophilic attack, and as such a high degree of diastereomeric excess would be expected.

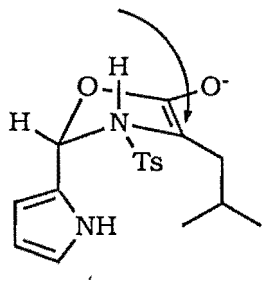

2.28

The pyrrole of the oxazolidinone **2.18** chiral template, could also act as a "diene" for a Diels-Alder reaction. Pyrroles do not usually undergo Diels-Alder reactions[6] but rather tend to react with the dienophile by conjugate addition. Cases where pyrrole acts as a dienophile have been reported[16]. Approach of the dieneophile to the diene may be influenced by the configuration of the oxazolidinone, if a Diels-Alder reaction was to proceed.

No attempt has been made to optimise the yield of **2.18**.

2.2.2.2 *Mechanism for the Formation of the Pyrrylol Pyrazine* **2.19**

The pyrryl anion **2.16** can also attack the amino acid acid chloride through nitrogen to form the desired *N*-acylated-p-2-c, Scheme 2.17. This subsequently undergoes base promoted cyclisation to give the pyrrylol pyrazine **2.19.**

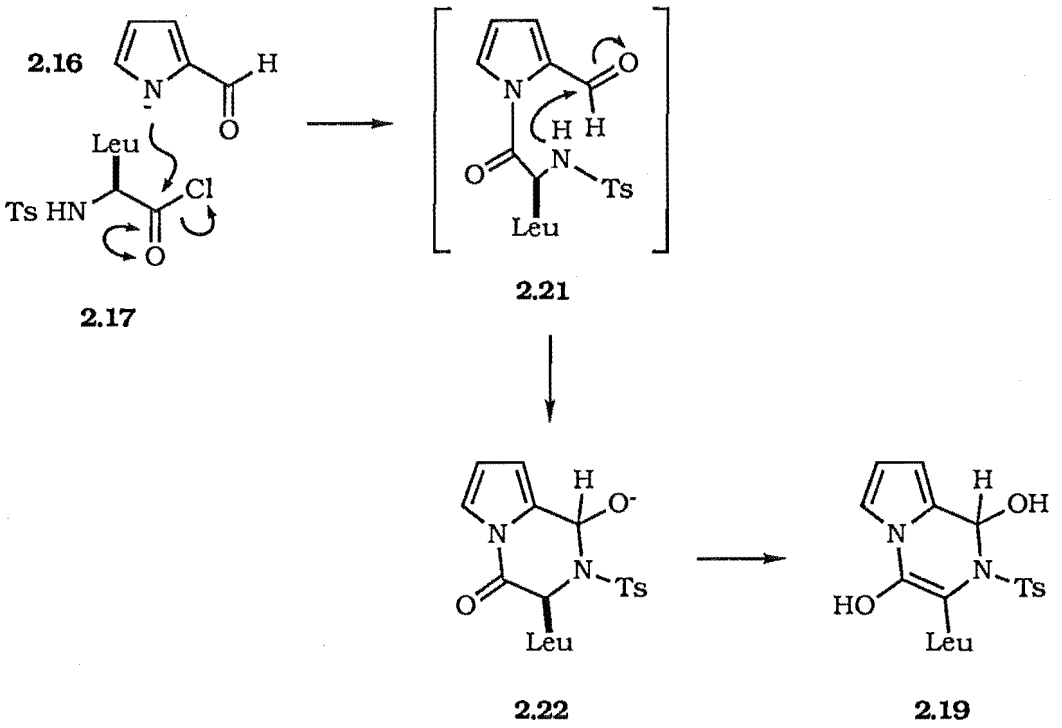

Scheme 2.17

2.2.3 NaH Reaction - Acylation of Pyrrole-2-Carboxaldehyde by Simple Activated Acyl Species

P-2-c was acylated with acetyl chloride in an attempt to improve an understanding of the NaH reaction described above, and to help clarify the assignment of ^{1}H NMR spectra. The pyrrole anion was formed using NaH, in an analogous reaction as above, Section 2.2.1. Acetyl chloride **2.23** (1.2equiv.) was added, and stirring continued for one hour, Scheme 2.18.

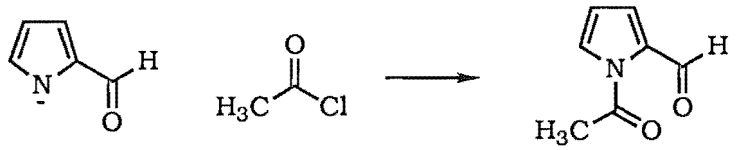

Scheme 2.18

During this time a large amount of black precipitate formed, again attributed to formation of a pyrrole polymer. Chromatography gave two pyrrolic compounds, the starting material p-2-c (21%), and the required *N*-acetyl-p-2-c (20%) **2.24**. The spectral data of the *N*-acetyl-p-2-c **2.24** were consistent with the same compound reported by Bohlmann[17].

2.2.4 NaH Reaction - Conclusion

The two competing pathways of pyrrylol pyrazine and oxazolidinone formation occur with an amino acid derived acid chloride. The desired *N*-acylated species, were only observed with the simple model acid chloride. A new methodology was therefore required for the acylation of p-2-c on nitrogen.

2.3 Alkali Metal Mediated Acylation of Pyrrole Derivatives

2.3.1 Methyl Lithium Mediated Acylation

Metallic potassium has been used extensively for the preparation of pyrryl-anion potassium salts. We reasoned that MeLi would be a more convenient method for the production of lithium pyrryl-anion salts. Pyrrole **2.25** was dissolved in dry ether at -78°C under nitrogen, and treated with one equivalent of MeLi **2.26**. After five minutes hydrocinnamoyl chloride **2.27** was added to yield, after twenty four hours, the *N*-cinnamoyl-pyrrole **2.28**, Scheme 2.19, essentially pure by ^{1}H NMR spectroscopy (95% after chromatography).

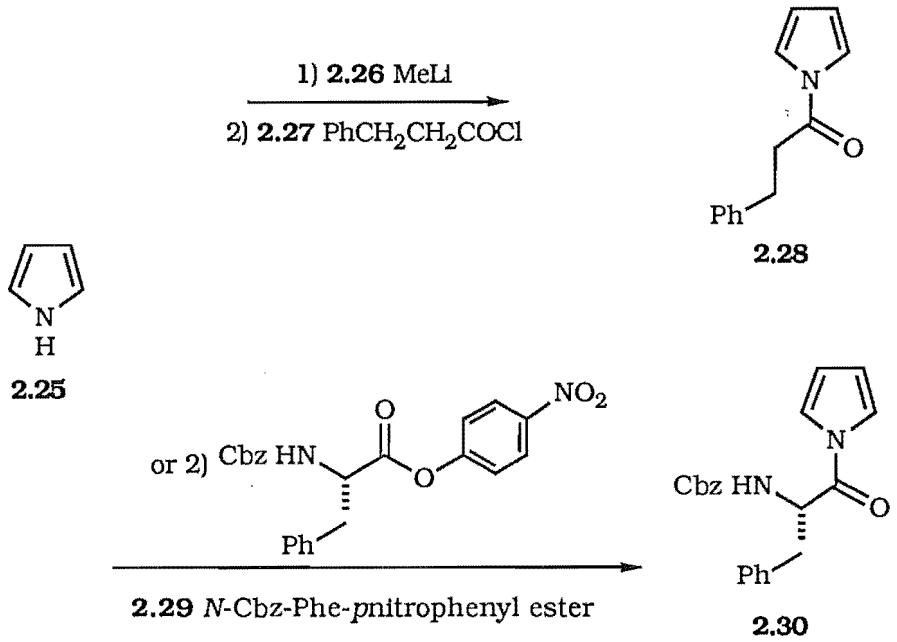

Scheme 2.19

A similar reaction using *N*-Cbz-L-Phe-*p*-nitrophenyl ester **2.29** (1equiv.) gave the desired *N*-acyl-pyrrole **2.30** and starting material. After chromatography, **2.30** was isolated in 48% yield. The ^{1}H NMR spectrum of **2.30** was consistent with *N*-acylation, the pyrrole signals of H-2 and H-3 that were observed, had shifted downfield and the characteristic triplets at 6.30ppm and 7.10ppm were found to be consistent with *N*-acylation [δ ($CDCl_3$) 6.30 (2H, t, *J*=2.4Hz, H-2); 7.10 (2H, t, *J*=2.3Hz, H-3)]. A similar ^{1}H NMR spectrum was observed for the *N*-acyl-pyrrole **2.28**.

Attempts to formylate the *N*-acyl-pyrroles **2.28** and **2.30** to yield the *N*-acyl-p-2-c **2.31** and **2.33** precursors to the desired hydroxymethyl pyrroles **2.32** and **2.34**, Scheme 2.20, are discussed in Section 2.6.

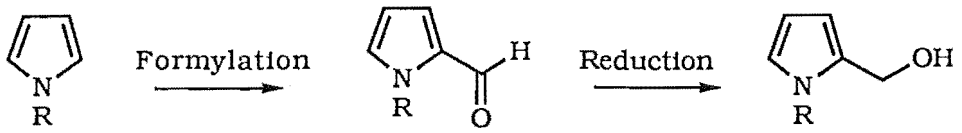

2.28 R=$COCH_2CH_2Ph$ **2.31** R=$COCH_2CH_2Ph$ **2.32** R=$COCH_2CH_2Ph$
2.30 R=CO-Phe-Cbz-*N* **2.33** R=CO-Phe-Cbz-*N* **2.34** R=CO-Phe-Cbz-*N*

Scheme 2.20

The MeLi reaction was then attempted on p-2-c. Addition of MeLi (1equiv. in ether) to p-2-c in dry ether at -78°C, produced a pale blue solution after five minutes.

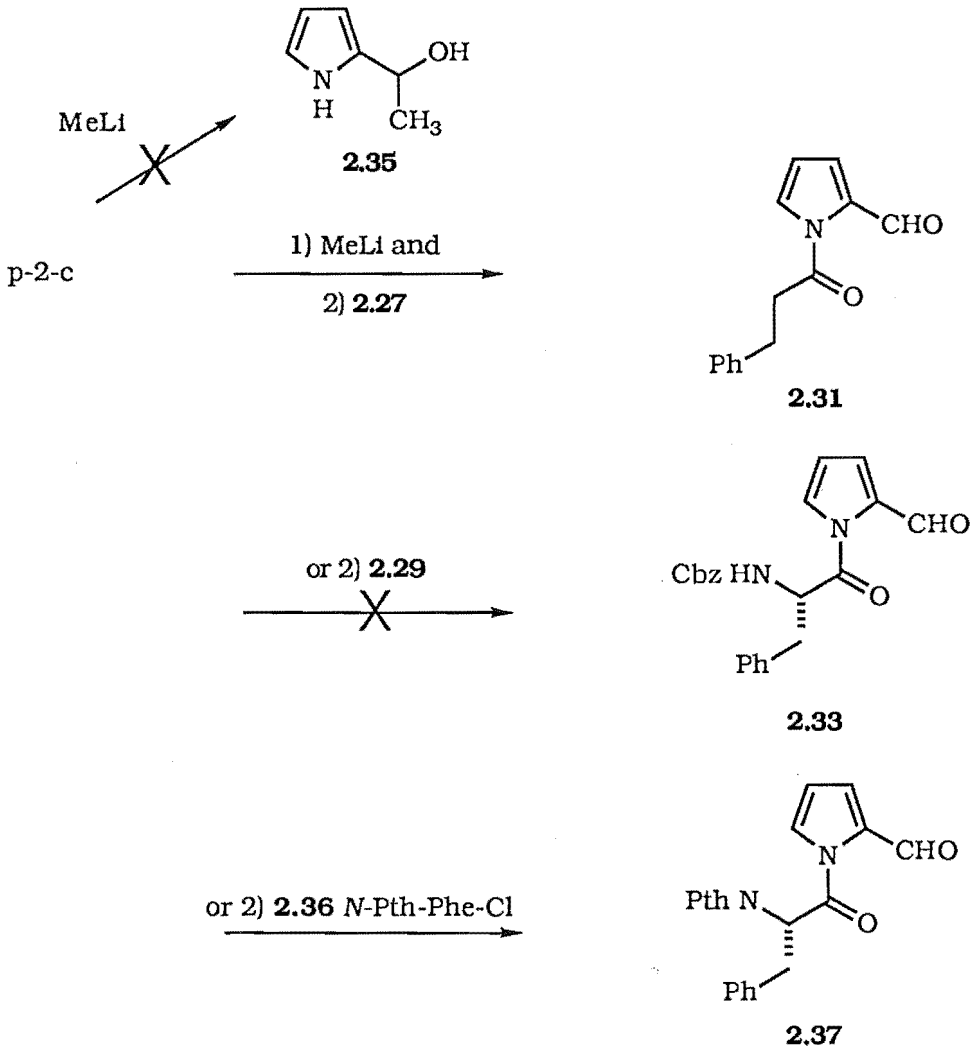

Scheme 2.21

The addition of hydrocinnamoyl chloride **2.27** to the pyrryl anion and subsequent work up afforded the *N*-cinnamoyl-p-2-c **2.31** in 89% yield after

chromatography. The result was surprising as it was expected that the MeLi may undergo nucleophilic addition at the formyl group to give the secondary alcohol **2.35**, Scheme 2.21.

The lack of this substitution suggests that the *N*-acylation occurs via the pyrrole/lithium enolate **2.38** with either a reversible attack at oxygen and acyl transfer to nitrogen, or direct acylation on nitrogen. This is further evidence of the non-aldehydic nature of p-2-c as described in Section 2.1.1.

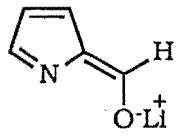

2.38

The extension of this reaction to the amino acid derivative required for enzyme recognition purposes was then attempted. Preparation of the lithium salt of p-2-c, as above, followed by addition of *N*-Cbz-Phe-*p*-nitrophenyl ester **2.29**, produced a yellow colour within five minutes. ^{1}H NMR spectral analysis of an aliquot at fifteen minutes, one hour and one day showed no sign of the desired *N*-acylated product **2.33**. The less reactive oxazolone **2.39** was thought to be forming on addition of the amino acid derivative to the MeLi. This is discussed in detail in Section 2.4.7.1.

The addition of *N*-Pth-Phe-Cl **2.36** to the p-2-c salt produced, within ten minutes, 90% by NMR spectrum of the *N*-acylated-p-2-c **2.37** (remaining 10% as p-2-c). A discussion of the characteristics of this product is found in the DMAP methodology section, Section 2.4.2.

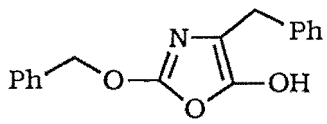

2.39

The MeLi reactions were quenched at -78°C as it was thought that the decomposition product of MeLi, LiOH, may cause deacylation of the product *N*-acyl species.

The high yield of the desired *N*-acylated amino acid pyrrole derivatives **2.31** and **2.37** using MeLi to form the anion of p-2-c therefore provides a viable synthesis of the desired *N*-acylated pyrrole derivatives that have been designed as enzyme inactivators, see Section 1.1.

2.3.2 n-Butyl Lithium Mediated Acylation

The reaction of p-2-c with n-BuLi followed by the addition of hydrocinnamoyl chloride at -78°C was also attempted. ^{1}H NMR spectral analysis indicated the *N*-acyl species **2.31** had formed in 80% yield, in addition to 20% p-2-c.

Reaction of BuLi and *N*-Cbz-Phe-*p*-nitrophenyl ester with p-2-c produced no acylated product after twenty four hours. The failure of this reaction again pointed to oxazolone **2.39** formation, discussed in Section 2.4.7.3.

The MeLi reaction had been found to proceed more efficiently and was therefore used in preference to n-BuLi.

2.4 The DMAP Methodology of Acylation Promotion

A 1969 paper by Steglich and Höfle[18] identified *N,N*-Dimethyl-4-pyridinamine (DMAP **2.40**, Scheme 2.22) as an effective, high yielding, acylating catalyst (0.1equiv. with respect to the species being acylated); a two fold excess of triethyamine (TEA) is also added to the reaction.

DMAP is believed to act in a similar manner to pyridine in promoting acylation reactions. The enhanced reactivity of DMAP over pyridine is not a result of increasing basicity (DMAP pK_b=9.70, pyridine pK_b=5.29), but is due to the high concentration of *N*-acyl pyridinium salts **2.41** formed, which are very effective acylating agents, Scheme 2.22[19].

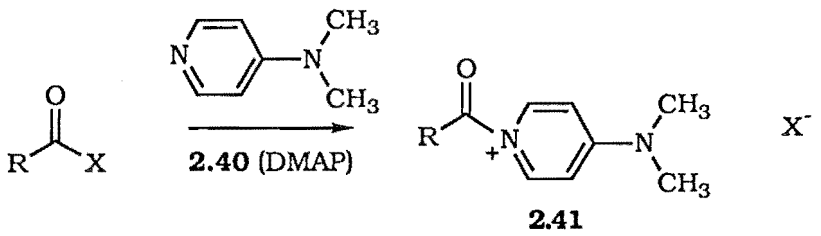

Scheme 2.22

2.4.1 DMAP Mediated *N*-Acylation of Pyrrole-2-Carboxaldehyde

Acetyl chloride (1.1equiv.) was added to p-2-c, TEA (1.5equiv.,) and DMAP (0.1equiv.) in dry CH_2Cl_2; a general reaction is described in Table 2.1 below. The resultant deep yellow solution was then stirred for twenty four hours. Washing with citric acid (10% solution in water), effectively removed the TEA and the DMAP. The *N*-acetyl-p-2-c **2.24** was isolated as a crystalline solid (63%).

A further reaction using acetic anhydride was attempted to test the generality of the methodology. The addition of Ac_2O (1.1equiv.) to p-2-c, TEA and DMAP in CH_2Cl_2 gave a quantitative yield of the *N*-acetyl-p-2-c **2.24**. The enhanced yield over the acetyl chloride reaction (63%), was surprising and warranted further investigation.

2.4.1.1 *Effect of Base on Yield of DMAP Catalysed Reaction of Pyrrole-2-Carboxaldehyde*

A series of acylating agents were investigated using the p-2-c/DMAP system. The non-nucleophilic hindered base *N,N*-diisopropylethyl amine (Hünigs base) was also investigated. Each reaction used the methodology discussed in the previous section. The results for these reaction are recorded

as isolated yields in Table 2.1.

Effect of Binding Base on Yields in the DMAP Reaction with Pyrrole-2-Carboxaldehyde

Isolated Yield (%)

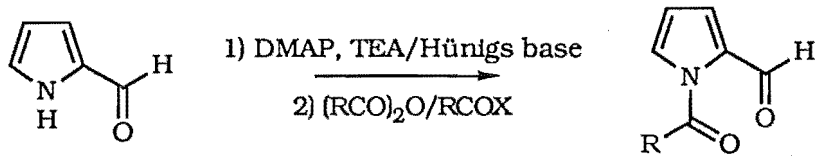

Activated Acyl Species	R		TEA	Hünigs Base
$(CH_3CO)_2O$	$-CH_3$	**2.24**	Quant.	58
$(CH_3CH_2CO)_2O$	$-CH_2CH_3$	**2.42**	Quant.	53
CH_3COCl	$-CH_3$	**2.24**	50	Quant.
CH_3CH_2COCl	$-CH_2CH_3$	**2.42**	45	90
PhCOCl	-Ph	**2.43**	45	Quant.
$PhCH_2CH_2COCl$	$-CH_2CH_2Ph$	**2.31**	50	95

Quant. = Quantitative Yield

The pyrrole **2.44** in the presence of DMAP and TEA was acylated by acetyl chloride, producing the *N*-acetylated pyrrole **2.45** in 95% isolated yield, Table 2.2. The reaction indicated that a wide variety of pyrrole derivatives have the possibility of being *N*-acylated by the DMAP reaction.

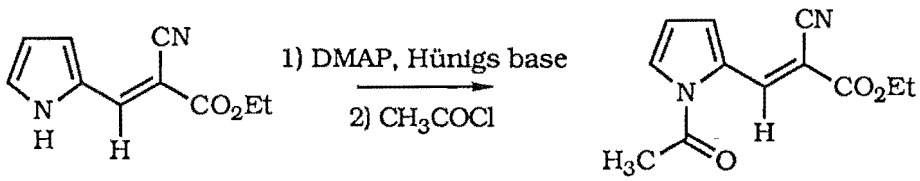

2.44 **2.45**

Scheme 2.23

Effect of Binding Base on Yields in the DMAP Reaction with Pyrrole 2.44

Activated Acyl Species		TEA	Hünigs Base
$(CH_3CO)_2O$	**2.45**	95	58
CH_3COCl		55	Quant.

Quant. = Quantitative Yield

Table 2.2

A clear trend emerges from these data: acid chlorides generally gave a lower yield of the *N*-acylated pyrrole product using DMAP and TEA, rather than DMAP and Hünigs base. However, high yields of *N*-acylated pyrrole product were obtained using the corresponding acid anhydrides with DMAP and TEA, while lower yields were obtained in the reactions using Hünigs base. Where decreased conversion to the *N*-acylated pyrrole product was observed, the yields were not increased with longer reaction times. This protocol was used throughout the subsequent work.

The hindered Hünigs base may help to stabilise the more reactive acid chloride and hence a higher yield is observed than in the corresponding reaction using TEA.

2.4.2 *N*-Acylation of Pyrrole-2-Carboxaldehyde with Amino Acids

The use of MeLi to promote *N*-acylation of pyrrole, but not p-2-c, with amino acids has been discussed, Section 2.3. The DMAP reaction was developed for the acylation of p-2-c with simple acylating agents. The methodology was now in place to extend the *N*-acylating species to an amino acid. Phenylalanine (Phe) was chosen since both serine proteases and the HIV protease cleave on the carboxyl side of an aromatic amino acid.

2.4.2.1 *Phthalyl Protected Phenylalanine Amino Acid*

The phthalyl (Pth) group was used in the initial extension studies. The *N*-Pth-Phe-Cl acid chloride **2.36** was prepared from *N*-Pth-Phe-OH using DMF and oxalyl chloride. *N*-Pth-Phe-Cl was added slowly to a stirred solution of p-2-c, Hünigs base and DMAP in CH_2Cl_2 under nitrogen, Scheme 2.24.

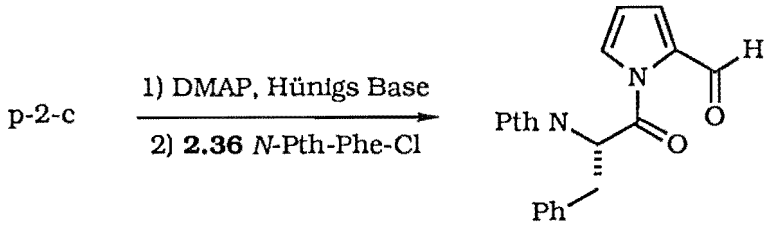

2.37

Scheme 2.24

An immediate colour change was observed. Colourless, to yellow, to green and finally to black over five minutes. The reaction mixture was stirred for twenty four hours and worked up as before. The ^{1}H NMR spectrum did not show a 9.54ppm signal due to the p-2-c. A new signal at 10.17ppm and a triplet (J=3.4Hz) at 6.19ppm were evident and indicated that *N*-acylation of p-2-c had occurred to give **2.37**; see Section 2.7.1 for more detailed NMR spectral analysis. The yield of the reaction was low (<15%), due to polymer formation.

The order of reagent addition was changed in an attempt to minimise polymer formation. A similar reaction was attempted where p-2-c, DMAP, and Hünigs base in CH_2Cl_2, were added dropwise to the stirred solution of ice cold acid chloride. Again a deep yellow/brown solution resulted over ten minutes. After fifteen minutes an aliquot was removed from the mixture that showed by ^{1}H NMR spectroscopy essentially 100% conversion to an *N*-acylated pyrrole. A signal at 9.54ppm (p-2-c) was not observed whereas a downfield signal at 10.17ppm and a triplet (J=3.4Hz) at 6.19ppm were observed. The product *N*-acyl-pyrrole **2.37** was isolated in a preparative experiment, but proved to be unstable to chromatography.

The product was unstable and deacylation occurred after three days in a freezer. Therefore, it was decided to reduce the *N*-acyl-pyrrole **2.37** without further purification, as discussed in Section 2.4.4. The hydroxymethyl pyrrole was expected to be more resistant to deacylation, as explained in Section 2.1.2.

2.4.3 DMAP *N*-Acylation of Pyrrole

The most widely used method for preparation of *N*-acylated pyrrole is the acylation of the potassium salt of pyrrole[20]. The reaction is tedious and the yields are low[21]. The use of acyl imidazole as an acylating agent of pyrrole at reflux has also been reported[21]. This method is not useful for products that are heat sensitive or for species that will not form the acylated imidazole.

Another acylation reaction involves MeLi as previously found in this work, Section 2.3.1.

The DMAP methodology was shown to be very effective when applied to pyrrole. Ac_2O was added to pyrrole, TEA and DMAP in CH_2Cl_2 to give the *N*-acetyl-pyrrole **2.46** in 54% yield. The NMR spectral data were consistent with that reported elsewhere[22].

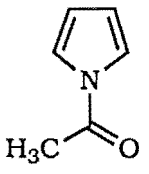

2.46

2.4.4 Reduction of *N*-Acylated Formyl Pyrrole Derivatives

Standard methods for the reduction of formyl pyrroles use $NaBH_4$ in aqueous solution[23].

However, it was decided not to use aqueous conditions to limit problems with decomposition of the sensitive amino acid-pyrrole system.

2.4.4.1 *Sodium Borohydride Reduction of N-Acyl-Pyrrole-2-Carboxaldehyde's*

The reduction of related formyl pyrroles with $NaBH_4$ in CH_2Cl_2/MeOH has been reported[24].

The *N*-acetyl-p-2-c **2.24** was reduced under the same conditions, Scheme 2.25.

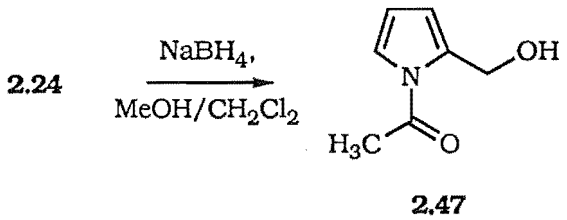

2.47

Scheme 2.25

The ^1H NMR spectrum of the crude reaction mixture gave no evidence of the starting material -C*H*O signal at 10.30ppm. Chromatography of the crude sample gave two fractions.

The NMR spectrum of the first fraction showed a new broad doublet (J=6.0Hz) at 4.63ppm. This fraction was isolated in 84% yield and identified as the desired *N*-acetyl hydroxymethyl pyrrole **2.47**. A detailed NMR spectral study of this and other hydroxymethyl pyrroles is found in Section 2.7.2.

The second fraction was identified as the formyl pyrrole, p-2-c (13%) the result of deacylation rather than reduction. This compound is clearly produced under the reduction conditions, as the starting material contained no p-2-c.

The deacylation of *N*-acetyl-p-2-c **2.24** was studied by ^1H NMR

spectroscopy. The aldehyde in d_4-MeOH slowly hydrolysed to p-2-c (30% after one hour). Acetate was also observed on standing. *N*-acetyl-p-2-c does not undergo deacylation in $CDCl_3$; however the addition of one equivalent of NaOH caused total deacylation to p-2-c and acetate in ten minutes, see Sections 4.2 and 4.3 for similar experiments.

The formyl group of the *N*-acylated formyl pyrrole increases ring delocalisation, Figure 2.8, and hence makes the amide bond more susceptible to nucleophilic attack and subsequent deacylation.

The reduction of amino acid derived pyrrole derivative **2.37** was then attempted.

2.4.4.2 *$NaBH_4$ Reduction of Amino Acid Pyrrole Derivatives* **2.37**

The reduction of the amino acid aldehyde **2.37** using $NaBH_4$ in $MeOH/CH_2Cl_2$, as above, produced a polymeric species, p-2-c and the unstable acetal **2.49**, Scheme 2.26, [δ ($CDCl_3$) 3.29 (3H, s, OMe); 3.45 (3H, s, OMe); 3.56 (2H, m, CH_2-Ph); 5.66 (1H, m, Phe-CH); 6.14 (1H, t, *J*=3.4Hz, H-4); 6.47 (1H, m, H-3); 7.07 (1H, dd, *J*=3.4 &1.6Hz, H-5); 7.11-7.21 (5H, m, Phe-Ph); 7.69 (2H, dd, *J*=5.4 & 2.5Hz, Pth-CH); 7.77 (2H, dd, *J*=5.3 & 2.6, Pth-CH)]. There was no evidence of the desired reduced amino acid pyrrole **2.51**. The formation of the acetal **2.49** is consistent with *N*-acylation increasing the carbonyl character of the formyl group. The acyl group decreases the contribution of resonance structure **2.48**, Scheme 2.26, due to the delocalisation of the nitrogen lone pair as in structure **2.50**; see Section 2.7.3.2 for supporting UV data.

The complex electronic structure of the π pyrrole system, is again demonstrated by the stability of the pyrrole derivatives and their subsequent reaction.

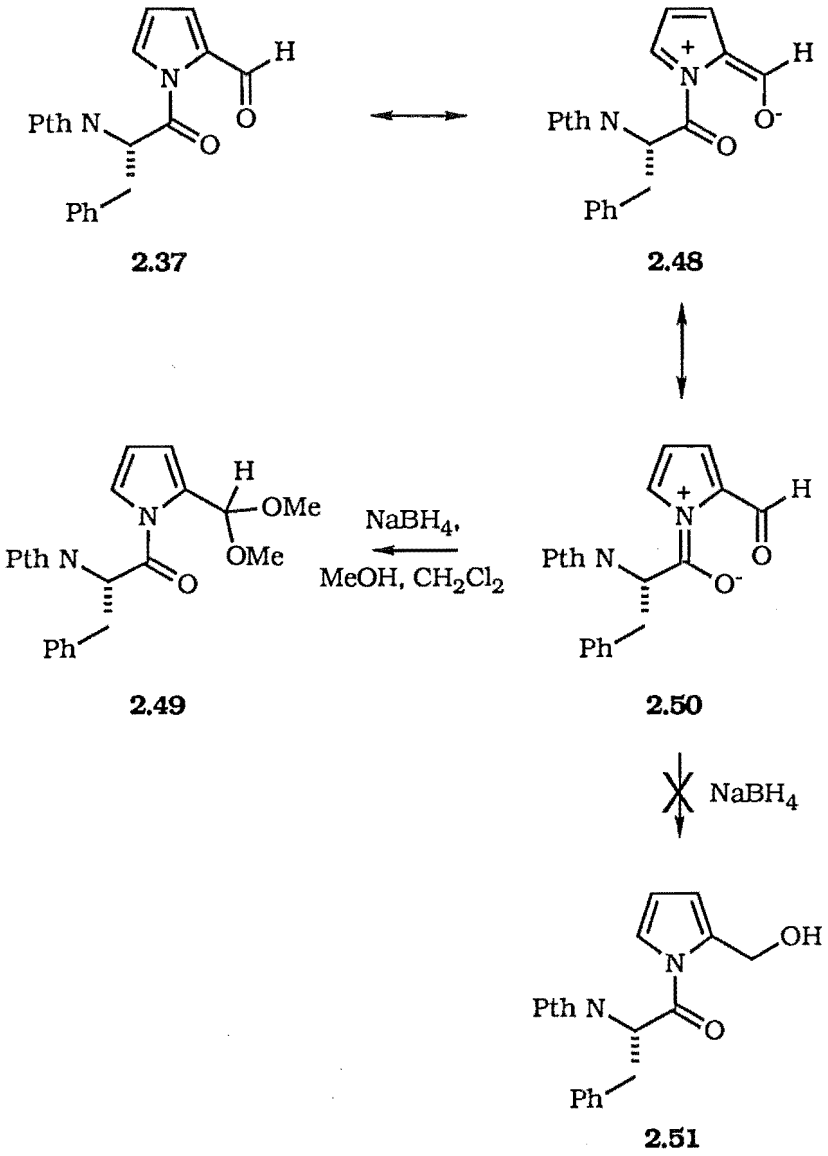

2.37 **2.48** **2.49** **2.50** **2.51**

Scheme 2.26

2.4.4.3 *Reduction of* **2.37** *with LiAlH4*

The attempted reduction of the amino acid pyrrole aldehyde **2.37** using $LiAlH_4$ in dry ether gave only starting material. A literature report suggests that *N*-acyl-pyrroles are hydrolysed by $LiAlH_4$ to give deacylated pyrrole and an aldehyde or primary alcohol[25] this was not observed for this system.

2.4.5 Zinc Borohydride Reduction of the *N*-Amino Acid Formyl Pyrroles 2.31 and 2.37

A trial reduction of the formyl pyrrole **2.31** in dry ether with zinc borohydride[26] **2.51** (1.2equiv. in dry ether), Scheme 2.27, under dry nitrogen for thirty minutes afforded, after radial chromatography, the desired

hydroxymethyl pyrrole **2.32** in 90% yield.

The hydrocinnamoyl moiety ($COCH_2CH_2Ph$) has successfully been used as a Phe analogue in the inhibition of tRNA synthetase[27]. This species **2.32**, therefore, was expected to be a potential inhibitor of the proteolytic enzymes, chymotrypsin and HIV protease. The results of the assays on these enzymes are found in Chapter Five.

Reduction of the amino acid aldehyde **2.37** in dry ether with zinc borohydride **2.51** (1.2equiv. in dry ether), Scheme 2.27, under nitrogen for thirty minutes afforded, after radial chromatography, the desired hydroxymethyl pyrrole **2.52** in 62% yield.

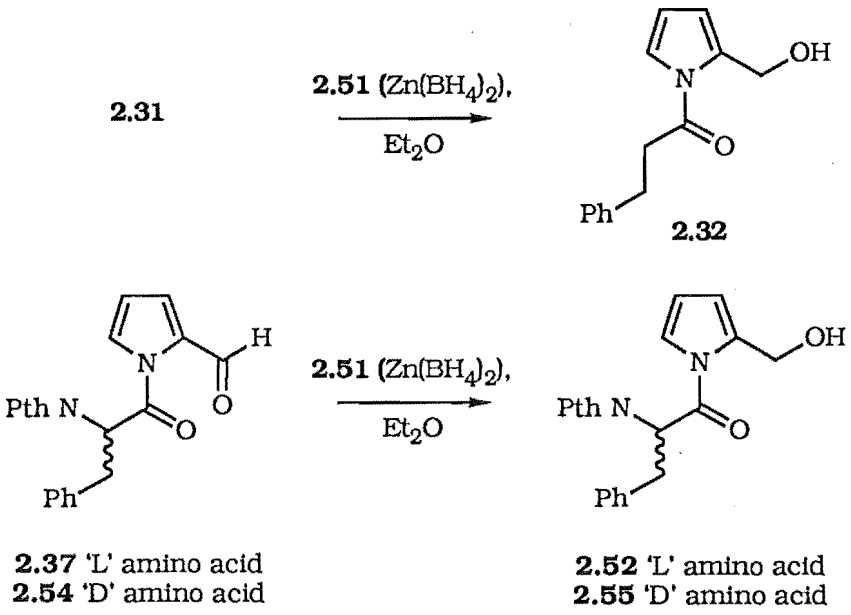

Scheme 2.27

The ^1H NMR spectrum was consistent with an *N*-acylated pyrrole and reduction to a hydroxymethyl pyrrole, NMR spectral analysis is described in Section 2.7.4. This mauve amorphous solid resisted all attempts at crystallisation but was nevertheless remarkably stable. Little decomposition was observed over six months when stored under nitrogen in a freezer.

The hydroxymethyl pyrrole **2.52** exhibited the characteristics necessary to give mechanism based inactivation of a protease. The pyrrole ring deactivated by the *N*-acylated amino acid, and a leaving group at the 2-position, allows azafulvene formation on enzymic deacylation. This compound was tested against the HIV protease and α-chymotrypsin, see Sections 5.1 and 5.2.

2.4.6 Determination of Enantiomeric Excess of the Amino Acid-Pyrrole Derivative

For the designed hydroxymethyl pyrrole derivatives, it is required that no racemisation of the amino acid should occur. We therefore designed the following experiment to determine the enantiomeric excess.

The enantiomeric excess of the L-amino acid hydroxymethyl pyrrole derivative **2.52** was determined by conversion to the corresponding camphanate **2.53** using (-)-camphanic acid under Mitsunobu conditions[28], Scheme 2.28. A detailed ^1H NMR spectral analysis of the camphanate made from the L-derivative **2.53** determined the enantiomeric excess to be 90%. The analogous reaction sequence starting with D-Phe, followed by *N*-protection with *N*-carbethoxyphthalimide[29], acid chloride formation and reaction with p-2-c, Hünigs base and DMAP gave **2.54**. The $Zn(BH_4)_2$ reduction with the final Mitsunobu reaction formed the camphanate to give the D-amino acid derivative **2.56** as a reference for the calculation. Figure 2.29 shows the ^1H NMR spectra of the camphanate methyl signal region and the pyr-CH_2 region for the two camphanates **2.53** and **2.56**.

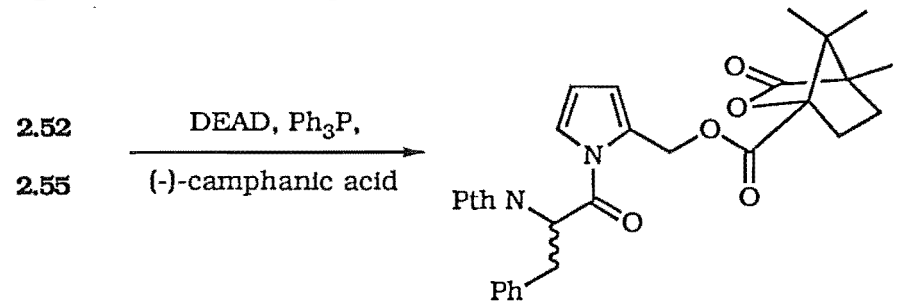

2.53 'L' amino acid
2.56 'D' amino acid

Scheme 2.28

^1H NMR Spectra of Camphanate Methyl Region of Camphanates 2.53 and 2.56

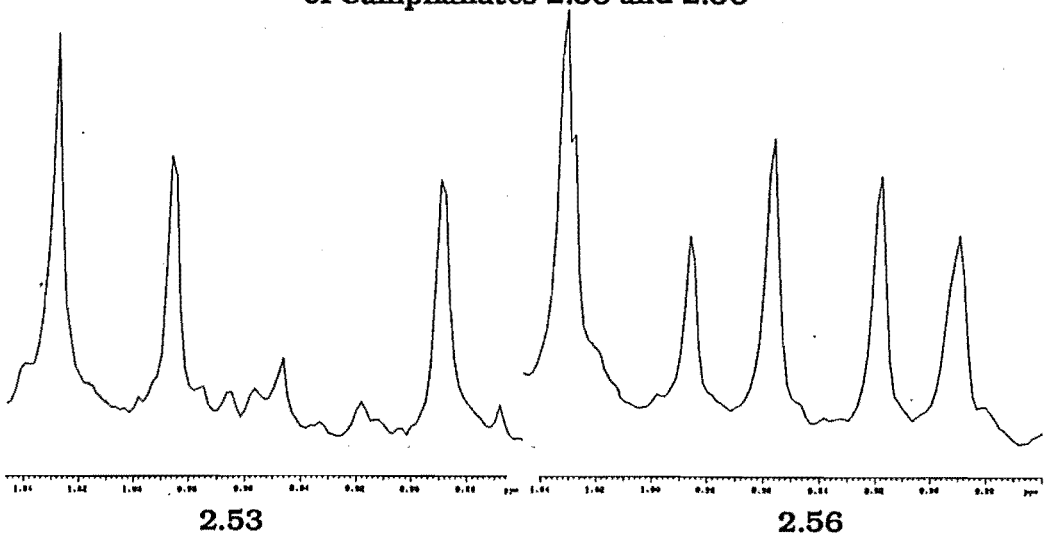

^{1}H NMR Spectra of Camphanate pyr-CH_2 Region of Camphanates 2.53 and 2.56

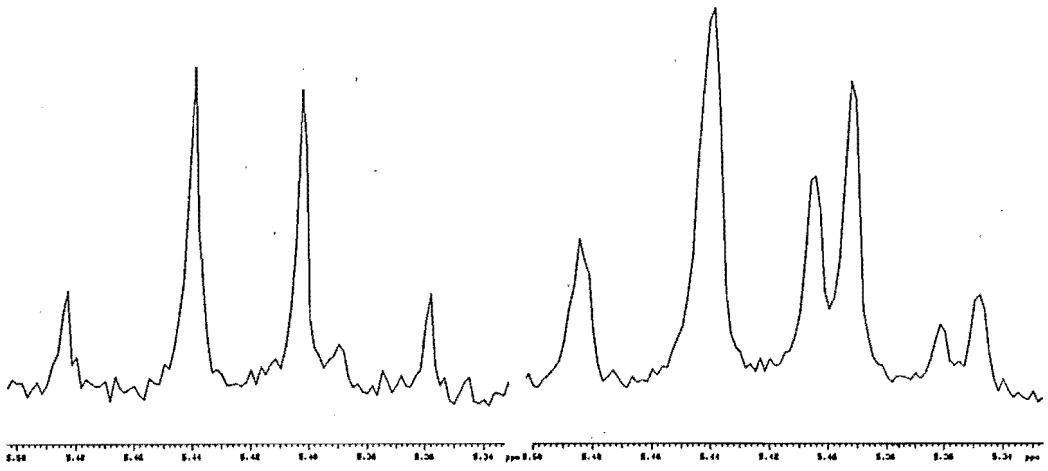

2.53 **2.56**

Figure 2.29

Table 2.3 shows a comparison of the ^{1}H NMR spectra of the two isomers.

Selected ^{1}H NMR Spectral Data for the *N*-Acylated Camphanates 2.53 and 2.56

Origin of Signal	L isomer 2.53 δ (ppm)	D isomer 2.56 δ (ppm)
camphanate-CH_3	0.89	0.92
camphanate-CH_3	0.99	0.96
camphanate-CH_3	1.03	1.03
pyrrole-CH_2-CO	5.35	5.34
pyrrole-CH_2-CO	5.49	5.50
pyrrole H-4*	6.09	6.09

*In table to show that the spectra referencing was correct

Table 2.3

The data in Table 2.3 summarises the major differences in ^{1}H NMR spectra of the two isomers. The ^{1}H NMR spectrum of the 'L' amino acid based compound **2.53** indicated a 95:5 (L:D) ratio. A ratio of 65:35 (D:L) was determined for the 'D' derived hydroxymethyl pyrrole **2.56**. The optical rotary

dispersion (ORD) spectra of all of the amino acid derivatives used in the formation of the camphanates **2.53** and **2.56** was measured to pin-point the source of racemisation in the 'D' series; these data are expressed in Table 2.4.

ORD data from Phenylalanine Derivatives

[(c1, MeOH), $[\alpha]_D^{25}$]

Pyrrole derivative	D		lit. value	L		lit. value
Phe-OH	+31•	**2.57**	+33(*c*2, H_2O)*	-34•		-33(*c*2, H_2O)*
N-Pth-Phe-OH	+98	**2.59**	+212(c1, EtOH)†	-217•		-212(c1.9, EtOH)†
N-(*N*-Pth-Phe)-p-2-c	+196	**2.54**		-210	**2.37**	
N-(*N*-Pth-Phe)-p-2-OH	+180	**2.55**		-195	**2.52**	
N-(*N*-Pth-Phe)-p-2-O-camph	+114	**2.55**		-90	**2.53**	

•Obtained from Sigma Chemical Co.; *Sigma Chemical Co.; †From [30]

Table 2.4

Racemisation has clearly occurred in the preparation of the protected amino acid *N*-Phthalyl D-amino acid **2.59** via *N*-carbethoxy phthalimide **2.58**, Scheme 2.30.

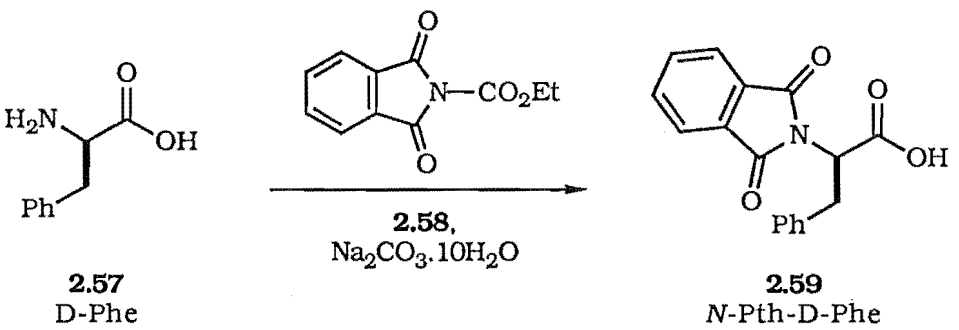

2.57
D-Phe

2.59
N-Pth-D-Phe

Scheme 2.30

The 'L' version of the protected amino acid, *N*-Pth-L-Phe-OH, was obtained from the Sigma Chemical Company. Repeating the sequence with optically pure[31] *N*-Pth protected D-Phe amino acid was not felt necessary as the 'L' and 'D' series camphanates, **2.53** and **2.56** respectively, had clearly distinguishable ^1H NMR spectral signals, Figure 2.29.

The high enantiomeric excess found in the 'L' derivative **2.53** clearly shows that the steps involved in the synthesis of *N*-acylated hydroxymethyl pyrroles did not cause racemisation of the amino acid α-carbon during the synthesis. This finding will therefore allow the production of this class of inhibitor in high optical purity.

N-Pth protected dipeptide acid chlorides, and other *N*-Pth protected amino acids were also tried using the DMAP methodology to *N*-acylate p-2-c. This is discussed in Section 3.3.

2.4.7 Deprotection of *N*-Phthalalyl Protected Amino Acid Pyrrole Derivative 2.52

The phthalyl protecting group of **2.52** proved to be difficult to remove. Conditions tried included those described as mild[32], $NaBH_4$/2-propanol followed by hot acetic acid. The traditional methods of hydrazinolysis[33], and acid catalysed hydrolysis[34] were considered to be detrimental to the pyrrole.

These results were expected, but are unfortunate as extension in the *N*-direction from the pyrrole would be most advantageous for recognition of the inhibitor by the targeted enzyme. The HIV protease, for example, requires up to four amino acids in the *N*-direction from the scissile bond, the P_1-P_4 subsites, to make an adequate inhibitor; see Section 1.2 for a discussion. At present there is only one amino acid and a large *N*-protecting group, both of which are consistent with known inhibitors of the HIV-1 protease, Section 1.2.4 and Section 3.2.5.

We therefore tried to extend the reaction to the benzyloxycarbonyl (Cbz) protecting group.

2.4.7.1 *N-Cbz Protection of the Acylated Amino Acid Phenylalanine*

We expected that an analogous reaction using an activated ester of an *N*-protected amino acid, eg: the conveniently crystalline *p*-nitrophenyl ester, would yield the desired *N*-acyl product, Scheme 2.31.

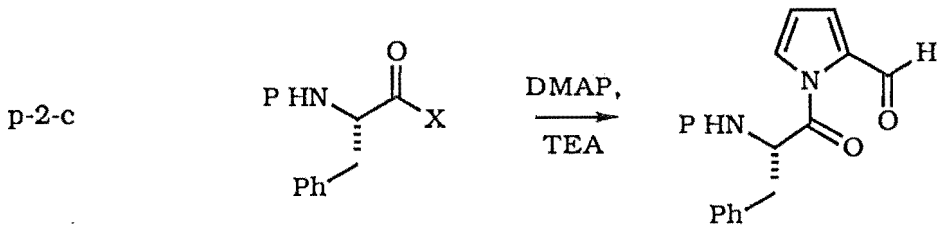

2.29 P=Cbz, X=*p*nitrophenyl ester
2.60 P=Fmoc, X=Cl

2.33 P=Cbz
2.61 P=Fmoc

Scheme 2.31

The DMAP methodology was used in an attempt to *N*-acylate p-2-c. Addition of *N*-Cbz-Phe-*p*-nitrophenyl ester **2.29** to the pyrrole solution produced a yellow colour that intensified over twenty four hours. This colour was attributed to the release of *p*-nitrophenol. During the standard DMAP work up the organic layer was washed with water until the yellow colour had been removed from the washings. The ^{1}H NMR spectrum of this, was consistent with the desired *N*-acylated pyrrole **2.33**, ie: a downfield shift of the of -C*H*O signal to 10.38ppm and shifts downfield, as well as characteristic multiplicity changes to the pyrrole H-3, H-4, H-5 signals [δ ($CDCl_3$) 6.34 (1H, t, *J*=3.6Hz, H-4); 7.04 (1H, m, H-3); 7.21 (1H, dd, *J*=3.1 & 1.7Hz, H-5)].

This reaction was repeated many times after this initial success. However problems were encountered with the reproducibility. The yield (by ^{1}H NMR spectrum) was at best 13% *N*-(*N*-Cbz-Phe)-p-2-c **2.33**, with 87% p-2-c. The following modifications were attempted in order to improve the reproducibility:

1) amino acid and DMAP were scrupulously dried by recrystallisation followed by drying under high vacuum for twenty four hours,

2) p-2-c and TEA were freshly distiled,

3) the reaction was performed in a "dry box",

4) freshly activated 4Å molecular sieves were added to the reaction,

5) the reaction carried out at reflux,

6) varying the amounts of each reagent and solvent,

7) glassware both washed in strong acid and strong base respectively,

8) the addition of water to the reaction mixture,

9) altering the order of addition of reagents, all to no avail. There was no doubt that the first reaction, and several of the later reactions, gave the desired *N*-acylated pyrrole derivative **2.33**. The assumption was that the problem was in the source of the starting materials. The p-2-c in the first

successful reaction was obtained from Aldrich Chemical Company, whereas in subsequent reactions it was prepared from Vilsmeier-Haack formylation of pyrrole[35]. The amino acid, obtained from Sigma, was also of different batches.

This reaction was not pursued further due to the problems of reproducibility.

2.4.7.2 *N-(9-Fluorenylmethyl)oxycarbonyl (Fmoc) Protection of the Acylated Amino Acid Phenylalanine*

N-Fmoc protected amino acids have received much attention in peptide synthesis due to ease of deprotection. Addition of a solution of *N*-Fmoc-Phe-Cl[36] **2.60**, Scheme 2.31, to p-2-c under the DMAP conditions produced no sign of *N*-acylated product **2.61**, there was full recovery of p-2-c.

2.4.7.3 *Loss of Activity of Cbz and Fmoc Amino Acid Acylating Agents and Possible Methods to Overcome this Problem*

The use of an N^{α}-urethane, eg: Cbz, protected amino acid acid chlorides had been limited since the necessary basic co-reagent, DMAP, causes immediate conversion of the amino acid to the corresponding oxazolone[37] **2.39**, Scheme 2.32.

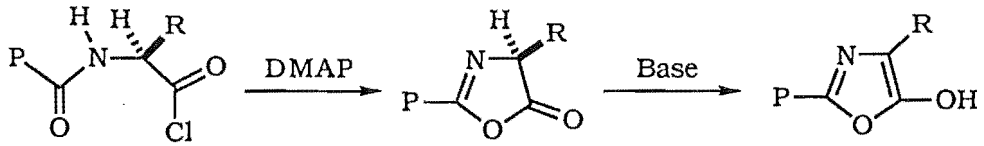

P= Fmoc, Cbz, Boc

2.39

Scheme 2.32

Oxazolones are more sluggish than the parent acid chloride to further acylation and result in racemisation. Extension of amino acid chain in the *N*-direction (Figure 2.9) required the removal of the protecting group.

The oxazolone **2.39** was assumed to have formed on the addition of DMAP to the activated amino acid derivatives. Carpino[36] also indicated that the formation of the oxazolone is overcome by the slow addition of the amino acid acid chloride to the compound that is to be acylated. Here, direct reaction of the pyrrole with the acid chloride competes favourably with oxazolone formation. This order of addition is opposite to that used in the *N*-Pth protected case where high yields of the *N*-acyl product were observed, Section 2.4.2.1. The DMAP reaction produced no *N*-acylated product on the reversal of addition as described above.

Carpino also suggested that α-amino acid fluorides do not undergo

oxazolone formation. The acid fluoride is expected to acylate the pyrrole derivative readily, this the reaction was not attempted[38].

Activation of amino acids by DCC **2.62** and HOBt[39] **2.64**, Scheme 2.33, was also attempted. The formation of the HOBt/amino acid complex **2.65**, Scheme 2.33, has been shown to depress oxazolone formation, Scheme 2.32.

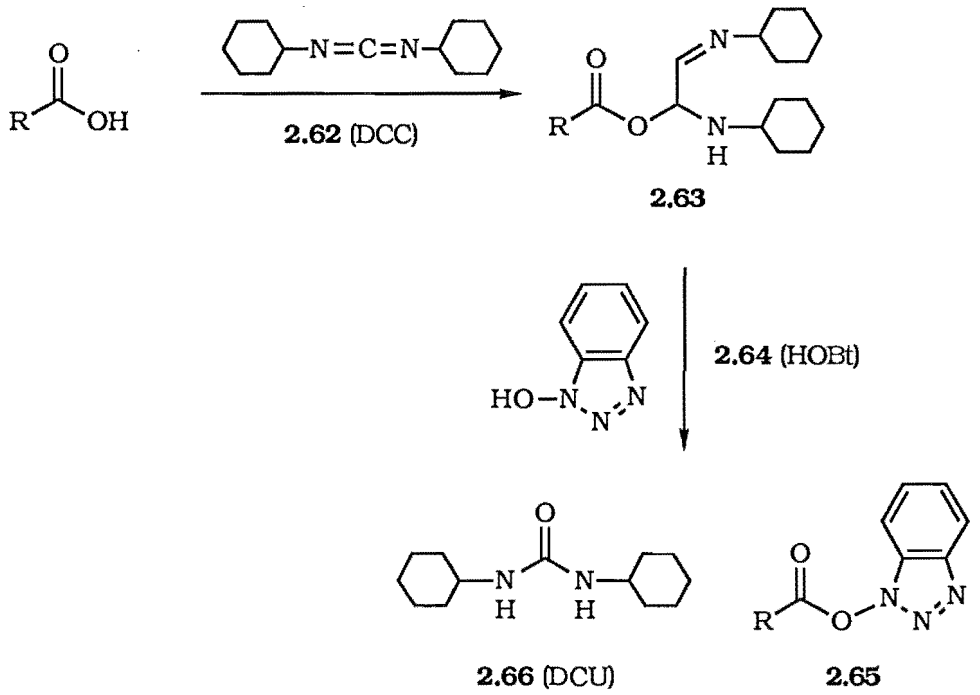

Scheme 2.33

One equivalent each of HOBt **2.64** and DCC **2.62** were added to the free *N*-Cbz-Phe-OH and a white solid, attributed to the DCU **2.66**, formed, indicating formation of the activated amino acid, eg: **2.65**. This was followed by the addition of the necessary reagents for the DMAP promoted acylation of pyrrole. The ^{1}H NMR spectrum of aliquots of this mixture did not show evidence of *N*-acylated product after fifteen minutes, three hours and twenty four hours. We were forced to conclude that the HOBt activated amino acid species was not reactive enough to acylate p-2-c.

2.5 Protection of the Pyrrole-2-Carboxaldehyde Formyl Group - Acetal Studies

The NaH and MeLi studies indicated that the pyrrole aldehyde played a part to the detriment of the *N*-acylation reaction via reaction through oxygen. Electron and/or resonance donating substituents at the 2-position of the pyrrole have been found to activate the nitrogen towards nucleophilic attack.

Protection of the formyl group by acetal formation was not expected to alter the electron density on the pyrrole nitrogen. The p-2-acetal **2.67**, Scheme 2.34, described by Loader[40] was prepared by the method described as indirect. The acetal was shown to be stable and survived the DMAP conditions.

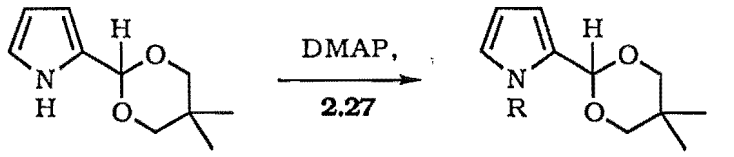

2.67 **2.68** R= $COCH_2CH_2Ph$

Scheme 2.34

The addition of one equivalent of hydrocinnamoyl chloride to p-2-acetal **2.67** using the DMAP methodology produced no evidence by ^1H NMR spectrum of the desired *N*-acylated species **2.68**. This reaction was attempted several times without any success. Nor was success obtained with the MeLi promoted acylation of **2.67**. The ^1H NMR spectrum signal for the pyr-C*H*-acetal was expected at 5.8-5.9ppm with similar shifts and multiplicity of H-3, H-4 and H-5, as observed in the *N*-acylated-p-2-c derivatives, Section 2.7.1.

The continual lack of products from the reaction with the acetal forced the conclusion that acetal formation removes sufficient electron density from the pyrrole nitrogen so as to deactivate it towards the acylation reactions. The use of acetal protected p-2-c was therefore discontinued.

2.6 Formylation of *N*-Acyl-Pyrrole Derivatives

The *N*-acylation of pyrrole itself was moderately successful via both the DMAP and MeLi methods, Section 2.3.1. and Section 2.4.3. The Vilsmeier-Haack formylation of the product **2.28** and **2.30**, Scheme 2.35, only resulted in the formation of p-2-c and polymer. No evidence for the desired formyl pyrroles **2.31** or **2.33** was observed.

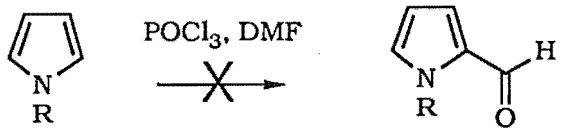

2.28 R=$COCH_2CH_2Ph$
2.30 R=CO-Phe-Cbz-*N*

2.31 R=$COCH_2CH_2Ph$
2.33 R=CO-Phe-Cbz-*N*

Scheme 2.35

A recent report indicated that formylation of aromatic compounds using the trifluoromethanesulfonic anhydride/DMF complex[41] proceeds in higher yields than the standard Vilsmeier-Haack reaction. This reaction was considered, but not attempted.

2.7 Spectroscopic Data of Pyrrole Derivatives

The formyl pyrroles **3.44**, **3.52**, **3.54** and **3.56** and the hydroxymethyl pyrroles **3.45**, **3.53**, **3.55** and **3.57** are described in Chapter Three, they are included in the NMR spectral discussion, below, for completeness.

2.7.1 NMR Analysis of the *N*-Acylated Pyrrole-2-Carboxaldehyde's

2.7.1.1 *N-Acyl-Pyrrole-2-Carboxaldehyde ^1H NMR Spectral Signal Positions*

^1H NMR spectral analysis of the *N*-acylated-p-2-c species **2.24**, **2.31**, **2.37**, **2.42**, **2.43**, **3.44**, **3.52**, **3.54** and **3.56** showed that the H-3 and H-5 pyrrole ring protons of the *N*-acylated pyrroles were downfield. They ranged from 7.12-7.26ppm for H-3 and 7.25-7.43ppm for H-5. An upfield signal for H-4 was observed at 6.25-6.39ppm, and the formyl signal was found in the range 10.04-10.34ppm. This data is tabulated in Table 2.5, and a representative ^1H NMR spectra is shown in the Figure 2.36 of the *N*-acetyl-p-2-c **2.24**.

^1H NMR Spectra of *N*-Acetyl-Pyrrole-2-Carboxaldehyde 2.24

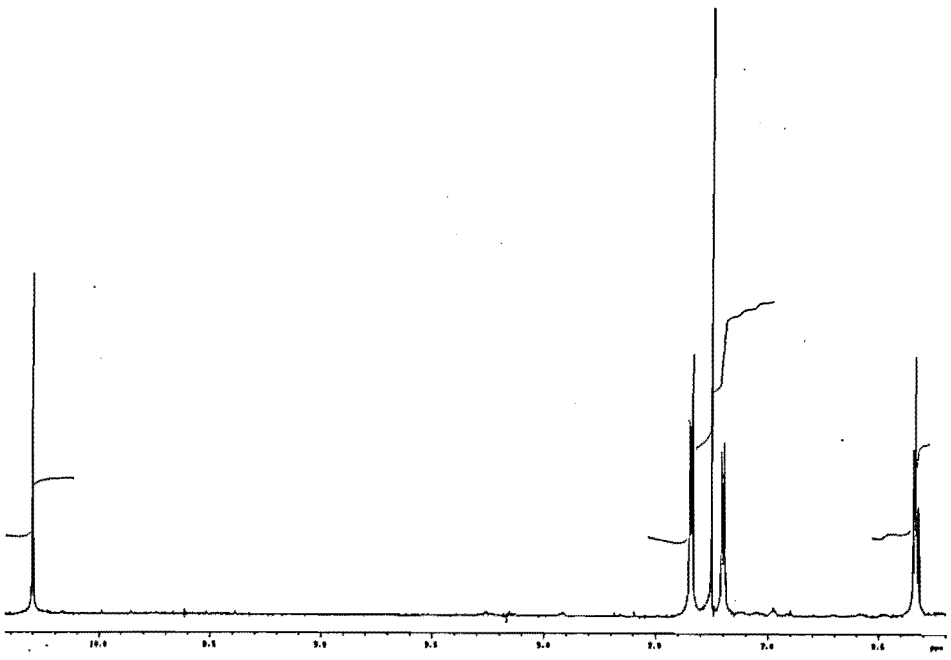

2.24

Figure 2.36

^{1}H NMR Spectral Data for *N*-Acylated-Pyrrole-2-Carboxaldehyde's

[δ ppm (300MHz), $CDCl_3$, TMS internal standard]

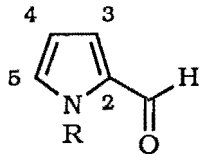

R group		H-3	H-4	H-5	-C*H*O
H		7.03	6.38	7.17	9.55
-$COCH_3$[12]	**2.24**	7.21	6.35	7.35	10.29
-$COCH_2CH_3$	**2.42**	7.26	6.39	7.43	10.34
-COPh	**2.43**	7.22	6.38	7.31	10.04
-$COCH_2CH_2Ph$	**2.31**	7.21	6.33	7.32	10.29
-CO-(Phe-Pth-*N*)	**2.37**	7.07	6.19	7.18	10.10
-$COCH_2CH(CH_3)_2$	**3.56**	7.12	6.25	7.25	10.32
-CO-(Leu-Pth-*N*)	**3.44**	7.16	6.31	7.29	10.14
-$CO(CH_2)_{10}CH_3$	**3.52**	7.22	6.35	7.35	10.32
-$CO(CH_2)_4CO_2Me$	**3.54**	7.23	6.36	7.36	10.30
Average Position:		7.19	6.32	7.32	10.24
Δ with respect to p-2-c:		+0.16	+0.06	+0.15	+0.69

Table 2.5

The signals for the formyl pyrroles, Table 2.5, are shifted with respect to the free p-2-c on average +0.16ppm for H-3, +0.06ppm for H-4, +0.15ppm for H-5 and +0.69ppm for -C*H*O. These downfield shifts indicate that the protons are deshielded by *N*-acylation, since the nitrogen lone pair is delocalised into the amide bond to give ring deactivation, see Section 2.1.2. This pattern of pyrrole NMR spectral signals was consistent with *N*-acylation.

Studies by Jones[42] on *N*-acylated pyrrole derivatives concluded that the variation in ^{1}H NMR chemical shifts may be directly correlated with the π electron density at the ring protons and with the varying electronegativity of the pyrrole nitrogen, as described in Section 2.1.2. Toube[7], Section 2.1.1, found that the relatively large formyl proton deshielding by the anisotropic *N*-acyl carbonyl group caused a downfield shift of all the pyrrole protons and in particular the aldehyde proton. The *N*-acylation work described here was found to be consistent with both these conclusions.

2.7.1.2 *Pyrrole Protons Resonance Multiplicity*

The multiplicity of the pyrrole proton signals were characteristically altered on *N*-acylation. The ^{1}H NMR spectrum of p-2-c, Figure 2.37, showed that the pyrrole proton H-3, H-4 and H-5 were coupled to each other and to the N*H* of the pyrrole.

^{1}H NMR Spectra of Pyrrole-2-Carboxaldehyde

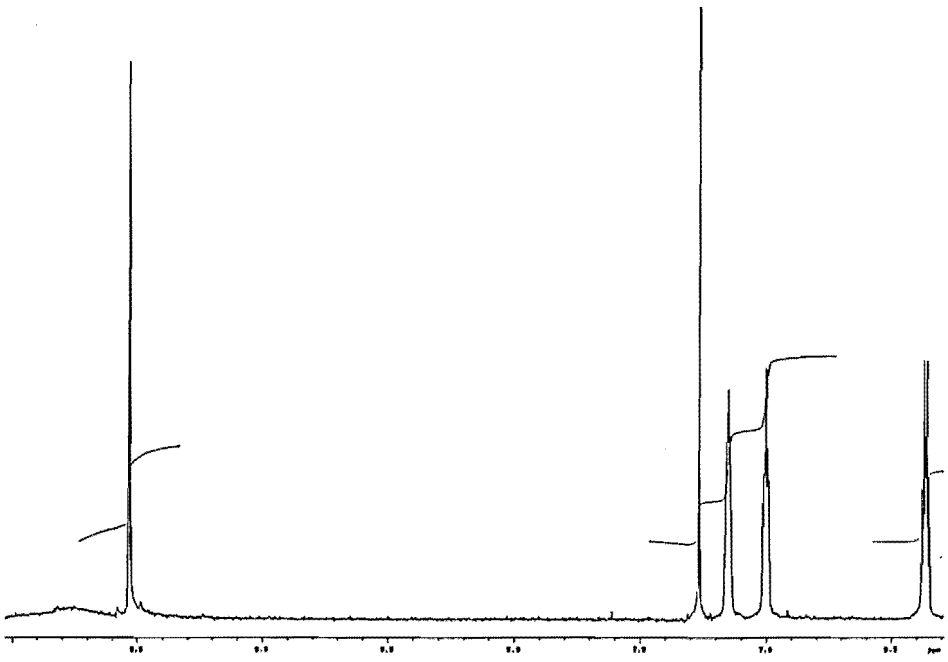

Pyrrole-2-Carboxaldehyde (p-2-c)

Figure 2.37

The H-5 signal is further coupled to the formyl group via the "zig-zag"[8] arrangement. Irradiation of the broad pyrrole-N*H* signal at approximately 10ppm simplifies the multiplet due to H-3, H-4 to a doublet of doublets (*J*=3.5 & 1.0Hz) and H-5 to a very broad singlet. *N*-Acylated pyrroles produce a similar result on irradiation of the N*H* resonances, the multiples of H-3 and H-4 simplify, while H-5 appears as doublet of doublets'. In addition, the pyrrole ^{1}H NMR spectrum signals shift downfield. The coupling constants for the *N*-acylated pyrroles synthesised are summarised in Table 2.6.

NMR Spectral *J* Coupling Constants (Hz) for
***N*-Acylated-Pyrrole-2-Carboxaldehyde's**
[δ ppm (300MHz), $CDCl_3$, TMS internal standard]

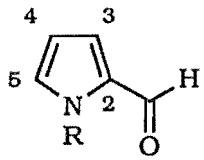

R group		H-3	H-4	H-5
H		m	m	m
$-COCH_3$[12]	**2.24**	dd	dd	dd
		3.5 & 2.0	3.5 & 3.5	3.5 & 2.0
$-COCH_2CH_3$	**2.42**	dd	dd	dd
		3.7 & 1.6	3.7 & 3.2	3.2 & 1.7
-COPh	**2.43**	dd	dd	dd
		3.1 & 1.5	3.5 & 3.1	3.7 & 1.6
$-COCH_2CH_2Ph$	**2.31**	dd	t	dd
		3.1 & 1.6	3.1	3.1 & 1.7
-CO-(Phe-Pth-*N*)	**2.37**	dd	t	dd
		3.4 & 2.2	3.4	3.4 & 2.3
$-COCH_2CH(CH_3)_2$	**3.56**	dd	t	dd
		3.5 & 1.5	3.5	3.5 & 1.5
-CO-(Leu-Pth-*N*)	**3.44**	dd	t	dd
		3.5 & 1.5	3.5	5.8 & 3.1
$-CO(CH_2)_{10}CH_3$	**3.52**	dd	t	dd
		3.8 & 1.8	3.7	3.7 & 1.9
$-CO(CH_2)_4CO_2Me$	**3.54**	dd	t	dd
		3.5 & 1.5	3.5	3.5 & 1.5

Table 2.6

2.7.1.3 *Carbon Spectra of N-Acylated Formyl Pyrrole Derivatives*

The ^{13}C NMR spectra showed the same effects of *N*-acylation as the ^{1}H NMR spectra did, there are downfield signal shifts corresponding to *N*-acylation. These observations are summarised in Table 2.7. This again demonstrates that the amide bond deactivates the pyrrole ring by an increase in the electron delocalisation.

^{13}C NMR Spectral data for *N*-Acylated-Pyrrole-2-Carboxaldehyde's

[δ ppm (75MHz), $CDCl_3$, $CDCl_3$ internal reference]

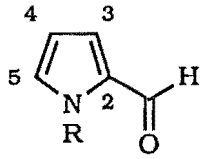

R		C-2 δ	C-3 δ	C-4 δ	C-5 δ	-CHO δ
H		132.6	121.4	111.4	126.4	179.3
$-COCH_3$	**2.24**	135.5	122.8	112.8	126.6	182.4
$-COCH_2CH_3$	**2.42**	135.7	122.5	112.8	125.9	182.6
-COPh	**2.43**	135.3	122.8	112.0	129.3	181.0
$-COCH_2CH_2Ph$	**2.31**	139.7	122.9	112.8	125.9	182.4
-CO-(Phe-Pth-*N*)	**2.37**	135.6	122.9	113.3	125.7	181.6
-CO-(Leu-Pth-*N*)	**3.44**	135.3	122.6	113.2	125.5	181.6
$-COCH_2CH(CH_3)_2$	**3.56**	135.4	122.0	112.4	126.0	182.4
$-CO(CH_2)_{10}CH_3$	**3.52**	135.7	122.4	112.7	125.9	182.6
$-CO(CH_2)_4CO_2Me$	**3.54**	135.6	122.8	112.8	126.0	182.4
Average Position:		135.5	122.6	112.8	126.3	182.1
Δ with respect to p-2-c:		+3.1	+1.2	+1.4	-0.1	+2.8

Table 2.7

2.7.2 NMR Spectral Analysis of the *N*-Acyl Hydroxymethyl Pyrroles

2.7.2.1 *N-Acyl Hydroxymethyl Pyrrole Proton Signal Positions*

The pyrrole proton resonances for H-3, H-4 and H-5 of the hydroxymethyl pyrroles **2.32**, **2.47**, **2.51**, **3.43**, **3.53** and **3.57** occur at similar chemical shifts to p-2-c. The doublet of doublets observed for the pyrrole H-5 shifted upfield by 0.25ppm to 7.07ppm, H-4 moved on average upfield by 0.15ppm to 6.17ppm. A most remarkable shift was observed for that of H-3, the signal moved upfield by 0.98ppm, with respect to the *N*-acylated formyl derivative, with a multiplicity increase from a doublet of doublets to a multiplet, Figure 2.38. This H-3 shift, is in contrast to that of p-2-c where there are two downfield (H-3, H-5) and one upfield signal (H-4). The

hydroxymethyl pyrrole compounds have one downfield (H-5) and two upfield signals (H-3, H-4). A representative ^{1}H NMR spectra of **2.47** is shown in Figure 2.38, p-2-c is in Figure 2.37 above for comparison.

^{1}H NMR Spectra of *N*-Acetyl-Hydroxymethyl Pyrrole 2.47

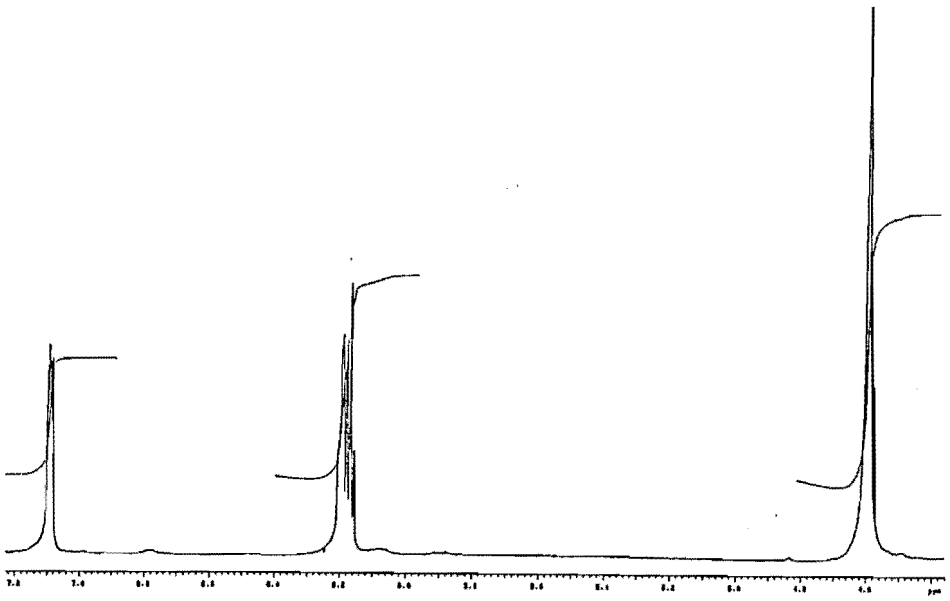

2.47

Figure 2.38

A representative example of all hydroxymethyl pyrroles, the *N*-(*N*-Pth-Phe)-p-2-OH **2.51** system is described here: irradiation of the broad singlet due to C*H*$_2$OH at 4.59ppm collapsed the H-3 signal (6.14ppm) to a doublet of doublets (*J*=3.4 & 1.4Hz), suggesting that the C*H*$_2$OH signal is coupled to H-3, two bonds distant. A very broad singlet at 3.66ppm was assigned to the O*H* on the basis that irradiation of this signal at 3.66ppm collapsed the broad singlet at 4.59ppm (C*H*$_2$OH) to a sharp singlet.

The overall upfield shifts are indicative of the loss of the aldehyde carbonyl. This causes the ring system to have an increase in electron density[42] due to the loss of the inductive formyl substituent. The reduction of the formyl group causes a decrease in the number of resonance contributors, and therefore an increase in the ring electron density, see Section 2.1.1.

The shifted upfield ^{1}H NMR spectral signals of the *N*-acylated hydroxymethyl pyrroles are represented in Table 2.8.

^{1}H NMR Spectral data for *N*-Acylated Hydroxymethyl Pyrroles

[δ ppm (300MHz), $CDCl_3$, TMS internal standard, multiplicity, (*J* Coupling in Hz)]

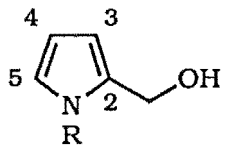

R group		H-3	H-4	H-5	CH_2OH
H		6.14, m	6.12, m	6.78, m	4.62, bs
$-COCH_3$	**2.47**	6.24, m	6.21, t 3.3	7.08, dd 3.4 & 1.6	4.63, d 6.0
$-COCH_2CH_2Ph$	**2.32**	6.21, m	6.17, t 3.3	7.06, dd 3.3 & 1.6	4.62, bs
-CO-(Phe-Pth-*N*)	**2.51**	6.14, dd 3.4 & 1.4	6.05, t 3.4	6.93, dd 3.4 & 1.5	4.59, bs
-CO-(Leu-Pth-*N*)	**3.43**	6.22, m	6.17, t 3.5	7.06, dd 3.4 & 1.5	4.63, bs
$-COCH_2CH(CH_3)_2$	**3.57**	6.22, m	6.19, t 3.5	7.11, dd 3.5 & 2.0	4.63, bs
$-CO(CH_2)_{10}CH_3$	**3.53**	6.22, m	6.19, t 3.0	7.12, dd 3.0 & 1.0	4.62, bs
$-CO(CH_2)_4CO_2Me$	**3.55**	6.23, m	6.21, t 3.5	7.11, dd 3.5 & 2.0	4.63, bs
Average Position:		6.21	6.17	7.07	4.62
Δ with respect to average *N*-Acyl-p-2-c:		-0.98	-0.15	-0.25	n.a.

Table 2.8

The coupling values of the pyrrole protons are also represented in Table 2.8.

The ^{13}C NMR spectral signals for the hydroxymethyl pyrroles produced by formyl reduction are given in Table 2.9.

^{13}C NMR Spectral data for *N*-Acylated Hydroxymethyl Pyrroles

[δ ppm (75MHz), $CDCl_3$, $CDCl_3$ internal reference]

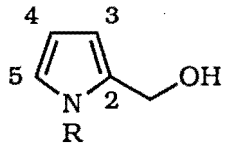

R		C-2 δ	C-3 δ	C-4 δ	C-5 δ	CH_2OH δ
$-COCH_3$	**2.47**	135.6	114.8	112.3	121.7	57.9
$-COCH_2CH_2Ph$	**2.32**	135.5	114.5	112.2	120.7	57.9
-CO-(Phe-Pth-*N*)	**2.51**	135.9	114.9	113.1	120.2	57.6
-CO-(Leu-Pth-*N*)	**3.45**	136.1	114.9	113.0	120.1	57.6
$-COCH_2CH(CH_3)_2$	**3.57**	135.4	114.5	111.9	121.0	57.9
$-CO(CH_2)_{10}CH_3$	**3.53**	135.5	114.4	111.9	120.9	57.9
$-CO(CH_2)_4CO_2Me$	**3.55**	135.5	114.6	112.2	120.8	57.9
Average Position:		135.6	114.7	112.4	120.8	57.8
Δ with respect to average *N*-Acyl-p-2-c:		+0.1	-7.9	-0.4	-5.5	n.a.

Table 2.9

2.7.3.1 *IR Spectroscopy of the N-Acylated Pyrrole Derivatives*

The formyl group of p-2-c is less aldehyde like in nature than other aliphatic aldehydes due to the deactivation by the π electron system, Figure 2.2, Section 2.1.1. This is manifested in the UV, IR and the NMR spectra (Section 2.7.1) of the *N*-acyl-pyrrole derivatives.

The p-2-c carbonyl stretching frequency is lowered to $1667cm^{-1}$ on *N*-acylation, as discussed in Section 2.1.1. This is due to the pyrrole nitrogen lone pair being delocalised into the π system and to the *N*-acyl group. The effect is to increase the stretching frequency of the formyl carbonyl to a more aldehyde like position. The figures in Table 2.10 show the increase in the aldehyde IR stretching frequency and the amide stretching frequency on *N*-acylation of p-2-c.

IR Stretching Frequencies for the Carbonyl Groups of *N*-Acylated-Pyrrole-2-Carboxaldehyde's

(FTIR, neat, cm^{-1})

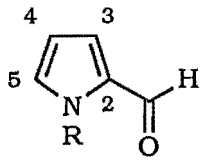

R		-CHO	R-CO
$-COCH_3$	**2.47**	1730	1670[11]
$-COCH_2CH_3$	**2.42**	1725	1655
-COPh	**2.43**	1770	1677
$-COCH_2CH_2Ph$	**2.31**	1729	1654
-CO-Phe-*N*-Pth	**2.51**	1732	1660
-CO-Leu-*N*-Pth	**3.44**	1738	1668
$-COCH_2CH(CH_3)_2$	**3.56**	1727	1665
$-CO(CH_2)_4CO_2Me$	**3.54**	1731	1651
$-CO(CH_2)_{10}CH_3$	**3.52**	1738	1660

Table 2.10

There is a uniform increase in wave number as the formyl becomes more aldehyde like in nature, as would be expected by the increased delocalised system that approximates a true aldehyde, more closely.

2.7.3.2 *UV Spectroscopy of N-Acylated Pyrrole Derivatives*

A decrease in λ_{max} of the UV spectra of **2.32**, **2.42**, **2.43**, **2.51**, **3.44** and **3.56** relative to p-2-c, was consistent with a decrease in conjugation between the pyrrole ring and the formyl substituent. This is due to an increased electron withdrawing capability of the *N*-acyl species, as exemplified by the *N*-Pth protecting group. The largest λ_{max} decrease, Table 2.11, is observed when the R group is -COPh. A similar large shift was observed where R was $-N(Me)_2$, that was explained via steric interactions that lead to a 64° out of planar twist[43]. The same argument can be applied to the case where R is -COPh **2.43**.

Table 2.11 shows that as the electron withdrawing ability of the *N*-acyl group increases, a decrease in λ_{max} is observed.

UV Spectra of *N*-Acylated Pyrrole Derivatives (nm)

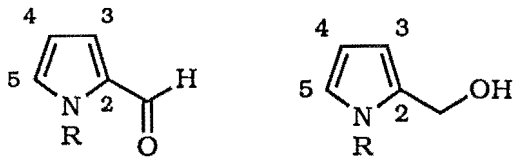

R	λ_{max} -CHO		λ_{max} -CH_2OH
-$COCH_2CH_3$* **2.42**	296		n.r.
-$COCH_2CH_2Ph$* **2.31**	296	**2.32**	285
-$COCH_2CH(CH_3)_2$* **3.56**	297	**3.57**	283
-CO-(Leu-*N*-Pth)† **3.44**	285	**3.45**	283
-CO-(Phe-*N*-Pth)† **2.51**	279	**2.52**	279
-COPh* **2.43**	273		301≠
-$N(CH_3)_2$*	268≠		not available

[c=1, * $CHCl_3$; † MeOH; n.r. Corresponding Aldehyde Not Reduced ; ≠ From [9]]

Table 2.11

Reduction of the *N*-acyl formyl pyrroles to *N*-acyl hydroxymethyl pyrroles, **2.32**, **2.42**, **2.43**, **2.51**, **3.45** and **3.57**, causes an increase in the λ_{max}. This is consistent with loss of the formyl group and hence in conjugation.

2.7.3.3 *Thin Layer Chromatography - TLC*

Throughout the pyrrole acylation work, extensive use of TLC monitoring and the Ehrlich reaction[44], Section 2.7.3.4 was employed.

A standard solvent system of ethyl acetate: petroleum ether= 1:2 was found to resolve the pyrrolic species under investigation, satisfactorily. Table 2.12 indicates the R_f values of the series of *N*-cinnamoyl pyrrole derivatives. The series is representative of the *N*-acyl-pyrrole derivatives that were studied.

Generally, *N*-acylation of p-2-c lowered the R_f; reduction of the formyl group lowered the R_f further.

Effect of Various *N*-Cinnamoyl Pyrrole Derivatives 2.31 and 2.32 on R_f and the Rate of Colour Formation in the Ehrlich Reaction

pyrrole derivative		R_f	Ehrlich Reaction
p-2-c		0.48	++
N-cinnamoyl-p-2-c	**2.31**	0.46	+
N-cinnamoyl-p-2-OH	**2.32**	0.40	++

+++, Instantaneous development of colour:

++, full colour developed within 30 seconds: +, full colour in five minutes

Table 2.12

2.7.3.4 *The Ehrlich Reaction*

Further valuable information was gained from the staining of the TLC plate. Once the UV active species were identified, the TLC plate was dipped in an ethanolic solution of 4-dimethylamino benzaldehyde containing a catalytic amount of HCl (the Ehrlich reaction[44]). This produced a red-purple spot that has been attributed to formation of an azafulvene like structure[45] **2.69**, Scheme 2.38.

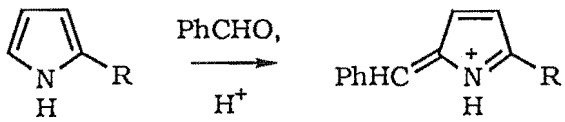

2.69

Scheme 2.38

The rate of formation of the spot depends to a large extent on the electronic character and orientation of the substituents on the pyrrole ring[46]. The greater the amount of electron donating ability of the substituent on the pyrrole, the greater the rate of colour formation. Derivatives with electron withdrawing substituents do not couple as readily with the reagent and therefore colour formation is slower.

The Ehrlich data in Table 2.12 have been described along the same lines by Badger[46]. Reducing the electron density of the pyrrole ring by *N*-acylation slows down the appearance of the colour. Reduction of the formyl to the alcohol results in the loss of some of the electron withdrawing ability, ie: an increase in the ring electron density, as a consequence a positive Ehrlich test is observed at approximately the same rate as the unsubstituted p-2-c.

A combination of the Ehrlich reaction and TLC monitoring was found to be a useful technique in determining the reaction progression.

2.8 Conclusion

The designed mechanism based inhibitors, Section 1.1, require that an acyl species be placed on the nitrogen of a pyrrole. A synthetic methodology has been developed for a variety of different acylating agents. Ultimately the amino acid chain, will be extended, in the *N*-direction (Figure 2.9) to aid in enzyme recognition, see the next chapter.

The DMAP methodology developed successfully places acyl groups on the nitrogen of pyrrole derivatives. No racemisation of amino acids was observed in the case of **2.51** using the DMAP method and thus satisfies one of the criteria for the *N*-acylation of pyrroles. The method also is versatile with both simple, and amino acid based acylating agents being promoted to *N*-acylate several pyrrole derivatives in good yields, eg: p-2-c, pyrrole and **2.44**. MeLi was also found to promote *N*-acylation of pyrrole derivatives.

Amino acids with a proton on nitrogen seem to cause oxazolone **2.39** formation and loss of activity of the amino acid. Oxazolone formation was manifest by decreased yields of *N*-acyl-pyrrole derivatives. There is evidence that amino acid acid fluorides do not undergo the same oxazolone formation as the acid chloride and therefore are expected to act as good acylating agents under DMAP conditions.

The MeLi reaction would appear to overcome the problem of placing a removable amino acid protecting group on pyrrole with *N*-Cbz-Phe-*p*-nitrophenyl ester, eg: **2.30**, however MeLi mediated acylation of p-2-c with *N*-Cbz-Phe-*p*-nitrophenyl ester does not proceed. The Vilsmeier-Haack formylation of *N*-acylated pyrrole **2.30** did not work. There exists the possibility that formylation with triflic anhydride may be successful.

Thus, there are a few possible reactions which may in the future allow additional amino acids to be added to extend the peptide sequence in the *N*-direction, Figure 2.9.

2.9 References to Chapter Two

[1] Candy, C. F.; Jones, R. A.; Wright, P. H. *J. Chem. Soc. (C)* **1970**, 2563-2567.

[2] Menger, F. M.; Donohue, J. A. *J. Am. Chem. Soc.* **1973**, *95*, 432-437.

[3] Nicolaou, K. C.; Claremon, D. A.; Papahatjis, D. P. *Tetrahedron Lett.* **1981**, *22*, 4647-4650.

[4] Kipping, F. S. *J. Chem. Soc. (Lond).* **1894**, 480-503.

[5] Moon, M. W.; Bell, L. T.; Webster, D. M. *J. Org. Chem.* **1974**, *39*, 315-318.

[6] Gilchrist, T. L. *Heterocyclic Chemistry*; Pitman: London, 1985.

[7] Coumbarides, G. S.; Mercey, J. M.; Toube, T. P. *J. Chem. Res. (S)* **1990**, 151.

[8] Banwell, C. N.; Sheppard, N. *Faraday Discuss. Chem. Soc.* **1962**, *34*, 115-126.

[9] Abell, A. D. Post Doctoral Thesis, Cambridge, England, 1986.

[10] Jones, A. R.; Bean, G. P. *The Chemistry of Pyrroles*; Academic Press Inc.: London, 1977; p472.

[11] Bray, B. L.; Muchowski, J. M. *J. Org. Chem.* **1988**, *53*, 6115-6118.

[12] *Comprehensive Hetrocyclic Chemistry*, Vol. 6, Part 4B; Katritzky, A. R., Rees, C. W., Editorial Chairmen; Pergamon: Oxford, 1984.

[13] Bray, B. L.; Hess, P.; Muchowski, J. M.; Scheller, M. E. *Helv. Chim. Acta.* **1988**, *71*, 2053-2057.

[14] Williams, R. M. *Synthesis of Optically Active α-Amino Acids*; Pergamon: Oxford, 1989; pp. 62-84.

[15] Williams, R. M. *Synthesis of Optically Active α-Amino Acids*; Pergamon: Oxford, 1989; p79.

[16] Wagner-Jauregg, T. *Synthesis* **1980**, 165-214.

[17] Nickisch, K.; Klose, W.; Bohlmann, F. *Chem. Ber.* **1980**, *113*, 2036-2037.

[18] Steglich, W.; Höfle, G. *Angew. Chem., Int. Ed. Engl.* **1969**, *8*, 981.

[19] Fieser, M.; Danheiser, R. L.; Roush, W. *Reagents for Organic Synthesis*, Vol 9, John Wiley & Sons: New York, 1981; p179.

[20] *Beilsteins Handbuch der Organischen Chemie*, Band XX, Springer: Berlin, 1935; p165.

[21] Reddy, G. S. *Chem. Ind. (London)* **1965**, 1426-1427.

[22] Uny, R. W.; Jones, R. A. *Aust. J. Chem.* **1965**, *18*, 363-371.

[23] Silverstein, R. M.; Ryskiewicz, E. E.; Chaikin, S. W. *J. Am. Chem. Soc.* **1954**, *76*, 4485-4486.

[24] Schauder, J-R; Jendrezejewski, S.; Abell, A.; Hart, G. J.; Battersby, A. R. *J. Chem. Soc., Chem. Commun.* **1987**, 436-438.

[25] Lee, S. D.; Brook, M. A.; Chan, T. H. *Tetrahedron Lett.* **1983**, *24*, 1569-1572.

[26] Gensler, W. J.; Johnson, F. A.; Sloan, D. B. *J. Am. Chem. Soc.* **1960**, *82*, 6074-6081.

[27] Scudar, P. *J. Mol. Biol.* **1973**, *76*, 123-129.

[28] Mitsunobu, O. *Synthesis* **1981**, 1-28.

[29] Bodanszky, M.; Bodanszky, A. *The Practice of Peptide Synthesis*; Springer-Verlag: Berlin, 1984; p10.

[30] Wünsch, E. *Houben-Weyl: Methoden der Organischen Chemie* Vol. 15, Part1, Georg Thieme: Stuttagart, 1974; pp. 250-257.

[31] Hoogwater, D. A.; Reinhoudt, D. N.; Lie, T. S.; Gunneweg, J. J.; Beyerman, H. C. *Recueil* **1973**, *92*, 819-825.

[32] Osby, J. O.; Martin, M. G.; Ganem, B. *Tetrahedron Lett.* **1984**, *25*, 2093-2096.

[33] Bodanszky, M.; Bodanszky, A. *The Practice of Peptide Synthesis*; Springer-Verlag: Berlin, 1984; p163.

[34] Bodanszky, M.; Bodanszky, A. *The Practice of Peptide Synthesis*; Springer-Verlag: Berlin, 1984; p179.

[35] *Organic Syntheses*, Col. Vol. 4; John Wiley & Sons: New York, 1963; pp. 831-833.

[36] Carpino, L. A.; Cohen, B. J.; Stephens Jr, K. E.; Sadat-Aalaee, S. Y.; Tein, J-H.; Landridge, D. C. *J. Org. Chem.* **1986**, *51*, 3732-3734.

[37] Carpino, L. A.; Sadat-Aalaee, D.; Chao, H. G.; DeSelms, R. H. *J. Am. Chem. Soc.* **1990**, *112*, 9651-9652.

[38] Olah, G. A.; Nojima, M.; Kerekes, I. *Synthesis* **1973**, 487-488.

[39] Windridge, G. C.; Jorgensen, E. C. *J. Am. Chem. Soc.* **1971**, *93*, 6318-6319.

[40] Loader, C. E.; Anderson, H. J. *Synthesis* **1987**, 295-297.

[41] Martinez, A. G.; Alvarez, R. M.; Barcina, J. O.; Cerero, S. de la M.; Vilar, E. T.; Fraile, A. G.; Hanack, M.; Subramanian, L. R. *J. Chem. Soc., Chem. Commun.* **1990**, 1571-1572.

[42] Jones, A. R.; Spotswood, T. McL.; Cheuychit, P. *Tetrahedron* **1967**, *23*, 4469-4479.

[43] Abell, A. D. Post Doctoral Thesis, Cambridge, England, 1986; p17.

[44] Fischer, H.; Orth, H. *Die Chem des Pyrrols*, Vol II, Akademische Verlag: Leipzig, 1934.

[45] Jones, A. R.; Bean, G. P. *The Chemistry of Pyrroles*; Academic Press Inc.: London, 1977.

[46] Badger, G. M.; Harris, R. L. N.; Jones, R. A. *Aust. J. Chem.* **1964**, *17*, 1022-1027.

Chapter Three

Extension of Amino Acid Sequence

3.1 The Requirement to Extend the Amino Acid Chain in the *C*- and *N*-Direction

The DMAP methodology described in Section 2.4 allows access to 2-substituted pyrroles *N*-acylated with a *N*-Pth protected amino acid, eg: **2.52** as described in Section 2.4.3.1. This represents the first requirement for the synthesis of the designed enzyme inhibitors, Section 1.1. The amino acid Phe would occupy the P_1 subsite and pyrrole (Pyr), the P_1' subsite and allow for partial enzyme recognition. The 2-pyrrole substituent allows the release of latent reactivity in the form of an azafulvene **1.3** on cleavage of the amino acid-pyrrole bond.

A large well defined hydrophobic pocket of chymotrypsin is known to accept Phe. This and other serine proteases also have an antiparallel β-sheet arrangement in the S_1-S_3 subsites, see Section 1.2.2. This is particularly important in the hydrogen bonding of the substrate (or inhibitor)[1]. The S_2' enzyme subsite is also hydrophobic in nature. X-Ray crystal structures of chymotrypsin show multiple hydrogen bonding to the backbone of the enzyme. Chymotrypsin inhibition studies have shown that residues as far removed from the active site as P_{14}', are important to binding[2]. Residues closer to the scissile bond at positions P_4, P_2, P_2' and P_3', have also been found to be important to recognition. X-Ray crystal structures of HIV protease-inhibitor complexes also show multiple hydrogen bonding between the inhibitor and the enzyme. The C_2 type inhibitors, Section 1.2.4, of HIV protease, are the only potent inhibitors, containing as few as two amino acid residues.

The hydroxymethyl pyrrole compounds, eg: **2.52** lack the extended peptide like sequence, eg: **3.1** Figure 3.1, usually found in the normal substrate of chymotrypsin and HIV protease.

3.2 Increase of Enzyme Recognition: Extension in the C-Direction of Pyrrole Derivatives

Replacement of Pro for Pyr, as in **3.2**, Figure 3.1, does not produce a mechanism based inhibitor, as there is no leaving group for azafulvene formation.

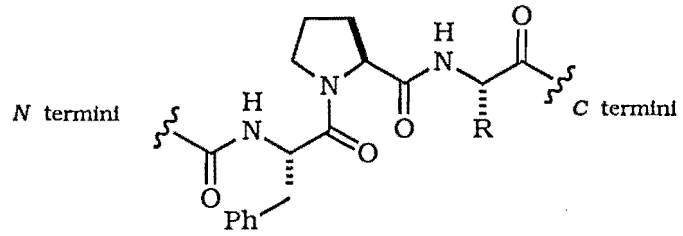

3.1
Natural Substrate

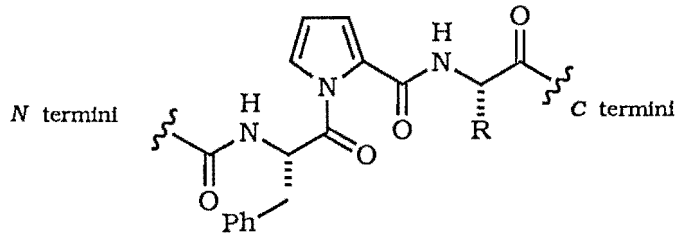

3.2
Peptide "Sense"

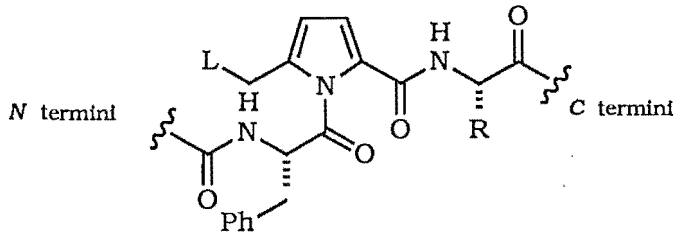

3.3
Peptide "Sense"

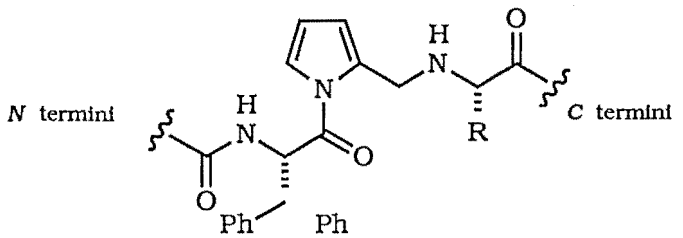

3.4
Peptide "Sense"

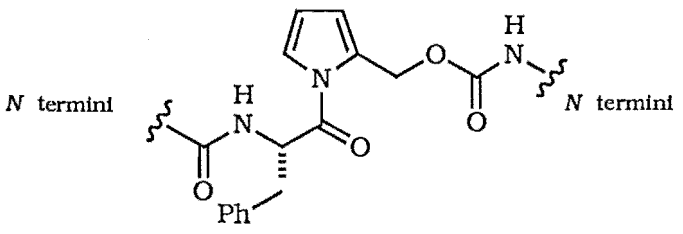

3.5
Peptide "Anti-Sense"

Figure 3.1

The addition of a leaving group, pyr-CH_2L, to the *N*-acylated pyrrole

amide as in **3.3**, Figure 3.1, would then produce an inhibitor in the correct "sense", while maintaining the ability to form an azafulvene.

Replacement of the hydroxyl group of hydroxymethyl pyrrole with an amino acid would form a pseudo dipeptide with the correct "sense", relative to the substrate, ie: *N*→*C*, **3.4** Figure 3.1.

Esterification of a hydroxymethyl pyrrole, eg: **3.5**, using Mitsunobu conditions as described for the formation of the camphanate **2.53**, Section 2.4.6, would produce a pseudo dipeptide in the "anti-sense" direction, ie: *C*→*N*, **3.5** Figure 3.1.

The relationship between a proline based natural peptide **3.1**, in the correct sense, and the "sense" **3.3**, **3.4** and "anti-sense" **3.5** pyrrole based mechanism based inhibitors described above, is summarised in Figure 3.1.

3.2.1 Extension of the Pyrrole in the C-Direction - Peptide "Sense"

Removal of the carbonyl group on the *C* side of pyrrole, outlined in **3.2** Figure 3.2, would result in an pyrrole-amine **3.4**. This exhibits all the characteristics required of a potential protease mechanism based inhibitor.

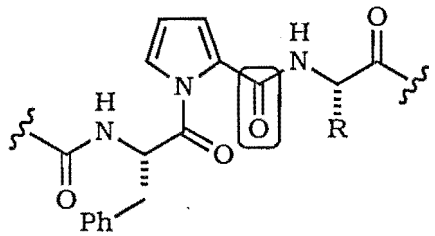

3.2

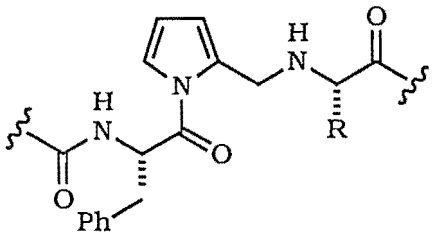

3.4

Figure 3.2

These include a suitably positioned leaving group for azafulvene formation, extended sites for hydrogen bonding to the enzyme active site and the possibility of further amino acid extension. Extension in the *C*-direction in this fashion was planned in accordance with the retrosynthesis presented in Scheme 3.3.

Disconnection of the pyrrole-amine bond of **3.6** yields the *N*-acylated imine pyrrole derivative **3.7**. The synthesis of the imine **3.7** can be envisaged via either the non-acylated p-2-c, eg: **3.8** pathway *a*, or via the *N*-acylated p-2-c, eg: **3.9** pathway *b*. Subsequent selective reduction of the *N*-acylated imine **3.7** would then produce the desired amine **3.6**.

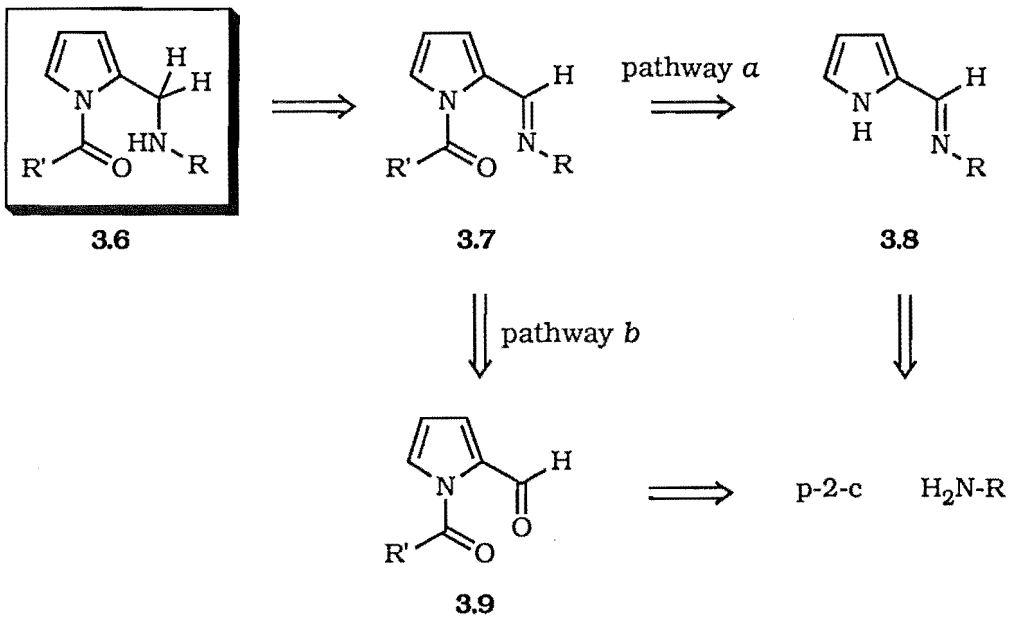

3.6 **3.7** **3.8** **3.9**

Scheme 3.3

Acylation on the pyrrole nitrogen of the p-2-imine **3.8** using the DMAP methodology, pathway *a*, Scheme 3.4, to give **3.7**, followed by reduction, would give the desired amine **3.6**, Scheme 3.4. Acylation on the pyrrole nitrogen of the intermediate imine was expected to behave similarly to the acylation of the formyl pyrrole, p-2-c.

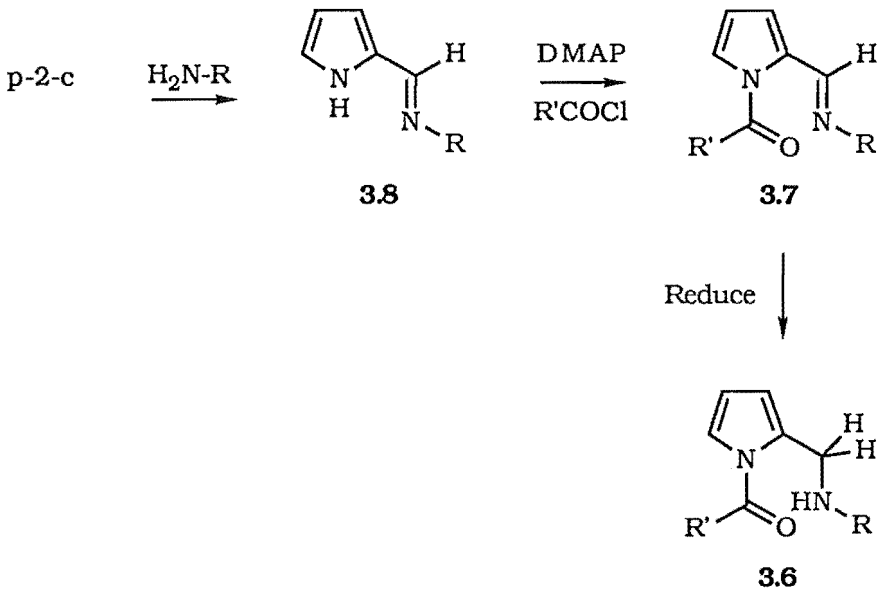

3.8 **3.7** **3.6**

Scheme 3.4

3.2.1.1 *Formation of Pyrrole-2-Imines from P-2-C*

Imine formation is well known[3,4,5] and occurs via a tetrahedral species **3.10**, Scheme 3.5.

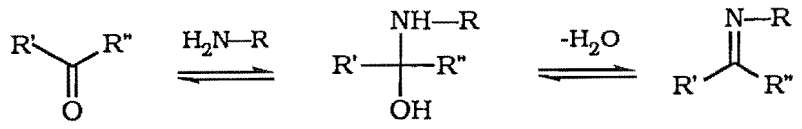

3.10 imine

Scheme 3.5

Imines formed from aromatic amines or aldehydes are usually stable and readily isolated, and are referred to as Schiff bases. Slow or unreactive systems have been found to form the desired imine when the equilibrium is shifted to the right by removal of water.

Stirring p-2-c with one equivalent of the *C* protected amino acid H_2N-Ala-OEt **3.11** generated from the hydrochloride salt, Scheme 3.6, did not however, yield the desired imine **3.12**.

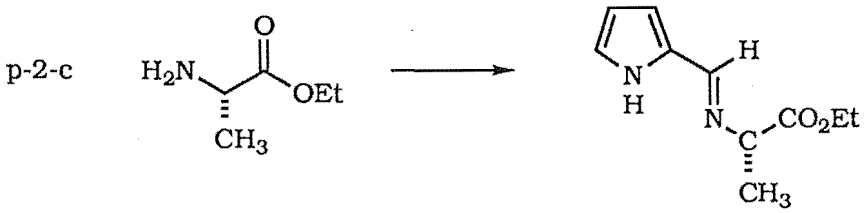

3.11 **3.12**

Scheme 3.6

Similar reactions where the water produced was removed in the presence of $MgSO_4$ or activated 4Å molecular sieves, did not produce the desired imine **3.12** either. Brunner[3] described several methods for the formation of imines, eg: **3.13**, including pyrrolic imines similar to those required in the present study.

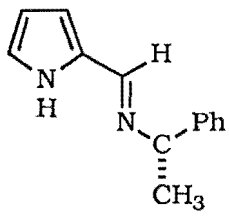

3.13

A similar reaction to that reported by Brunner was attempted using one equivalent each of HCl.H_2N-Ala-OEt and p-2-c in Benzene/MeOH=2:1, containing one equivalent of TEA. The ^{1}H NMR spectrum of the crude reaction mixture after twenty four hours indicated 78% of p-2-Ala-OEt imine **3.12**, Scheme 3.6. The remaining 22% was starting p-2-c. A diagnostic ^{1}H NMR spectral signal for the pyr-C*H*=N-R signal was observed at 8.05ppm.

Polymeric species were also formed, as apparent by the large amount of insoluble black precipitate in the crude reaction mixture. A polymer also

formed over three days in the NMR tube containing the imine, this was possibly due to traces of hydrochloric acid in the $CDCl_3$.

Azeotropic removal of water from p-2-c and the amino acid in pentane at reflux using a modified Dean-Stark apparatus produced 90% of the desired imine **3.12**. Similar azeotrope reactions in CH_2Cl_2, benzene and $CHCl_3$ did not produce the imine. The reflux of p-2-c in pentane with the free amino acid Ala did not yield the corresponding imine.

The addition of Ts-OH to the azeotrope reactions, described above, gave no apparent increase in the yield of the imine **3.12**.

The synthesised p-2-Ala-OEt imine **3.12** was found to be unstable on silica and after five days storage as a solid, decomposed. The crude reaction mixture was sufficiently clean to allow characterization of the imine, once the polymer had been removed by filtration. The ^1H NMR spectrum of **3.12** lacked the formyl resonance, as described in the reduction work of Section 2.7.2. The H-3, H-4 and H-5 signals shifted upfield, as did the NH signal with respect to p-2-c, see Section 3.2.1.2. The nitrogen withdraws less electron density from the pyrrole ring than the oxygen of the formyl derivatives, and therefore canonical forms of the type **2.14**, Figure 2.8, are less important.

Imine formation using the non-amino acid based amine, isobutylamine **3.14**, and azeotropic removal of water produced 100% ^1H NMR spectral yield of the desired p-2-isoBuNH_2 imine **3.15**, Scheme 3.7.

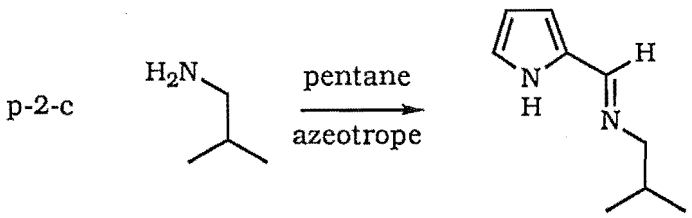

3.14 **3.15**

Scheme 3.7

Polymer was again formed, decreasing the yield of the imine. The continued formation of pyrrole decomposition polymers meant that yields of the final imine were drastically reduced. This is not the only work in the area of pyrrole imine formation in which trouble was reported with decomposition of product to polymer. Battersby also reported[6] a similar phenomenon, as described in Section 3.2.1.4.

The p-2-isoBuNH_2 imine **3.15** was found to be unstable to chromatographic separation, but was fully characterised by ^1H NMR spectroscopy. The H-3, H-4 and H-5 ^1H NMR spectral signals again were

consistent with the absence of a formyl group. See Table 3.1 for a summary.

Unlike the Ala based imine **3.12**, the isobutylamine based imine **3.15** does not present the possibility of further amino acid extension.

3.2.1.2 *NMR Spectral Comparison of Pyrrole-2-Imines*

Table 3.1 summarises the ^{1}H NMR spectra of imines **3.12** and **3.15**. The average signal position is presented in Table 2.7.1.1 for comparison with p-2-c.

Comparison of ^{1}H NMR Spectral Signals from Pyrrole-2-Imines 3.12 and 3.15

Pyrrole Derivative	H-3 δ	H-4 δ	H-5 δ	pyr-C*H* δ
3.12	6.56	6.26	6.96	8.05
3.15	6.46	6.22	6.86	8.01
p-2-c	7.03	6.38	7.17	9.55
average *N*-acyl-p-2-c*	7.19	6.32	7.32	10.24

* Data from Section 2.7.1.1

Table 3.1

3.2.1.3 *N-Acylation of Pyrrole-2-Imines*

The DMAP methodology described in Section 2.4 was expected to allow ready acylation of the imines **3.12** and **3.15**. Reaction of freshly prepared p-2-Ala-OEt imine **3.12**, with DMAP, TEA and acetyl chloride failed to yield the desired *N*-acyl imine **3.16**, Scheme 3.8. The only products detected were *N*-acetyl-p-2-c **2.24** and p-2-c. Similar results were observed for the DMAP promoted acylation of the non-amino acid p-2-isoBuNH$_2$ imine **3.15**.

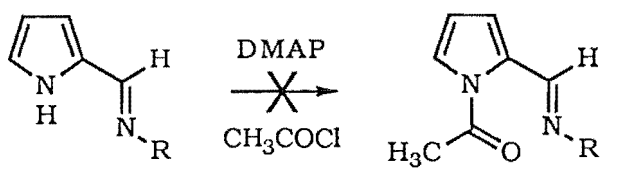

3.12 R=Ala-OEt
3.15 R=$CH_2CH(CH_3)_2$

3.16 R=Ala-OEt
3.17 R=$CH_2CH(CH_3)_2$

Scheme 3.8

Imine hydrolysis occurred, either under the DMAP conditions to give the p-2-c, which was subsequently *N*-acylated to give **2.24**, or alternatively the acylation of the imine occurred with subsequent hydrolysis to the aldehyde. The fact that the desired *N*-acyl-p-2-imines **3.16** or **3.17** were not observed, tends to eliminate the latter hypothesis. *N*-Acylation of the p-2-imine's pathway *a*, Scheme 3.3, was therefore discontinued in favour of the strategy depicted in pathway *b* of the retrosynthesis, Scheme 3.3.

3.2.1.4 *Imine Formation from N-Acylated Pyrrole-2-Carboxaldehyde*

An alternative strategy for the formation of the desired *N*-acyl-p-2-imine **3.7**, pathway *b*, Scheme 3.3, was to form the imine of the *N*-acylated-p-2-c **2.31**, Scheme 3.9.

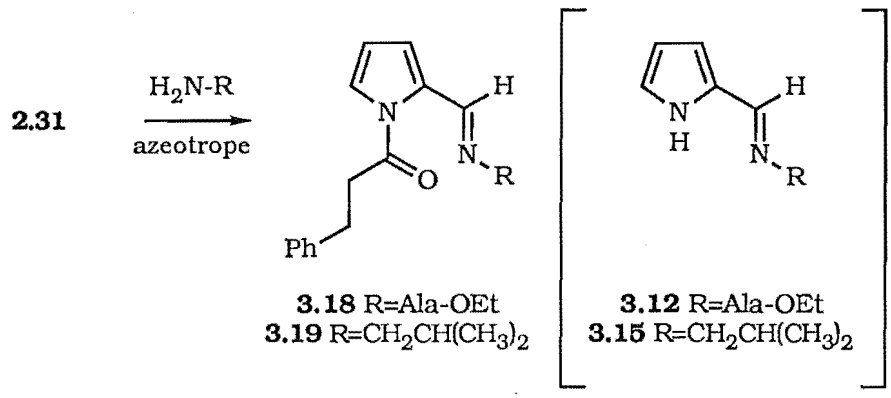

3.18 R=Ala-OEt
3.19 R=$CH_2CH(CH_3)_2$

3.12 R=Ala-OEt
3.15 R=$CH_2CH(CH_3)_2$

Scheme 3.9

The *N*-cinnamoyl-p-2-c **2.31**, dissolved in pentane containing one equivalent each of HCl.H_2N-Ala-OEt and TEA, was heated under reflux with a modified Dean-Stark apparatus. After twenty-four hours a ^{1}H NMR spectrum of an aliquot of the crude reaction showed that the imine **3.18** had not formed and that only starting materials were present. Further reflux for two days showed that the non-acylated p-2-imine **3.12** had produced 50% yield. The remainder of the ^{1}H NMR spectrum was consistent with p-2-c.

The addition of one equivalent of titanium isopropoxide has been reported[7] to increase the rate of imine formation, see Section 3.2.2. An increase in the rate of formation of the non-acylated imine **3.12** production to 60% over one hour was observed when this procedure was applied to the present study. There was no evidence of the desired *N*-acylated imine **3.18** in this reaction. The final yield of non-acylated imine **3.12** was 65%, by ^{1}H NMR spectroscopy. The remaining material was p-2-c.

Isobutylamine was used in an attempt to form the *N*-acylated imine from the *N*-acylated formyl pyrrole **2.31**. High yields and a rapid rate were

observed without the addition of titanium isopropoxide. The non-acylated imine **3.15** formed in 100% yield within one hour. No evidence for the desired *N*-acylated p-2-imine **3.19** was obtained.

An essentially quantitative conversion of **2.31** to the corresponding non-acylated imines **3.12** and **3.15**, by reaction with H_2N-Ala-CO_2Et and isobutylamine, respectively, Reaction 1, Scheme 3.10, was observed. As previously described, Section 3.2.1.1, there was found to be a great deal of polymer and p-2-c formed in the reaction where the imine formation reaction was attempted using a non-acylated pyrrole, eg: p-2-c, Reaction 2, Scheme 3.10.

Reaction 1:

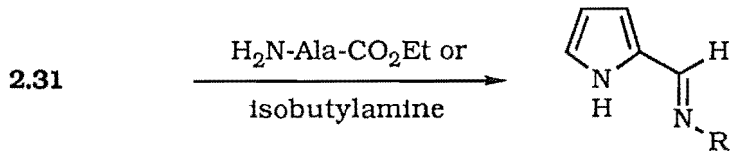

Reaction 2:

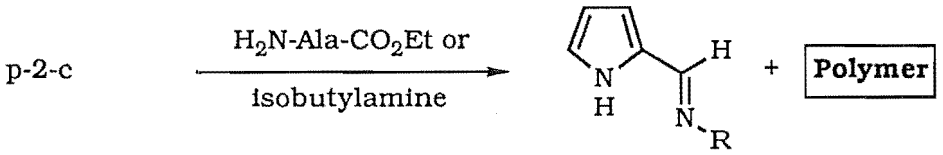

3.12 R=Ala-OEt
3.15 R=$CH_2CH(CH_3)_2$

Scheme 3.10

The yield of non-*N*-acylated pyrrolic imines **3.12** and **3.15** was found to increase, and the amount of polymer decrease, on using an *N*-acylated pyrrole derivative for the imine formation. This again provides evidence for the more aldehyde like nature of the pyrrole formyl group on *N*-acylation of the pyrrole, Section 2.1.2. Miller and Battersby[6] found in the synthesis of precursors to porphyrins, that the pyrrolylmethyl peptide analogues **3.23** were formed via similar imine compounds, **3.21**, Scheme 3.11. Their reactions proceeded to give low yields with much decomposition product, the same result observed in this study, Section 3.2.1.1.

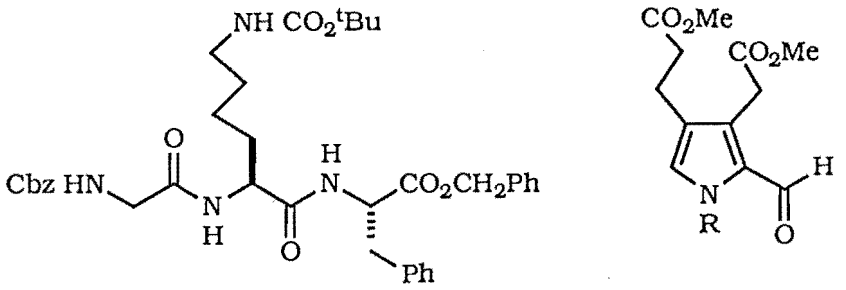

3.20

3.21 R=H
3.22 R=$COCH_3$

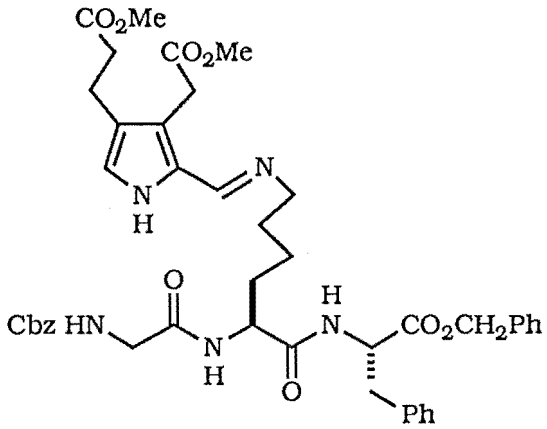

3.23

Scheme 3.11

On the basis of the results of the imine work presented in this thesis, it is suggested that the synthesis of imines of p-2-c (and derivatives) is best carried out using an acylated derivative of p-2-c, eg: **3.22**, Scheme 3.11. The *N*-acyl group would be expected to hydrolyse during the reaction to give the desired imine **3.23** in high yield.

3.2.3 *In Situ* Reduction of the Pyrrolic Imine to Pyrrolic Amine

Ultimately imines of the type **3.24** were to be reduced to the amine, eg: **3.25**, Scheme 3.12, to incorporate a residue at the P_2' subsite (see Section 1.2.4). Pyr occupies the P_1' subsite, while providing a leaving group for azafulvene formation.

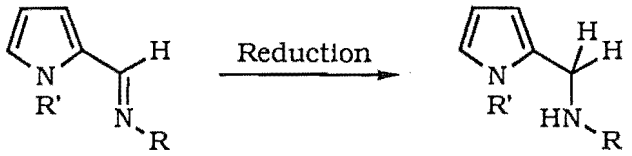

3.24 **3.25**

Scheme 3.12

Sodium cyanoborohydride has been reported to reduce carbonyls directly to an amine via an *in situ* generation of the imine[8]. Mattson[7] found that titanium(IV) isopropoxide enhances the rate and yield of the *in situ* reduction with unreactive aldehydes. The titanium reagent is thought to function by forming a stable tetrahedral complex **3.26**, Scheme 3.13. Reduction of the titanium complex then produces the amine **3.25**.

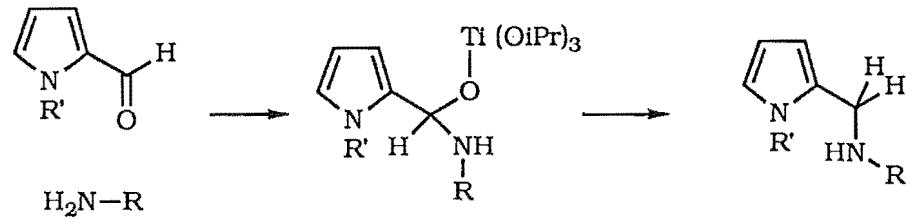

3.26 **3.25**

Scheme 3.13

Titanium isopropoxide was also used in Section 3.2.1.4 successfully to increase the yield of the pyrrole imine **3.12**.

N-acetyl-p-2-c **2.24** followed by one equivalent of H_2N-Ala-OEt were added to 1.25 equivalents of titanium isopropoxide and the resulting viscous solution was stirred under nitrogen for one hour. Absolute ethanol was added, followed by sodium cyanoborohydride. A ^1H NMR spectrum of the crude reaction mixture showed that the non-acylated amine **3.27** accounted for 80% of the pyrrolic content, Scheme 3.14, while the remaining 20% was starting material, *N*-acetyl-p-2-c **2.24**.

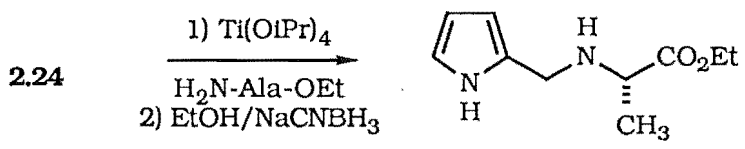

3.27

Scheme 3.14

The corresponding reaction of p-2-c and H_2N-Ala-OEt in the presence of titanium isopropoxide was not attempted, as the results from Section 3.2.1.3, indicated polymer formation would occur.

Numerous attempts to isolate the amine **3.27** failed, with the recovery of polymer and a low yield of p-2-c. This decomposition was rationalised as occurring via azafulvene formation, see Section 2.2.2.1 and Section 4.3.2.1 for a similar polymer formation. The reductive amination reaction was attempted on the *N*-cinnamoyl-p-2-c **2.31** using HCl.H_2N-Ala-OEt amino acid and one equivalent of TEA. The products from this reaction were again: p-2-c and some polymeric species.

The *N*-acylation of the pyrrole starting material was expected to decrease spontaneous azafulvene formation. The DMAP promoted *N*-acylation of the pyrrole-2-amine **3.27**, from the dry crude reaction mixture did not proceed, as was found in work reported in Section 3.2.1.3.

3.2.4 Amide Extension in the C-Direction

Extension to a true peptide like compound, structure **3.2**, Figure 3.1, would be possible if the carboxyl group was retained for peptide extension as in **3.3**, Scheme 3.15. This compound would have the recognition aspects of the designed mechanism based inhibitor and a suitable leaving group for azafulvene formation. Scheme 3.15 depicts the series of reactions that are required to form the desired mechanism based inhibitor **3.33**. The leaving group would be introduced either via pathways *a* or *b*, Scheme 3.15.

3.2.4.1 *Preliminary Studies*

A literature report indicated that coupling pyrrole-2-carboxylic acid (p-2-COOH **3.29**) couples with amino acid hydrochloride's in the presence of DCC and TEA to give the amide linkages[9], Scheme 3.16. Stirring p-2-COOH with an equivalent each of HCl.H_2N-Gly-OEt, DCC and TEA for twelve hours in CH_2Cl_2, gave the amide **3.28** in 75% isolated yield, Scheme 3.16.

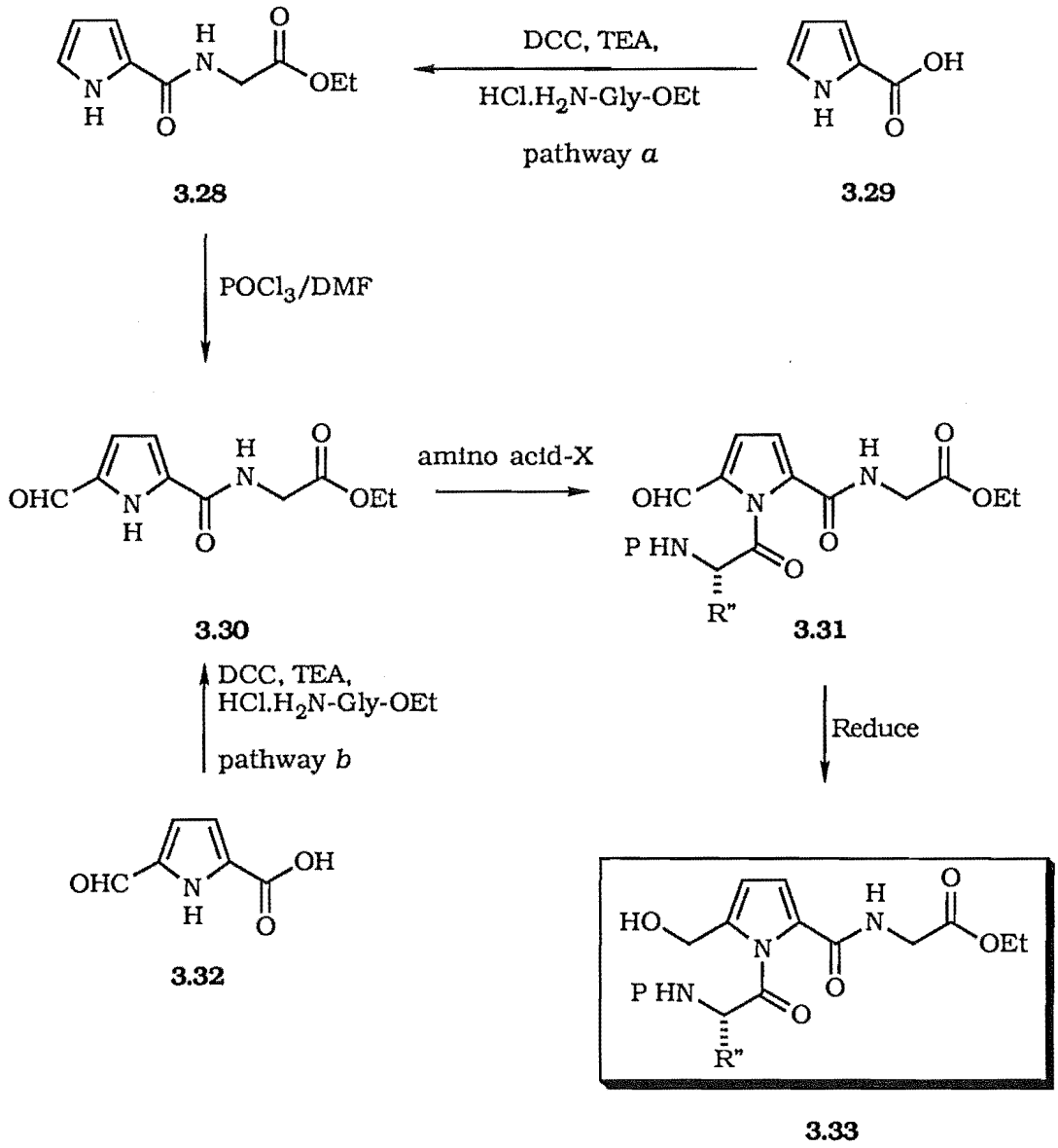

Scheme 3.15

The amide **3.34**, Scheme 3.16 prepared from isobutylamine was also formed under the same conditions. The ^1H NMR spectral yield of this pyrrole amide was 22%, the remaining material was p-2-COOH. Polymer was also evident. Since there was no improvement in the yield over the amino acid based amide **3.28**, no isolation attempts were made in this series.

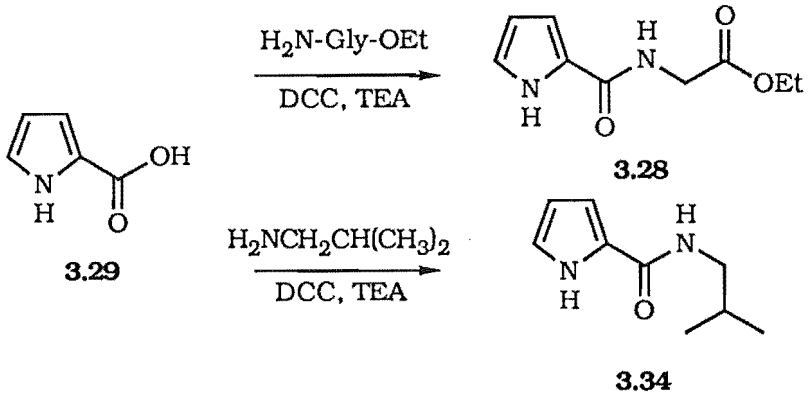

Scheme 3.16

Attempts to *N*-acylate the amide **3.28** with acetyl chloride using either the DMAP methodology, Section 2.4, or the NaH reaction, Section 2.2, were unsuccessful and yielded only polymer and p-2-COOH.

The amide **3.28** lacks a leaving group to allow azafulvene formation as required for the designed mechanism based inhibitor. Formylation[10] at the pyrrole 5-position with ensuing reduction, could provide this leaving group, Scheme 3.17.

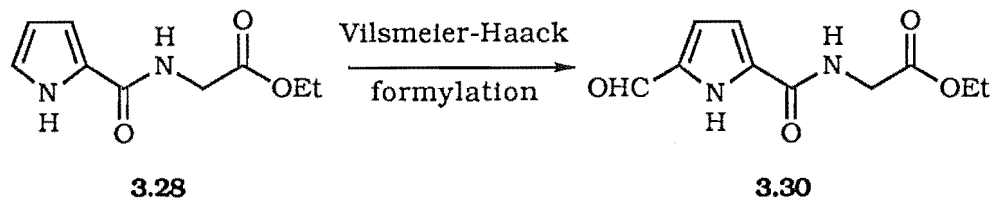

Scheme 3.17

Preliminary Vilsmeier-Haack formylation of the amide **3.28** produced what appeared to be the formyl pyrrole **3.30** in approximately 10%. No acylation was attempted of this amide species. Clearly, the ideas outlined in Scheme 3.15 warrant further investigation.

3.2.5 Extension of the Pyrrole *C*-Direction in the Peptide Anti-Sense

Structure **3.5**, Figure 3.1, describes what has been termed an "anti-sense" peptide where the the final inhibitor would possess two *N* termini. These compounds still provide the possibility of enzyme recognition through hydrogen bonding. "Anti-sense" compounds have been developed by Erikson and Kempf to produce viable and potent inhibitors of the HIV protease, Figure

3.18[11].

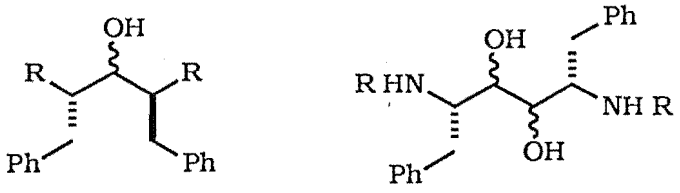

3.34
"pseudo symmetrical"

3.35
"symmetrical"

Figure 3.18

The Kempf inhibitors were designed to utilise the known C_2 symmetry of the HIV protease. The positioning of the C_2 axis was based on modelling studies and the fact that the two catalytic aspartic acids of the protease are close to the C_2 axis of the enzyme. It has also been observed in other aspartic acid protease inhibitors (renin inhibitors[12]) that the P region is more important for recognition than the P' region. The final inhibitors provide two distinct, chemically stable, pseudo-symmetric (**3.34**, Figure 3.18) or symmetric (**3.35**, Figure 3.18) units.

Although chymotrypsin lacks the C_2 symmetry of the HIV protease, it was still considered that the "anti-sense" extension would provide possible sites for hydrogen bonding to the enzyme.

Using the knowledge that inhibitors of HIV protease have been developed with the peptides in the "anti-sense" fashion, the esterification of hydroxymethyl pyrroles, eg: **2.32** was attempted. Standard esterification reactions of alcohols via an activated acylating agent and pyridine[13] or DMAP as promoters are well known. A trial acylation of *N*-cinnamoyl-p-2-OH **2.32** using acetyl chloride was attempted. Dissolution of **2.32** in CH_2Cl_2 containing one equivalent each of DMAP and TEA was followed by the addition of acetyl chloride. The desired *O*-acetylated *N*-acylated pyrrole derivative, *N*-cinnamoyl-p-2-OAc **3.36**, Scheme 3.19, was isolated in 87% yield.

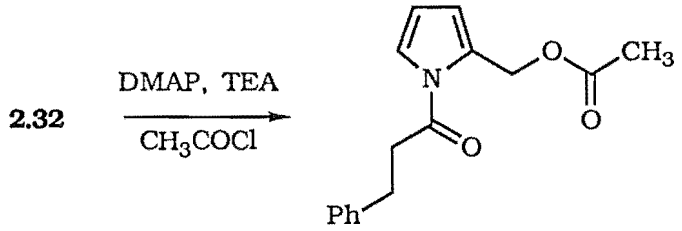

3.36

Scheme 3.19

The reaction was again tried, using *N*-Fmoc-Phe-Cl as the acylating agent, as ultimately an amino acid is required for extension of the recognition sequence. Chromatography resulted in a 20% yield of **3.37**. A good deal of other amino acid remnants were observed in the ^{1}H NMR spectrum and some pyrrolic polymer filtered off during work up.

An alternative procedure using the Mitsunobu conditions was attempted as outlined in Scheme 3.20.

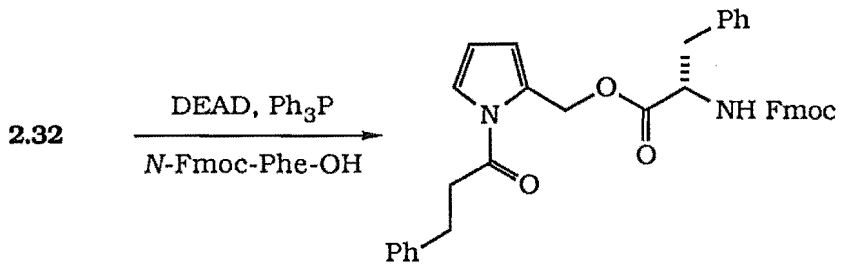

3.37

Scheme 3.20

N-Cinnamoyl-p-2-OH **2.32** was treated under Mitsunobu conditions and after three hours the ^{1}H NMR spectrum showed clean conversion to the desired ester. Chromatography of the crude product gave the dipeptide **3.37** in 73% isolated yield. This method of esterification was used in all the subsequent esterification reactions.

The C_2 symmetry based inhibitors of Kempf and Erickson[11,14] showed that although one amino acid extension from the scissile bond to the P_1' subsite produced satisfactory inhibition, two amino acids in the P_1' and P_2' subsites terminating with the Cbz group produced more potent inhibitors. The IC_{50} values for compounds where amino acids were added in the "sense" direction for P interactions and "anti-sense" for the P' interactions of **3.34** are presented in Table 3.2.

IC_{50} Values of HIV Protease for Various Substituents on 3.34

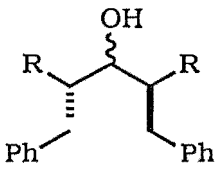

Substituent (R)	**IC_{50}, nM**
Ac-	>10000
Ac-Val-	12
Ac-Val-Val-	10
N-Cbz-Val-	3.0
N-Cbz-Ile-	4.9
N-Cbz-Leu-	>100

Table 3.2

A trial Mitsunobu esterification with the dipeptide *N*-Cbz-Phe-Ala-OH gave the tripeptide *N*-cinnamoyl-p-2-O-Phe-Ala-Cbz **3.38**, in 69% isolated yield.

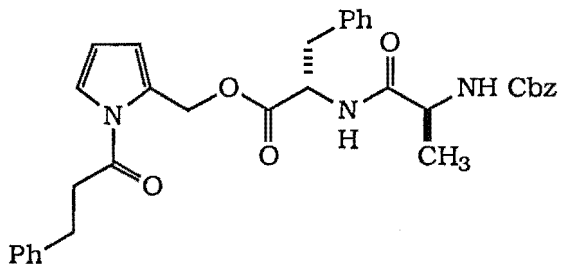

3.38

Erickson and Kempf found that the most potent HIV protease inhibitors were obtained when the amino acid Val occupied the P_1' and P_2' subsites. Chymotrypsin inhibition is also known to be dependent on residues other than the primary P_1 (Phe) residue, Section 1.2.2, and Section 3.1. Hence the Mitsunobu reaction using *N*-(*N*-Pth-Phe)-p-2-OH **2.52** and the amino acid *N*-Cbz-Val-Val-OH produced the tetrapeptide *N*-(*N*-Pth-Phe)-p-2-O-Val-Val-Cbz (20%) **3.39**.

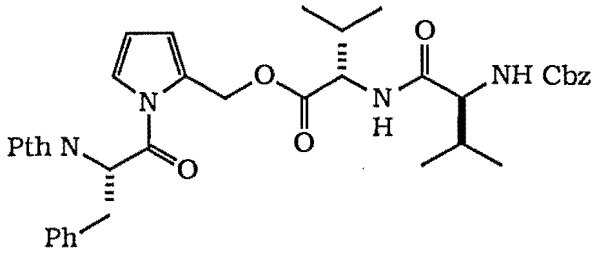

3.39

This compound was the most advanced potential inhibitor developed in this work, and as such was tested for enzyme activity against chymotrypsin and HIV protease, Section 5.1 and Section 5.2.

3.3 Increase of Enzyme Recognition: Extension in the *N*-Direction of Pyrrole Derivatives

The successful *N*-acylation of p-2-c with *N*-Pth-Phe-Cl **2.36**, Section 2.4.2.1, suggested that other amino acids protected by Pth would also *N*-acylate p-2-c. The *N*-acylation of p-2-c by these amino acids would provide evidence for the generality of the DMAP methodology.

3.3.1 *N*-Direction Amino Acid Modification

DMAP was used to promote the *N*-acylation of p-2-c with amino acid acid chlorides derived from *N*-Pth-Gly-OH **3.40** and *N*-Pth-Leu-OH **3.41**. The product *N*-acylated formyl pyrrole derivatives **3.42** and **3.44**, Scheme 3.21, that were produced, both had the characteristic triplet for H-4 at 6.38ppm (J=3.5Hz) and 6.31ppm (J=3.5Hz), respectively and the downfield shifted -C*H*O signal, 10.16ppm and 10.14ppm, respectively.

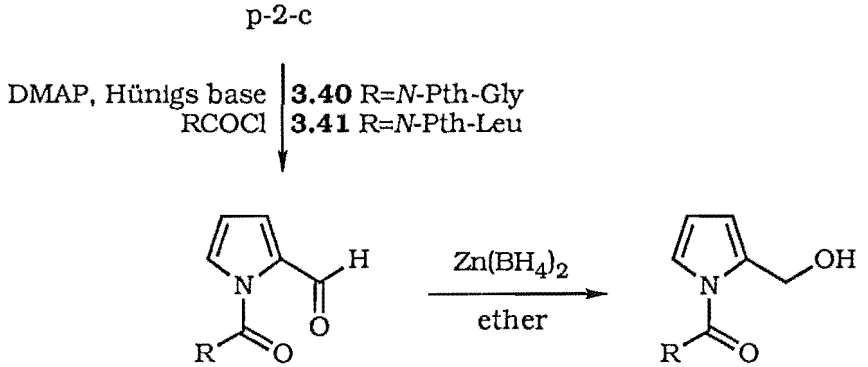

3.42 R=*N*-Pth-Gly
3.44 R=*N*-Pth-Leu

3.43 R=*N*-Pth-Gly
3.45 R=*N*-Pth-Leu

Scheme 3.21

Zinc borohydride reduction of the formyl derivatives **3.42** and **3.44** proceeded to give the corresponding hydroxymethyl pyrroles **3.43** (22%) and **3.45** (87%), respectively. The ^{1}H NMR spectra, again showed the characteristic pyr-CH_2OH signal at 4.63ppm for both compounds. The Gly derived pyrrole **3.43**, was found to be unstable and decomposed to polymer and p-2-c in twenty four hours.

The success in placing the *N*-Pth protected amino acids on the pyrrole nitrogen using the DMAP methodology suggested that a similar reaction might work with a *N*-Pth protected dipeptide. The addition of an

THE LIBRARY
UNIVERSITY OF CANTERBURY
CHRISTCHURCH, N.Z.

extra amino acid in the pyrrole *N*-direction would be advantageous to enzyme recognition, Section 1.2.

N-Pth-Gly-Phe-Cl, prepared from *N*-Pth-Gly-Phe-OH using oxalyl chloride/DMF, was added to a solution of DMAP, p-2-c and Hünigs base in CH_2Cl_2. A black precipitate formed. ^1H NMR spectroscopy gave strong evidence of the desired *N*-acylated pyrrole **3.46**, Figure 3.22, with a signal at 10.17ppm consistent with *N*-acylated formyl pyrrole. The triplet at 6.34ppm (J=3.1Hz) also gave credence to *N*-acylation.

This compound decomposed rapidly and was not fully characterised. Reduction of the freshly prepared crude aldehyde **3.46**, with zinc borohydride also presented problems. Strong evidence was again observed in the crude ^1H NMR spectrum for the desired hydroxymethyl pyrrole **3.47**, Figure 3.22. A characteristic singlet at 4.56ppm was consistent with pyr-CH_2OH. A triplet at 6.25ppm due to H-4 (J=3.0Hz) was also consistent with the other *N*-acylated hydroxymethyl pyrroles discussed previously, Section 2.7.2. This species was the only hydroxymethyl pyrrole to decompose on chromatography, p-2-c being the only pyrrole compound recovered (21%). *N*-Cbz-Ala-Phe-Cl was also used in an analogous reaction. This reaction produced no evidence of the desired *N*-acylated pyrrole **3.48**.

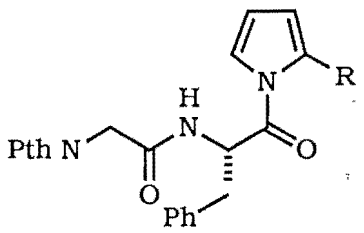

3.46 R=CHO
3.47 R=CH_2OH

Figure 3.22

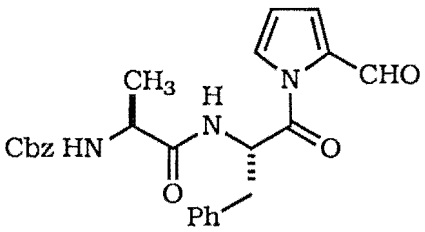

3.48

3.3.2 *N*-Direction Non-Amino Acid Modification

Many non-amino acid inhibitors of the HIV protease and chymotrypsin have been reported, Section 1.2.2 and 1.2.4. The carboxylates are thought to span, and block the active site of HIV protease[15], Section 1.2.4. The charged residues at the end of the active site are postulated to interact with the carboxylates thus holding the inhibitors in place. The DMAP methodology was thought capable of promoting the acylation of activated acyl species, with the long chain acid chlorides on pyrrole nitrogen.

The acid chlorides of lauric acid **3.49** and adipic acid monomethyl ester **3.50** were prepared from the corresponding acids. The DMAP reaction under normal conditions, ie: those in which the acid chloride was added to the p-2-c, Hünigs base and DMAP solution produced the *N*-lauralyl-p-2-c **3.52** and *N*-adipic monomethyl ester-p-2-c **3.54** in 90% and 89%, respectively,

Scheme 3.23.

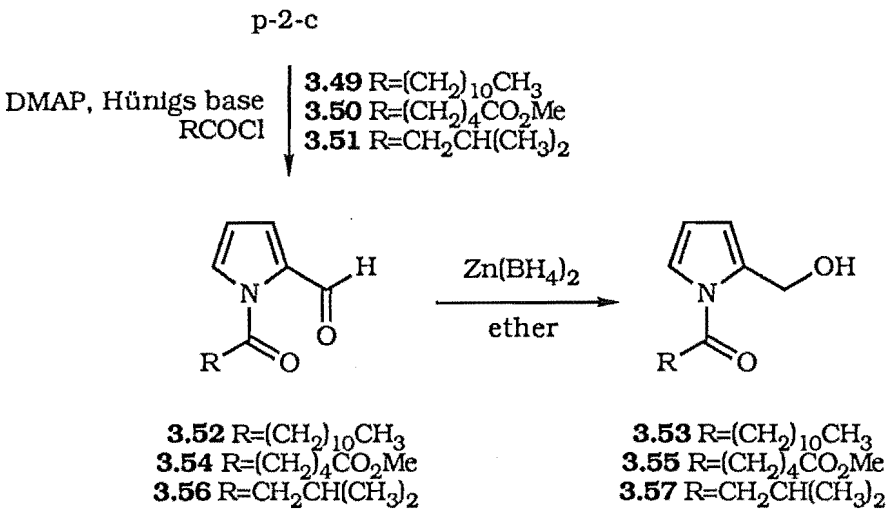

Scheme 3.23

The reduction of **3.52** and **3.54** with zinc borohydride produced after chromatography the desired hydroxymethyl pyrroles **3.53** (58%) and **3.55** (45%) respectively, Scheme 3.23. These derivatives were tested for activity against the HIV protease and chymotrypsin, Section 5.2 and Section 5.1.

The formyl pyrrole **3.56** was prepared from the DMAP mediated reaction of p-2-c with isovaleryl chloride **3.51** and Hünigs base. The desired formyl pyrrole **3.56** was isolated in 88% yield. Zinc borohydride reduction gave the hydroxymethyl pyrrole **3.57** in 90% after chromatography.

These long chain examples and the amino acid derivatives clearly demonstrate that the DMAP methodology is a versatile procedure for the *N*-acylation of pyrrole derivatives.

3.4 Conclusion

Extension of the amino acid chains in the *N*- and *C*-direction is known to be important in the recognition of an inhibitor by a protease. The work presented in this chapter was designed to incorporate these recognition features.

Unfortunately, the *C*-direction extension in a "peptide like sense" was not practical. The imine, eg: **3.12**, formation from p-2-c proved difficult, as was the acylation of this imine. The alternative imine formation, eg: **3.18**, from an *N*-acylated-p-2-c produced in high yields, the non-acylated pyrrole imines, eg: **3.12** and **3.15**. This may be useful in solving some of the problems that are often experienced in pyrrole chemistry.

The amine **3.27** was formed from the imine **3.12**, but was unstable in solution and could not be purified nor acylated.

N-Acylation of the amide **3.28** suffered a similar fate. Encouraging results were obtained from formylation of the amino acid amide **3.28**. The formylation at the 5-position of pyrrole-2-amide, eg: **3.30**, can be expected to increase the ability for acylation to occur on nitrogen. The formylation would also provide a position for the leaving group necessary for azafulvene formation. This work should be investigated further.

Extension of the pyrrole in the *C*-direction in the "anti-peptide sense" produced a series of peptides up to four amino acids, eg: **3.39**, that would occupy the P_1-P_3' subsites. The hydroxymethyl pyrrole compounds were esterified via the Mitsunobu reaction conditions in high yields. The new pseudo peptides were tested against the HIV protease, Section 5.2 and α-chymotrypsin, Section 5.1.

Extensions of the pyrrole in the *N*-direction by modification of the pyrrole *N*-acyl group to a non-amino acid species was based on known HIV protease inhibitors. The two long chain hydroxymethyl pyrrole compounds **3.53** and **3.55** produced in this portion of work were found to be active against α-chymotrypsin, this is discussed in Section 5.1.

3.5 References to Chapter Three

[1] Fersht, A. *Enzyme Structure and Mechanism*, Second Ed.; W. H. Freeman: New York, 1985.

[2] Laskowski, M.; Tashiro, M.; Empie, M. W.; Park, S. J.; Kato, I.; Ardelt, W.; Wieczork, M.; in *Proteinase Inhibitors: Medical and Biological Aspects*; Springer-Verlag: Tokyo, 1983.

[3] Brunner, H.; Reiter, B.; Riepl, G. *Chem. Ber.* **1984**, *117*, 1330-1354.

[4] McIntire, F. C. *J. Am. Chem. Soc.* **1947**, *69*, 1377-1380.

[5] March, J. *Advanced Organic Chemistry*, Third Ed.; John Wiley & Sons: New York, 1985; p797.

[6] Miller, A. D.; Leeper, F. J.; Battersby, A. R. *J. Chem. Soc. Perkin Trans. 1* **1989**, 1943-1956.

[7] Mattson, R. J.; Pham, K. M.; Leuck, D. J.; Cowen, K. A. *J. Org. Chem.* **1990**, *55*, 2552-2554.

[8] Borch, R. F.; Bernstein, M. D.; Durst, H. D. *J. Am. Chem. Soc.* **1971**, *93*, 2897-2904.

[9] Kasum, B.; Prager, R. H.; Tsopelas, C. *Aust. J. Chem.* **1990**, *43*, 355-365.

[10] Martínez, A. G.; Alvarez, R. M.; Barcina, J. O.; de la Cerero, S.; Vilar, E. T.; Fraile, A. G.; Hanack, M.; Subramanian, L. R. *J. Chem. Soc., Chem. Commun.* **1990**, 1571-1572.

[11] Kempf, D. J.; Norbeck, D. W.; Codacovi, L-M.; Wang, X. C.; Kohlbrenner, W. E.; Wideburg, N. E.; Paul, D. A.; Knigge, M. F.; Vasavanonda, S.; Craig-Kennard, A.; Saldivar, A.; Rosenbrook Jr, W.; Clement, J. J.; Plattner, J. J.; Erickson, J. *J. Med. Chem.* **1990**, *33*, 2687-2689.

[12] Greenlee, W. J. *Med. Res. Rev.* **1990**, *10*, 173-236.

[13] Fieser, L. F.; Fieser, M. *Reagents for Organic Synthesis*, Vol 1.; John Wiley and Sons: New York, 1967; p958.

[14] Erickson, J.; Neidhart, D. J.; VanDrie, J.; Kempf, D. J.; Wang, X. C.; Norbeck, D. W.; Plattner, J. J.; Rittenhouse, J. W.; Turon, M.; Wideburg, N.; Kohlbrenner, W. E.; Simmer, R.; Helfrich, R.; Paul, D. A.; Knigge, M. *Science* **1990**, *249*, 527-533.

[15] Brinkworth, R. I.; Woon, T. C.; Fairlie, D. P. *Biochem. Biophys. Res. Commun.* **1991**, *176*, 241-246.

Chapter Four

Protease Inhibitor Properties

4.1 Hydrolysis Study

A model hydrolysis system was designed to mimic enzyme action and to help understand the mechanism of the deacylation of *N*-acylated pyrroles[1], a key step in the proposed mechanism of inactivation.

Potassium hydroxide was used to mimic the active site catalytic residues of the protease, Ser195 of chymotrypsin and Asp25 and Asp225 of the HIV-1 protease. Reactions described in later sections of this work, Section 4.3.4, have an added external nucleophile, n-butylamine. This was designed to mimic the nucleophilic residues, His57 of chymotrypsin and Thr26 or the bound water of the HIV protease, causing covalent inactivation, found in the enzyme. These nucleophilic residues are considered the likely candidates to attack the azafulvene **1.3** produced on cleavage of the amino acid-pyrrole amide bond, Figure 4.1.

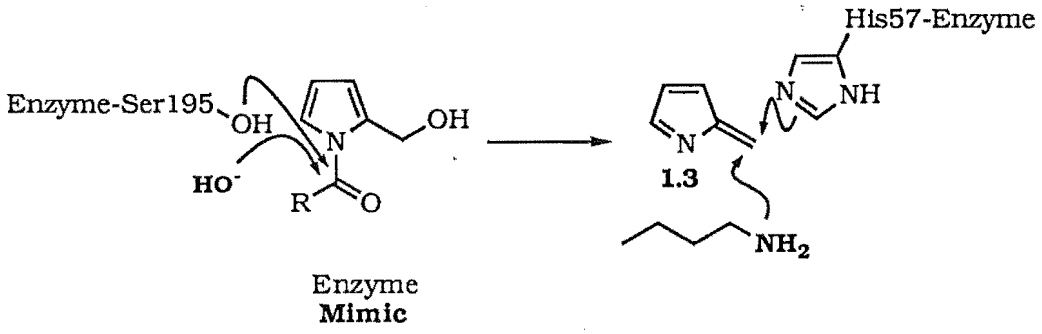

Figure 4.1

The general reaction scheme for the hydrolysis study was as follows: The *N*-acyl pyrrole under study was dissolved in d_4-methanol (0.6mL) or d_3-acetonitrile (0.6mL) in an NMR tube. To this was added an equivalent of the external nucleophile followed by the calculated amount of KOH. ^{1}H NMR spectra were recorded at appropriate times over twenty four hours or until no further significant reaction was observed. The reaction was monitored, and NMR spectral yields were obtained by integration of the pyr-C*H*$_2$X ^{1}H NMR resonances of all pyrrolic reaction species, relative to an internal standard, CH_2Cl_2. The structures of all compounds formed in these reactions were confirmed by comparison with authentic samples or by full characterisation.

N-Acylation of 2-substituted pyrroles suppresses azafulvene formation, see Section 2.1.2 and Section 4.7.1. This is extremely important for the proposed mechanism of the inhibitors since release of the azafulvene before delivery to the enzyme would decrease the effectiveness of the inhibitor. The aim of the hydrolysis study was to analyse the subsequent reactions and

products formed on amide hydrolysis. The stability of the *N*-acylated pyrroles under the conditions of the hydrolysis study, without hydroxide present, is therefore central to the effectiveness of the study. The *N*-acylated pyrroles were subjected to the hydrolysis study conditions, without hydroxide, to ensure that no reaction occurred. The findings from these studies are described below.

4.2 Hydrolysis of *N*-Acyl Pyrrole 2.32 in d4-Methanol

The stability of *N*-acylated pyrrole **2.32** under the hydrolysis conditions was determined. A sample of **2.32** was left in d_4-methanol in an NMR tube at 23°C. The pyr-CH_2OH, resonance of **2.32**, 4.62ppm, was monitored over twenty four hours. The ^{1}H NMR spectrum was unchanged after this period. The addition of a twenty five fold excess of KOH produced an immediate deacylation to give hydroxymethyl pyrrole **4.1**[2], pyr-CH_2OH 4.50ppm, in 100% NMR yield [^{1}H NMR (d_4-MeOH) δ 4.50 (2H, s, pyr-CH_2OH); 5.99 (1H, t, *J*=2.6Hz, H-4); 6.07 (1H, m, H-3); 6.67 (1H, m, H-5)]. Within fifty minutes the species **4.1** had equilibrated with the methoxymethyl pyrrole **4.2**, pyr-CH_2OMe 4.36ppm, Scheme 4.2. [^{1}H (d_4-MeOH) δ 3.59 (3H, s, OMe); 4.36 (2H, s, pyr-CH_2OMe); 6.00 (1H, t, *J*=3.1Hz, H-4); 6.04 (1H, m, H-3); 6.70 (1H, m, H-5)]. Compounds **4.1** and **4.2** were present in a ratio of 2:3 (**4.2**:**4.1**). This ratio remained unchanged over two days.

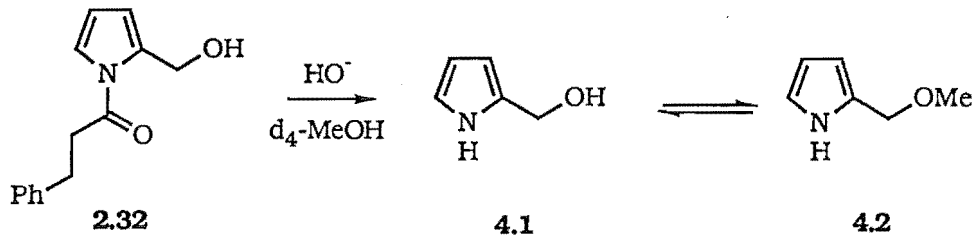

2.32 **4.1** **4.2**

Scheme 4.2

A second experiment was carried out in which the amount of HO^- was reduced to one equivalent (KOH in D_2O), represented in Figure 4.3.

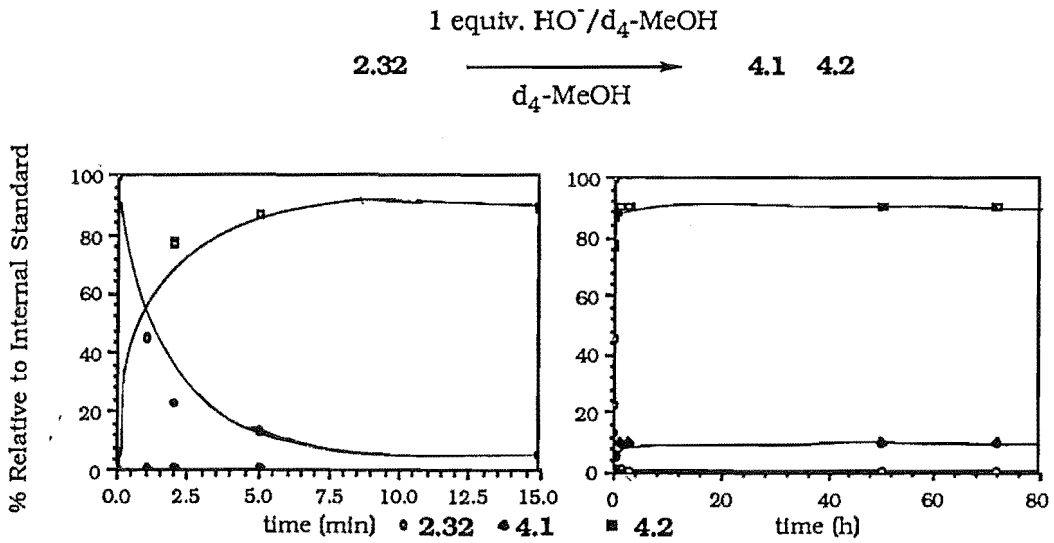

Figure 4.3

As expected the deacylation was slower with starting material **2.32** still present after fifteen minutes. The product ratio of **4.1** to **4.2** after sixty minutes was also lower at 9:1 (**4.2**:**4.1**). This ratio remained unchanged over two days.

Hydrocinnamate **4.3** was also evident in the ^{1}H NMR spectrum. Over two hours a three proton singlet at 3.67ppm appeared. This and other related signals compared directly to authentic methyl hydrocinnamate **4.4**, [^{1}H NMR (d_4-MeOH) δ 2.64 (2H, t, *J*=7.5Hz, CH_2-Ph); 2.96 (2H, t, *J*=7.6Hz, CO-CH_2); 3.67 (3H, s, OCH_3); 7.20-7.32 (5H, m, Ph)].

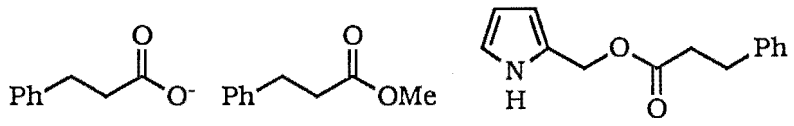

4.3 **4.4** **4.5**

The *O*-acyl pyrrole derivative **4.5**, discussed in Section 4.3.2, was not observed in any of the hydrolysis studies conducted in d_4-methanol.

The conclusion drawn from these experiments is that deacylation of **2.32** leads directly to **4.1**, Scheme 4.4, which subsequently decomposes to the azafulvene **1.3**, which is trapped by either HO^- or MeO^- to give **4.1** or the methoxymethyl pyrrole **4.2**, respectively, see Section 4.5.1 for a discussion.

The *N*-acyl pyrroles are stable in the absence of hydroxide.

The rate determining step in the hydrolysis of **2.32** is the formation of **1.3**, while the subsequent attack on **1.3** by a nucleophile is fast, Scheme 4.4.

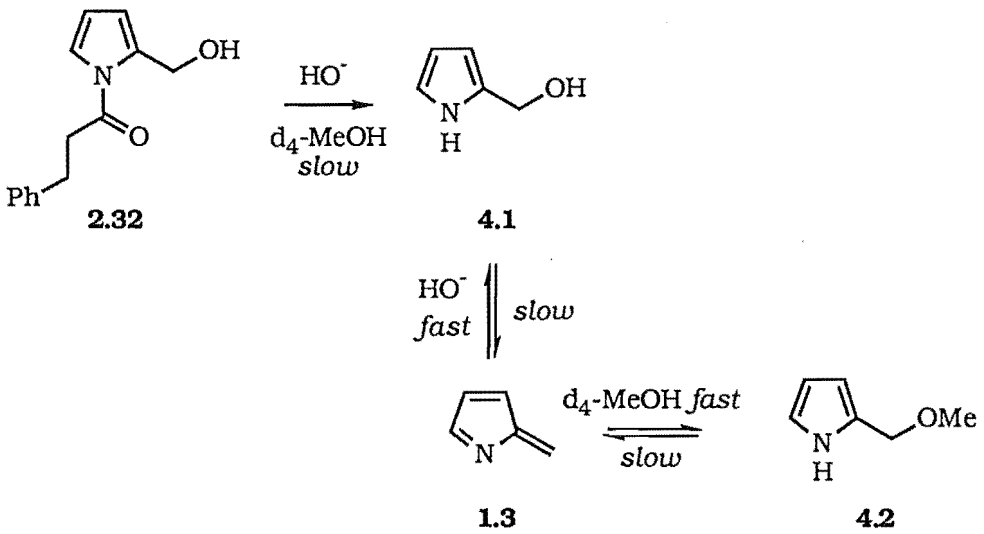

2.32 **4.1** **1.3** **4.2**

Scheme 4.4

Nucleophilic attack on pyrroles of this type are known to be S_N1 in

nature[3]. Kinetic analysis has indicated that hydroxymethyl pyrroles react by an S_N1 mechanism[3]. Thus although MeO^- is a better nucleophile than HO^-[14], the formation of **4.2** and **4.1** respectively are dependent only on the concentration of each of the nucleophilic species.

To confirm the S_N1 nature of the reaction, it was reasoned that if the concentration of methanol was decreased with respect to HO^- then the final equilibrium would favour the hydroxymethyl pyrrole **4.1**. This was achieved by "diluting" the d_4-methanol with the non-nucleophilic, di-polar, aprotic solvent, d_3-acetonitrile.

4.3 Hydrolysis of *N*-Acyl Pyrrole 2.32 in d3-Acetonitrile

The following work describes the hydrolysis study in d_3-acetonitrile (0.6mL). The HO^- added is dissolved in either d_4-methanol or D_2O, the total volume of either solvent does not exceed 30μL. Therefore the solvent, d_3-acetonitrile, is in vast excess in all cases.

4.3.1 HO^- dissolved in d_4-Methanol

The addition of one equivalent of the HO^- (KOH in d_4-MeOH) to the *N*-acylated pyrrole **2.32** in d_3-acetonitrile solvent resulted in deacylation to give **4.1** and **4.2** as predicted. The major product of the reaction was the methoxymethyl pyrrole **4.2**, which equilibrated over one hour with the hydroxymethyl pyrrole **4.1** to give a final ratio of 7:3 (**4.2**:**4.1**), Figure 4.5.

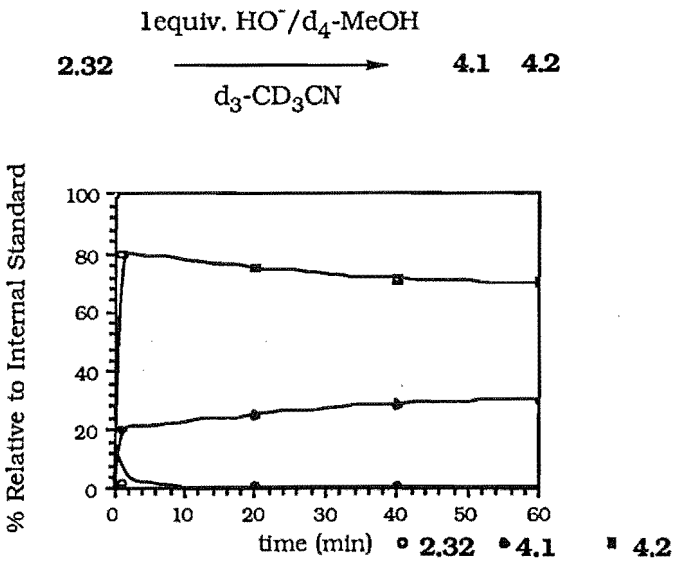

Figure 4.5

Figure 4.5 shows a rapid formation of **4.2** to a maximum of 80% at t=2 min. This decreased over one hour to give a final equilibrium concentration of 7:3 (**4.2**:**4.1**), which has **4.2** lower than the 9:1 (**4.2**:**4.1**) ratio observed in d_4-methanol experiment. Starting material **2.32** was totally consumed within twenty minutes.

This result is consistent with the proposal that nucleophilic attack on **1.3** occurs via an S_N1 like mechanism - a lower concentration of methanol results in a lower equilibrium concentration of **4.2**, while a higher concentration of HO^- leads to a higher equilibrium concentration of **4.1**. The final ratio of products was 7:3 (**4.2**:**4.1**) in the d_3-acetonitrile experiment.

A competition therefore exists between the HO^-/H_2O and $MeO^-/MeOH$ nucleophiles in these reactions.

4.3.2 HO^- dissolved in D_2O

The KOH was dissolved in D_2O rather than d_4-methanol to avoid the complication of an extra nucleophile. This enabled the direct observation of HO^- action on **2.32**.

No hydrolysis of **2.32** in d_3-acetonitrile and D_2O occurred on standing at 23°C for three days, thus satisfying the criterion described in Section 4.1, in that the hydrolysis of **2.32** would be solely due to HO^- mimicking the active site of an enzyme.

4.3.2.1 *One Equivalent HO^- in D_2O*

The addition of one equivalent of HO^- (KOH in D_2O) to **2.32** resulted in 80% deacylation of the starting material **2.32** after ten minutes.

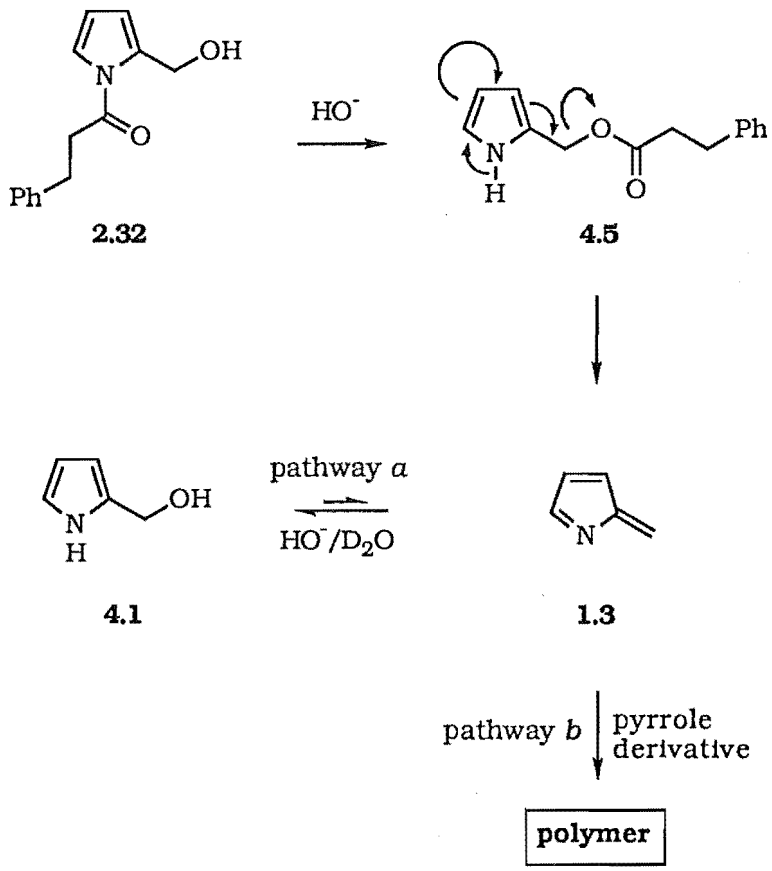

2.32 **4.5**

4.1 **1.3**

Scheme 4.6

The *O*-acyl pyrrole derivative **4.5**, pyr-CH_2OR, 5.07ppm appeared as **2.32** was consumed, Scheme 4.6. A full description of compound **4.5** is given

in Section 4.3.2.3. The species **4.5** appeared to form via an intramolecular acyl transfer reaction, see Section 4.5 for a full discussion.

Figure 4.7 presents the data for the hydrolysis of **2.32** and its subsequent reactions. Compound **4.5** reached a maximum of 80% with respect to the internal standard, CH_2Cl_2, in ten minutes. This slowly decreased over three hours while the pyr-CH_2OH (4.50ppm) resonance for hydroxymethyl pyrrole **4.1** increased at the same rate as the resonance of **4.5** decreased. During the initial five minutes of reaction there was **no** evidence of **4.1**, while **2.32** was completely deacylated. Thus the direct deacylation of **2.32** to **4.1**, as observed in the d_4-methanol, does not occur in d_3-acetonitrile.

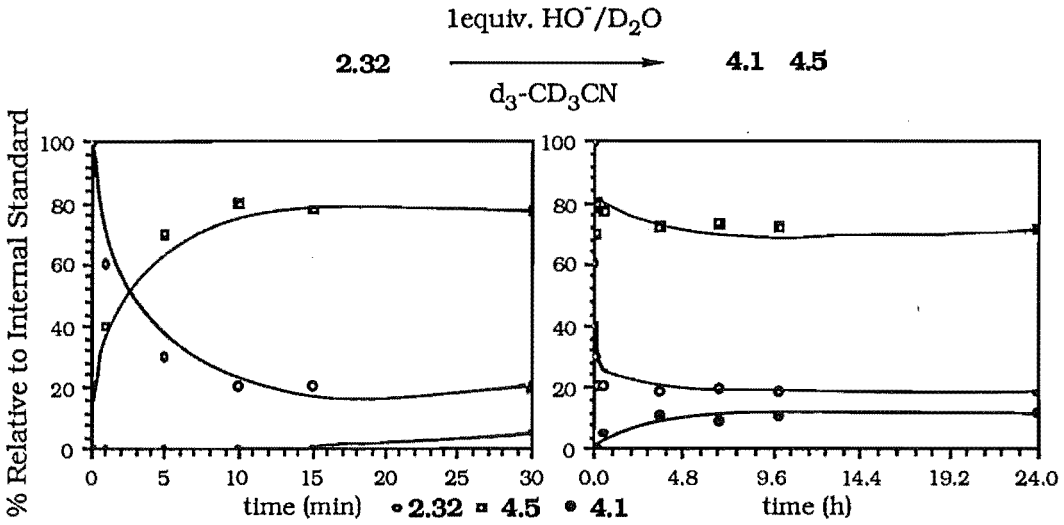

Figure 4.7

The formation of hydroxymethyl pyrrole **4.1**, from the *O*-acyl pyrrole derivative **4.5**, can therefore be attributed to attack of HO^-/D_2O on the azafulvene **1.3**, formed from **4.5**, pathway *a* Scheme 4.6. The relative percentages of reaction products after four days was 18% **2.32**, 71% **4.5** and 12% **4.1**.

During this and the other hydrolysis reactions, the d_3-acetonitrile solution was observed to became darker and the NMR tube stained. This observation can be attributed to polymer formation, pathway *b*, Scheme 4.6. Polymer formation is also discussed in Sections 2.4.2.1 and 3.2.1.1. However, in these cases polymer formation was acid catalysed. The polymer formed here is under basic conditions and therefore another mechanism must be operating, this is discussed in Section 4.3.3. The percentages and ratios of pyrroles given in this chapter ignores polymer formation.

4.3.2.2 *Two Equivalents HO^- in D_2O*

A reaction of **2.32** in d_3-acetonitrile with two equivalents of HO^- (KOH in D_2O) gave a more rapid deacylation and *N*- to *O*- acyl transfer to give the *O*-acyl pyrrole derivative **4.5**. Within one minute there was no evidence of starting material **2.32**, while **4.5** reached a maximum of 93%, Figure 4.8. The final substitution product **4.1** increased as an equilibrium between **4.1** and the *O*-acyl pyrrole derivative **4.5** was established, Scheme 4.6; the equilibrated finally was established at 2:3 (**4.5**:**4.1**) after twenty four hours.

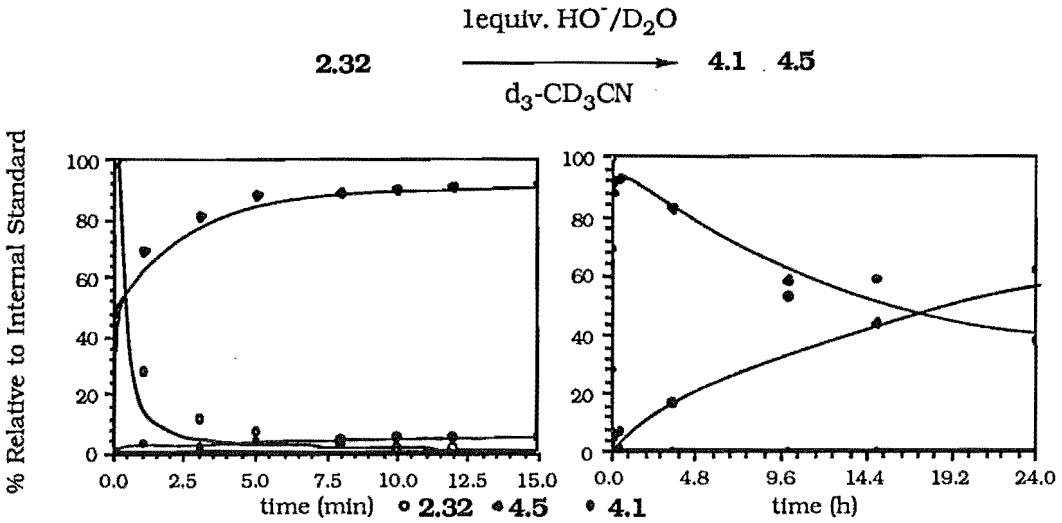

Figure 4.8

The excess HO^- precludes pyrrole polymer formation.

4.3.2.3 *Characterisation of the O-Acyl Pyrrole Derivative* **4.5**

Deacylation of **2.32** in d_3-acetonitrile with one equivalent of HO^- was carried out at -20°C. The starting material **2.32** was converted cleanly to the *O*-acyl pyrrole derivative **4.5** in approximately ten minutes, Figure 4.9.

The *O*-acyl pyrrole was stable at -20°C in the absence of an excess of HO^-, and thus a ^{13}C NMR spectrum was obtained.

The ^1H and ^{13}C NMR spectra were consistent with a 2-substituted pyrrole, without an *N*-acyl group. The ^1H NMR spectra showed H-3 (dd, *J*=2.5 & 1.5Hz), and H-4 (t, *J*=2.2Hz), upfield H-5 as a dd (*J*=2.3 & 1.5Hz) downfield. A similar result was obtained from the ^{13}C NMR spectra with C-3 (108.9ppm) and C-4 (106.9ppm) upfield and C-5 (118.2ppm) downfield. This pattern was similar to that observed for p-2-c, Section 2.7. The ^{13}C NMR spectrum showed a signal was consistent with other acylated pyrroles, described in Section 3.2.5, for the pyr-CH_2OR at 58.0ppm.

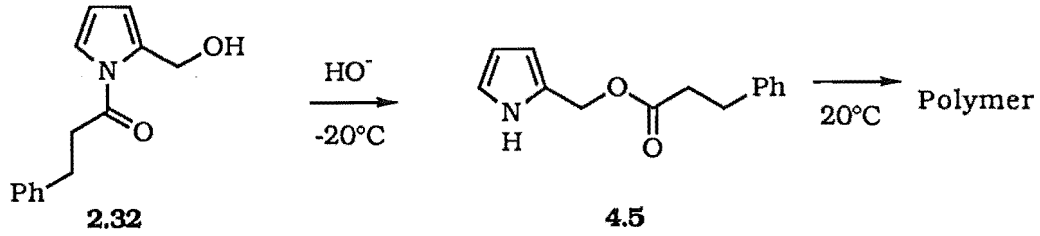

2.32 **4.5**

Figure 4.9

After obtaining the ^{13}C NMR spectrum at -20°C, the solution was allowed to warm to room temperature. Within five minutes the colour of the solution intensified and the NMR tube became stained, providing evidence that the *O*-acyl pyrrole derivative **4.5** was forming a polymer via the azafulvene **1.3**, see Section 4.3.2.1 and Schemes 4.6 and 4.9.

4.3.3 Pyrrolic Polymer Formed in Base

The production of polymers in pyrrole chemistry is common. As described in the *N*-acylation work (Section 2.2.2.1), many polymeric pyrrole species were formed in the initial stages of this research work. However, pyrrole polymers are commonly formed under acid catalysis rather than under basic conditions as described in the present hydrolysis study. The formation of pyrrole polymers under basic conditions is strongly suggestive of azafulvene formation. The subsequent attack on the azafulvene by further pyrroles forms the polymer observed in the hydrolysis reactions.

4.3.4 Addition of an External Nucleophile to the Deacylation of 2.32 in d_3-Acetonitrile

Further evidence for azafulvene formation was necessary as its formation was central to the proposed mechanism of protease inhibition. An alcohol will not normally react with a primary amine, Figure 4.10, under the conditions of the hydrolysis study.

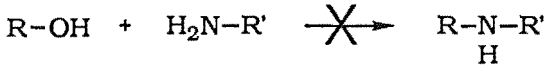

Figure 4.10

An added external nucleophile, such as n-butylamine, in a deacylation reaction of **2.32** would be expected to trap the electrophilic azafulvene **1.3**, as

it was produced from the *O*-acyl pyrrole derivative **4.5**, via pathway *a*, Scheme 4.11. Alternatively, **1.3** produced directly via the deacylation of **2.32**, pathway *b*, Scheme 4.11, would also be trapped.

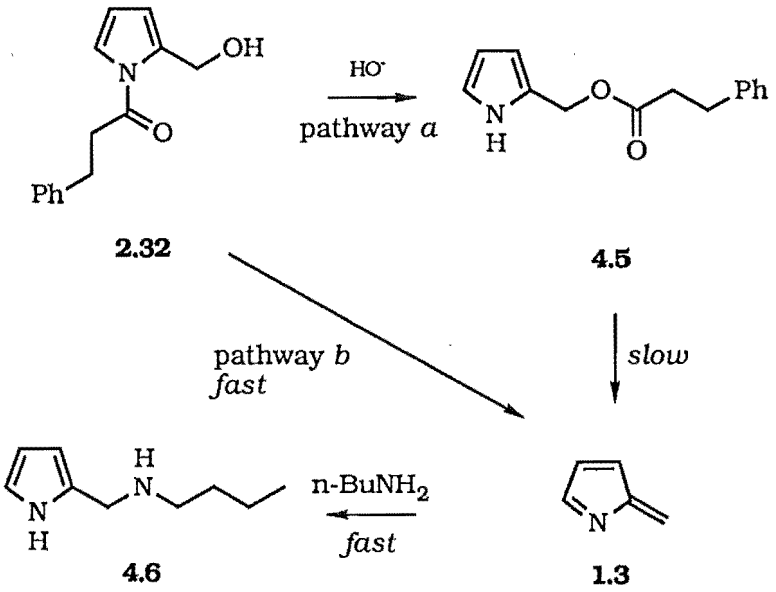

Scheme 4.11

The external nucleophile was designed to mimic an active site nucleophilic residue of the target protease, eg: His57 of chymotrypsin and Thr26 or the bound water of HIV protease, as described in Section 4.1. Trapping the azafulvene **1.3** by the amine would therefore mimic one of these nucleophilic residues, and demonstrate that the latent reactivity is released on the hydrolysis of a hydroxymethyl pyrrole in the form of the azafulvene **1.3**.

An equivalent of n-butylamine was added to the solution of **2.32** in d_3-acetonitrile. The addition of one equivalent of HO^- (KOH in D_2O) to the solution then caused a rapid, partial conversion of **2.32** to **4.5** as observed previously, Section 4.3.2. Over one hour the pyr-CH_2OR ^{1}H NMR resonance of **4.5** decreased and a corresponding signal of the pyrrole amine **4.6**, pyr-CH_2NHR 3.62ppm, increased. Figure 4.12 depicts a series of ^{1}H NMR spectra observed for this reaction.

^{1}H NMR Spectra of 2.32, 4.5 and 4.6 Over One Hour for the Hydrolysis of 2.32 with HO^-

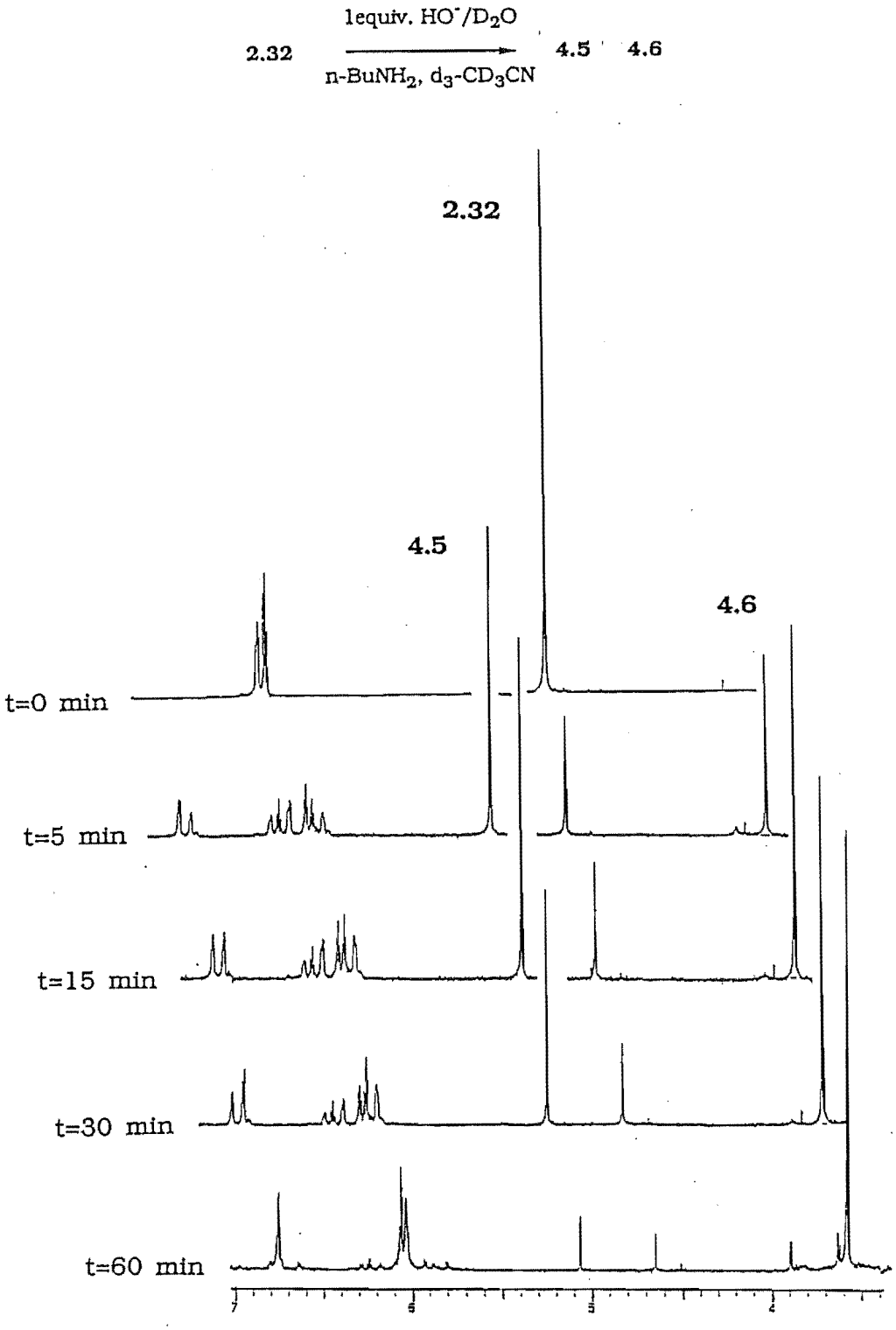

Figure 4.12

Approximately 10% of the amine **4.6** was observed after one minute. Since the *O*-acyl pyrrole derivative **4.5** reacts slowly to give **4.6**, it is suggested that HO^- causes a rapid deacylation of **2.32** to form the azafulvene **1.3**, which

yields **4.6** on attack by n-butylamine, pathway *b* Scheme 4.11. Two competing pathways for the formation of **4.6** therefore exist.

Furthermore, the rates at which the signals for **4.5** and **4.6** decrease and increase respectively, Figure 4.13, after two minutes, suggests that once the *O*-acyl pyrrole derivative **4.5** has formed, the amine **4.6** is only formed by the subsequent formation of **1.3** from **4.5**. The formation of the azafulvene **1.3** from **4.5** is slow relative to pathway *b*, Figure 4.11.

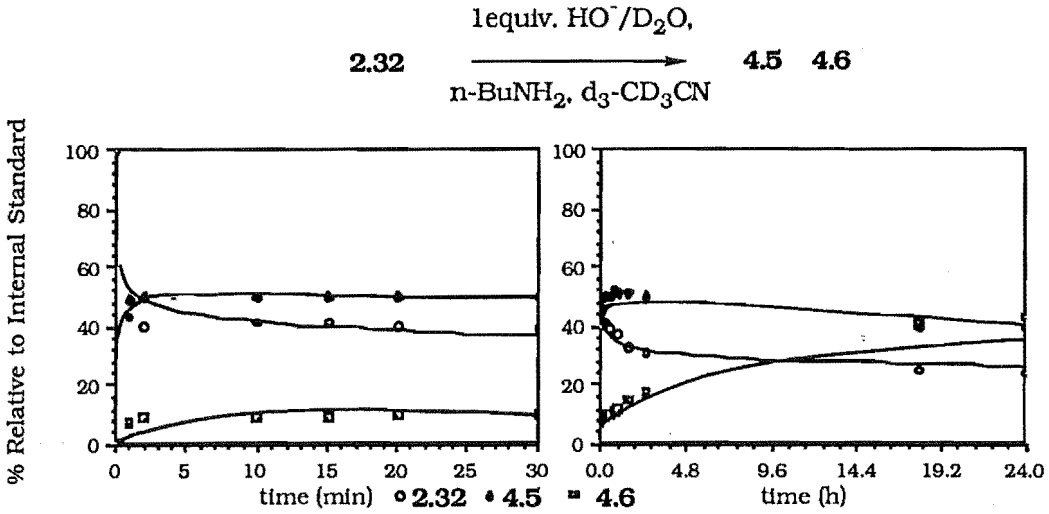

Figure 4.13

The kinetic analysis experiments, see Section 4.4, found, when two or more equivalents of HO^- were added to **2.32**, in this hydrolysis study, the pyrrole amine **4.6**, was the only pyrrole species existing after three hours.

The amine **4.6** was isolated, by the removal of solvents from the completed reaction, t=5 days. ^1H, ^{13}C NMR spectra and a high resolution mass measurement were consistent with the proposed structure **4.6**. The ^1H NMR resonances for the pyrrole protons were consistent with absence of an *N*-acyl group. H-3 (δ 6.03, m) and H-4 (δ 6.06, t, *J*=2.9Hz) were upfield while H-5 (δ 6.67, m) was downfield, relative to a *N*-acylated pyrrole, eg: **2.32**. This pattern is similar to p-2-c, discussed in Section 2.7. The increased multiplicity of H-3 and H-5 relative to a non-*N*-acylated pyrrole is due to coupling to the N*H*.

The reaction did not go to completion with one equivalent of HO^-. 10% of both the *N*-acylated pyrrole **2.32** and the *O*-acyl pyrrole derivative **4.5** remained after three days. A second equivalent of HO^- would, therefore appear necessary for the complete hydrolysis of **2.32**. Amide hydrolysis is typically described as a second order process with respect to HO^-, this is discussed in Section 4.5.

4.3.4.1 *Monitoring the Formation of* **4.6** *and* **4.3** *in the Deacylation of* **2.32**

The deacylation of **2.32** was also monitored via the appearance of hydrocinnamate **4.3** in the ^{1}H NMR spectra time course study. Species **4.3** is the non-pyrrole product formed from the deacylation of **2.32**. Integration of the pyrrole amine **4.6** signals [^{1}H NMR (d_3-CD_3CN) δ 0.87 (3H, t, *J*=7.3Hz); 1.26-1.42 (4H, m, $CH_2CH_2CH_2CH_3$); 2.90 (2H, dt, *J*=7.4Hz, $NHCH_2$); 3.62 (2H, s, pyr-CH_2NH); 6.03 (1H, m, H-3); 6.06 (1H, t, *J*=2.9Hz, H-4); 6.67 (1H, m, H-5)] with respect to those of the hydrocinnamate **4.3** [^{1}H NMR (d_3-CD_3CN) δ 2.44 (2H, t, *J*=8.4Hz, Ph-CH_2); 2.88 (2H, t, *J*=8.4Hz, CO-CH_2); 7.29-7.32 (5H, m, Ph)] indicated a ratio of 1:1. The observation was carried out at the completion of the reaction. A decrease in the ratio of **4.6** to **4.3** would suggest that polymer formation was occurring, rather than the formation of the desired pyrrole amine **4.6**. Under the hydrolysis conditions of this study a decrease in the ratio of the hydrocinnamate **4.3** relative to **4.6** would be unlikely, as there was no methanol present to allow formation of the methyl hydrocinnamate **4.6**, as was observed in the case presented in Section 4.2. The ^{1}H NMR spectral ratio of **4.6**:**4.3** remained at 1:1, giving strong evidence that no polymer was formed. The lack of colour in the NMR sample gave further support to the absence of polymerisation.

4.3.5 Stability of *N*-Acylated Hydroxymethyl Pyrroles

The stability of *N*-acylated hydroxymethyl pyrroles in the presence of solvent and weak bases is of paramount importance to the succesful use of these compounds as mechanism based inhibitors, Section 1.1. The premature release of the latent reactivity would result in non-specific interactions. The *N*-acylation of pyrrole suppresses the formation of the reactive azafulvene; therefore a hydroxymethyl pyrrole would not be expected to react, in the absence of hydroxide. The hydrolysis study mimics the enzyme: the hydroxide is designed to mimic the active site catalytic residue and the n-butylamine a nucleophilic residue within the enzyme, see Section 4.1. The stability of an *N*-acylated hydroxymethyl pyrrole was observed when the hydroxymethyl pyrrole **2.32** was subjected to the following conditions: The *N*-acylated hydroxymethyl pyrrole **2.32** was dissolved in d_3-acetonitrile (0.6mL) containing D_2O (50μL) and n-butylamine (50μL). No change in the ^{1}H NMR spectrum was observed over two months. We therefore concluded that the deacylation of *N*-acylated hydroxymethyl pyrrole **2.32**, as described in Section 4.2 and 4.3, was the result of HO^- catalysis. The hydroxymethyl pyrrole is therefore stable in a solution of D_2O/n-butylamine in the absence of HO^-.

4.4 Deacylation of 4.5: Kinetic Analysis

The rate constant with respect to HO^- concentration for the deacylation of **4.5** in d_3-acetonitrile containing n-butylamine (1equiv.) at 23.1°C was determined.

Compound **2.32** was dissolved in d_3-acetonitrile (0.6mL). One equivalent of n-butylamine was added and the solution was well mixed. Either one, one and a half, two or three equivalents of HO^- (KOH in D_2O) were added in separate experiments, followed by vigorous shaking. The reaction was followed by recording the ^1H NMR spectra at t=0.5 min and subsequently at one minute intervals until the reaction slowed. ^1H NMR spectrum were then recorded at two, five, ten and/or fifteen minutes intervals as indicated in Table 4.1. The reaction was followed for two hours, or until no further significant reaction was observed.

1) One Equivalent HO^-: As described previously, Section 4.3.4, one equivalent of HO^- caused immediate deacylation of **2.32** to give **4.5** and subsequently **4.6**. The level of **2.32** decreased to a minimum of 10%, as **4.5** reached a maximum of 80%. The level of **4.5** subsequently decreased over twenty four hours to 10%. **4.6** steadily increased to reach a maximum of 80%. After three days these ratios were unchanged.

2) One and a Half Equivalents HO^-: A similar result to that above was observed. The addition of one and a half equivalents of HO^- caused immediate deacylation of **2.32** to give **4.5** with the subsequent formation of **4.6**. Compound **2.32** was fully deacylated to **4.5** within two minutes. After one hour 80% **4.5** was converted to **4.6**, Section 4.3.2.2. The final ratio was 8:2 **(4.6:4.5)**.

2) Two Equivalents HO^-: Two equivalents of HO^- gave total conversion of the starting material **2.32** to **4.5** within one minute. 90% of **4.5** was subsequently converted to the pyrrole amine **4.6**. The ratios remained fixed at 9:1 **(4.6:4.5)**.

3) Three Equivalents HO^-: The only species remaining after thirty minutes hydrolysis with three equivalents of HO^- was the pyrrole amine **4.6**.

The observed rate obtained from these deacylations is detailed in Table 4.2.

4.4.1 Determination of Rate of Decomposition of 4.5

The observed rate, k, of deacylation of **4.5** was obtained using the following method:

1) The data for the kinetic analysis of **4.5** were based on the absorbance of the two proton pyr-C*H*$_2$OCOCH$_2$CH$_2$Ph singlet (5.07ppm).

2) Each ^{1}H NMR spectrum was placed in an array using Varian NMR spectrometer software. The signal at 5.07ppm was highlighted, and the full raw data, Table 4.1, were produced using a program provided in the Varian software[4] based on work by Gelan[5].

^{1}H NMR Spectral Absorbance at 5.07ppm for Kinetic Analysis of the Hydrolysis of 4.5† in d$_3$-Acetonitrile

Raw Data from One Experiment at Each Concentration Shown

Time t (min)	1 Equiv. HO$^-$	1.5 Equiv. HO$^-$	2 Equiv. HO$^-$	3 Equiv. HO$^-$
0	112.0	165.1	135.4	155.7
1	98.6	154.8	116.4	106.7
1.5				83.8
2	89.6	156.0	100.5	74.2
2.5				72.4
3	77.3	147.0	91.9	60.9
4			88.4	54.1
5	76.4	147.7	83.5	45.0
6				43.5
7		146.4	79.3	27.4
8			67.5	23.0
10	75.2	145.6	64.5	21.1
13		138.9	63.8	17.6
15	73.9	136.3	59.7	4.5
30	68.3	135.1	56.4	0•
45	64.9	132.9		
60	59.4	132.0	55.4	
90	56.0	129.8	54.1•	
120	54.7	118.9•		
1 (day)	21.4•			
Abs$_\infty$	21	130	56	0

† Data Collected at 23.1°C; • End of Data Collection

Table 4.1

3) The absorbance at t=infinity (Abs_∞) was determined by observation of the accompanying graph, eg: Figure 4.14, that was produced from the calculation of the raw data.

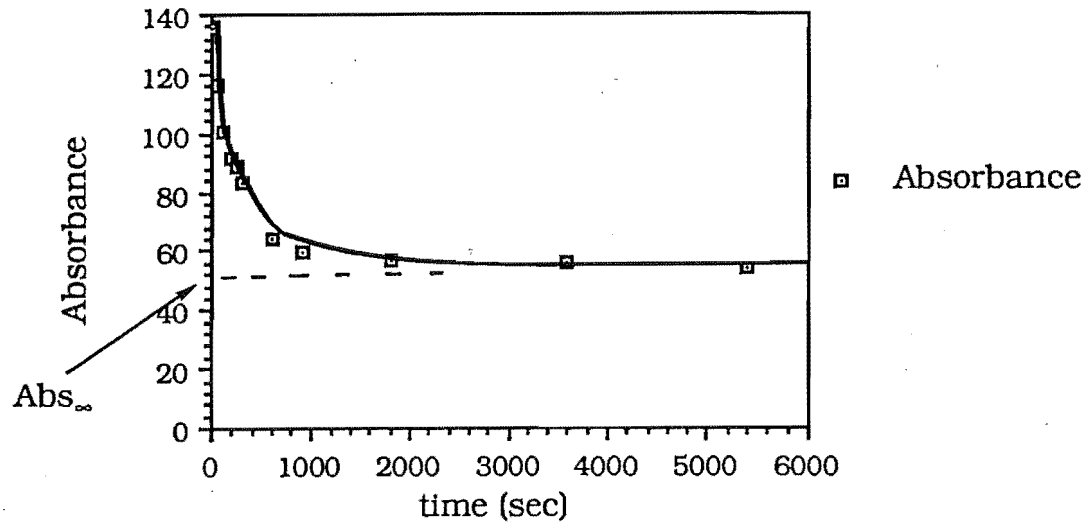

Figure 4.14

4) The observed rate, k, was then obtained using the formula given in Figure 4.15.

$$kt = \ln\left(\frac{Abs_0 - Abs_\infty}{Abs_t - Abs_\infty}\right)$$

Figure 4.15

Abs_0 is the absorbance at time t=0, Abs_∞ the absorbance at t=∞, Abs_t is the absorbance at a given time t and k is the observed rate. The observed rate in Table 4.2 was obtained for the various HO^- concentrations using this formula, and the data presented in Table 4.1.

Observed Rate of Hydrolysis of 4.5 with respect to HO^- Concentration

Concentration HO^- (M)	Equivalents HO^-	Observed Rate k
$0.66x10^{-3}$	1	$1.34x10^{-3}$
	1	$1.33x10^{-3}$
	1	$1.30x10^{-3}$
$0.95x10^{-3}$	1.5	$1.98x10^{-3}$
$1.29x10^{-3}$	2	$2.79x10^{-3}$
	2	$2.81x10^{-3}$
$1.90x10^{-3}$	3	$3.96x10^{-3}$

Table 4.2

5) The rate of disappearance of **4.5** was found to increase linearly with increasing HO^- concentration. The plot of k_{obs} versus HO^- concentration gave a straight line, Figure 4.16, and the slope 0.458x represents $k_{OH}[HO^-]$ or the k_{obs} with respect to decomposition of **4.5.**

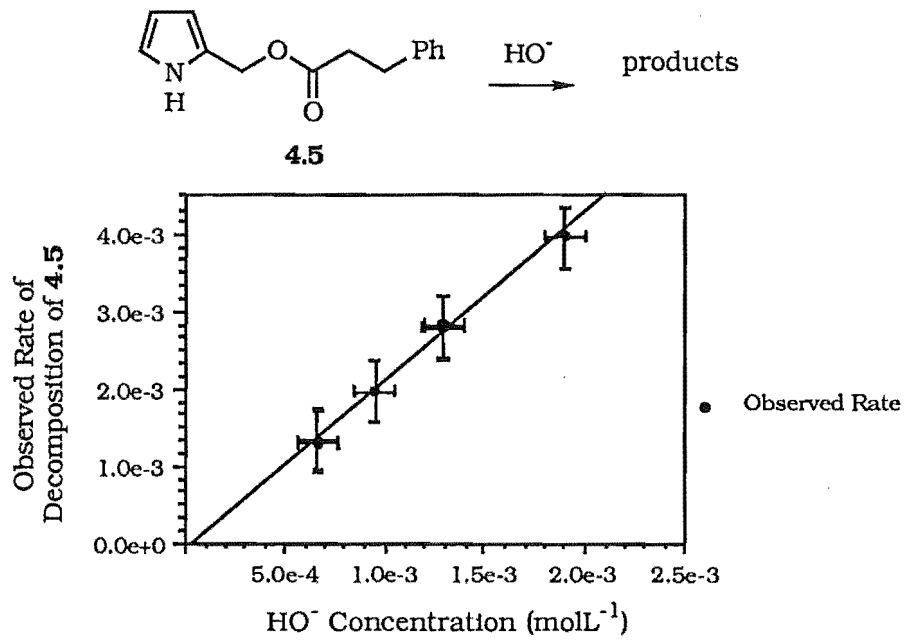

Figure 4.16

The deacylation of **4.5** is therefore first order with respect to HO^- at zero to three equivalents of HO^- and has a rate constant of $k=0.458s^{-1}$.

Reactions can be forced to adopt pseudo-first order kinetics by using a large excess (greater than ten equivalents) of reagent for ease of kinetic analysis. The graph in Figure 4.16, is linear up to three equivalents of added HO^-, indicating that the deacylation of the *O*-acyl pyrrole derivative **4.5** is genuinely first order with respect to HO^-.

A Y axis intercept of $4.285x10^{-5}$ indicated that there is no background hydrolysis within experimental error of zero, ie: $k_{obs}=0$ at zero HO^- concentration. This observation reinforces the evidence that the hydroxymethyl pyrrole **2.32** is stable in solution, Section 4.3.5.

The overall rate of the deacylation reaction could be obtained using the equation given in Figure 4.17.

$$\text{Rate}= k_{HO^-}[\mathbf{2.32}][\mathbf{4.5}][\mathbf{4.6}][HO^-]$$

Figure 4.17

A kinetic analysis as outline in Figure 4.17 was not carried out. The hydrolysis of the pyrrole amide bond is likely to be first order at low HO^- concentrations and second order at higher HO^- concentrations[1], this will be discussed in detail in Section 4.5. The added complexity creates kinetics that are difficult to study. In any event, a simple analysis was deemed sufficient to establish the feasibility of the proposed mode of enzyme inhibition.

The overall mechanism of the reaction is discussed in Section 4.5.

4.5 A Mechanistic Summary of the Deacylation of *N*-Acyl Hydroxymethyl Pyrrole 2.32

The overall mechanism of *N*-acyl hydroxymethyl pyrrole **2.32** deacylation under various solvent conditions, outlined in this section, is complex. The mechanism can be simplified into two separate sections. One is the mechanism in d_4-methanol, Section 4.5.1, the second in d_3-acetonitrile, Section 4.5.2.

There are two aspects to the reaction of **2.32** with HO^- in d_3-acetonitrile. The first involves the hydrolysis of the pyrrole-amide bond, and the second, the subsequent reactions of the *O*-acyl pyrrole derivative **4.5**.

The experimental observation that **2.32** is stable in solutions of d_4-MeOH/D_2O, d_3-acetonitrile/D_2O and d_3-acetonitrile/D_2O/n-butylamine for extended periods, confirms the conclusion that *N*-acylation of a 2-substituted pyrrole suppresses azafulvene formation and hence subsequent reaction, Section 2.1.2, and 1.2.4 and 4.7.1. A hydroxymethyl pyrrole, eg: **2.32**, would not be an effective mechanism based inhibitor if the latent reactivity was released before delivery to the targeted enzyme.

4.5.1 Amide Hydrolysis in d_4-Methanol

The addition of HO^- to compound **2.32**, in d_4-methanol results in deacylation via either pathway *a*, or by pathway *b* Scheme 4.18, to give the hydroxymethyl pyrrole **4.1** and the methoxymethyl pyrrole **4.2**.

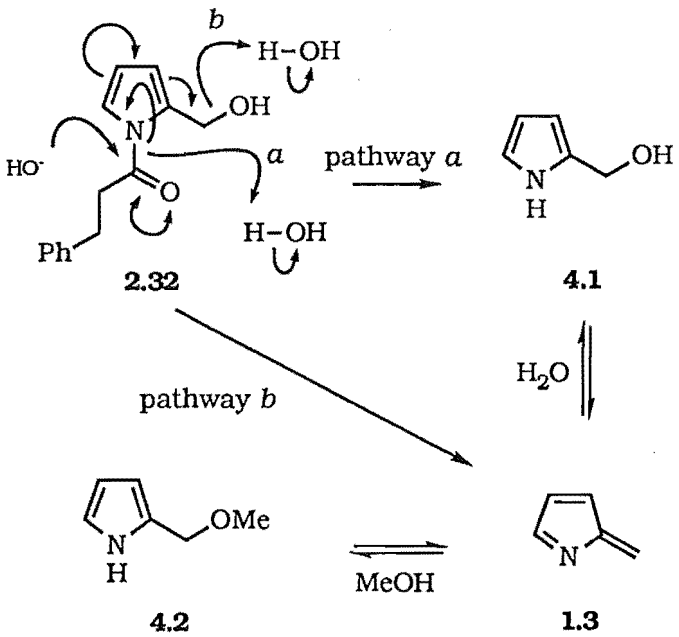

Scheme 4.18

Pathway *a:* The initial hydrolysis product via this pathway would be the hydroxymethyl pyrrole **4.1**. There would be no evidence of the methoxymethyl pyrrole **4.2**.

Pathway *b:* The methoxymethyl pyrrole **4.2** would be observed in the initial stages of the hydrolysis, if the hydrolysis was occurring via pathway *b*, ie: an acyl loss with concerted azafulvene formation. This would also signify that **4.1** was forming via the azafulvene **1.3** and not from the loss of the acyl group from the pyrrole nitrogen.

The deacylation of **2.32** initially produced a trace, but NMR observable amount of **4.1**. Compound **4.2** was not observed initially, Section 4.2. This suggests an initial acyl loss to give **4.1**, without immediate azafulvene formation. An equilibrium is then established (within two minutes) between **4.2** and **4.1** most probably through the azafulvene **1.3**. Nucleophilic attack on **1.3** occurs via either HO^-, to return to hydroxymethyl pyrrole **4.1**, or methanol to produce the methoxymethyl pyrrole **4.2**. Compound **4.2** was not observed initially, even with a vast excess of methanol over HO^-.

Therefore, it is proposed that the deacylation of **2.32** in d_4-methanol proceeds via pathway *a*, Scheme 4.18, to give the hydroxymethyl pyrrole **4.1**. This then undergoes azafulvene **1.3** formation to give an equilibrium mixture of **4.2** and **4.1**. Further support is obtained in the reaction of **2.32** with KOH/d_4-MeOH in d_3-acetonitrile. Again a trace amount of **4.1** was initially produced on deacylation of **2.32**. A rapid build up of **4.2** was only observed after two minutes. The small amount of **4.1** (<5%) is postulated to form directly from the initial deacylation of **2.32**. The equilibrium favours **4.2** over **4.1** since methanol is in excess, Section 4.3.1; formation of **4.4** requires pathway *a*. This is consistent with an S_N1 like mechanism via the azafulvene **1.3** as described in Section 4.2.

4.5.2 Amide Hydrolysis in d_3-Acetonitrile

The deacylation of **2.32** with one or more equivalents of KOH in D_2O (trace, 10μL) in d_3-acetonitrile (0.6mL) resulted in an *N*- to *O*- acyl transfer to give compound **4.5**. This acyl transfer can occur via an intramolecular mechanism, either by participation of the hydroxymethyl group, pathway *c*, Scheme 4.19, or via the tetrahedral intermediate **4.8**, pathway *d*, Scheme 4.19. The intermolecular pathways *b* and *e* are also possible.

Scheme 4.19 summarises the reactions in d_3-acetonitrile, Section 4.3. Pathways *a* and *b* were also postulated for the d_4-methanol reactions, Section

4.2.

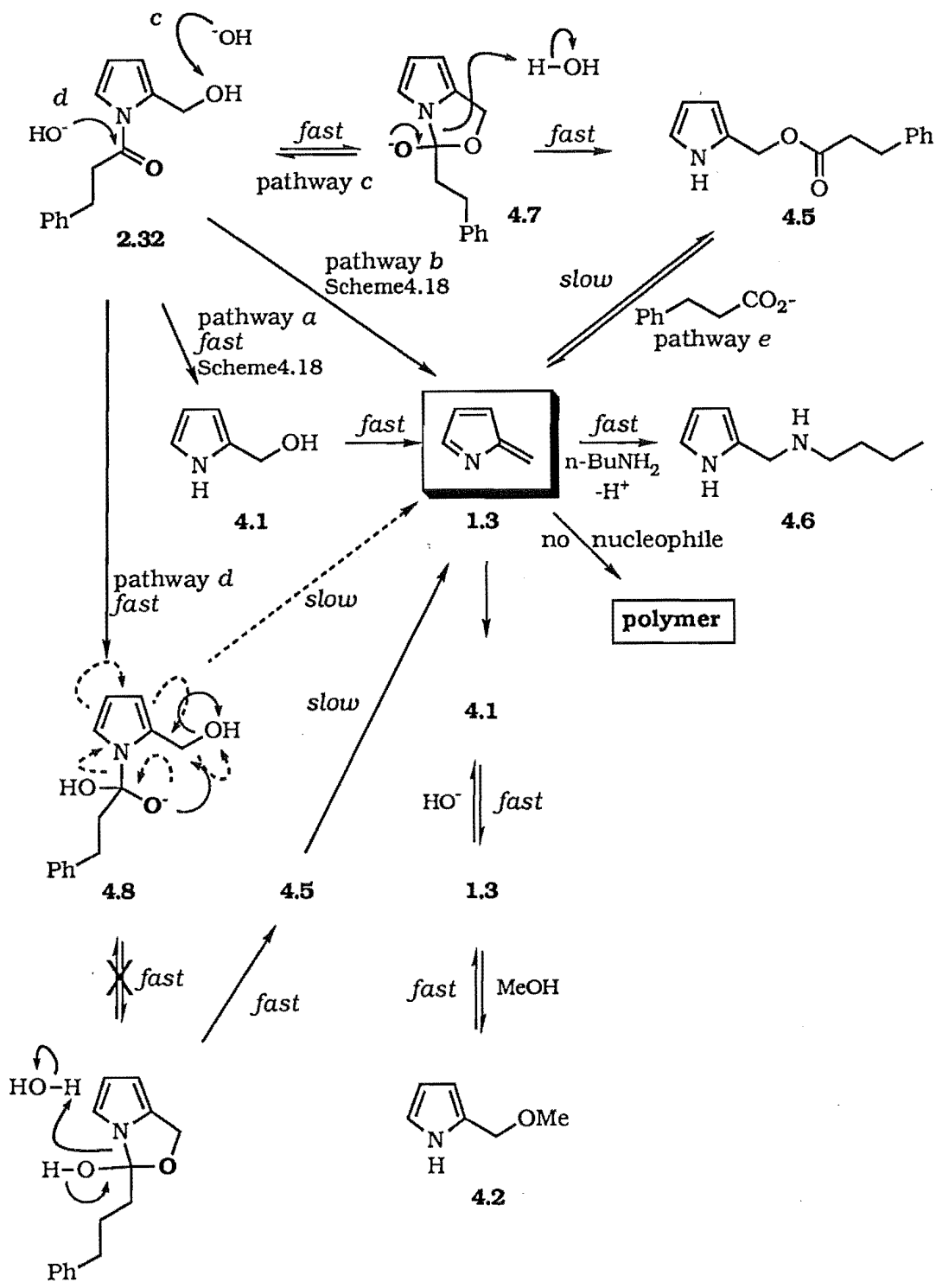

Scheme 4.19

Only the second of these mechanisms, pathway c, does not involve cleavage of the hydroxymethyl pyrrole group. Studies on the elucidation of the mechanism is presented in Section 4.6.

4.5.2.1 *Amide Hydrolysis and O-Acyl Pyrrole Derivative* **4.5** *Formation: Reaction Cube Analysis*

The hydrolysis of an amide bond is generally second order with respect to HO^-[6,7], although some first order cases are known[8].

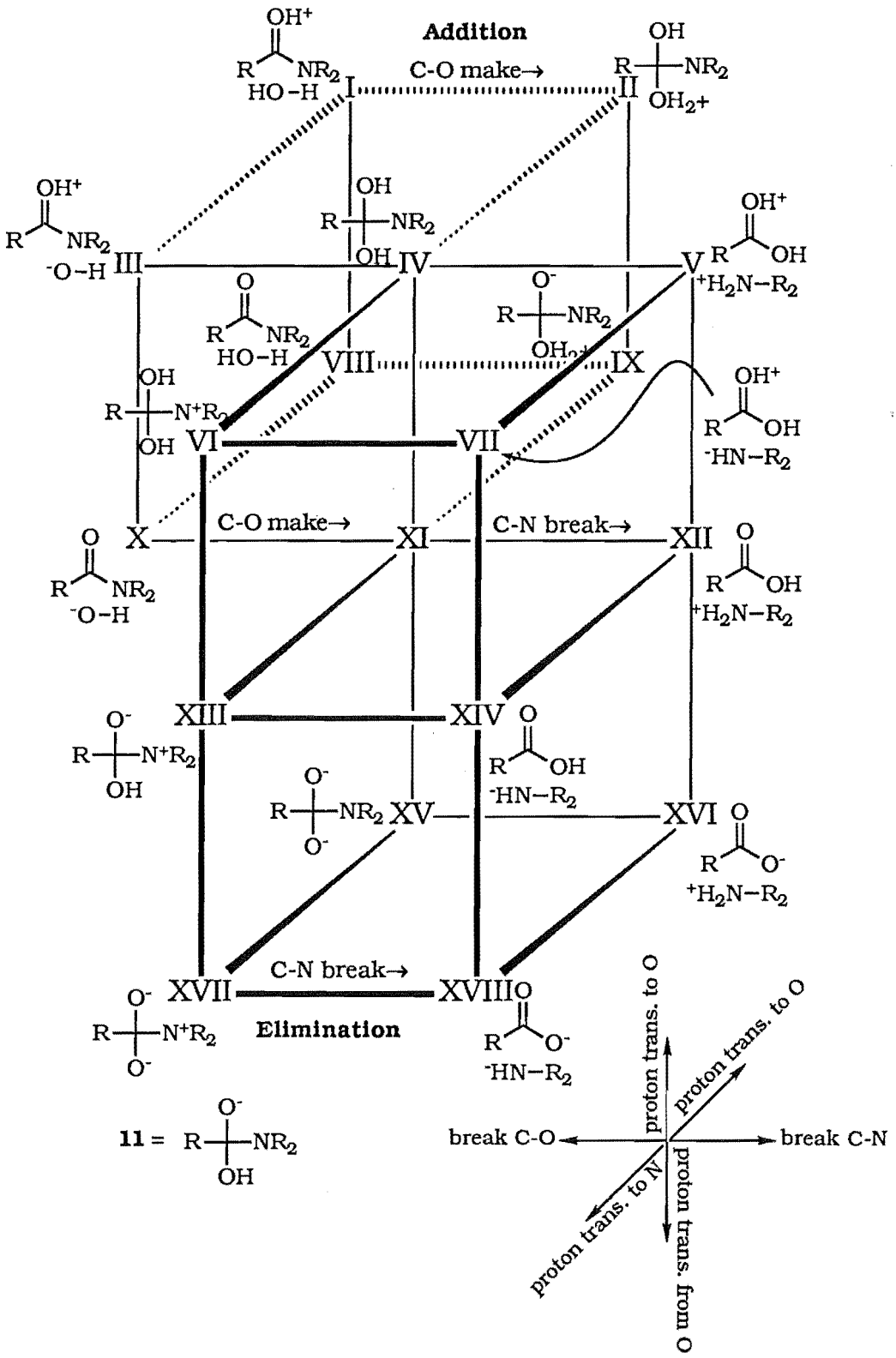

Figure 4.20

The hydrolysis of compound **4.5** was shown to be first order. The reaction cube[9] presented in Figure 4.20 outlines a typical amide hydrolysis. The complex amide bond hydrolysis mechanism is represented simply by a reaction cube of this type.

A reaction cube, in which one face represents the charge types of the reactants (points I, III, VIII, X on the reaction cube, Figure 4.20) and the opposite face represents the corresponding charge types of products (V, VII, XVI, XVIII), can be used to display the multiple mechanistic paths of familiar reactions and systematically to generate mechanistic hypotheses for new reactions[9,10]. The cube describes the interrelation of all charge types of both reactants and products. Each charge type can be related to any of the others by either an edge, face diagonal or body diagonal operation, eg: the points I and II, on an edge, are related by a C-O bond forming step. Cubes can be constructed for each process involved in a possible mechanism.

Amide hydrolysis can be described with three cubes. One cube describes the addition of a nucleophile to the amide bond and the second cube describes elimination of a tetrahedral intermediate to give the hydrolysis products. Since amide hydrolysis can also occur in basic media a third cube is required to describe any dianionic tetrahedral intermediates that may be involved. The corner of each of the three cubes represents a potential intermediate in the reaction. A reaction cube is relatively easy to create, and can simplify the complexity of a mechanism, eg: amide hydrolysis has 31 edge, 34 face and 12 body diagonal processes available. Each process relates to a possible mechanistic pathway available for the reaction to undergo.

The two cubes of addition and elimination for amide hydrolysis share a common edge: IV, XI. The cube for dianionic tetrahedral intermediates is placed on the bottom of the elimination cube. Further reaction of these possible intermediates leads to, in this case, the *O*-acyl pyrrole derivative **4.5**. Figure 4.20 shows six of nine product charge types: V, VII, XII, XIV, XVI, XVIII. There are eight tetrahedral charged intermediates: II, IV, VI, IX, XI, XIII, XV, XVII of which only four are important for hydrolysis in base: IV, XI, XIII, XV.

The amide hydrolysis in the reaction cube of Figure 4.20, was used to described the initial *N*-acyl to *O*-acyl transfer reaction of compound **2.32** to give **4.5**. This requires cleavage of the pyrN-C(O^-) bond, but not the pyr-CH_2O-C(O^-)(R)N bond, **4.9**.

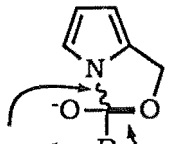

this bond to break — this bond can not break

4.9

This requirement necessitates that the tetrahedral species XV, Figure 4.20, is not an intermediate on the pathway. The C-O bond, of **4.9**, is broken in the formation of the species represented at point XV, and as such the -$OCOCH_2CH_2Ph$ group would be lost.

The *N*- to *O*- acyl transfer to give **4.5** that accompanies amide hydrolysis can conveniently be depicted by the simplified reaction cube given in Figure 4.21.

The attack of HO^- on the amide gives XI in the reaction cube of Figure 4.21.

The neutral *N*-acyl hydroxymethyl pyrrole **2.32** is represented at corner X and is the starting point for this cube. Under the basic conditions of the current study, C-O bond formation occurs to give the structure at position XI. There are three possible pathways, in line with the guide lines established above, that will ultimately produce the *O*-acyl pyrrole derivative **4.5** point XIV, Figure 4.21. There are seven possible routes under basic conditions for the formation of **4.5** but these include the species XV, Figure 4.20, and therefore the final products result in the loss of -$OCOCH_2CH_2Ph$.

The three routes are:

1) XI, IV, XIV — A proton transfer to *O* to give IV, which is followed by a concerted C-N bond cleavage and a proton transfer from *O* to *N*.

2) XI, XIII, XIV — From XI, a proton transfer to *N* gives XIII. A C-N bond cleavage follows to give XIV as the final structure.

3) XI, XIV — A concerted C-N cleavage, with a proton transfer to *N* to yield XIV.

Each of these routes is possible and accounts for the observed products in the reaction.

The *O*-acyl pyrrole derivative **4.5**, represented at point XIV in Figure 4.21, can lose hydrocinnamate via **1.3** to give the pyrrolic amine **4.6**, as described in Section 4.4 (first order with respect to the concentration of HO^-).

The hydrolysis of a pyrrole-amide bond is second order with respect to HO^- at high HO^- concentration[1,11]. When the leaving group of the nitrogen containing species is electron rich, a proton transfer to the nitrogen must occur, as in the case of pyrroles. This proton transfer must occur, even in base, for the N-C bond finally to break. This proton transfer is often the rate determining step[12,13]. Ingold[14] has classified the hydrolysis of amides and

esters; under this classification, amide hydrolysis in basic conditions occurs via the $B_{AC}2$ mechanism. This is a unimolecular base catalysed hydrolysis with acyl loss via a tetrahedral intermediate.

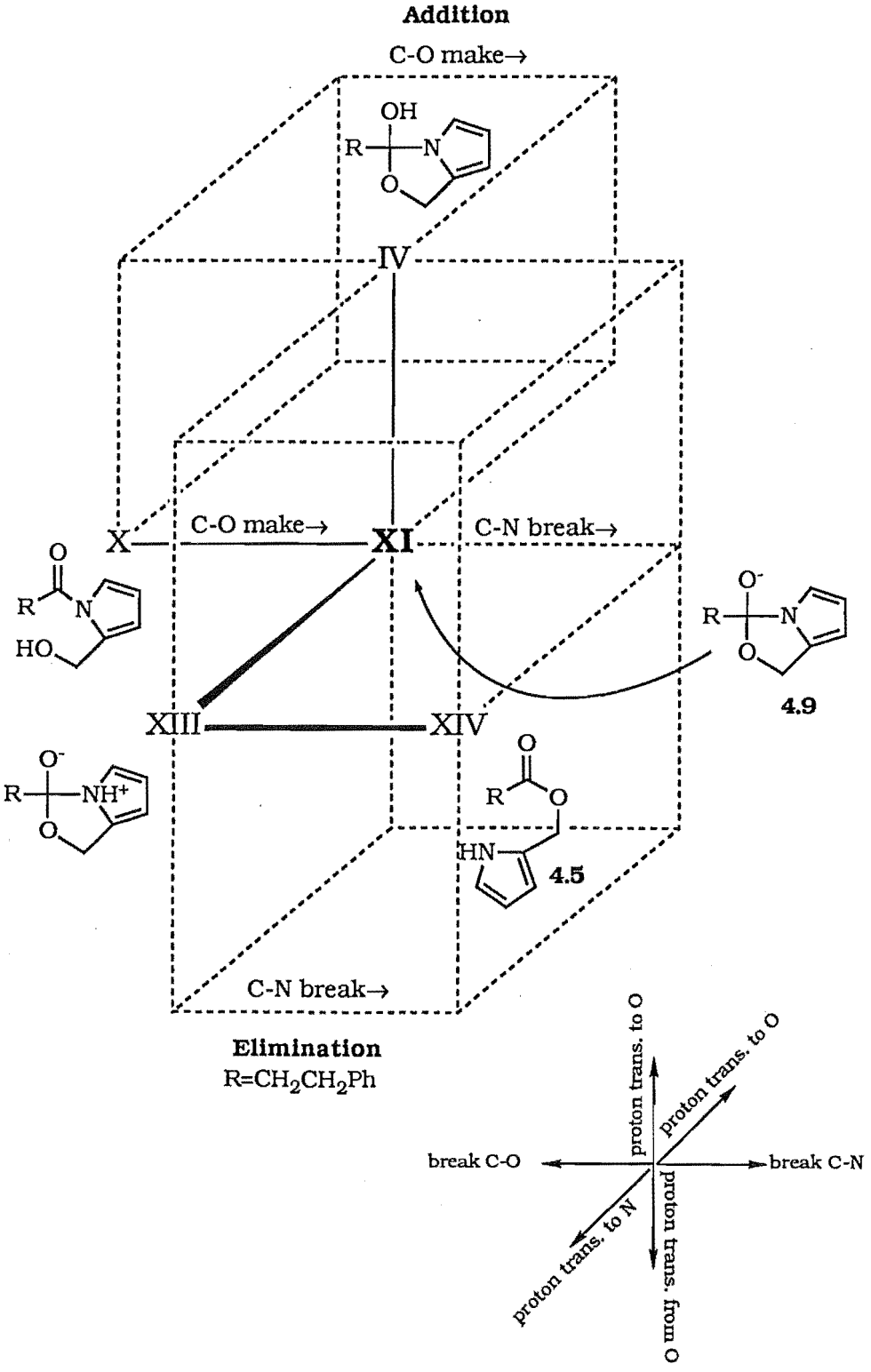

Figure 4.21

4.6 Elucidation of the Mechanism of *O*-Acyl Transfer to give 4.5

4.6.1 Theory Behind the use of Chiral Hydroxymethyl Pyrroles to Elucidate the O-Acyl Transfer Mechanism to give 4.5

The acyl transfer from **2.32** to **4.5** can be intramolecular, via either attack of the hydroxymethyl group on the amide carbonyl, pathway *c*, Scheme 4.19, or via the tetrahedral intermediate **4.8** pathway *d*, Scheme 4.19, with hydroxide attack at the amide carbonyl. Pathways *b* and *e* are also possible to give a third option via the intermolecular trapping of the acyl group by **1.3**.

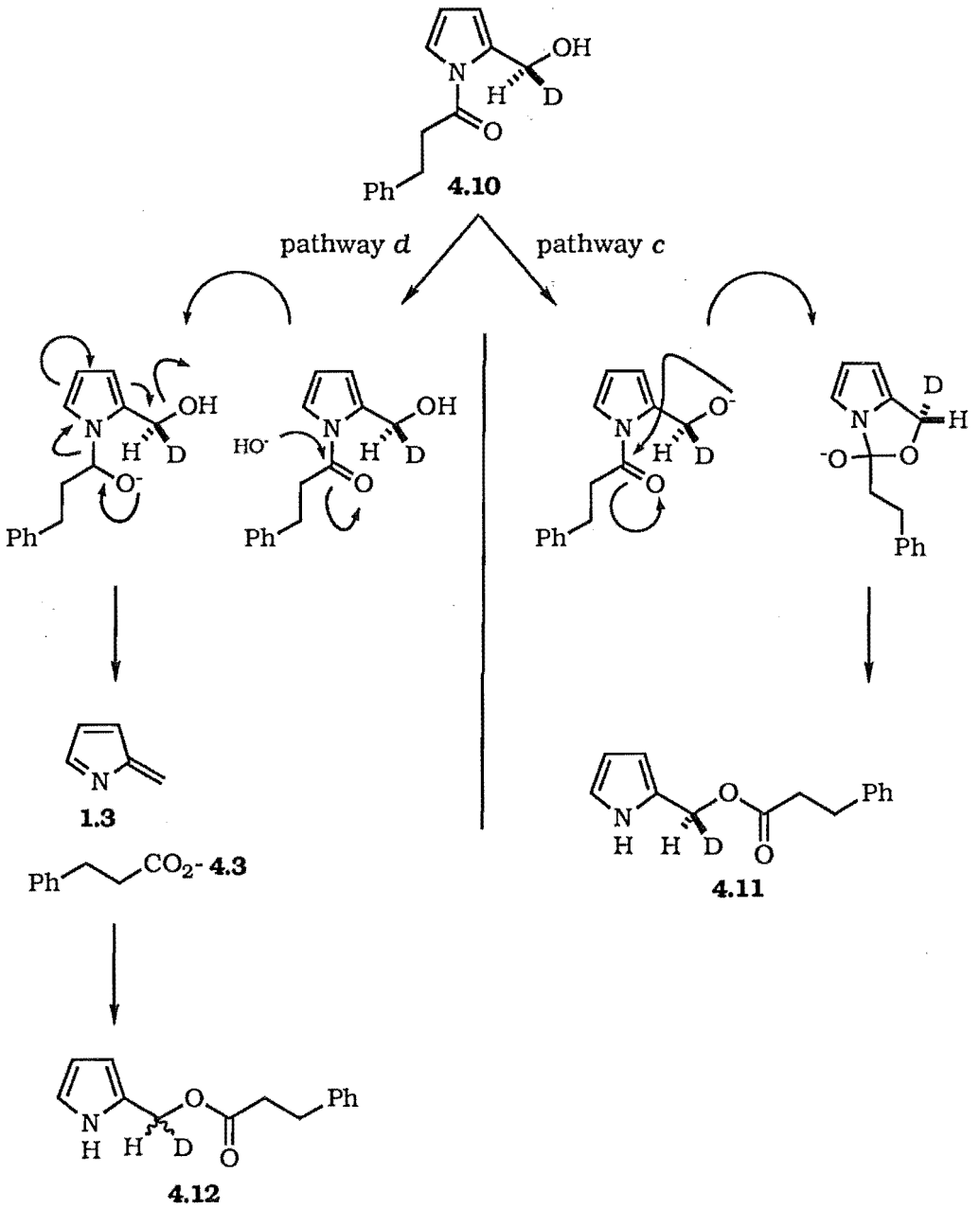

Scheme 4.22

As stated earlier, only the second of these mechanisms, pathway *c*, does not involve cleavage of the hydroxymethyl pyrrole group.

The optically active, deuterated hydroxymethyl pyrrole **4.10** was

prepared to elucidate the mechanism, pathway *c* or *d*, of the *O*-acyl transfer. The observation of the -CHD- group in the products from the hydrolysis via pathway *c* and *d* described above is given here:

1) The reaction via pathway *c* would proceed with retention of configuration at the 2-methylene position of **4.11**, as the CHD-OH bond is not broken.

2) Formation of **4.12** via the azafulvene **1.3**, pathway *d*, would result in the racemisation of the -CHD- group.

This is summarised in Scheme 4.22.

3) An S_N2 displacement would also give inversion of configuration of the methylene position of **4.11**. The S_N2 mechanism was considered unlikely. The *N*-acylation of the hydroxymethyl pyrrole, eg: **2.32** was intended to discourage an S_N2 type mechanism. This is experimentally shown in Section 4.7.1, where displacement of the OH via the Mitsunobu reaction (known to favour an S_N2 process) occurs with S_N1 character indicating azafulvene chemistry[15].

Since enantiomers are not distinguishable by ^1H NMR spectroscopy in the absence of a further chiral species (eg: solvent, shift reagent) the direct observation of the configuration of the -CHD- group of the chiral pyrrole products **4.11** and **4.12** is not possible. Diastereoisomers are, however, NMR distinguishable, this is expected in the case where the signals are anisochrouous.

Initial experiments using chiral shift reagents[16,17] to separate the ^1H NMR spectra of the products **4.11** and **4.12** were unsuccessful. The obvious solution to the problem of observing the -CHD- group configuration was to use a chiral *N*-acyl group. A chiral *N*-acyl group would cause diastereoisomers to be formed and hence the -CHD- signal should be clearly resolved. The chiral *N*-acyl group, *N*-Pth-Leu, was chosen. A trial deacylation of the non-labelled hydroxymethyl pyrrole *N*-(*N*-Pth-Leu)-p-2-OH **3.45** in d_3-acetonitrile containing HO^- (1 equiv. KOH in D_2O) gave **4.13** after five minutes. **4.13** produced from this reaction was analogous to the deacylation of **2.32** to give **4.5** discussed in Section 4.3.

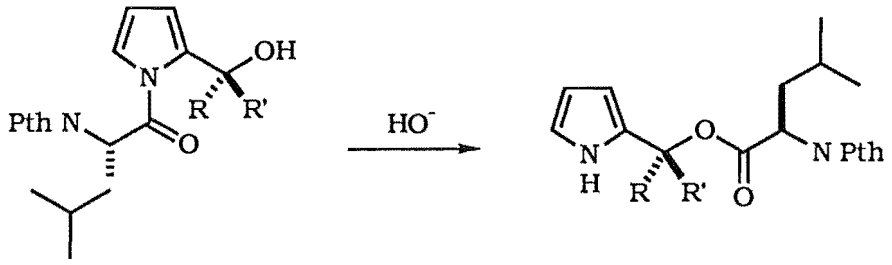

3.45 R=R'=H
4.14 R=H, R'=D

4.13 R=R'=H

Scheme 4.23

The doublets due to pyr-CH_2OR group of the *O*-acylated pyrrole derivative **4.13** at 5.09ppm and 5.13ppm were clearly resolved. The ^{1}H NMR spectrum of **4.13** is shown in Figure 4.30.

The clear doublet observed for **4.13** indicated that an analogous reaction using optically pure, deuterated hydroxymethyl pyrrole **4.14**, as in Scheme 4.23, would give clear evidence as to the stereochemical fate of the pyr-CH_2R group of the *O*-acylated pyrrole derivative produced on the hydrolysis of **4.14**.

4.6.2 Preparation of the Chiral Hydroxymethyl Pyrrole Derivative 4.14

The DMAP methodology, described in Section 2.4, was employed in the synthesis of the chiral *N*-acylated formyl pyrrole **4.16**, Scheme 4.24.

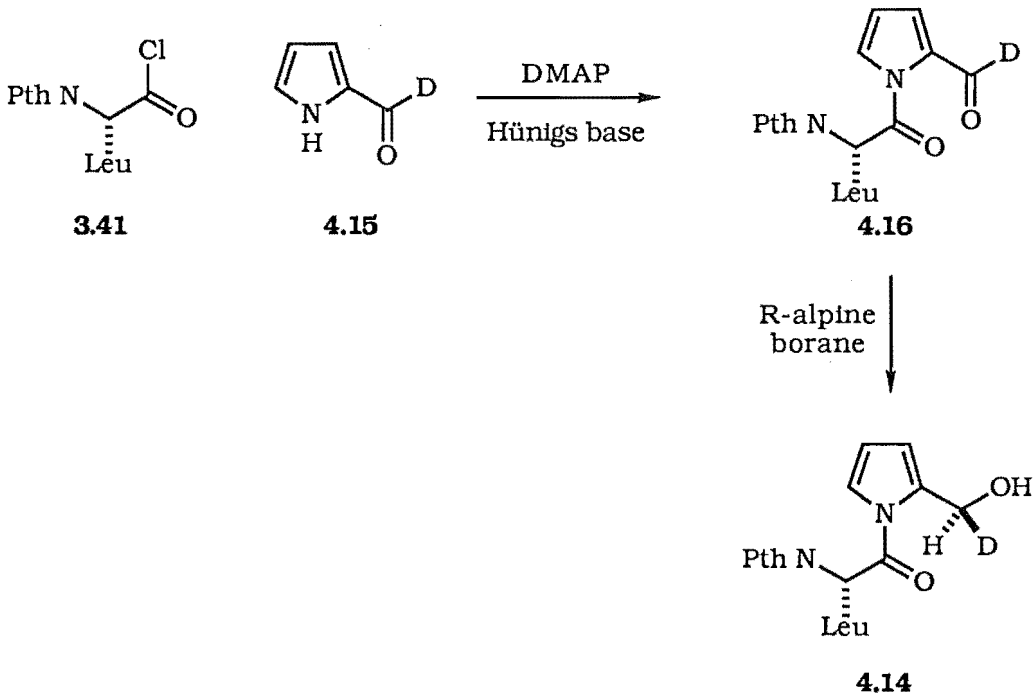

3.41 **4.15** **4.16**

4.14

Scheme 4.24

D_1-Pyrrole-2-carboxaldehyde **4.15** (p-2-CDO) was prepared via the Vilsmeier-Haack formylation of pyrrole using d_7-DMF. The addition of p-2-CDO **4.15**, DMAP and Hünigs base to *N*-Pth-Leu-Cl **3.41** caused polymerisation.

A report on microscale preparations of acid chlorides under the same oxalyl chloride/DMF conditions used here, indicated that *N*-(chloromethylene)-*N*-methanaminium chloride **4.17** was a likely product in the oxalyl chloride/DMF preparation of **3.41**[18].

Compound **4.17** is more reactive than an acid chloride and hence reacts preferentially with alcohols to produce alkyl halides[19]. **4.17** was conveniently removed in a hexane preparation of the acid chloride, by filtering.

We found that when the crude reaction from the oxalyl chloride/DMF reaction conducted in benzene was evaporated to dryness and hexane added, the required acid chloride was taken into the organic layer. An insoluble yellow oil remained in the reaction vessel; the ^{1}H NMR spectrum of this oil indicated the presence of **4.17**.

Use of the purified acid chloride in the DMAP reaction with p-2-CDO **4.15**, Scheme 4.24, gave the desired *N*-acylated p-2-CDO **4.16** in high yield. Inspection of the ^{1}H NMR spectrum of the failed preparations of **4.16** showed signals due to **4.17** [^{1}H NMR δ 1.93, 2.93, 3.01, 8.05][18]. The acid chloride formation is probably best carried out in hexane.

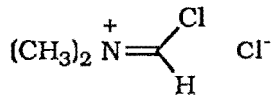

chloromethylene

4.17

R-Alpine borane[20] reduction [(+)-α-pinene and 9-BBN, Scheme 4.24] of the aldehyde **4.16** gave the chiral hydroxymethyl pyrrole **4.14** in 51% yield, after silica chromatography. The ^{1}H NMR spectrum of **4.14** showed a one proton singlet corresponding to pyr-C*H*DOH at 4.63ppm. The ^{1}H NMR spectrum of the unlabelled *N*-(*N*-Pth-Leu)-p-2-OH **3.45**, Section 3.3.1 had a two proton singlet in the same position.

R-Alpine borane is known to yield 'S' alcohols[21,22] on reduction of the corresponding aldehyde. The determination of the absolute stereochemistry in this work was not possible. The assumption was that R-alpine borane reduced the formyl group of **4.16** in the same sense as reported in a related system[21], ie: to give the 'S' stereochemistry, as drawn in **4.14**. In any event the exact chirality was not important in the present studies.

4.6.3 Hydrolysis of Chiral Hydroxymethyl Pyrrole Derivative 4.14

(S)-*N*-(*N*-Pth-Leu)-p-2-CHDOH **4.14**, Section 4.6.2, was dissolved in d_3-acetonitrile and HO^- (1equiv. KOH in D_2O) was added. The ^{1}H NMR

spectrum after fifteen minutes showed one signal at 5.08ppm indicating one diastereoisomer **4.19**, Figure 4.25.

^{1}H NMR Spectra of Methylene Region of
O-Acetylated Pyrrole 4.19

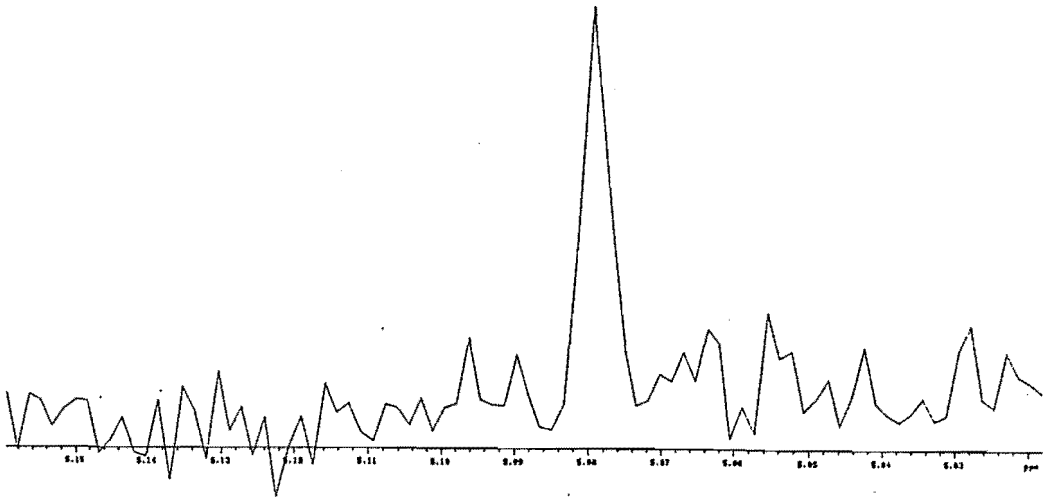

Figure 4.25

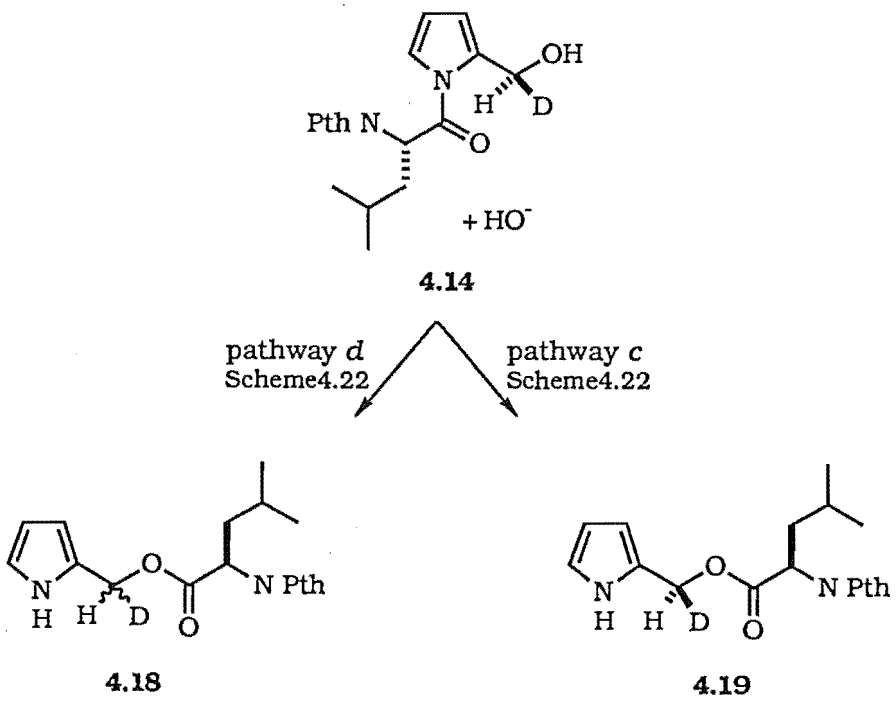

Scheme 4.26

Racemisation had clearly not occurred to give **4.18**. This implies that the formation of the *O*-acylated pyrrole derivative, eg: **4.5** did not form via an azafulvene, as in pathway *d* Scheme 4.26. The determination of the configuration of **4.19** is described in Section 4.6.4.

The mechanism of formation of **4.5** must therefore be via a pathway analogous to pathway *c*, Scheme 4.26 or much less likely via an S_N2 displacement, see Section 4.6.1 for a discussion. The *N*- to *O*- acyl transfer occurs via an intramolecular attack of the hydroxymethyl group on the amide carbonyl.

4.6.4 Determination of the Configuration of the Chiral H-6 Position of the Pyrrole Derivatives 4.14 and 4.19

The direct observation of the configuration of the 2-methylene position of pyrroles **4.14** and **4.19** was not possible. The configuration was determined by analogy with other known examples[21,22]. The following three observations were used to determine the configuration of the -CHD- group.

1) R-Alpine borane is known to reduce aldehydes to alcohols with the 'S' configuration.

2) The pyrrole camphanate derivative **4.20**, Scheme 4.27, had been prepared in optical purity via R-alpine borane reduction[23]. Ozonolysis of **4.20** produced one of the two enantiomeric glycolates **4.21** or **4.22**; each has a known ^1H NMR spectrum. The ^1H NMR spectrum of the glycol was compared to the known standards **4.21** and **4.22**. The chirality of the camphanate **4.20** was determined as the 'S' configuration.

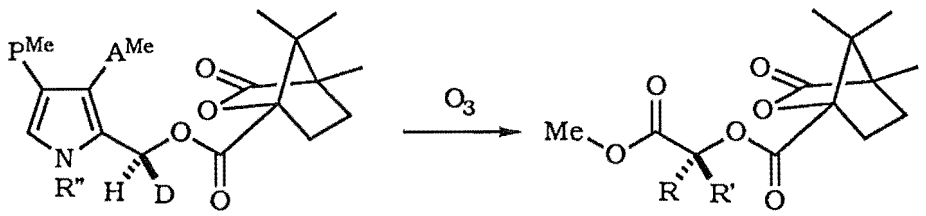

4.20
P^{Me}=$CH_2CH_2CO_2Me$
A^{Me}=CH_2CO_2Me
R"=SO_2Me or SO_2CF_3

4.21 R=H, R'=D
4.22 R=D, R'=H

Scheme 4.27

The ozonolysis reaction is relatively simple; however the yields are very low (<10%), and hence the reaction was not attempted in the present study.

3) A further analogy was derived from the corresponding series using the optically active hydroxymethyl pyrrole **4.10** as the base pyrrole.

3a) The racemic camphanate **4.25** was synthesised by the reduction of **4.23** with $Zn(BH_4)_2$, Scheme 4.28, as described in Section 2.4.5, followed by camphanate **4.25** formation with (-)-camphanic chloride and DMAP, Section 3.2.5. ^1H NMR spectral analysis identified the camphanate **4.25** pyr-C*H*DO-camph signals at 5.38ppm and 5.39ppm in a ratio of 1:1 for the 'R' and 'S' isomers, Figure 4.34.

3b) The optically active camphanate **4.26** was prepared from the reaction of (-)-camphanic chloride and DMAP with the chiral hydroxymethyl pyrrole **4.10**, Scheme 4.28. ^1H NMR spectral analysis of the optically active, labelled pyrrole camphanate **4.26** gave a singlet at 5.38ppm for the pyr-C*H*DO-camph proton, Figure 4.34. Using the knowledge that R-alpine borane reduces aldehydes to the 'S' alcohol we attributed the upfield signal to the 'S' enantiomer.

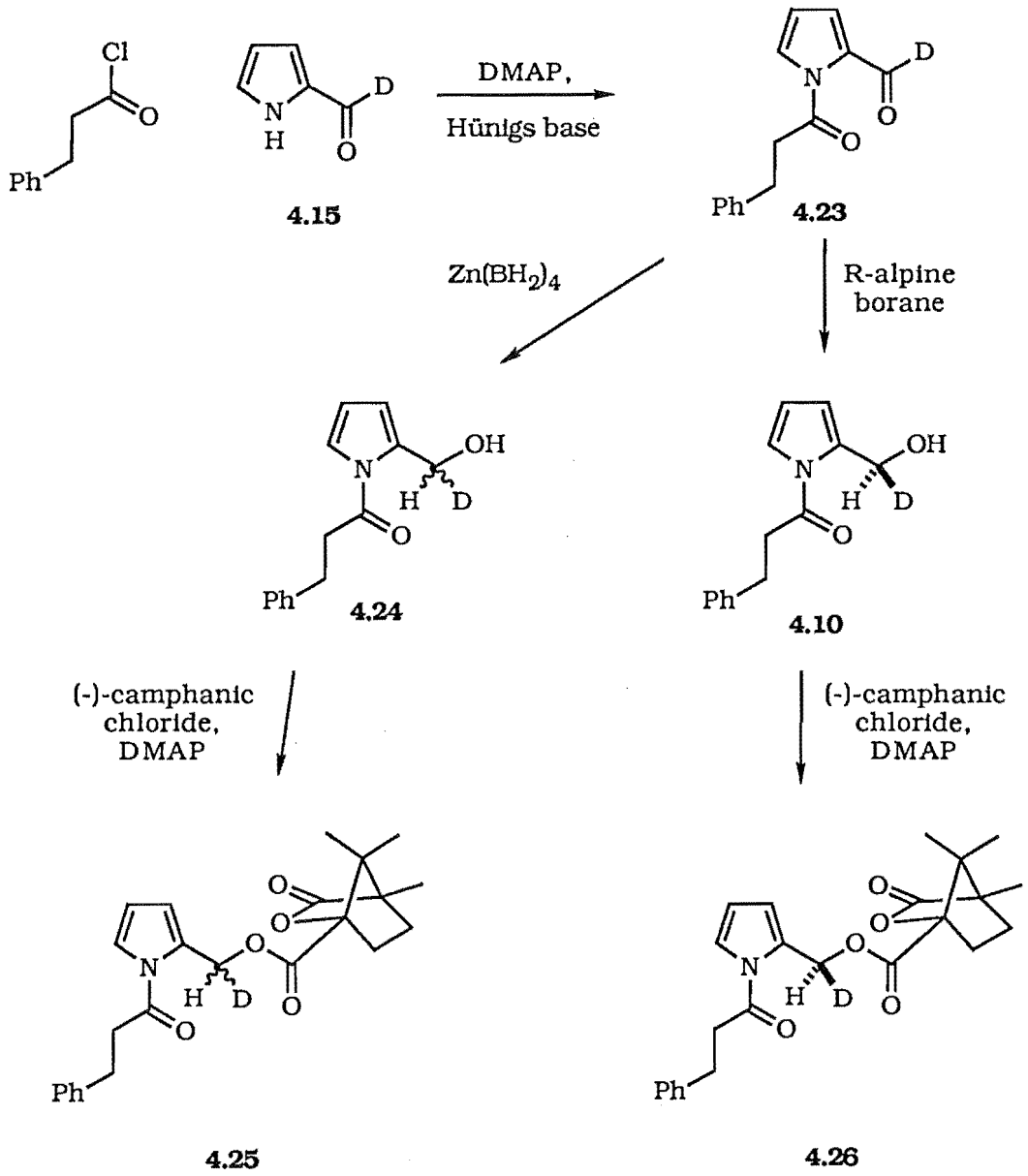

Scheme 4.28

Using the information given in steps 1) to 3b) above, the configuration of the -CHD- group of the labelled *O*-acyl pyrrole derivative **4.19** was determined as follows:

1) The achiral, non-labelled hydroxymethyl pyrrole *N*-(*N*-Pth-Leu)-p-2-OH **3.45** was deacylated by the addition of HO^- (1equiv. KOH in D_2O) in d_3-acetonitrile, Scheme 4.29, to give **4.13**. The well resolved doublet of pyr-CH_2OR was centred at 5.09ppm and 5.13ppm, Figure 4.30.

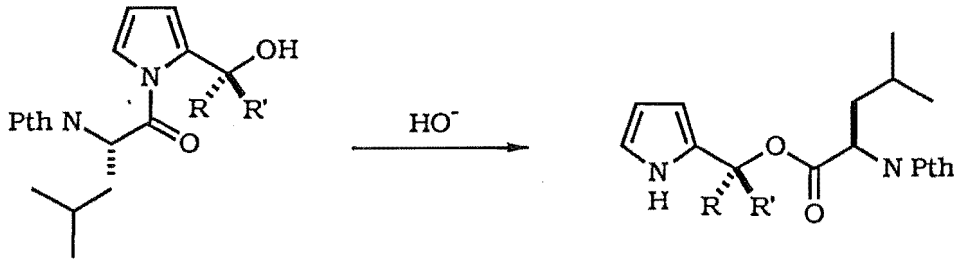

3.45 R=H, R'=H
4.14 R=H, R'=D

4.13 R=H, R'=H
4.18 R=D, R'=H
4.19 R=H, R'=D

Scheme 4.29

^{1}H NMR Spectra of Methylene Region of O-Acetylated Pyrrole Esters 4.13 and 4.19

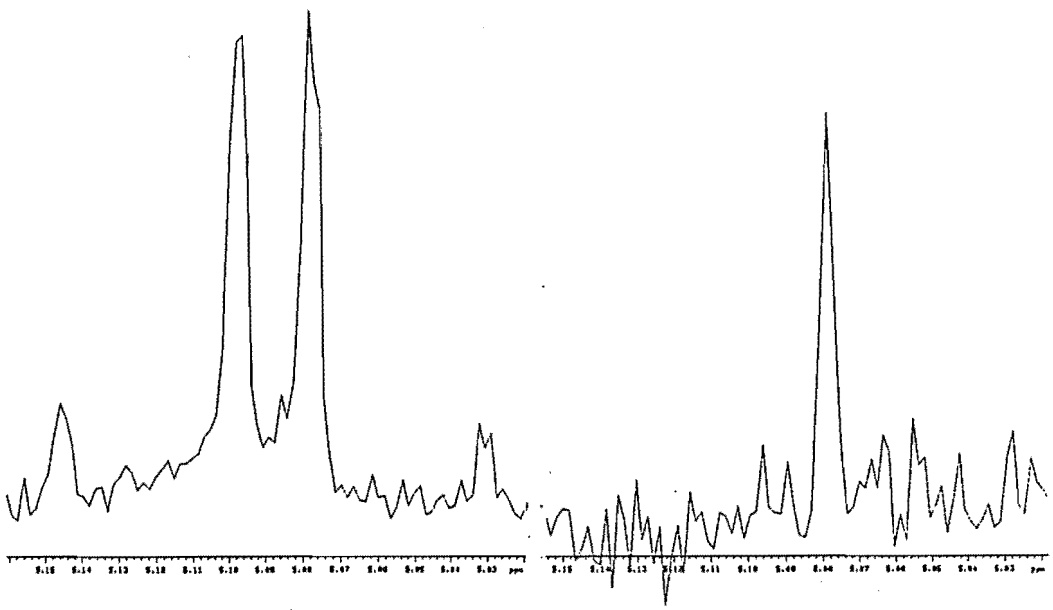

4.13 **4.19**

Figure 4.30

2) Hydrolysis of the labelled *N*-(*N*-Pth-Leu)-p-2-CHDOH **4.14**, as described above, gave the *O*-acyl pyrrole derivative, eg: **4.19**, Scheme 4.29. ^{1}H NMR spectral analysis of the labelled *O*-acyl pyrrole derivative gave an upfield signal at 5.09ppm, Figure 4.30. Therefore the chirality was assigned as 'S' for the product **4.19**.

The single signal indicates that the reaction to form **4.19** (and **4.5**) proceeds with retention of configuration and therefore most likely via an

intramolecular reaction, pathway *c* Scheme 4.19. This also gives further support to the notion that an S_N2 mechanism is not operating in the *N*- to *O*-acyl transfer reaction.

4.6.5 Hydrolysis of *O*-Acetylated Pyrrole 3.36

Hydrolysis of **3.36** in d_3-acetonitrile with HO^- (1equiv. KOH in D_2O) containing one equivalent of n-butylamine gave a slow conversion to **4.6**, to give a final ratio of 7:3 (**4.6**:**3.36**) after three hours, Figure 4.31. No other pyrroles were observed by ^1H NMR spectroscopy.

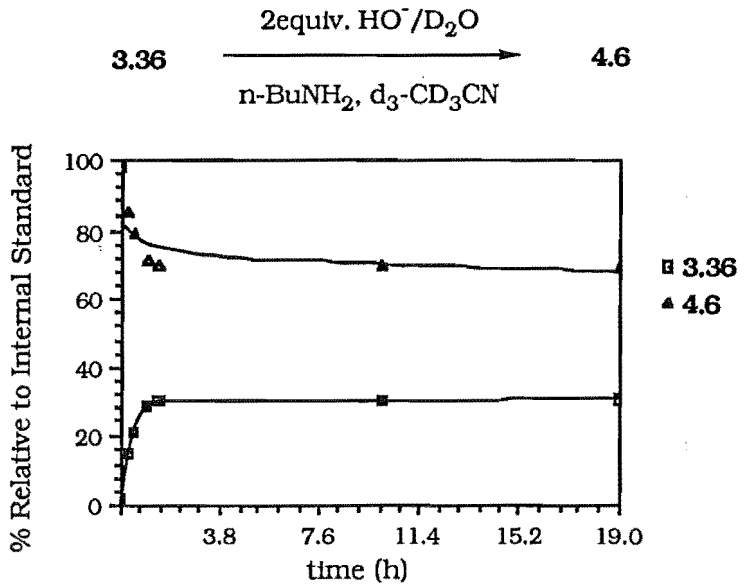

Figure 4.31

As described in Section 4.5.2, two pathways for the formation of **4.6** are possible. The first involves the *N*- to *O*- acyl transfer via the intramolecular attack by the hydroxymethyl group, pathway *c* Scheme 4.19. The second slower pathway, previously occurred only before the *O*-acyl pyrrole derivative **4.5** had formed. The slow rate observed on the hydrolysis of **3.36** is equivalent to this process. The mechanism of formation of **4.6** in this case, is therefore likely to be via pathway *b* Scheme 4.19.

4.6.6 Summary of the Evidence for Intramolecular Acyl Transfer

The rate of hydrolysis of **3.36**, Section 4.6.5, indicates that hydroxide attack on hydroxymethyl pyrroles, occur at the CH_2OH group. The rate observed for the protected hydroxymethyl pyrrole is consistent with intramolecular acyl transfer.

The chiral labelling experiment showed that the pyr-CHDR centre is not racemised during the formation of **4.19** under hydrolysis of **4.14**. The mechanism of formation of **4.19** (and **4.5**) is therefore via an intramolecular reaction, pathway *c* Scheme 4.19.

This hydrolysis provides an example of neighbouring group participation in the hydrolysis of an amide bond. Other nucleophilic substitutions, are known to be catalysed by the presence of a neighbouring nucleophile. The hydrolysis of phthalamic acid **4.27**, Scheme 4.32, has been shown to be 10^5 times faster than benzamide ($PhCONH_2$) at a similar pH[6].

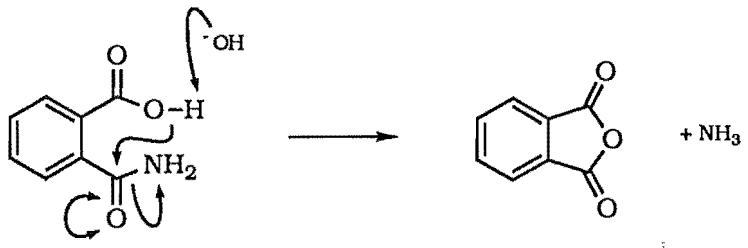

4.27

Scheme 4.32

The rate enhancement of phthalamic acid **4.27** over benzamide is not the result of the electron withdrawing ability of the -COOH group, but is an example of neighbouring group participation. Another good example is the catalytic triad of serine protease.

This form of catalysis has been suggested in the nucleophilic hydrolysis of esters and amides by enzymes[24]. The catalytic triad of serine proteases, Section 1.2.2, consists of an arrangement of nucleophilic residues that are able to promote neighbouring group participation in the cleavage of peptide bonds.

4.7 Azafulvene Chemistry: Experimental Evidence

4.7.1 The Suppression of Azafulvene Formation by *N*-Acylation of Hydroxymethyl Pyrroles

The *N*-acylation of pyrroles with a 2-substituted leaving group, has been shown to suppress the formation of azafulvenes, Section 2.1.2. Pyrrole *N*-acylation removes electron density from the nitrogen thereby decreasing the ability of the nitrogen lone pair to promote azafulvene formation. The more electron withdrawing the *N*-acyl substituent, the more suppressed the pyrrole is to azafulvene formation, see Section 2.1.2 for a discussion.

4.7.1.1 *Stability of N-Acylated Hydroxymethyl Pyrrole* **2.32** *with respect to 2-Hydroxymethyl Pyrrole* **4.1**

The observation that the hydroxymethyl pyrrole **2.32** dissolved in d_3-acetonitrile did not react with n-butylamine or with D_2O in the absence of HO^- supports the theory that *N*-acylation of 2-substituted pyrroles suppresses azafulvene formation, Section 1.1. Nucleophilic displacement at the 2-methylene group of pyrrole **2.32** does not occur due to *N*-acylation, only after the *N*-acyl group is removed, eg: as in **4.5**, does reaction occur.

This was demonstrated when the hydroxymethyl pyrrole **4.1**[2] was prepared independently by zinc borohydride reduction of p-2-c, see Section 2.4.5. The p-2-c was dissolved in d_3-acetonitrile and ^1H NMR spectra were recorded over two hours. During the first hour the signal for pyr-CH_2OH 4.62ppm (d_3-CD_3CN) gradually decreased, while the baseline noise increased. At the end of the second hour, the baseline noise obscured all of the pyrrole signals. This was accompanied by an intense colour in the NMR tube attributed to pyrrole polymer formation, see Sections 2.4.2, 3.2.1.4 and 4.3.2.1.

The *N*-acylated pyrrole **2.32** was found to be stable under the same conditions (and conditions with n-butylamine present) for two days. This indicates that a non-*N*-acylated pyrrole undergoes azafulvene formation readily, while *N*-acylation of 2-substituted pyrroles suppresses azafulvene formation.

4.7.1.2 *Labelled Hydroxymethyl Pyrroles* **4.10** *and* **4.24** *used to Determine the Stereochemical Consequence of Azafulvene Chemistry*

The labelled formyl pyrrole **4.23** was prepared using the DMAP methodology, Section 2.4. Hydrocinnamoyl chloride was added to p-2-CDO **4.15** in the presence of DMAP and Hünigs base. The resultant deuterated

formyl pyrrole **4.23** was then reduced under each of the conditions, outline in Scheme 4.33 and summarized below:

1) Achirally with $Zn(BH_4)_2$ in ether, to give the racemic deuterated hydroxymethyl pyrroles **4.24**, and

2) Chirally with R-alpine borane to give the 'S' labelled hydroxymethyl pyrrole **4.10** (R-alpine borane is known to reduce aldehydes to alcohols with the 'S' configuration).

The conformation at the 2-methylene position was then determined by making the camphanate derivatives **4.25**, **4.26** and **4.28**.

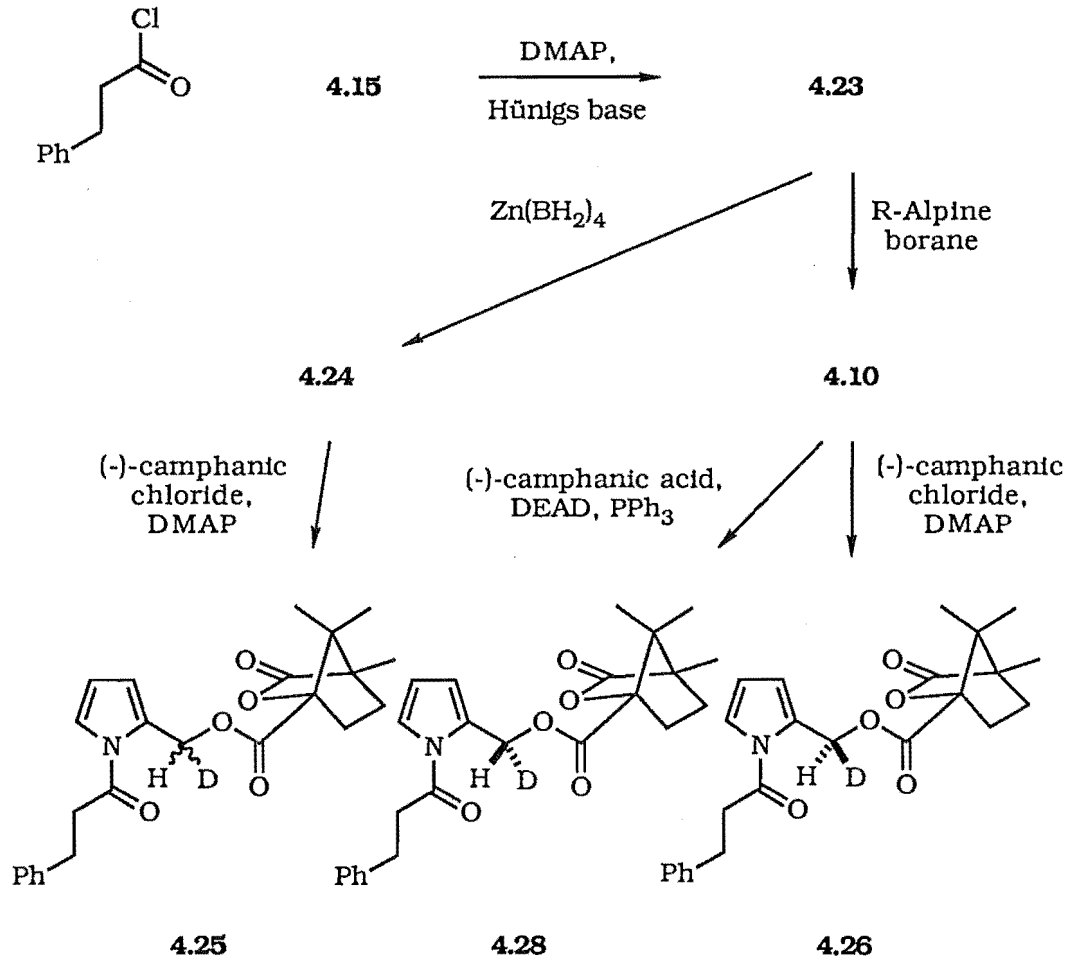

Scheme 4.33

Hydroxymethyl pyrroles **4.10** and **4.24** were dissolved in CH_2Cl_2 followed by the addition of one equivalent of (-)-camphanic chloride and DMAP to give the desired camphanates **4.26** and **4.25**, respectively. The hydroxymethyl pyrrole **4.10** was also subjected to camphanate formation under the Mitsunobu conditions[25] (the addition of excess DEAD, PPh_3 and (-)-

camphanic acid to **4.10** in THF) to give the camphanate **4.28.**

^{1}H NMR spectral analysis of the resultant camphanates **4.25, 4.26** and **4.28** was performed to determine the stereochemical fate of the -CHD- group in the formation of the camphanates **4.26** and **4.28.**

1) The achiral camphanate **4.25** was used as a reference as signals for the pyr-C*H*DO-camph group of both enantiomers were evident at 5.38ppm and 5.39ppm, Figure 4.34. The upfield signal at 5.38ppm was assigned to the 'S' enantiomer by analogy with *N*-(*N*-Pth-Leu)-p-2-CHDOH **4.14**, Section 4.7.1.2.

2a) The chiral labelled camphanate **4.26** prepared by the acid chloride/DMAP method showed a single one proton signal at 5.38ppm, Figure 4.34. The acid chloride/DMAP method ensures the racemisation does not occur, since the CHD-OH bond is not broken, azafulvene chemistry is therefore not possible.

2b) The labelled camphanate **4.28** prepared from the Mitsunobu reaction showed two signals, a downfield signal at 5.39ppm and an upfield signal at 5.38ppm for pyr-C*H*DO-camph, Figure 4.34.

^{1}H NMR Spectra of pyr-C*H*DO-camph Signal for the Camphanates: 4.25, 4.26 and 4.28

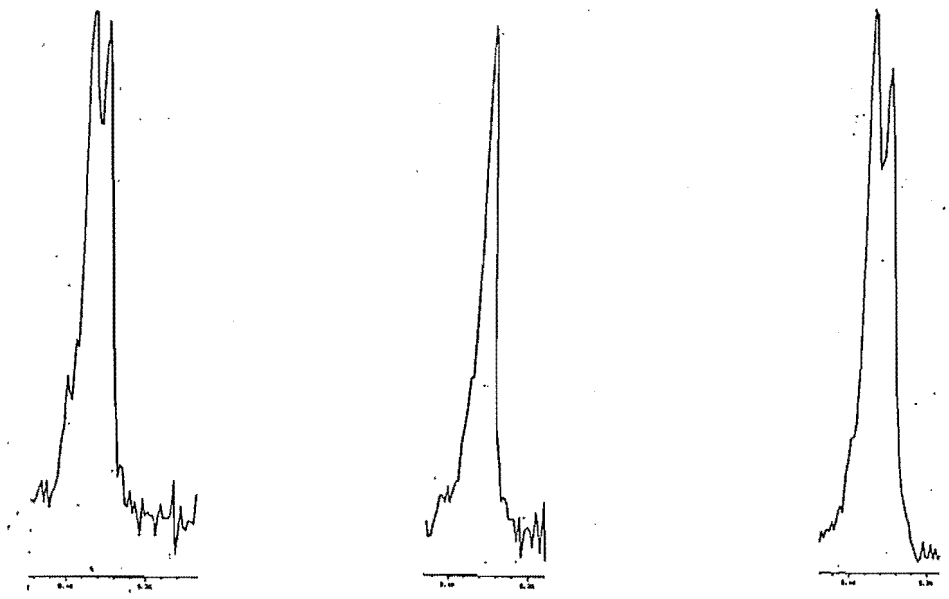

4.25 **4.26** **4.28**

Figure 4.34

The high stability of hydroxymethyl pyrroles towards nucleophilic displacement was evidenced by the lack of reaction of the pyrrole **2.32** after several months in a solution containing n-butylamine, Section 4.3.4. The Mitsunobu reaction forces a nucleophilic displacement to occur without HO^-. The Mitsunobu conditions are known to favour an S_N2 mechanism. The formation of **4.28** under S_N2 conditions would yield a ^1H NMR spectrum with a single downfield signal at 5.39ppm, the result of inversion. Similarly, if the displacement occurred solely due to azafulvene chemistry, a one to one ratio of 'S' (5.38ppm) to 'R' (5.39ppm) signals would be expected.

^1H NMR spectral analysis of the camphanate **4.28** from the Mitsunobu reaction showed two signals at 5.38ppm and 5.39ppm, Figure 4.34. The signal at 5.39ppm (61%) indicated an inversion of configuration, ie: an S_N2 reaction had occurred to give the 'R' configuration. The signal at 5.38ppm (39%) indicates that azafulvene chemistry was also evident during the camphanate formation.

Since a single signal was not observed from the Mitsunobu reaction we concluded that azafulvene chemistry had occurred, in part, to give the 'S' enantiomer. However, the ratio of 61:39 ('R':'S') indicates that azafulvene formation had been partially suppressed by *N*-acylation of pyrrole.

This result also discounts the S_N2 mechanism for *O*-acyl pyrrole derivative **4.5** formation, eg: even under Mitsunobu conditions, which give the best possible chance for an S_N2 process, azafulvene chemistry still occurs to a significant extent.

The more strongly electron withdrawing the *N*-acyl group, the greater the expected suppression of azafulvene formation. The suppression of azafulvene formation by *N*-acylation of 2-substituted pyrroles is supported by other work[21] in which the mesylate (SO_2Me) and triflate (SO_2CF_3) groups were placed on the pyrrole nitrogen to give **4.20**, Scheme 4.27.

A similar camphanate formation to that described in the present study using the 'S' labelled hydroxymethyl pyrrole enantiomer, gave the 'R' camphanate **4.20** in 96% enantiomeric excess via the Mitsunobu reaction. The configuration was confirmed by the degradation to the corresponding glycolate **4.21** of which the chirality and ^1H NMR spectra are known; this is described in Section 4.7.1.2.

4.7.2 Azafulvene 1.3 Formation: Evidence from Hydrolysis of Hydroxymethyl Pyrroles

4.7.2.1 *Racemisation of Chiral Labelled -CHD- Group of Hydroxymethyl Pyrrole* **4.14**

The *N*-acylation of pyrroles has been shown to suppress azafulvene formation, Sections 1.2.4, 2.1.2 and 4.7.1. We required evidence that the postulated azafulvene **1.3** does form on deacylation of *N*-acyl pyrroles.

Azafulvene formation was shown by Battersby[26] to occur in the release of hydroxymethylbilane **4.30**, Scheme 4.35, after assembly from porphobilinogen (PBG, **4.29**) in the enzyme hydroxymethylbilane synthase[23]. The release of the bilane was postulated to occur via the azafulvene **4.31**.

The reaction of chiral [11-D_1-R] or [11-D_1-S] labelled PBG gave a racemic product **4.33** at the 11-PBG position, under non-enzymic conditions. The chirality is retained when the cyclisation is carried out in the presence of hydroxymethylbilane synthase to produce **4.32**.

It was suggested that in the active site of an enzyme the attack is carried out stereospecifically to give **4.32**, while attack in solution would occur from both faces of the azafulvene, thus leading to the racemic product **4.33**.

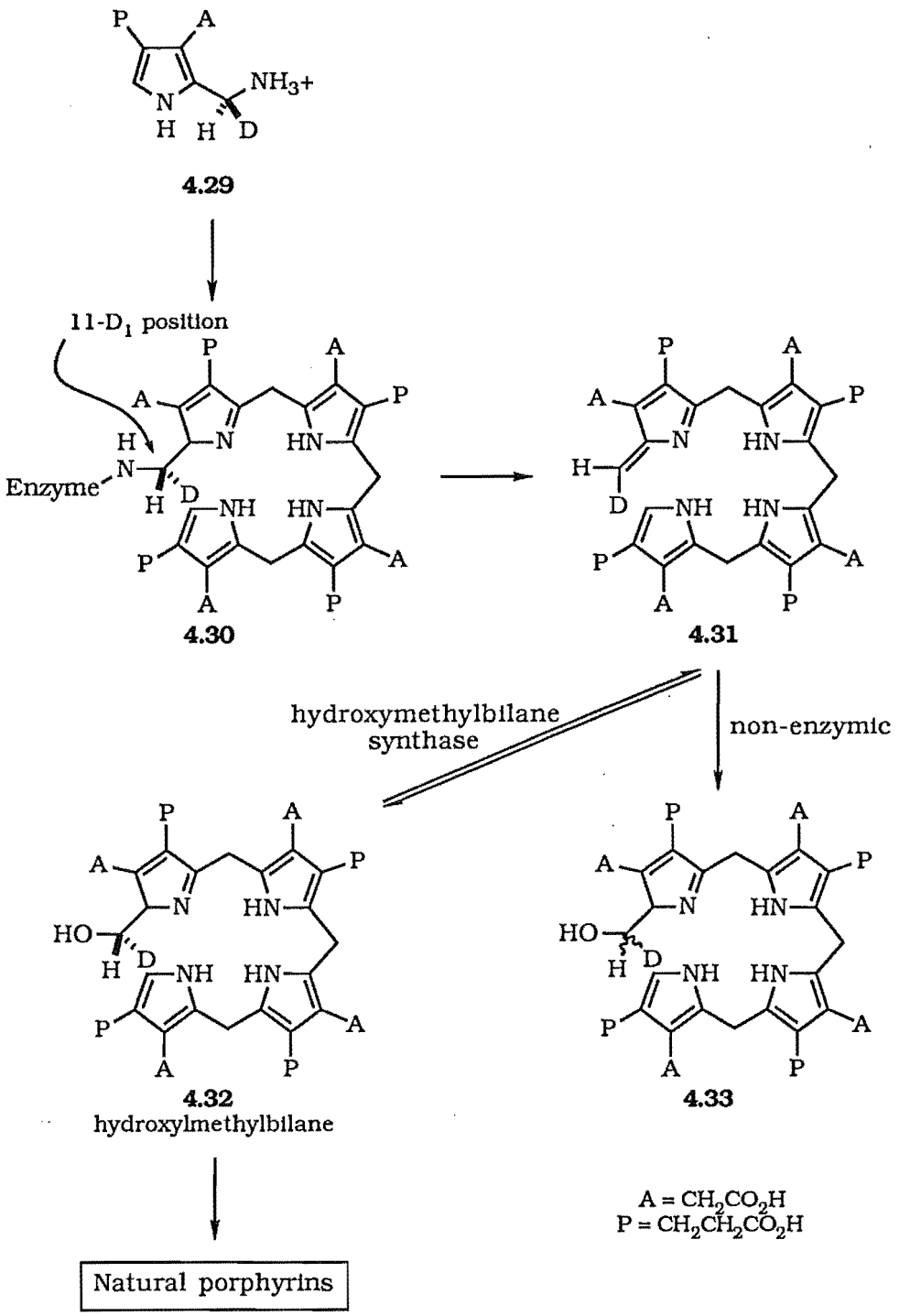

Scheme 4.35

Chiral labelling was also used in the current work, to gain an insight into the reactions of hydroxymethyl pyrroles, eg: **2.32**, with a nucleophile, eg: an amine. The amine was designed to mimic a nucleophilic residue of an enzyme, that is expected to react with the electrophilic azafulvene to give enzyme inhibition.

A trial reaction using the unlabelled hydroxymethyl pyrrole **3.45**, Scheme 4.36, in the presence of racemic *sec*-butylamine and HO^-, showed a

clearly resolved doublet centred at 3.54ppm and 3.56ppm, Figure 4.37 for pyr-CH_2NHR group of **4.35**. Therefore, the hydrolysis using the optically active, labelled hydroxymethyl pyrrole **4.14** and optically active (S)-(+)-*sec*-butylamine would clearly indicate the stereochemical outcome of the chiral centre.

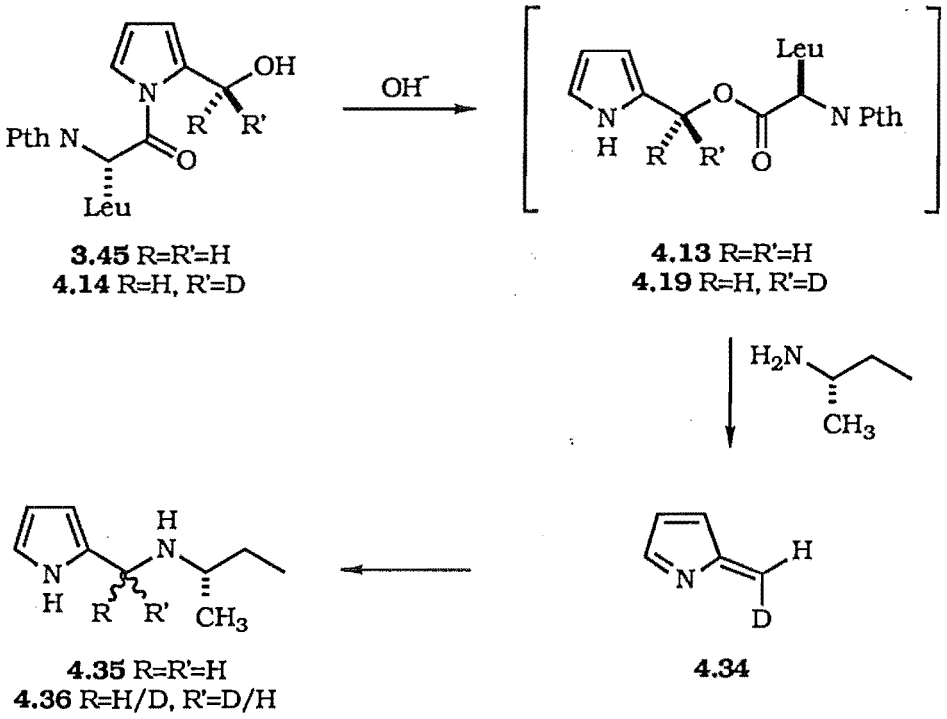

3.45 R=R'=H
4.14 R=H, R'=D

4.13 R=R'=H
4.19 R=H, R'=D

4.35 R=R'=H
4.36 R=H/D, R'=D/H

4.34

Scheme 4.36

^{1}H NMR Spectra of Methylene Region of Pyrrole Amines 4.35 and 4.36

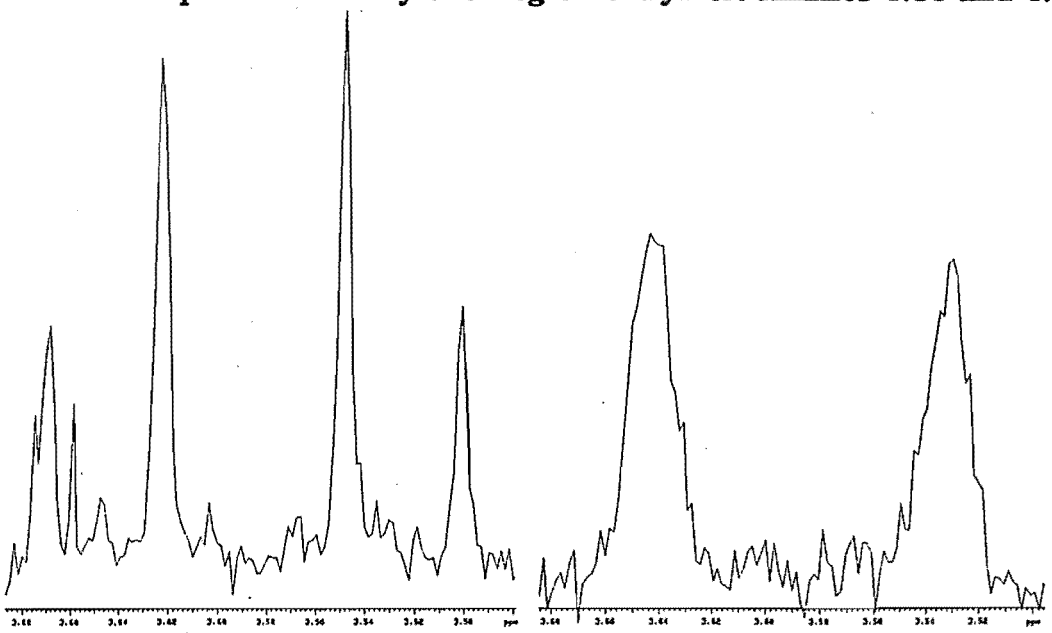

4.35 **4.36**

Figure 4.37

The hydroxymethyl pyrrole **4.14** was subjected to the hydrolysis conditions described in Section 4.6.2. Addition of the chiral amine (S)-(+)-*sec*-butylamine to **4.14** in d_3-acetonitrile was followed by HO^- (1equiv. KOH in D_2O). The deacylation immediately produced the *O*-acylated pyrrole derivative **4.19**, shown previously to be the 'S' enantiomer, Section 4.7.1.2.

The desired labelled amine **4.36** was also formed within ten minutes. ^1H NMR spectral analysis of **4.36** showed two, one proton signals at 3.54ppm and 3.56ppm, Figure 4.37. This clearly indicated that racemisation of the -CHD- group has occurred.

Therefore there is strong evidence that the azafulvene **4.34** does form on the hydrolysis of **4.14**. The hydrolysis of **4.14** forms the optically active **4.19**. This then deacylates to give the azafulvene **4.34**, in which subsequent nucleophilic attack on **4.34** by *sec*-butylamine clearly shows racemisation of the -CHD- group.

The implication is that enzymic catalysed cleavage of the amino acid-pyrrole bond will release the latent reactivity thereby allowing inhibition.

4.7.2.2 *Formation of Pyrrole Amine* **4.6**, **4.35** *and* **4.36**

Evidence that the azafulvene **1.3** forms is obtained when the reaction between an alcohol and a primary amine does not give a secondary amine, Scheme 4.38, is considered, see Section 4.3.4.

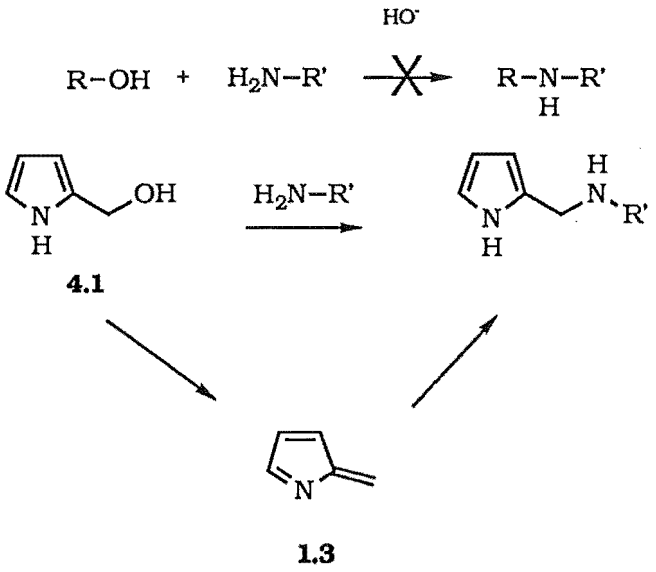

Scheme 4.38

The pyrrole amines **4.6**, **4.35** and **4.36** are suggested to form via attack of an added external nucleophile, n-butylamine and *sec*-butylamine, respectively on the azafulvene **1.3**. It is felt that this reaction can only occur

via the azafulvene.

When the reaction was carried out, without sufficient nucleophile being present, the azafulvene was attacked by the hydroxymethyl pyrrole **4.1** to produce polymeric pyrrole material, as evidenced by the colour of the solution and the staining of the NMR tube. Base catalysed pyrrole polymer formation is strongly suggestive of azafulvene formation.

4.8 Conclusion

The hydrolysis studies discussed in this chapter have shown that the deacylation of hydroxymethyl pyrrole derivatives, eg: **2.32**, produces an electrophilic species, probably the azafulvene **1.3**. This electrophilic species is rapidly trapped either by an external nucleophile, added to mimic an enzyme's nucleophilic residues, or by another hydroxymethyl pyrrole to give polymeric products. The activation of **2.32** proceeds, in part, by an initial *N*- to *O*- acyl transfer, with the subsequent release of the postulated azafulvene **1.3**.

The decomposition of **4.5** to produce the hydroxymethyl pyrrole amine **4.6** was shown to be first order with respect to HO^- concentration from zero to three equivalents.

The use of optically active, deuterated hydroxymethyl pyrrole derivatives enabled the elucidation of the stereochemical fate of the pyr-CH_2OR group in nucleophilic displacement reactions and the deacylation reactions catalysed by HO^-. The results suggest that HO^- attacks the hydroxymethyl pyrrole, followed by attack of the oxyanion at the amide carbonyl in an intramolecular cyclisation. The cyclised product is not observed, but rapidly breaks down to produce **4.19** with *retention* of configuration.

N-Acylation of hydroxymethyl pyrroles was shown to suppress azafulvene formation. There was no reaction of **2.32** in a n-butylamine solution after two months. Deacylation of the pyrrole by HO^- caused rapid formation of products produced via the displacement of the OH group. The Mitsunobu reaction was also shown to proceed with partial S_N2 character if azafulvene formation had not been suppressed by *N*-acylation, racemisation would have occurred. A full S_N2 process would have occurred if no azafulvene chemistry was involved, thus resulting in exclusive inversion of chirality.

The azafulvene **1.3** was shown to form, since the pyrrole amine pyr-C*H*DNHR group of **4.36** was found to have racemised.

The designed mechanism based inhibitors are expected to produce an azafulvene in the enzymes' active site, Section 1.1. This may then be attacked by a further nucleophilic residue on the enzyme, thus binding the pyrrole to the enzyme. The end result should be inhibition of the enzyme.

4.9 References to Chapter Four

[1] Brown, R. S.; Bennet, A. J.; Slebocka-Tilk, H.; Jodhan, A. *J. Am. Chem. Soc.* **1992**, *114*, 3092-3098.

[2] Silverstein, R. M.; Ryskiewicz, E. E.; Chaikin, S. W. *J. Am. Chem. Soc.* **1954**, *76*, 4485-4486.

[3] Jones, A. R. *The Chemistry of Heterocyclic Compounds*; Vol. 48; John Wiley and Sons: New York, 1990.

[4] *VNMR*, Version 4.1, Varian Nuclear Magnetic Resonance Instruments; California: 1992.

[5] Gelan, J.; Limburgs Universitair Centrum; Belgium.

[6] March, J. *Advanced Organic Chemistry*, Third Ed; John Wiley & Sons: New York, 1985; p340.

[7] Slebocka-Tilk, H.; Bennet, A. J.; Hogg, H. J.; Brown, R. S. *J. Am. Chem. Soc.* **1991**, *113*, 1288-1294.

[8] DeWolfe, R. H.; Newcomb, R. C. *J. Org. Chem.* **1971**, *36*, 3870-3878.

[9] Scudder, P. H. *J. Org. Chem.* **1990**, *55*, 4238-4240.

[10] Okuyama, T.; Gandour, R. D.; Fueno, T. *Chem. Lett.* **1990**, 273-276.

[11] Menger, F. M.; Donohue, J. A. *J. Am. Chem. Soc.* **1973**, *95*, 432-437.

[12] Schowen, R. L.; Jayaraman, H.; Kershner, L. *J. Am. Chem. Soc.* **1966**, *88*, 3373-3375.

[13] Gani, V.; Viout, P. *Tetrahedron* **1976**, *32*, 2883-2889.

[14] Ingold, C. K. *Structure and Mecanism in Organic Chemistry*, 2nd Ed; Cornell University Press: New York, 1969.

[15] Jones, A. R.; Bean, G. P. *The Chemistry of Pyrroles*; Academic Press Inc.: London, 1977; pp151-163.

[16] Campbell, J. R. *Aldrichimica Acta* **1971**, *4*, 55-60.

[17] Kime, K. A.; Sievers, R. E. *Aldrichimica Acta* **1977**, *10*, 54-62.

[18] Ward, D. E.; Rhee, C. K. *Tetrahedron Lett.* **1991**, *32*, 7165-7166.

[19] Bosshard, H. H.; Mory, R.; Schmid M.; Zollinger, H. *Helv. Chim. Acta* **1959**, *42*, 1653-1658.

[20] Midland, M. M.; Tramontano, A.; Zderic, S. A. *J. Chem. Soc. Chem. Commun.* **1977**, 5211-5215.

[21] Abell, A. D. Post-Doctoral Thesis, Cambridge, England, 1986.

[22] Midland, M. M.; Tramontano, A.; Zedric, S. A. *J. Chem. Soc. Chem. Commun.* **1979**, 2352-2354.

[23] Schauder, J-R.; Jendrezejewski, S.; Abell, A.; Hart, G. J.; Battersby, A. R. *J. Chem. Soc., Chem. Commun.* **1987**, 436-438.

[24] March, J. *Advanced Organic Chemistry*, Third Edition; John Wiley & Sons: New York, 1985; p294.

[25] Mitsunobu, O. *Synthesis* **1981**, 1-28.

[26] Neidhart, W.; Anderson, P. C.; Hart, G. J.; Battersby, A. R. *J. Chem. Soc., Chem. Commun.* **1985**, 924-927.

Chapter Five

Enzyme Testing and Molecular Modelling

5.1 α-Chymotrypsin Assay of Selected Hydroxymethyl Pyrroles

The pyrroles **2.52**, **2.55**, **3.39**, **3.45**, **3.53** and **3.55**, Figure 5.1, were tested as potential inhibitors of α-chymotrypsin as outlined by Cannell[1,2]. The α-chymotrypsin assay was based on a colourimetric technique, where enzymic release of a coloured derivative, from the substrate, indicates activity.

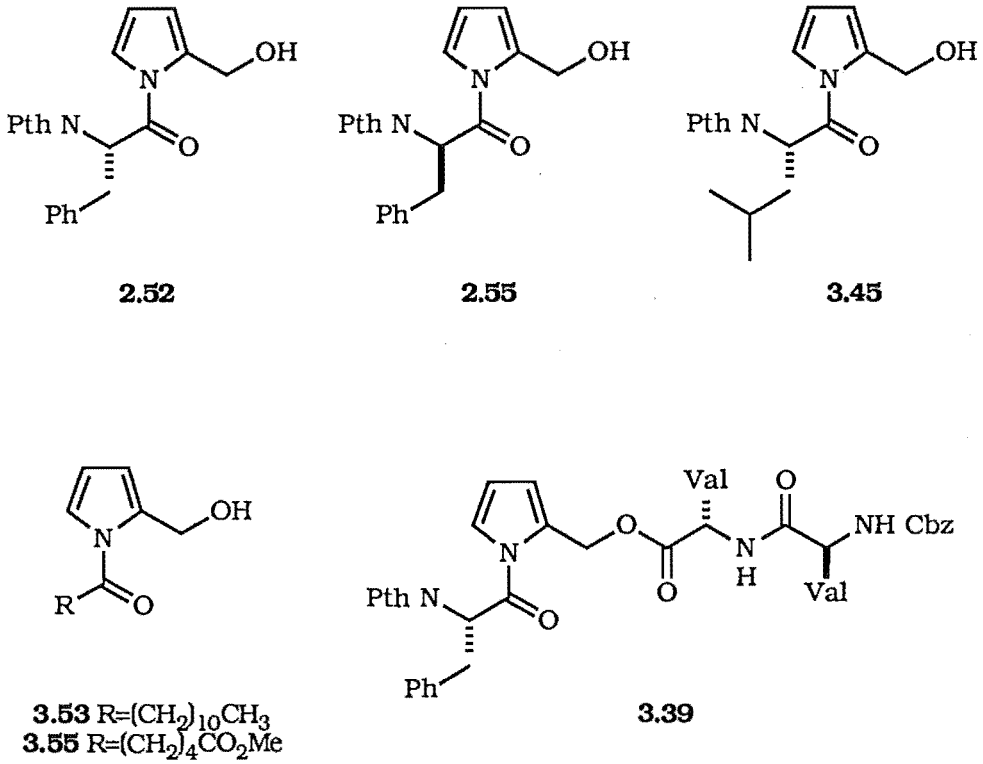

Figure 5.1

Solutions of the pyrroles to be tested were made up to 12.5μg mL^{-1} and 125μg mL^{-1} as standard solutions in methanol. The buffer, Tris-HCl (pH 7.6), the pyrrole test solution and an α-chymotrypsin solution (50mM in Tris-HCl buffer, pH 7.6) were added to each well of a microtitre plate. Preincubation of this solution at 37°C for thirty minutes was followed by the addition of the substrate *N*-succinyl-phenylalanine-4-nitroanilide **5.1**, Scheme 5.2. The enzyme and test solutions were preincubated to ensure maximum inhibition before addition of the substrate. After the addition of the substrate **5.1**, the optical density was measured over approximately two hours. The absorbance was read at 410nm at t=0, and after incubation at 37°C when significant colour change had taken place.

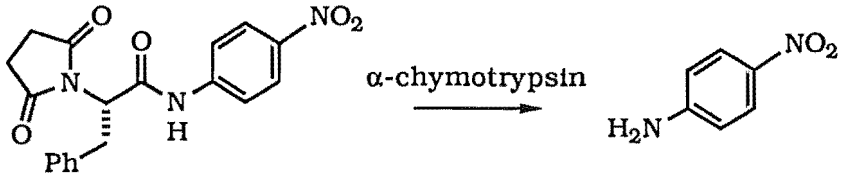

5.1 **5.2**

Scheme 5.2

Control samples were included in all assay cases and each sample was tested in duplicate. Methanol was used to dissolve the proposed inhibitor and for subsequent sample dilution as it was water soluble and hence compatible with the assay system.

The assay was based on the breakdown of the colourimetric substrate **5.1** by the enzyme to produce a coloured product **5.2**, Scheme 5.2. The colour development, due to enzymic release of 4-nitroanilide **5.2**, indicated that the enzyme was active. Lack of colour development, therefore, indicated inhibition.

The results obtained, Table 5.1, indicate that the pyrrole derivatives designed as mechanism based inhibitors of proteolytic enzymes, Section 1.2, are modest inhibitors of α-chymotrypsin.

Compound	**% Inhibition** ($12.5\mu g\ mL^{-1}$)	**% Inhibition** ($125\mu g\ mL^{-1}$)
2.52	24.1	42.9
2.55	15.2	31.8
3.45	20.5	24.7
3.53	14.3	53.3*
3.55	22.8	9.2
3.39	42.9	95.4*

* Precipitation occurs in Reaction Well.

Table 5.1

These data are represented in Figure 5.3.

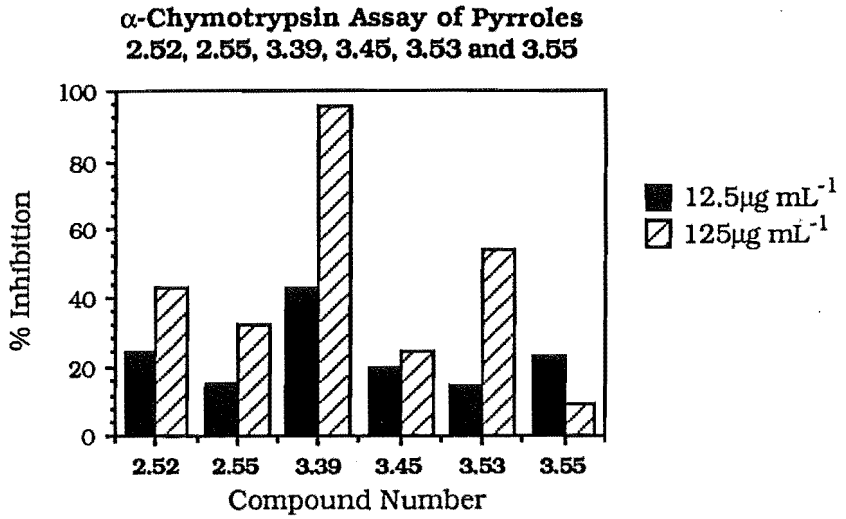

Figure 5.3

There is a 150% decrease in the activity of the 'D' amino acid hydroxymethyl pyrrole **2.55** with respect to the 'L' derivative **2.52**, Figure 5.4. The value represented here for the 'D' amino acid **2.55** has been corrected for the 35% 'L' component, caused by racemisation, Section 2.4.6. The decrease indicates that the natural amino acid configuration is important for enzyme recognition, as would be expected in an enzyme system.

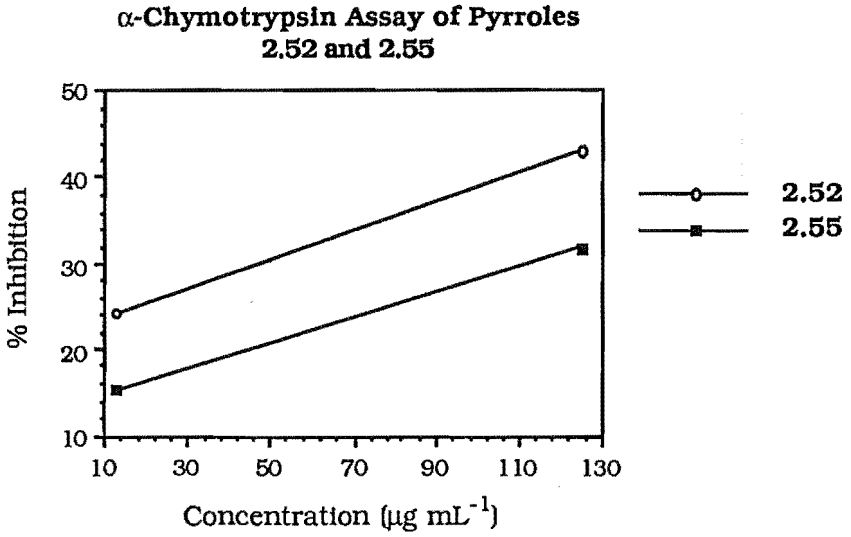

Figure 5.4

The 'L'-Phe derivative **2.52** shows 42.9% inhibition at 125μg ml^{-1}. The tetrapeptide **3.39** also shows 42.9% inhibition, but at a lower concentration. This inhibition is the best observed, excluding the derivatives that precipitated. The inhibition is consistent with the known fact that α-chymotrypsin cleaves amide bonds on the *C*-terminal side of aromatic amino

acids, Section 1.2.3. The extension of the peptide chain in **3.39** to increase hydrogen bonding to the enzyme, also increases the inhibition of the enzyme.

The inhibitor properties of the other pyrrole derivatives are satisfactory, since they are not ideally suited for targeting α-chymotrypsin. The precipitation of **3.39** and **3.53** in the reaction well, indicates that the compounds are unstable (or not soluble) to the assay conditions. The same result is observed and discussed in Section 5.2.

The results shown in Table 5.1 indicate that the compounds designed as mechanism based inhibitors of proteases were active against α-chymotrypsin.

Potential lead compounds have been established. These pyrroles contain the required aspects that were incorporated into the designed mechanism based inhibitors, Section 1.1. The latent reactivity is contained in the *N*-acylated, 2-substituted pyrrole. The hydroxymethyl pyrroles **2.52**, **2.55**, **3.45**, **3.53** and **3.55** contain the latent reactivity. There is however little opportunity for hydrogen bonding to the enzyme. This has been shown to be important to the inhibition of α-chymotrypsin, Section 1.2.1 and to the HIV protease, Section 1.2.3. Hydrogen bonding has been addressed in the extension in the *C*-direction, P_1' and P_2' residues, by the addition of the dipeptide Cbz-Val-Val-OH to give **3.39**. To make a better inhibitor of α-chymotrypsin, additional hydrogen bonding must be included by further extension in the P_x' direction. The effect of varying the residues in the P_x' direction should also be examined. The methodology outlined in Chapter Two and Three enables this to be possible. The removal of the *N*-Pth protecting group would also enable extension in the *N*-direction, by adding more P_x residues. This possibility was described in Section 2.4.7.

5.2 HIV-1 Protease Assay of Selected Hydroxymethyl Pyrroles

The selected pyrroles **2.32**, **2.52**, **3.39**, **3.53** and **3.55** were tested against the HIV-1 protease[3]. The testing conditions used were first described by Dreyer[4]. The compound under study was dissolved in DMSO and placed in the acidic MENDT buffer (50mM Mes. pH 6.0/1mM EDTA/200mM NaCl/1mM dithiothreitol/0.1% Triton X-100). The inhibition of the HIV-1 protease was observed by incubating the protease (110ng) at 37°C for one hour with 2μg of the polyprotein p55, a substrate for the HIV-1 protease, Section 1.2.3. Reactions were quenched by boiling for two minutes in $NaDodSO_4$/PAGE buffer. The rates of cleavage were determined by HPLC analysis of the peptidolysis products.

Initial results of the simple, non-peptide based, potential inhibitor **2.32** and the one amino acid hydroxymethyl pyrrole **2.52** showed that there was no inhibition at concentrations <1mg mL^{-1}. There was slight inhibition above these concentrations. This was encouraging as **2.32** and **2.52** showed some similarity to a HIV-1 protease substrate, Section 1.2.3, but lacked the extended hydrogen bonding also known to be important for inhibition of the protease[5,6]. The improvement of the proposed inhibitor is possible by the addition of extended hydrogen bonding positions in the molecule, and overall hydrophobic interactions within the enzyme/inhibitor complex.

The synthesis of the tetrapeptide pyrrole derivative **3.39**, as described in Section 3.2.5, and the long chain derivatives, **3.53** and **3.55**, Section 3.3.2, were thought of as the next generation of inhibitors.

The C_2 inhibitors[7], Section 1.2.3 and Section 3.2.5 showed that amino acid extension in the "anti-sense" fashion produced potent inhibitors of HIV-1 protease. The tetrapeptide **3.39** was synthesised along these lines, it contains the crucial P_1 and P_1' interactions of Phe and "Pro"[8] respectively, Section 1.2.3. The extension of the peptide chain in the C-direction, Section 3.2.5, increases the important hydrogen bonding interactions between the inhibitor and enzyme at the P_2' and P_3' subsites. The large aromatic amino acid protecting group, Pth, at the P_2 subsite is also consistent with known inhibitors of the HIV-1 protease[9].

The long chain hydroxymethyl pyrrole **3.53** was designed on the basis of the known inhibitors cerulenin **5.3**, and **5.4**[10], Figure 5.5.

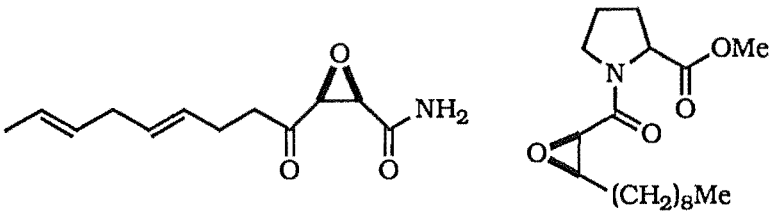

cerulenin **5.3** **5.4**

Figure 5.5

This work found that an eleven carbon chain was the optimal length for inhibition of the HIV-1 protease, using long chain aliphatic residues, eg: **5.3**, Figure 5.6.

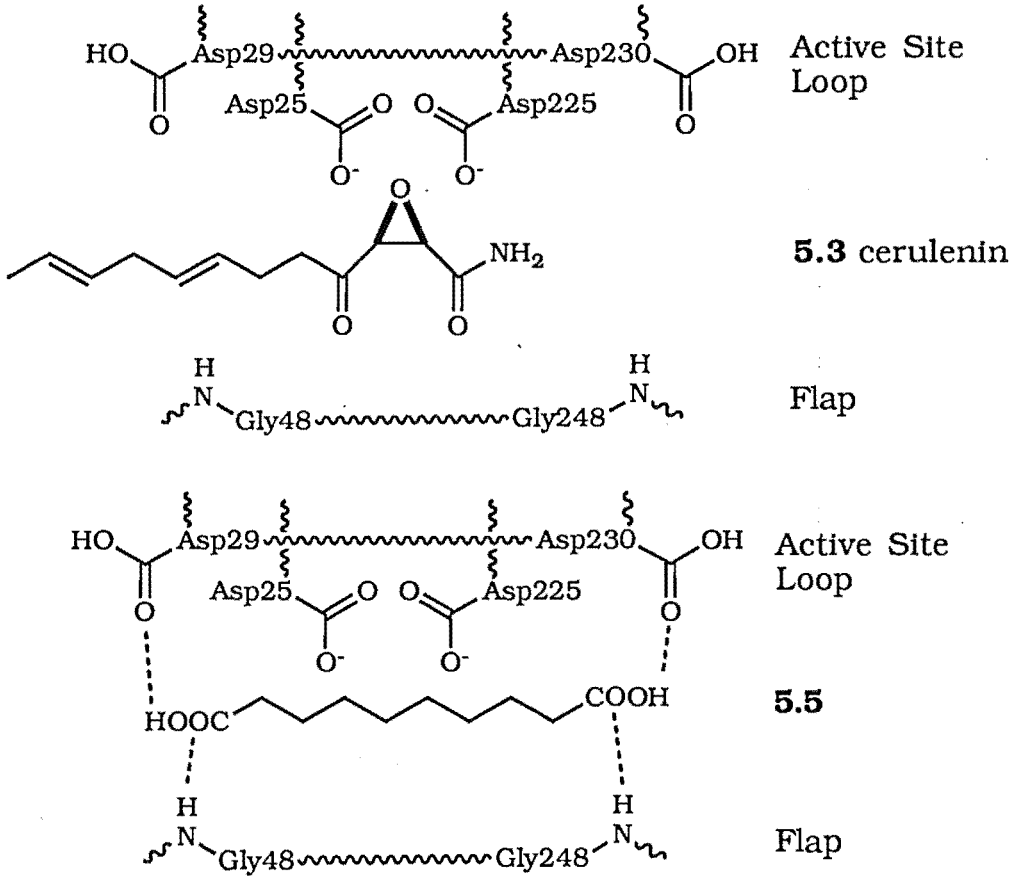

Figure 5.6

The researchers postulated that the interaction between the hydrophobic chain and the HIV proteases' hydrophobic pocket, was responsible for the inhibition. In general, they found that a hydrophobic residue of a correct length is required for efficient inhibition of the HIV protease[10].

In contrast to the long chain hydrophobic residues described above

are the shorter chained carboxylates[11]. This work found that the inhibition of the HIV-1 protease was likely to occur via interaction of the carboxylates, eg: **5.5**, Figure 5.6, with the charged residues at the ends of the hydrophobic tube created around the active site of the HIV-1 protease, Section 1.2.4. The optimal length was found to be eight CH_2 groups flanked at each end by a terminal carboxylic acid group.

The shorter chain *N*-acylated methyl ester hydroxymethyl pyrrole **3.55** was designed on the basis of the work of non-peptide carboxylates. It was proposed that four CH_2 groups and the methyl ester would position the latent reactivity at the active site in the **3.55** proposed inhibitor.

The three inhibitors, **2.32**, **2.52**, **3.39**, **3.53** and **3.55**, were tested against an HIV-1 protease assay. All the pyrrole derivatives showed <1mg mL^{-1} inhibitory properties. The low activity of **2.32**, **2.52**, **3.39**, **3.53** and **3.55** was attributed to the instability of the pyrrole derivatives to the assay conditions.

5.2.1 Stability of Hydroxymethyl Pyrroles to Enzyme Assay Conditions

It was felt that the acidic conditions under which the assays were conducted caused the decomposition of hydroxymethyl pyrroles.

The stability of the hydroxymethyl pyrrole **2.52** was tested under the HIV-1 protease assay conditions. The hydroxymethyl pyrrole **2.52** was dissolved in DMSO and placed in an acidic buffer (potassium phthalate/phthalic acid pH 5.9) at 37°C for one hour. After fifteen minutes a precipitate had formed. This precipitate was insoluble in water and chloroform, and was attributed to the formation of a pyrrolic polymer.

The hydroxymethyl pyrrole compounds may be potential mechanism based inhibitors of HIV-1 protease. The decomposition of the inhibitor clearly shows that the inhibition of the enzymes under these conditions may not be observed due to the pyrrole polymer forming.

5.2.2 Increase in Stability of Hydroxymethyl Pyrrole Scissile Bond

The pyrrole derivatives were found to be unstable under the assay conditions described in Sections 5.1 and 5.2. The stability of the scissile bond to the assay conditions may be increased by the addition of electron donating substituents on the leaving group. The leaving group governs the lability of the amide bond. An increase in the electron density at the amino acid-pyrrole amide bond, would increase the stability of the amide bond. The most obvious target would be the methyl hydroxymethyl pyrrole derivative **5.6**.

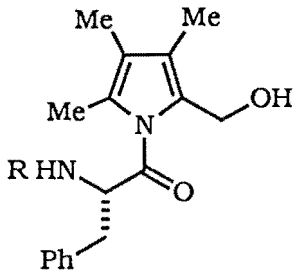

5.6

The methyl groups would not be expected to form destabilising interactions between the inhibitor and the enzyme. An increase in electron density would be expected to stabilise this bond and thereby increasing the stability of the proposed hydroxymethyl pyrrole inhibitors to the assay conditions. This aspect of work was not attempted.

5.3 Molecular Modelling of a Simple Hydroxymethyl Pyrrole 5.7

Molecular modelling and associated graphics is frequently used to visualise enzyme-inhibitor interactions. The generation of low energy conformers of a potential inhibitor allows the observation of enzyme-inhibitor interactions[12]. There is no guarantee that the enzyme-inhibitor structure data obtained from the modelling, relate to the actual enzyme-inhibitor complex.

The simple hydroxymethyl pyrrole **5.7** was subjected to a modelling study, to give an indication of the possible interactions between the hydroxymethyl pyrroles and α-chymotrypsin and the HIV-1 protease.

5.3.1 Generation of Minimised Low Energy Conformers

The dipeptide H_2N-Phe-p-2-OH **5.7**, Figure 5.7, was constructed using the INSIGHTII package[13] and subjected to a Monte Carlo[14] conformational search by BATCHMIN[15,16] using the all atom AMBER force field[17]. All the rotatable bonds, Figure 5.7, were searched to find the set of low energy conformers.

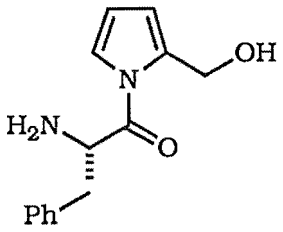

5.7
N-Pth-Phe-p-2-OH

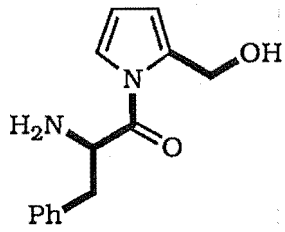

Bonds Rotated during Conformational Search

Figure 5.7

After fifteen hundred increments of a Monte Carlo search, 116 low energy conformers had been found. A further five hundred increments found no new low energy conformers. Each of these were minimised using a conjugate gradient minimisation until the minimisation had converged to a value of 0.01kJ mol^{-1} $Å^{-1}$. This was followed by a Full Matrix Newton-Rapson minimisation of each conformer until the gradient converged to <0.001kJ mol^{-1} $Å^{-1}$. A final second derivative analysis was performed on the output of the final Newton-Rapson minimisation to ensure that none of the conformers found were at turning points. The result from the grid search and subsequent minimisations gave twenty-two low energy conformers within 11kJ mol^{-1} of

the lowest energy conformer, these are shown in Figure 5.9.

5.3.2 Docking Calculations: Low Energy Conformers of 5.7 with HIV-1 Protease

A docking calculation evaluates the interaction energies of many orientations (conformers) between all the atoms of two molecules. The calculation determines those orientations with the lowest energy interactions. The interactions may point to a possible conformation of one molecule, that interacts with the second molecule better than any other conformation. A compound can therefore be synthesised with the conformation of the better interactions expressed.

The coulombic energy and the van der Waals potentials can readily be calculated. The combination of these energy terms can be thought of as an indication of the "goodness-of-fit" for a particular conformer in the active site. Ideally a docking interaction would be calculated while one molecule is moved in relation to the second molecule, in real time. The computation of the interactions is easy but computation time increases rapidly, with an increase in the size of the two molecules. An energy grid that encompasses the regions of interest of one molecule, eg: the active site of an enzyme, has been shown to approximate the whole molecule to a good degree[18]. The energies between the molecule being docked and the energy grid changes. The energy grid itself does not alter. This allows real time docking.

The X-ray crystal coordinates of the HIV-1 protease complexed with the JG-365 inhibitor, **1.40** (Brookhaven 7HVP[6]) were used in the following calculations[19].

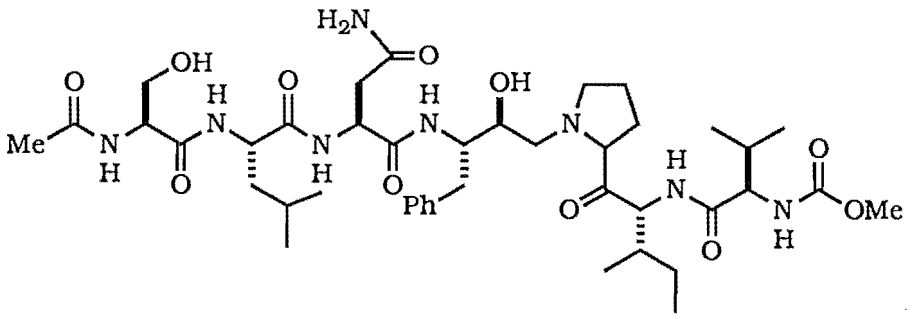

JG-365

1.40

An energy grid of the inhibited HIV-1 protease active site, was created taking all elements in a 4.2Å radius from the JG-365 inhibitor. This subset contained the bound water molecule and the two aspartic acids of the active

site. Three atoms from the proposed hydroxymethyl pyrrole inhibitor **5.7** were superimposed on corresponding atoms of the JG-365 inhibitor **1.40**, Figure 5.8. These three atoms from the JG-365 inhibitor were chosen because they positioned the Pyr "pseudo" amino acid of **5.7** at P_1' and the Phe in the vicinity of the P_1 subsite, as described in Section 1.2.4.

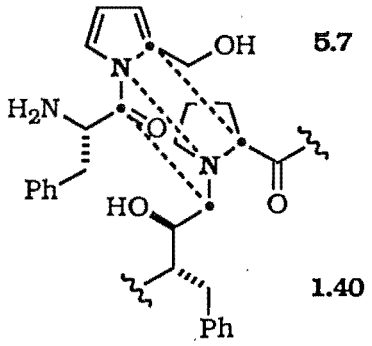

Figure 5.8

Each conformer was "docked" into the active site of the JG-365 inhibitor using the DOCKING protocol of the Biosym software. The values that the docking calculation produces are only relative to each conformer in the same series. This gives an indication of the "goodness-of-fit". The twenty-two low energy conformers depicted in Figure 5.9 are shown in order of increasing "docking energy". The lower the "docking energy" the more favourable are the interactions. The energy calculated by MACROMODEL is given in italics.

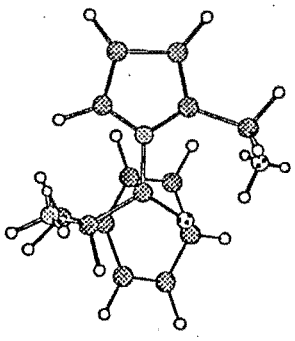

I*
3.113
114.5

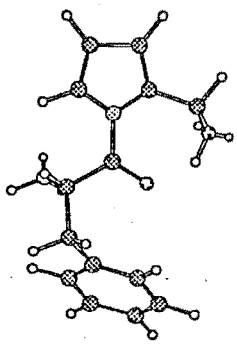

II*
3.442
119.0

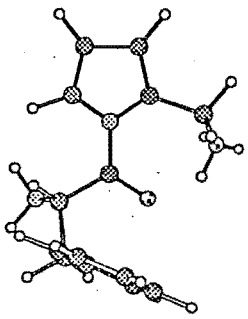

III*
3.585
118.9

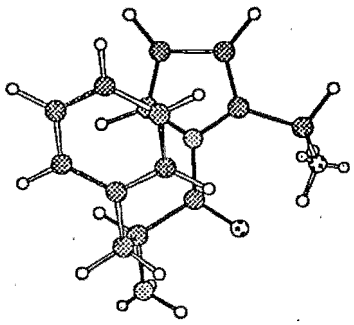

IV
3.603
115.7

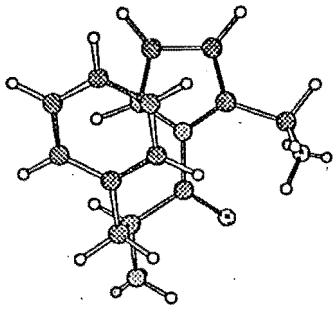

V
3.706
116.3

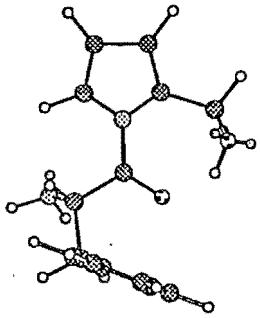

VI*
3.736
113.1

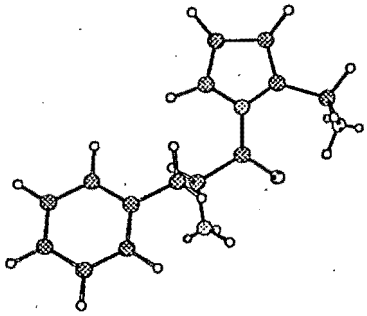

VII
3.791
119.8

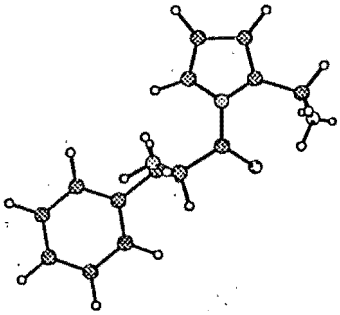

VIII
3.802
121.5

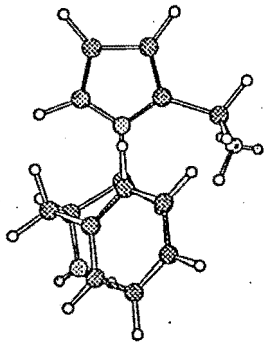

IX
3.802
116.2

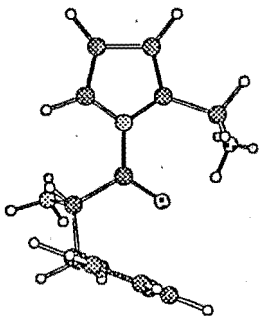

X
3.822
113.9

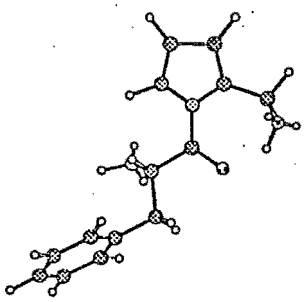

XI*
3.841
112.5

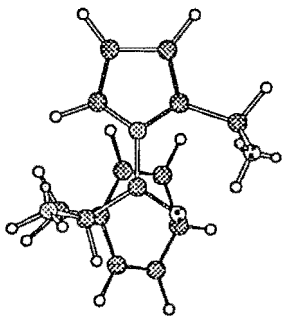

XII*
3.872
115.6

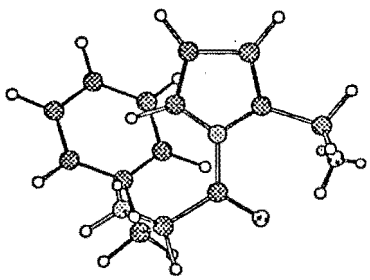

XIII
3.886
123.3

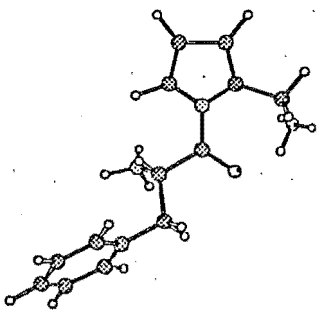

XIV*
3.990
112.8

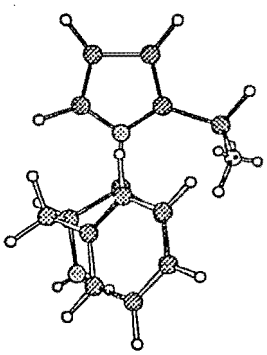

XV
4.053
114.9

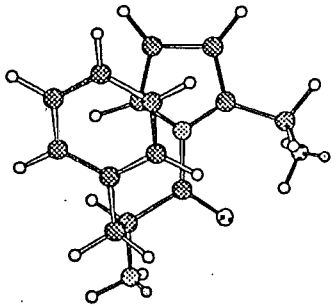

XVI
4.080
123.3

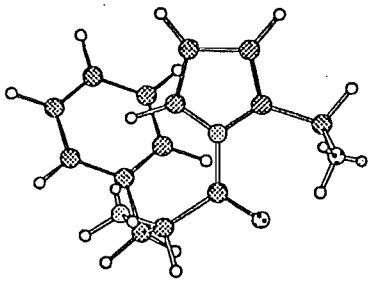

XVII
4.125
123.5

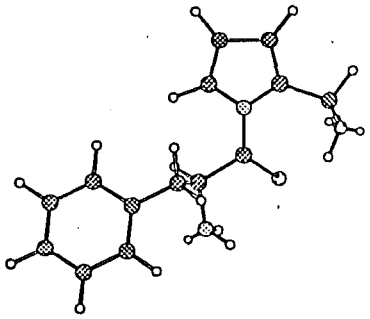

XVIII
4.135
119.8

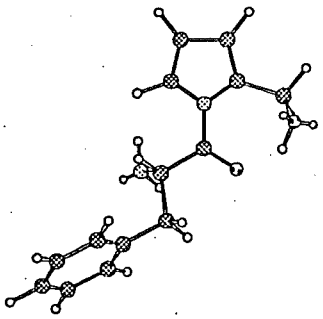

XIX
4.163
123.5

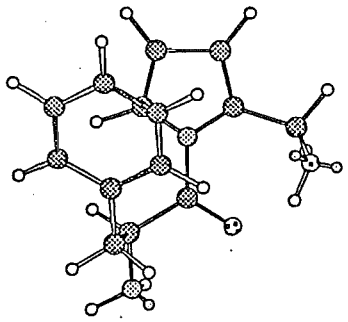

XX
4.270
122.8

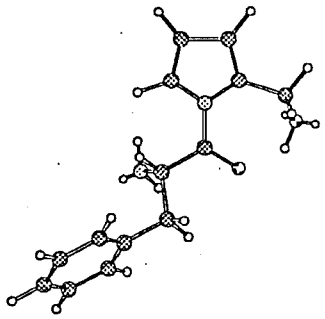

XXI*
5.005
123.2

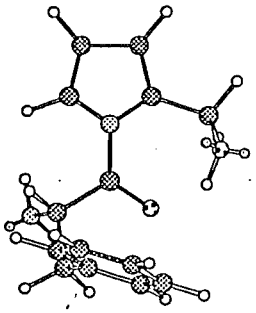

XXII
5.037
121.9

Figure 5.9

A visual inspection of the proposed inhibitor **5.7**, and the results from the non-bonding energies obtained in the docking calculations, suggests that the inhibitor does fit into the active site. The first three conformers (and those denoted with a * in Figure 5.9) have the phenyl ring of Phe (P_1) in the hydrophobic pocket (S_1) of the enzyme. The lowest non-bonded energy conformer that showed hydrogen bonding to both the water molecule and the aspartic acids was conformer II.

Computational time restraints did not permit a dynamics run of conformer II in the active site to see if the non-bonding interactions are improved[20] nor studies on α-chymotrypsin.

5.4 Conclusion

The assay results from α-chymotrypsin and HIV-1 protease are encouraging in regard to enzyme activity. Chymotrypsin is well known to cleave on the carboxyl side of aromatic amino acids, as is the HIV protease. The proposed mechanism based enzyme inhibitors have been shown to be active against these proteolytic enzymes. The inhibition of α-chymotrypsin was modest, while the inhibition of HIV-1 protease was very poor. This has been related to the instability of the hydroxymethyl pyrroles to the harsh assay conditions. No attempt has been made to optimise the activity.

An increase in activity of the hydroxymethyl pyrrole derivatives can be expected if more sites for hydrogen bonding are added to the proposed inhibitor, Chapter Three addresses this possibility. The alternative, and most important in regards to a useful pharmaceutical agent, is to increase the stability of the amino acid-pyrrole amide bond so that decomposition does not occur as readily. This may be possible by the introduction of methyl groups in to the pyrrole ring.

Molecular modelling was used as a tool to allowed the visualisation of a potential inhibitor in the active site of the HIV-1 protease. This result showed that the Phe can sit at the P_1 subsite with Pyr at the P_1' subsite, indicating favourable interactions for hydrolysis and release of the latent reactive group.

5.5 References to Chapter Five

[1] Cannell, R. J. P.; Kellam, S. J.; Owsianka, A. M.; Walker, J. M. *Planta Med.* **1988**, *54*, 10-14.

[2] Cannell, R. J. P.; Kellam, S. J.; Owsianka, A. M.; Walker, J. M. *J. Gen. Microbiol.* **1987**, *133*, 1701-1705.

[3] Testing completed at SmithKline Beecham Pharmaceuticals: King of Prussia, U.S.A.

[4] Dreyer, G. B.; Metcalf, B. W.; Tomaszek Jn, T. A.; Carr, T. J.; Chandler III, A. C.; Hyland, L.; Fakhoury, S. A.; Magaard, V. W.; Moore, M. L.; Strickler, J. E.; Debouck, C.; Meek, T. D. *Proc. Natl. Acad. Sci. USA* **1989**, *86*, 9752-9756.

[5] Miller, M.; Schneider, J.; Sathyanarayana, B. H.; Toth, M. V.; Marshall, G. R.; Clawson, L.; Selk, L.; Kent, S. B. H.; Wlodawer, A. *Science* **1989**, *246*, 1149-1153.

[6] Swain, A. L.; Miller, M. M.; Green, J.; Rich, D. H.; Schneider, J.; Kent, S. B. H.; Wlodawer, A. *Proc. Natl. Acad. Sci. USA* **1990**, *87*, 8805-8809.

[7] Kempf, D. J.; Norbeck, D. W.; Codacovi, L-M.; Wang, X. C.; Kohlbrenner, W. E.; Wideburg, N. E.; Paul, D. A.; Knigge, M. F.; Vasavanonda, S.; Craig-Kennard, A.; Saldivar, A.; Rosenbrook Jn, W.; Clement, J. J.; Plattner, J. J.; Erickson, J. *J. Med. Chem.* **1990**, *33*, 2687-2689.

[8] Huff, J. R. *J. Med. Chem.* **1991**, *34*, 2305-2314.

[9] Roberts, N. A.; Martin, J. A.; Kinchington, D.; Broadhurst, A. V.; Craig, J. C.; Duncan, I. B.; Galpin, S. A.; Handa, B. K.; Kay, J.; Kröhn, A.; Lambert, R. W.; Merrett, J. H.; Mills, J. S.; Parkes, K. E. B.; Redshaw, S.; Ritchie, A. J.; Taylor, D. L.; Thomas, G. J.; Machin, P. J. *Science* **1990**, *247*, 358-361.

[10] Blumenstein, J. J.; Copeland, T. D.; Oroszlan, S.; Michejda, C. J. *Biochem. & Biophys. Res. Comm.* **1989**, *2*, 980-987.

[11] Brinkworth, R. I.; Woon, T. C.; Fairlie, D. P. *Biochem. Biophys. Res. Commun.* **1991**, *176*, 241-246.

[12] Ferguson, D. M.; Radmer, R. J.; Kollman, P. A. *J. Med. Chem.* **1991**, *34*, 2654-2659.

[13] *InsightII* (V2.0.0) Biosym Technologies, Inc: San Deigo, 1991.

[14] Chang, G.; Guida, W. C.; Still, W. C. *J. Am. Chem. Soc.* **1989**, *111*, 4379-4386.

[15] *MacroModel Interactive Modeling System* (V3.1); Department of Chemistry, Columbia University: New York, 1991.

[16] Mohamadi, F.; Richards, N. G. J.; Guida, W. C.; Liskamp, R.; Lipton, M.; Caufield, C.; Chang, G.; Hendrickson, T.; Still, W. C. *J. Comput. Chem.* **1990**, *11*, 440-467.

[17] Weiner, S. T.; Kollman, P. A.; Nguyen, D. T.; Case, D. A. *J. Comput. Chem.* **1986**, *7*, 230-252.

[18] *Discover: Users Manual* (V2.7), Biosym Technologies, Inc: San Deigo, 1992.

[19] Crystal coordinates supplied by Prof. Amy Swain, NCI-Frederick Cancer Research and Develpoment Center, USA.

[20] Kahn, M.; Nakanishi, H.; Chrusciel, R. A.; Fitzpatrick, D.; Johnson, M. E. *J. Med. Chem.* **1991**, *34*, 3395-3399.

EXPERIMENTAL

6.1 General Experimental

Melting points were recorded on a Reichert micro heating stage and are uncorrected. Infrared spectra were observed either on a PYE Unicam SP3-300 Infrared Spectrophotometer and referenced on the polystyrene absorbance at 1603cm^{-1}, or on a Perkin-Elmer 1600 Series FTIR (denoted in the text as FTIR). UV spectra were observed in either $CHCl_3$ or MeOH, as indicated in the text, on a Perkin-Elmer Lambda 2 UV/Vis spectrometer. ORD spectra were measured on a JASCO J-20C Recording Spectropolarimeter in MeOH at 589nm.

^1H and ^{13}C NMR spectra were measured on a Varian CFT300 NMR spectrometer operating at 300MHz for proton spectra and 75MHz for carbon spectra, in $CDCl_3$ unless otherwise stated. ^1H NMR spectra were referenced on the internal standard trimethylsilane, 0.00ppm, while ^{13}C NMR spectra were referenced on the center resonance of the $CDCl_3$ triplet at 77.01ppm. ^1H NMR spectra in d3-CD_3CN were referenced on the center peak of the CH_3CN signal at 2.00ppm and the corresponding ^{13}C NMR spectral signal at 117.7ppm. ^1H NMR spectra in d4-MeOH were referenced on the center peak of the CH_3OH signal at 3.30ppm and the corresponding ^{13}C NMR spectral signal at 49.3ppm. Complete NMR assignment was based on COSY[1], DEPT[2] and HETCOR[3] (^{13}C-^1H) correlation experiments and NOE enhancement[4] relationships.

Mass spectra were obtained using a Kratos MS80RFA magnetic sector, double focusing mass spectrometer.

Solvents were purified by standard techiniques[5]. The amino acids were obtained from the Sigma Chemical Company, with the exception of Cbz-Val-Val-OH which was purchased from BACHEM Feinchemikalien AG, Switzerland. All other reagents were prepared by standard literature methods or obtained from the Aldrich Chemical Company.

All reactions were carried out under a dry N_2 atmosphere.

Reaction work up usually entailed drying the organic phase (Na_2SO_4), filtration, followed by evaporation under reduced pressure (Büchi Rotory Evaporator, H_2O pump vacuum). Preparative chromatography was carried out using a Chromatotron (Harrison Research Inc.), a centrifugally accelerated, radial, thin layer chromatograph, using glass plates coated with Merck Silica Gel (60 PF_{254}) containing Florisil at 2mm thickness. Visualisation was achieved using an ultraviolet lamp at λ=254nm.

6.1.1 Naming of Compounds Described in the Experimental

For ease of comparison, the simple pyrrole derivatives and 1-amino

acyl pyrroles are named as pyrroles, the larger pyrrole esters are named as amino acid esters.

The pyrrole ring system and the aromatic rings are numbered as depicted in Figure 6.1.

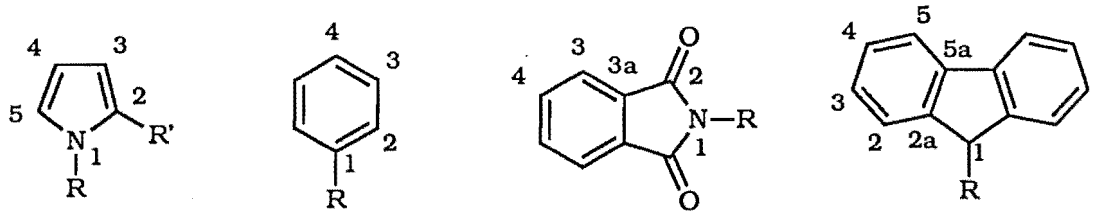

Figure 6.1

The pyrrole ring components are described as H-x or C-x, while the aromatic rings are described as Phe-aromHx (phenylalanine aromatic ring), Cbz-aromHx (benzyloxycarbonyl aromatic ring), Fmoc-aromHx (for Fmoc protected amino acids), Ts-aromHx (tosyl aromatic ring) and Ph-aromHx (for other aromatic rings). The corresponding carbons are described as Phe-aromCx, etc.

6.1.2 General Procedure for the Preparation of Amino Acid Acid Chlorides

The amino acid acid chlorides (with the exception of *N*-Fmoc-Phe-Cl[6]) used in this work were prepared under the following conditions.

General Procedure:

DMF (20μL, 1 drop), followed by freshly distiled oxalyl chloride (5equiv.) were added to the free amino acid (1equiv.) suspended in benzene (10mL, freshly distiled from CaH_2) under N_2. The resultant solution was stirred for 1 h at rt, the benzene was removed (H_2O pump) and the solvent (10mL) used in the subsequent reaction was added. Further evaporation under reduced pressure gave a quantitative yield of the amino acid acid chloride. The resultant acid chlorides derived from Ts and Cbz protecting groups were generally yellow oils, while those from Pth and Fmoc were white solids.

***N*-Ts-Leu-Cl**

^{1}H NMR δ 0.88 (3H, d, *J*=6.5Hz, (Leu-CH_3)$_A$); 0.94 (3H, d, *J*=6.5Hz, (Leu-CH_3)$_B$); 1.53 (1H, m, A part ABX, Leu-CH_2); 1.57 (1H, m, B part ABX,

Leu-CH_2); 1.80 (1H, m, Leu-C*H*(CH_3)$_2$); 2.44 (3H, s, Ts-CH_3); 4.25 (1H, X part ABX, Leu-CH); 5.13 (1H, bd, *J*=10.5Hz, NH); 7.32 (2H, d, *J*=8.0Hz, Ts-aromH3); 7.73 (2H, d, *J*=8.0Hz, Ts-aromH2).

***N*-Pth-Phe-Cl**

^{1}H NMR δ 3.56 & 3.63 (2H, ABX, Phe-CH_2); 5.32 (1H, X part ABX, *J*=5.1Hz, Phe-CH); 7.13-7.21 (5H, m, Phe-arom); 7.74 (2H, dd, *J*=5.7 & 3.3Hz, Pth-aromH3); 7.83 (2H, dd, *J*=5.8 & 3.2Hz, Pth-aromH4).

***N*-Pth-Leu-Cl**

^{1}H NMR δ 0.95 (3H, d, *J*=5.0Hz, (Leu-CH_3)$_A$); 0.97 (3H, d, *J*=5.0Hz, (Leu-CH_3)$_B$); 1.55 (1H, m, C*H*(CH_3)$_2$); 2.05 (1H, A part ABX, m, Leu-CH_2); 2.38 (1H, B part ABX, m, Leu-CH_2); 5.12 (1H, X part ABX, J=4.5Hz, Leu-CH); 7.79 (2H, dd, *J*=5.7 & 2.5Hz, Pth-aromH3); 7.91 (2H, dd, *J*=5.7 & 2.6Hz, Pth-aromH4).

6.1.3 Non-Amino Acid Based Acid Chlorides

The acid chlorides, hydrocinnamyl chloride, isovaleryl chloride, lauralyl chloride, monomethyl adipyl chloride and (-)-camphanic chloride were prepared as follows.

General Procedure:

DMF (20μL, 1 drop) followed by freshly distiled oxalyl chloride (5equiv.) were added to the free acid (1equiv.) dissolved in benzene (10mL, freshly distiled from CaH_2) under N_2. The resultant solution was stirred for 1 h at rt, and the benzene was removed (H_2O pump). The crude acid chloride was distiled under high vacuum, and sealed under N_2. All of these acid chlorides are known compounds.

6.2 Work Described in Section 2.2

6.2.1 NaH Promoted Acylation of Pyrrole-2-Carboxaldehyde by *N*-Ts-Leu-Cl, described in Section 2.2.1

NaH (42mg, 0.88mmol as a 50% suspension in oil, washed twice with dry pentane) was added to a stirred solution of p-2-c (83mg, 0.87mmol) dissolved in THF (10mL, freshly distiled from sodium wire and benzophenone) in a flame dried, N_2 filled flask. The mixture was stirred under N_2 at rt for 15 min and the cooled to 0°C. Ts-Leu-Cl acid chloride **2.17** (388mg, 0.94mmol) was dissolved in dry THF (10mL) and added dropwise to the stirred mixture of the sodium salt of p-2-c, described above, at 0°C over 5 min. The addition of the acid chloride caused immediate production of a deep brown/black solution and an accompanying precipiate. After 15 min water (10mL) was added to quench the reaction; some effervescence was observed. The THF was removed under reduced pressure and CH_2Cl_2 (10mL) was added. The aqueous phase was re-extracted with CH_2Cl_2 (3x15mL) and the combined organic phases washed with water (2x10mL), dried, and filtered to removed the considerable amount of black precipitate. Repeated silica chromatography (EtOAc/Pet. Ether=1:2) produced two new pyrrole compounds.

(2R,4S)-4-(2-Methylpropyl)-2-pyrrol-2-yl-3-toluenesulfonyl-5-oxazolidinone 2.18 29mg (8%) as a mauve oil; R_f 0.48; $[\alpha]^{D}_{26}$ -17° (c1, MeOH); ^{1}H NMR δ 0.87 (3H, d, *J*=6.7Hz, Leu-CH_3); 0.95 (3H, d, *J*=6.6Hz, Leu-CH_3); 1.41 (1H, dd, *J*=11.9 & 9.0Hz, Leu-CH_2); 1.51 (2H, dd, *J*=11.8 & 5.7Hz, Leu-CH_2); 1.92 (1H, sept, *J*=6.6Hz, C*H*(CH_3)$_2$) 2.47 (3H, s, Ts-CH_3); 4.10 (1H, dd, *J*=9.0 & 5.8Hz, N-C*H*(Leu)-CO); 6.18 (1H, m, H-4); 6.24 (1H, m, H-3); 6.68 (1H, s, pyr-CH); 6.85 (1H, m, H-5); 7.39 (2H, d, *J*=8.5Hz, Ts-aromH3); 7.74 (2H, d, *J*=8.4Hz, Ts-aromH2); 8.56 (1H, bs, pyr-NH); ^{13}C NMR δ 21.6, (Leu-CH_3 & Ts-CH_3); 22.6, (Leu-CH_3); 24.2, (*C*H(CH_3)$_2$); 41.4, (Leu-CH_2); 56.2, (N-*C*H(Leu)-CO); 85.8, (pyr-CH); 107.6, (C-3); 109.1, (C-4); 119.8, (C-5); 126.5, (C-2); 127.7, (Ts-aromC2); 130.6, (Ts-aromC3); 132.9, (Ts-aromC4); 145.7, (Ts-aromC1); 172.0, (CO); FTIR (neat) 3394.2, 2923.5, 2854.0, 1798.3, 1711.3, 1462.5cm^{-1}; UV (MeOH) 250.4, 276.0, 300.8nm; *m/e* (FAB) 362 (M, 18.8%); 334 (M-CO, 11.4%); 285 (M-C_5H_4N, 61.6%); 239 (B, M-$C_6H_5NO_2$, 100%); HRMS (M) Found: 362.1300 (Calcd. for $C_{18}H_{22}N_2O_4S_1$ 362.1289).

dihydropyrryl piperazine **2.19**, 19mg (5%) as a brown oil; R_f 0.46; ^{1}H NMR δ 0.85 (3H, d, *J*=6.9Hz, Leu-CH_3); 0.93 (3H, d, *J*=6.7Hz, Leu-CH_3); 1.40

(1H, m, Leu-CH_2); 1.70 (1H, m, Leu-CH_2); 1.89 (1H, sept, *J*=7.0Hz, C*H*(CH_3)$_2$); 2.31 (3H, s, Ts-CH_3); 5.55 (1H, bm, pyr-C*H*(OH)-N); 6.05 (1H, m, H-4); 6.73 (1H, m, H-3); 6.99 (1H, m, H-5); 7.00 (2H, d, *J*=8.2Hz, Ts-aromH3); 7.35 (2H, *J*=8.3Hz, Ts-aromH2); 9.09 (1H, s, pyr-CH(O*H*)-N); ^{13}C NMR δ 21.4 (Leu-CH_3); 21.9 (Leu-CH_3); 24.4 (Ts-CH_3); 30.9 (*C*H(CH_3)$_2$); 44.1 (Leu-CH_2); 56.2 (pyr-*C*H(OH)-N); 85.5 (C=*C*(Leu)-N); 109.4 (C-4); 120.7 (C-3); 126.3 (Ts-aromC3); 126.5 (C-5); 129.1 (Ts-aromC2); 132.2 (C-2); 137.5 (Ts-aromC4); 142.8 (Ts-aromC1); 166.2 (pyr-*C*H(OH)-N); *m/e* (FAB) 363 (M+1, 36.2%); 362 (M, 10.1%); 345 (M+1-H_2O and M-NH_3, 17.4%); 240 (B, M+1-Ts, 100%); HRMS (FAB, M+1) Found 363.1373 (Calcd. for $C_{18}H_{23}N_2O_4S_1$ 363.1378).

6.2.2 NaH Promoted Acylation of Pyrrole-2-Carboxaldehyde with Acetyl Chloride to give 2.24, described in Section 2.2.3

Acetyl chloride (18μL, 0.25mmol, 1.2equiv.) was added dropwise to a stirred mixture of the sodium salt of p-2-c **2.16** as prepared above. A black solution and an accompanying precipiate was again observed after 15 min. Water (10mL) was added to quench the reaction, some effevessence was observed. Work up as described above produced *N*-acetyl-p-2-c **2.24** 5.5mg (20%) mp 75-77°C (lit: 76-78°C), ^1H NMR spectral data was consistent with that by reported Bohlman[7].

6.3 Work Described in Section 2.3

6.3.1 MeLi Promoted Acylation of Pyrrole Derivatives, described in Section 2.3.1

6.3.1.1 *Non-Amino Acid Acylating Agents to give* **2.28** *and* **2.31**

P-2-c (100mg, 1.05mmol) or pyrrole (73μL, 1.05mmol) was dissolved in dry ether (10mL) under N_2 at -78°C. MeLi (1.05mmol, 9.5mL of 0.11M solution in dry ether, 1equiv.) was added. The pale blue mixture was stirred for 5 min at -78°C, after which hydrocinnamoyl chloride (172μL, 1.16mmol, 1.1equiv.) was slowly added. After a further 10 min stirring, citric acid (2mL, 10% solution in H_2O) and H_2O (2mL) were added, and the solution was allowed to warm to rt, at which time EtOAc (15mL) was added. The organic phase was washed with citric acid (5mL, 10% solution in H_2O) and the aqueous phases combined and re-extracted with EtOAc (10mL). The combined organic phases were washed with citric acid (5mL, 10% solution in H_2O), water (2x10mL), dried and evaporated to dryness. Chromatography on silica (EtOAc/Pet. Ether=1:2) yielded the corresponding *N*-acylated pyrrole.

2.31 212mg (89%) data discussed in Section 6.4.1.1, and

1-(3-Phenylpropanoyl)-pyrrole 2.28 205mg (98%) as a pale brown solid; R_f 0.40; ^{1}H NMR δ 3.12 (2H, m, CH_2Ph); 3.14 (2H, m, COCH_2); 6.28 (2H, t, *J*=2.5Hz, H-2); 7.22 (2H, t, *J*=2.6Hz, H-3); 7.23-7.31 (5H, m, Ph); ^{13}C NMR δ 30.4 (CH_2Ph); 36.4 (COCH_2); 113.2 (C-3); 118.9 (C-2); 126.5 (Ph-aromC4); 128.4 (Ph-aromC2); 128.7 (Ph-aromC3); 140.2 (Ph-aromC1); 169.7 (CO); IR (nujol) 2870, 1742, 1479cm^{-1}; UV ($CHCl_3$) 291.5nm; *m/e* (EI, 50eV) 199 (M, 93%); 131 (M-$C_4H_6N_1^+$, 9.5%); 105 (M-$C_5H_4N_1O_1$, 45.9%); 91 (B, M-$C_6H_6N_1O_1$, 100%); 77 (B-CH_2, 24.6%); HRMS (M) Found 199.09971 (Calcd. for $C_{13}H_{13}N_1O_1$ 199.09971).

6.3.1.2 *Amino Acid Acylating Agent to give* **2.30**

Pyrrole (73μL, 1.05mmol) was dissolved in dry ether (10mL), under N_2 at -78°C. MeLi (1.05mmol, 9.5mL of 0.11M solution in dry ether, 1equiv.) was added. The pale blue solution was stirred for 5 min at -78°C, after which *N*-Cbz-Phe-*p*-nitrophenyl ester **2.29** (486mg, 1.16mmol, 1.1equiv.) was added portionwise. After 15 min citric acid (2mL, 10% solution in H_2O) and H_2O (2mL) were added. The solution was warmed to rt, at which time EtOAc (15mL) was added. The organic phase was washed with citric acid (5mL, 10% solution in H_2O). The aqueous phases were combined and re-extract with

EtOAc (10mL). The combined organic phases were washed with citric acid (5mL, 10% solution in H_2O), water (2x10mL), dried and evaporated to dryness. Chromatography (EtOAc/Pet. Ether=1:2) yielded the *N*-acylated pyrrole.

1-(*N*-Benzyloxycarbonyl-*L*-phenylalanyl)-pyrrole 2.30 251mg (48%) as a pale brown solid; R_f 0.31; $[\alpha]^D_{18}$ -21° (c1, MeOH); ^{1}H NMR δ 3.10 (2H, m, Phe-CH_2); 4.66 (1H, m, Phe-C*H*); 5.08 (2H, s, Cbz-CH_2); 5.60 (1H, bd, *J*=8.8Hz, NH); 6.30 (2H, t, *J*=2.4Hz, H-3); 7.10 (2H, t, *J*=2.3Hz, H-2); 7.20-7.25 (5H, m, Phe-arom); 7.30-7.37 (5H, m, Cbz-arom); ^{13}C NMR δ 39.3 (Phe-CH_2); 54.1 (Phe-CH); 67.0 (Cbz-CH_2); 113.9 (C-3); 122.1 (C-2); 127.0 (Phe-aromC4); 127.2 (Cbz-aromC2); 128.1 (Phe-C9); 128.3 (Cbz-aromC4); 128.4 (Phe-C8); 128.4 (Cbz-aromC3); 135.6 (Cbz-aromC1); 135.9 (Phe-aromC1); 155.7 (Cbz-OCO); 171.9 (CO); FTIR (nujol) 3342.3, 2920.6, 1760.4, 1693.7, 1529.7cm^{-1}; UV (MeOH) 293.6nm; *m/e* (EI, 70eV) 348 (M, 2.7%); 282 (M-$C_4H_4N_1$, 30.0%); 131 (282-$C_8H_9N_1O_2^+$, 8.8%); 91 (B, $PhCH_2$, 100%); HRMS (M) Found 348.14738 (Calcd. for $C_{21}H_{20}N_2O_3$ 348.14738).

6.3.1.3 *Attempted N-Acylation of P-2-C with N-Cbz-Phe-p-Nitrophenyl Ester* **2.29** *using MeLi as the Base*

MeLi (1.05mmol, 9.5mL of 0.11M solution in dry ether, 1equiv.) was added to p-2-c (100mg, 1.05mmol) dissolved in dry Et_2O (10mL). After 5 min stirring, *N*-Cbz-Phe-*p*-nitrophenyl ester **2.29** (486mg, 1.16mmol, 1.1equiv.) was added and stirring was continued for 15 min. The desired *N*-acylated-p-2-c **2.33** was not detected by ^{1}H NMR spectroscopy.

The identical reaction as above was set up. After addition of the activated amino acid, stirring was continued for 1 h. The desired *N*-acylated-p-2-c **2.33** was not detected by ^{1}H NMR spectroscopy.

The identical reaction as above was set up again. After addition of the activated amino acid stirring was continued for 24 h. The desired *N*-acylated-p-2-c **2.33** was not detected by ^{1}H NMR spectroscopy.

6.3.2 n-BuLi Promoted Acylation of P-2-C to give 2.31, described in Section 2.3.2

Identical reaction conditions using n-BuLi (1.6M in hexane) rather than MeLi, using hydrocinnamoyl chloride as the acylating agent gave **2.31** 148mg (62%)

6.4 Acylation Work Described in Section 2.4 and Section 3.2.5

6.4.1 Acylation of Pyrrole-2-Carboxaldehyde to give 2.31, 2.33, 2.37, 2.42, 2.43, 2.45, 2.54, 3.42, 3.44, 3.52, 3.54, 3.56 using the DMAP Methodology

6.4.1.1 *Non-Amino Acid Based Acylating Agents to give* **2.31, 2.42, 2.43, 2.45, 3.52, 3.54** and **3.56**, *described in Section 2.4.1*

General Procedure:

P-2-c (100mg, 1.05mmol) TEA (162µL, 1.16mmol, 1.1equiv.) [or Hünigs base (202µL, 1.16mmol, 1.1equiv.) for acid chlorides] and DMAP (13mg, 0.11mmol, 0.1equiv.) were stirring under N_2 at rt in CH_2Cl_2 (10mL, freshley distiled from CaH_2). After stirring for 5 min the acid chloride (or anhydride) (1.16mmol, 1.1equiv.) was slowly added. The resultant mixture was stirred for a further 24 h. EtOAc (30mL) was added and the organic phase was washed with citric acid (1x10mL, 10% solution in H_2O), water (2x10mL), dried and evaporated. The resultant oils were chromatographed (EtOAc/Pet. Ether=1:2) on silica to afford the *N*-acylated-p-2-c derivatives, as described below.

6.4.1.1.1 Formyl Pyrroles **2.31, 2.42, 2.43** and **2.45**, described in Section 2.4.1

1-Propanoyl-2-formylpyrrole 2.42, Acylating agent: CH_3CH_2COCl, gave 144mg (90%) mp 80-82°C (EtOAc/Pet. Ether, colourless crystals); R_f 0.42; ^1H NMR δ 1.37 (3H, t, *J*=7.3Hz, CH_2CH_3); 3.02 (2H, q, *J*=7.2Hz, CH_2CH_3); 6.39 (1H, dd, *J*=3.7 & 3.2Hz, H-4); 7.26 (1H, dd, *J*=3.7 & 1.6Hz, H-3); 7.43 (1H, dd, *J*=3.2 & 1.7Hz, H-5); 10.34 (1H, s, CHO); ^{13}C NMR δ 8.6 (CH_2CH_3); 29.4 (CH_2CH_3); 112.8 (C-4); 122.5 (C-3); 125.9 (C-5); 135.7 (C-2); 172.7 (CO); 182.6 (CHO); IR (nujol) 1725, 1655, 1540, 1450cm^{-1}; UV ($CHCl_3$) 296.4nm; *m/e* (EI, 70eV) 151 (M, 45.0%); 123 (M-CO, 12.4%); 95 (B,

$C_5H_5NO^+$, 100%); HRMS (M) Found 151.0634 (Calcd. for $C_8H_9N_1O_2$ 151.0633); Anal. Calcd. for $C_8H_9N_1O_2$ C 63.57; H 6.00; N 9.27; Found C 63.63; H 5.82; N 9.27.

1-Phenacyl-2-formylpyrrole[8] 2.43, Acylating agent: PhCOCl, gave 209mg (100%) mp 90-91°C (EtOAC/Pet. Ether, deep brown mass); R_f 0.45; ^{1}H NMR δ 6.38 (1H, dd, *J*=3.5 & 3.1Hz, H-4); 7.22 (1H, dd, *J*=3.1 & 1.5Hz, H-3); 7.31 (1H, dd, *J*=3.7 & 1.6Hz, H-5); 7.65-7.81 (1H, m, Ph); 10.04 (1H, s, CHO); ^{13}C NMR δ 112.0, (C-4), 122.8, (C-5), 128.4, (Ph-aromC1), 128.8, (Ph-aromC3), 129.3, (C-3), 130.1, (Ph-aromC2); 133.6, (Ph-aromC4), 135.3, (C-2), 171.8, (CO), 181.0, (CHO); IR (neat) 1677, 1770, 1595cm^{-1}; UV ($CHCl_3$) 273.5 nm.

Ethyl 3-(1-Acetylpyrrol-2-yl)-2-cyanoprop-2-enoate 2.45, Acylating agent: CH_3COCl, gave 117mg (95%) mp 101-102°C (EtOAc/Pet. Ether, very pale yellow crystals); R_f 0.18; ^{1}H NMR δ 1.40 (2H, t, *J*=7.1Hz, CH_2CH_3); 2.67 (3H, s, $COCH_3$); 4.38 (2H, q, *J*=7.1Hz, CH_2CH_3); 6.50 (1H, dd, *J*=4.0 & 3.5Hz, H-4); 7.43 (1H, dd, *J*=3.2 & 1.5Hz, H-5); 7.79 (1H, dd, *J*=3.8 & 1.5Hz, H-3); 9.11 (1H, s, pyr-C*H*); ^{13}C NMR δ 14.2 (CH_2CH_3); 24.4 ($COCH_3$); 62.4 (CH_2CH_3); 99.7 (*C*(CN)(CO_2Et)); 114.0 (C-4); 118.6 (CN); 122.9 (C-3); 127.1 (C-5); 129.0 (C-2); 143.9 (pyr-*C*H); 155.8 ($CO_2CH_2CH_3$); 163.2 ($COCH_3$); IR (nujol) 2215, 1730, 1710, 1590, 1445cm^{-1}; UV ($CHCl_3$) 356.1, 267.0nm; *m/e* (EI, 50eV) 232 (M, 15.8%); 190 (B, M-$COCH_2$, 100%); 162 (B-CO, 18.5%); 144 (B-$CO_2CH_2CH_3$, 34.5%); HRMS (M) Found: 232.0853 (Calcd. for $C_{12}H_{12}N_2O_3$ 232.0848); Anal. Calcd for $C_{12}H_{12}N_2O_3$ C 62.05; H 5.21; N 12.07; Found: C 62.10; H 5.39; N 11.96.

1-(3-Phenylpropanoyl)-2-formylpyrrole 2.31, Acylating agent: $PhCH_2CH_2COCl$[9], gave 63mg (95%) mp 89-90°C (CCl_4, pale yellow crystals); R_f 0.51; ^{1}H NMR δ 3.16 (2H, t, *J*=7.2Hz, $COCH_2$); 3.27 (2H, t, *J*=7.2Hz, CH_2Ph); 6.33 (1H, t, *J*=3.1Hz, H-4); 7.21 (1H, dd, *J*=3.1 & 1.6Hz, H-3); 7.24 (2H, m, Ph-aromH2); 7.24 (1H, m, Ph-aromH4); 7.31 (2H, m, Ph-aromH3); 7.32 (1H, dd, *J*=3.1 & 1.6Hz, H-5); 10.29 (1H, s, CHO); ^{13}C NMR δ 30.4 (CH_2Ph); 37.8 ($COCH_2$); 112.8 (C-4); 122.9 (C-3); 125.9 (C-5); 126.7 (Ph-aromC4); 128.4 (Ph-aromC2); 128.7 (Ph-aromC3); 128.9 (C-2); 139.7 (Ph-aromC1); 171.2 (CO); 182.4 (CHO); FTIR (KBr) 3114.0, 1729.5, 1654.2, 1540.2cm^{-1}; UV ($CHCl_3$) 256.8, 296.8nm; *m/e* (EI, 50eV) 227 (M, 40.9%); 167 (B-$C_{12}H_9N_1$, 2.8%); HRMS (M) Found: 227.0945 (Calcd. for $C_{14}H_{13}N_1O_2$ 227.0946); Anal. Calcd. for $C_{14}H_{13}N_1O_2$ C 73.98; H 5.77; N 6.17; Found C 73.71; H 5.69; N 6.07.

6.4.1.1.2 Formyl Pyrroles **3.52**, **3.54** and **3.56**, described in Section 3.3.2

1-(3-Methylbutanoyl)-2-formylpyrrole 3.56, Acylating agent: $(CH_3)_2CHCH_2COCl$ (Section 6.1.3) gave 180mg (88%) as an orange oil; R_f 0.56; ^1H NMR δ 1.06 (6H, d, *J*=6.8Hz, $CH(CH_3)_2$); 2.22 (1H, m, $CH(CH_3)_2$); 2.80 (2H, d, *J*=6.6Hz, $COCH_2CH$); 6.25 (1H, t, *J*=3.5Hz, H-4); 7.12 (1H, dd, *J*=3.5 & 1.5Hz, H-3); 7.25 (1H, dd, *J*=3.5 & 1.5Hz, H-5); 10.32 (1H, s, CHO); ^{13}C NMR δ 22.0 ($CH(CH_3)_2$); 25.3 ($CH(CH_3)_2$); 44.3 ($COCH_2CH$); 112.4 (C-4); 122.0 (C-3); 126.0 (C-5); 135.4 (C-2); 171.3 (CO); 182.4 (CHO); FTIR (neat) 2962.4, 2873.9, 1727.2, 1665.2, 1545.4cm^{-1}; UV ($CHCl_3$) 296.8, 258.4nm; *m/e* (EI, 50eV) 179 (M, 34.2%); 96 (B, M-$C_5H_7O^+$, 100%); 69 (B-HCN, 37.8%); HRMS (M) Found 179.09462 (Calcd. for $C_{10}H_{13}N_1O_2$ 179.09462).

1-(Undecanoyl)-2-formylpyrrole 3.52, Acylating agent: $CH_3(CH_2)_{10}COCl$ (Section 6.1.3) gave 520mg (90%) as a brown solid; mp 80-81°C; R_f 0.46; ^1H NMR δ 0.88 (3H, t, *J*=6.5Hz, CH_3); 1.22-1.26 (16H, m, $CH_2(CH_2)_8CH_3$); 1.81 (2H, pent, *J*=6.9Hz, $COCH_2CH_2$); 2.93 (2H, t, *J*=7.5Hz, $COCH_2$); 6.35 (1H, t, *J*=3.7Hz, H-4); 7.22 (1H, dd, *J*=3.8 & 1.8Hz, H-3); 7.35 (1H, dd, *J*=3.7 & 1.9Hz, H-5); 10.32 (1H, s, CHO); ^{13}C NMR δ 14.1 (CH_3); 22.7, 24.5, 29.0, 29.3 x2, 29.4, 29.6 x2 ($CH_2(CH_2)_8CH_3$); 31.9 ($COCH_2CH_2$); 36.0 ($COCH_2$); 112.7 (C-4); 122.4 (C-3); 125.9 (C-5); 135.7 (C-2); 172.1 (CO); 182.6 (CHO); FTIR (KBr) 3127, 2918, 1731, 1651, 1539, 1471cm^{-1}; UV ($CHCl_3$) 310.0, 266.0nm; *m/e* (EI, 70eV) 277 (M, 11.7%); 193 (M-$C_6H_{12}^+$, 2.7%); 183 (M-C_5H_4NO, 23.6%); 98 (B, 193-$C_5H_5NO^+$, 100%); 71 (B-HCN, 24.3%); HRMS (M) Found 277.20417 (Calcd. for $C_{17}H_{27}N_1O_2$ 277.20416).

1-((5-Methoxycarbonyl)hexanoyl)-2-formylpyrrole 3.54, Acylating agent: $CH_3OCO(CH_2)_4COCl$ (Section 6.1.3) gave 220mg (89%) as a black solid; R_f 0.36; ^1H NMR δ 1.55 (2H, m, $CH_2CH_2CO_2CH_3$); 1.78 (2H, m, $COCH_2CH_2$); 2.40 (2H, t, *J*=7.0Hz, $CH_2CO_2CH_3$); 2.98 (2H, t, *J*=7.5Hz, $COCH_2$); 3.69 (3H, s, CO_2CH_3); 6.36 (1H, t, *J*=3.5Hz, H-4); 7.23 (1H, dd, *J*=3.5 & 1.5Hz, H-3); 7.36 (1H, dd, *J*=3.5 & 1.5Hz, H-5); 10.30 (1H, s, CHO); ^{13}C NMR δ 23.8 ($COCH_2CH_2$); 24.2 ($CH_2CH_2CO_2CH_3$); 33.6 ($CH_2CO_2CH_3$); 35.6 ($COCH_2$); 51.6 (CO_2CH_3); 112.8 (C-4); 122.8 (C-3); 126.0 (C-5); 135.6 (C-2); 171.6 (pyr-CO); 173.6 (CO_2CH_3); 182.4 (CHO); FTIR (nujol) 2873.1, 1737.6, 1712.5, 1537.1, 1463.1cm^{-1}; UV ($CHCl_3$) 295.2, 267.2nm; *m/e* (EI, 70eV) 237 (M, 45.9%); 143 (M-C_5H_4NO, 89.5%); 111 (B, 143-CH_3OH, 100%); 96 ($C_5H_6NO^+$, 94.8%); 83 (B-C_2H_4, 58.1%); HRMS (M) Found 237.10010 (Calcd. for $C_{12}H_{15}N_1O_4$ 237.10009).

6.4.1.2 *Amino Acid Acid Chloride Acylating Agents in the Acylation of P-2-C*

and DMAP as the Base

General Procedure:

P-2-c (30mg, 0.31mmol), Hünigs base (54μL, 0.31mmol, 1equiv.) and DMAP (3.8mg, 0.03mmol, 0.1equiv.) in CH_2Cl_2 (5mL) were added dropwise, under N_2, over 5 min, to an ice cooled solution of amino acid acid chloride (0.31mmol) in CH_2Cl_2 (5mL). After 10 min, the resulting solution was poured onto citric acid (10mL, 10% solution in H_2O) and CH_2Cl_2 (10mL) was added. The organic phase was washed with citric acid (10mL, 10% solution in H_2O), H_2O (2x5mL), dried and evaporated (H_2O pump). The *N*-acylated amino acid pyrrole derivatives described below were unstable to preparative silica chromatography.

6.4.1.2.1 Formyl Pyrroles **2.37** and **2.54**, described in Section 2.4.2.1

1-(*N*-Phthalyl-L-phenylalanyl)-2-formylpyrrole 2.37, Acylating agent: *N*-Pth-L-Phe-Cl, ^{1}H NMR spectral data in Section 6.1.2, gave 109mg (95%) as an unstable brown solid; R_f 0.44; $[\alpha]^D_{26}$ -210° (c1, MeOH); ^{1}H NMR δ 3.53 (2H, m, A & B part ABX, Phe-CH); 5.77 (1H, X part ABX, *J*=9.2 & 6.4Hz, Phe-CH_2); 6.19 (1H, t, *J*=3.4Hz, H-4); 7.07 (1H, dd, *J*=3.4 & 2.2Hz, H-3); 7.08-7.11 (5H, m, Phe-arom); 7.18 (1H, dd, *J*=3.4 & 2.3Hz, H-5); 7.63 (2H, dd, *J*=5.5 & 2.6Hz, Pth-aromH3); 7.69 (2H, dd, *J*=5.5 & 2.6Hz, Pth-aromH4); 10.10 (1H, s, CHO); ^{13}C NMR δ 34.9 (Phe-CH_2); 54.2 (Phe-CH); 113.3 (C-4); 122.9 (C-3); 123.8 (Pth-aromC3); 125.7 (C-5); 127.2 (Phe-aromC4); 128.7 (Phe-aromC2); 129.1 (Phe-aromC3); 131.0 (Pth-aromC3a); 134.5 (Pth-aromC4); 135.3 (Phe-aromC1); 135.6 (C-2); 166.9 (Pth-CO); 167.7 (pyr-CO); 181.6 (CHO); FTIR (neat) 3166.9, 1780.9, 1716.1, 1660.4cm^{-1}; UV (CHCl3) 340.8, 279.2nm; *m/e* (EI, 70eV) 372 (M, 8%); 250 (M-$C_6H_4NO_2$, 72%); 225 (M-$C_8H_5NO_2^+$, 25%); 129 (225-$C_5H_6NO^+$, 16%); 95 (B, $C_5H_5NO^+$, 100%); HRMS (M) Found 372.11100 (Calcd. for $C_{22}H_{16}N_2O_4$ 372.11099).

1-(*N*-Phthalyl-D-phenylalanyl)-2-formylpyrrole 2.54, Acylating agent: *N*-Pth-D-Phe-Cl (Section 6.1.2) gave 102mg (88%); $[\alpha]^D_{26}$ +196° (c1, MeOH). Spectral data identical to the L-isomer above.

6.4.1.2.2 Formyl Pyrroles **3.42** and **3.44**, described in Section 3.3.1

1-(*N*-Phthalyl-L-leucyl)-2-formylpyrrole 3.44, Acylating agent: *N*-Pth-L-Leu-Cl gave 335mg (94%) as an orange oil; R_f 0.40; $[\alpha]^D_{26}$ -117° (c1, MeOH); ^{1}H NMR δ 0.98 (3H, d, *J*=6.5Hz, (Leu-CH_3)$_A$); 1.04 (3H, d, *J*=6.5Hz,

(Leu-CH_3)$_B$); 1.50 (1H, m, Leu-CH_2); 2.00 (1H, m, Leu-CH_2); 2.42 (1H, m, CH(CH_3)$_2$); 5.67 (1H, X part ABX, J=10.5 & 4.5Hz, Leu-CH); 6.31 (1H, t, J=3.5Hz, H-4); 7.16 (1H, dd, J=3.5 & 1.5Hz, H-3); 7.29 (1H, dd, J=3.4 & 1.6Hz, H-5); 7.77 (2H, dd, J=5.5 & 3.0Hz, Pth-H14); 7.85 (2H, dd, J=5.8 & 3.1Hz, Pth-H15); 10.14 (1H, s, CHO); ^{13}C NMR δ 21.4 (CH_3)$_B$); 23.0 (CH_3)$_A$); 24.9 (CH(CH_3)$_2$); 37.5 (Leu-CH_2); 51.5 (Leu-CH); 113.2 (C-4); 122.6 (C-3); 123.8 (Pth-C14); 125.5 (C-5); 131.5 (Pth-C13); 134.6 (Pth-C15); 135.3 (C-2); 167.3 (Pth-CO); 168.7 (CO); 181.6 (CHO); FTIR (neat) 2959.4, 1775.1, 1737.8, 1721.2, 1667.7cm^{-1}; UV (MeOH) 289.6, 239.2nm; *m/e* (EI, 70eV) 338 (M, 33.0%); 244 (M-$C_5H_5N_1O_1$, 72.2%); 216 (244-CO, 96.7%); 174 (216-$C_3H_6^+$, 77.3%); 160 (B, 216-$C_4H_8^+$, 100%); 148 (M-$(CO)_2NH_2^+$, 50.3%); HRMS (M) Found 338.12665 (Calcd. for $C_{19}H_{18}N_2O_4$ 338.12664).

1-(*N*-Phthalyl-glycyl)-2-formylpyrrole 3.42, gave 74mg (25%) as an unstable black solid; ^{1}H NMR δ 5.00 (2H, s, Gly-CH_2); 6.38 (1H, t, J=3.5Hz, H-4); 7.23 (1H, m, H-3); 7.28 (1H, dd, J=2.0 & 3.6Hz, H-5); 7.69 (2H, dd, J=5.3 & 3.0Hz, Pth-aromH4); 7.80 (2H, dd, J=5.4 &3.0Hz, Pth-aromH3); 10.16 (1H, s, CHO).

6.4.1.3 *p-Nitrophenyl Ester Activated Amino Acid as the Acylating Agent of P-2-C with DMAP as the Base to produce* **2.33**, *described in Section 2.4.7.1*

P-2-c (10mg, 0.12mmol), TEA (18μL, 0.13mmol, 1.2equiv.) and DMAP (1.3mg, 0.01mmol, 0.1eqiuv.) were stirred in CH_2Cl_2 (10mL) at rt under N_2. *N*-Cbz-Phe-*p*-nitrophenyl ester **2.29** (49mg, 0.12mmol, 1.1equiv.) was slowly added portionwise. Over 24 h a yellow colour intensified in the flask, that was attributed to the release of *p*-nitrophenol. Dilution with EtOAc (5mL), followed by citric acid (5mL, 10% solution in H_2O), and water (5mL units) until the yellow colour of the *p*-nitrophenol had been removed from the aqueous phase, followed by drying and evaporation. The aldehyde was unstable to preparative chromatography.

1-(*N*-Benzyloxycarbonyl-L-phenylalanyl)-2-formylpyrrole 2.33, gave 5mg (13%) as an unstable brown oil; R_f 0.49; ^{1}H NMR δ 3.13 (2H, m, Phe-CH_2); 4.72 (1H, m, Phe-CH); 5.12 (1H, s, Cbz-CH_2); 5.20 (1H, d, J=6.8Hz, NH); 6.34(1H, t, J=3.5Hz, H-4); 7.04 (1H, m, H-3); 7.21 (1H, dd, J=3.4 & 1.7Hz, H-5); 7.27-7.52 (10H, m, aromatics); 10.38 (1H, s, CHO); ^{13}C NMR δ 33.1 (Phe-CH_2); 54.2 (Phe-CH); 67.3 (Cbz-CH_2); 112.4 (C-4); 121.6 (C-3); 127.1 (C-5); 128.3 (Cbz-aromC2); 128.5 (Phe-aromC4); 128.5 (Cbz-aromC4); 128.6 (Cbz-aromC3); 128.8 (Phe-aromC2); 129.2 (Phe-aromC3); 132.1 (Cbz-aromC1); 135.3 (Cbz-aromC1); 135.5 (C-2); 155.8 (Cbz-CO); 172.0 (CO); 182.1

(CHO); HRES (M) Found 376.1424 (Calcd. for $C_{22}H_{20}N_2O_4$ 376.1423).

6.4.1.3.1 Further Attempts at Formation of **2.33**, described in Section 2.4.7.1

Modifications:

1) Reagents and conditions as described above, except that activated 4Å molecular sieves (100mg) were added. After 24 h ^{1}H NMR spectral analysis indicated 11% desired *N*-acyl-p-2-c, the remaining 89% was p-2-c.

2) Reagents and conditions as described above, except that TDA-1 (3.6μL, 0.01mmol, 0.1equiv.) was added. Stirring for 20 h showed no desired *N*-acyl-p-2-c by ^{1}H NMR spectroscopy, there was only p-2-c.

3) 1equiv. of DMAP was added rather than 0.1equiv. Stirring for 24 h gave 13% *N*-acylated product by ^{1}H NMR spectroscopy, the remaining 87% was p-2-c.

4) The solution of p-2-c (1equiv.), TEA (1.2equiv.), DMAP (0.1equiv.) and activated amino acid (1.1equiv.) was heated at reflux for 1 h, 5 h or 24 h, ^{1}H NMR spectral analysis at each interval showed 5%, 4% and 0% of **2.33** respectively. The remainder was p-2-c. At 24 h a noticable black precipitate had formed.

5) The amount of the activated amino acid was increased from 1.1equiv. to 2.2equiv. (98mg, 0.22mmol). Stirring for 24 h produced 8% of **2.33** by ^{1}H NMR spectral analysis, the remaining pyrrole was starting material.

6) The glassware used in the reaction was soaked in a KOH/EtOH solution for 24 h and then rigorously rinsed with distiled H_2O and dried, prior to use. The *N*-acylated p-2-c **2.33** was not evident by ^{1}H NMR spectroscopy after 24 h reaction.

7) The glassware used in the reaction was soaked in concentrated H_2SO_4 for 24 h and then rigorously rinsed with distiled H_2O and dried, prior to use. The *N*-acylated p-2-c **2.33** was not evident by ^{1}H NMR spectroscopy after 24 h reaction.

8) Freshly distiled TEA and CH_2Cl_2 were extensively deoxygenated with dry N_2. P-2-c, DMAP and amino acid were dried under high vacuum. Glassware was flame dried under vacuum and cooled under N_2. The reaction was performed in a freshly regenerated "dry box". The *N*-acylated p-2-c **2.33** was not evident by ^{1}H NMR spectroscopy after 24 h reaction.

9) H_2O (2.0μL, 0.11mmol, 1equiv.) was added to the reaction. The *N*-acylated p-2-c **2.33** was not evident by ^{1}H NMR spectroscopy after 24 h reaction.

10) P-2-c, DMAP and TEA were added to a stirred solution of the

activated amino acid. The *N*-acylated p-2-c **2.33** was not evident by ^{1}H NMR spectroscopy after 24 h reaction.

11) P-2-c and Cbz-Phe-OH (2equiv.) were dissolved in dry EtOAc (5mL), DCC (1equiv.) was slowly added. The *N*-acylated p-2-c **2.33** was not evident by ^{1}H NMR spectroscopy after 24 h reaction.

12) Number 11) above was repeated with the addition of HOBt (15mg, 0.11mmol, 1equiv.) before the DCC. The addition of DCC caused a white precipitate to form, indicating that the DCU had formed and therefore the activation of the amino acid. The *N*-acylated p-2-c **2.33** was not evident by ^{1}H NMR spectroscopy after 24 h reaction.

13) TEA was omitted from the reaction conditions. The *N*-acylated p-2-c **2.33** was not evident by ^{1}H NMR spectroscopy after 24 h or after 2 months reaction.

14) Penta-fluoro phenyl ester activated Phe[10] was added to p-2-c, DMAP and TE2. The *N*-acylated p-2-c **2.33** was not evident by ^{1}H NMR spectroscopy after 24 h reaction.

6.4.2 Reduction of *N*-Acylated Formyl Pyrroles 2.24, 2.31, 2.37, 2.54, 3.42, 3.44, 3.52, 3.54 and 3.56 to give Hydroxymethyl Pyrroles 2.47, 2.32, 2.52, 2.55, 3.43, 3.45, 3.53, 3.55 and 3.57

6.4.2.1 *Sodium Borohydride Reduction*[11] *of* **2.24** *to give* **2.47**, *described in Section 2.4.4.1*

$NaBH_4$ (8.7mg, 0.23mmol, 1.5equiv.) was added portionwise to *N*-acetyl-p-2-c **2.24** (20mg, 0.15mmol) in CH_2Cl_2/MeOH (2mL: 1mL) at 0°C under N_2. After 10 min the reaction was diluted with CH_2Cl_2 (5mL), the organic solvents were washed with oxalic acid (5mL, 5% solution in H_2O), water (2x10mL), then dried and evaporated to dryness. Chromatography yielded the hydroxymethyl pyrrole **2.47** (84%) with spectral data consistent with the literature[3].

A similar reaction with *N*-(*N*-Pth-Phe)-p-2-c **2.37** did not produce the desired hydroxymethyl pyrrole **2.52**.

6.4.2.2 *Zinc Borohydride Reduction of* **2.31**, **2.37**, **2.54** *to give* **2.32**, **2.52**, **2.55**, **3.43**, **3.45**, **3.53**, **3.55** and **3.57**, *described in Section 2.4.5*

General Procedure:

The *N*-amino acid acylated pyrrole (0.28mmol) was dissolved in dry Et_2O under N_2. $Zn(BH_4)_2$ (0.34mmol, 3.1mL of 0.11M solution in dry Et_2O, 1.2equiv.) was added and the resultant solution was stirred at rt for 30 min.

The Et_2O solution was decanted from the organic insoluble zinc salts. Further Et_2O (2x5mL) was added, decanted and combined with the previous washings. H_2O (2mL) and acetic acid (2mL, 10% solution in water) were carefully added to the Et_2O extracts. The separated aqueous phase was re-extracted with CH_2Cl_2 (2x5mL) and the combined organic solvents were washed with H_2O (2x10mL). The organic phase was dried and evaporated.$Zn(BH_4)_2$ (0.34mmol, 3.1mL of 0.11M solution in dry Et_2O, 1.2equiv.) was added and the resultant solution was stirred at rt for 30 min. The Et_2O solution was decanted from the organic insoluble zinc salts. Further Et_2O (2x5mL) was added, decanted and combined with the previous washings. H_2O (2mL) and acetic acid (2mL, 10% solution in water) were carefully added to the Et_2O extracts. The separated aqueous phase was re-extracted with CH_2Cl_2 (2x5mL) and the combined organic solvents were washed with H_2O (2x10mL). The organic phase was dried and evaporated. The resultant hydroxymethyl pyrroles were purified by silica chromatography (EtOAc/Pet. Ether=1:2).

6.4.2.2.1 Hydroxymethyl Pyrroles **2.32**, **2.52** and **2.55**, described in Section 2.4.5

1-(3-Phenylpropanoyl)-2-hydroxymethylpyrrole 2.32, gave 92mg (90%) as a mauve amorphous mass; R_f 0.33; ^1H NMR δ 3.08 (2H, dt, *J*=7.8 & 1.5Hz, CH_2Ph); 3.17 (2H, dt, *J*=7.8 & 1.5Hz, $COCH_2$); 3.71 (1H, bs, CH_2OH); 4.62 (2H, bs, CH_2OH); 6.17 (1H, t, *J*=3.3Hz, H-4); 6.21 (1H, m, H-3); 7.06 (1H, dd, *J*=3.3 & 1.6Hz, H-5); 7.22 (1H, m, Ph-aromH3); 7.28 (2H, m, Ph-aromH2); 7.30 (1H, m, Ph-aromH4); D_2O exchange: bs at 3.71ppm is removed and bs at 4.62ppm collapses to sharp s; ^1H NMR δ (d_3-CD_3CN) 3.10 (2H, t, *J*=7.5Hz, CH_2Ph); 3.31 (2H, t, *J*=7.5Hz, $COCH_2$); 3.48 (1H, t, *J*=7.0Hz, CH_2OH); 4.65 (2H, d, *J*=7.0Hz, CH_2OH); 6.24 (1H, t, *J*=3.5Hz, H-4); 6.29 (1H, m, H-3); 7.28 (1H, dd, *J*=3.5 & 1.6Hz, H-5); 7.30-7.38 (5H, m, Ph); ^{13}C NMR ($CDCl_3$) δ 30.3 (CH_2Ph); 37.4 ($COCH_2$); 57.9 (CH_2OH); 112.2 (C-4); 114.5 (C-3); 120.7 (C-5); 126.5 (Ph-aromC4); 128.3 (Ph-aromC2); 128.6 (Ph-aromH3); 135.5 (C-2); 139.9 (Ph-aromC1); 172.2 (CO); FTIR (neat) 3519.9, 1703.2, 1605.6, 1495.2, 1409.4cm^{-1}; UV ($CHCl_3$) 548.0, 480.8nm; *m/e* (EI, 50eV) 229 (M, 13.7%); 198 (M-CH_2=OH^+, 11.4%), 105 (M-$C_6H_6N_1O_2$, 33.2%), 97 (B, M-105-HCN, 100%); HRMS (M) Found 229.1103 (Calcd. for $C_{14}H_{15}N_1O_2$ 229.1103).

1-(*N*-Phthalyl-L-phenylalanyl)-2-hydroxymethylpyrrole 2.52, gave 26mg (62%) as a mauve solid; R_f 0.31; $[\alpha]^D_{26}$ -195° (c1, MeOH); ^1H NMR δ

3.52 (2H, d, *J*=7.8Hz, Phe-CH_2); 4.59 (2H, bs, CH_2OH); 5.59 (1H, t, *J*=7.8Hz, Phe-CH); 6.05 (1H, t, *J*=3.4Hz, H-4); 6.14 (1H, dd, *J*=3.4 & 1.4Hz, H-3); 6.93 (1H, dd, *J*=3.4 & 1.5Hz, H-5); 7.09-7.19 (5H, m, Phe-arom); 7.63 (2H, dd, *J*=5.6 & 3.0Hz, Pth-aromH4); 7.70 (2H, dd, *J*=5.6 & 3.0Hz, Pth-aromH3); ^{13}C NMR δ 35.0 (Phe-CH_2); 53.9 (Phe-CH); 57.6 (CH_2OH); 113.1 (C-4); 114.9 (C-3); 120.2 (C-5); 123.8 (Pth-aromC3); 127.2 (Phe-aromC4); 128.7 (Phe-aromC2); 129.2 (Phe-aromC3); 131.1 (Pth-aromC3a); 134.3 (Phe-aromC1); 134.5 (Pth-aromC4); 135.9 (C-2); 167.0 (Pth-CO); 168.4 (CO); FTIR (neat) 3477.8, 1772.1, 1713.9, 1613.6, 1494.2, 1454.5cm^{-1}; UV (MeOH) 486.4, 301.2nm; *m/e* (EI, 50eV) 374 (M, 14.0%); 278 (M-$C_4H_6N_1O_1$, 10.9%); 250 (B, 278-C=O, 100%); HRMS (M) Found 374.12665 (Calcd. for $C_{22}H_{18}N_2O_4$ 374.12665).

1-(*N*-Phthalyl-D-phenylalanyl)-2-hydroxymethylpyrrole 2.55, gave 26mg (62%) as a mauve solid; R_f 0.31; $[\alpha]^D_{26}$ +180° (*c*1, MeOH); Spectral data identical to the L-isomer, **2.52**, above.

6.4.2.2.2 Hydroxymethyl Pyrroles **3.43** and **3.45**, described in Section 3.3.1

1-(*N*-Phthalyl-glycyl)-2-hydroxymethylpyrrole 3.43, gave 16mg (22%) as an unstable black solid; ^1H NMR δ 4.63 (2H, s, CH_2OH); 5.03 (2H, s, Gly-CH_2); 6.31 (1H, m, H-3); 6.33 (1H, t, *J*=3.2Hz, H-4); 7.20 (1H, dd, *J*=3.3 & 1.6Hz, H-5); 7.80 (2H, dd, *J*=5.6 & 3.3Hz, Pth-aromH3); 7.94 (2H, dd, *J*=5.6 & 3.2Hz, Pth-aromH4); ^{13}C NMR δ 29.7 (Gly-CH_2); 58.4 (CH_2OH); 113.8 (C-4); 115.1 (C-3); 119.7 (C-5); 123.9 (Pth-aromC3); 131.9 (Pth-aromC3a); 134.5 (Pth-aromC4); 136.2 (C-2); 167.5 (Pth-CO); 170.0 (CO).

1-(*N*-Phthalyl-L-leucyl)-2-hydroxymethylpyrrole 3.45, gave 299mg (87%) as a deep yellow oil; R_f 0.48; $[\alpha]^D_{26}$ -114° (*c*1, MeOH); ^1H NMR δ 0.98 (3H, d, *J*=6.5Hz, $CH(CH_3)_A$); 1.05 (3H, d, *J*=6.5Hz, $CH(CH_3)_B$); 2.00 (2H, m, Leu-CH_2); 2.46 (1H, m, $CH(CH_3)_2$); 4.63 (2H, s, CH_2OH); 5.54 (1H, dd, *J*=10.5 & 4.5Hz, Leu-CH); 6.17 (1H, t, *J*=3.5Hz, H-4); 6.22 (1H, m, H-3); 7.06 (1H, dd, *J*=3.4 & 1.5Hz, H-5); 7.76 (2H, dd, *J*=5.5 & 3.4Hz, Pth-aromH3); 7.86 (2H, dd, *J*=5.6 & 3.4Hz, Pth-aromH4); ^{13}C NMR δ 21.4 ($CH(CH_3)_B$); 23.0 ($CH(CH_3)_A$); 25.0 ($CH(CH_3)_2$); 37.7 (Leu-CH_2); 51.3 (Leu-CH); 57.6 (CH_2OH); 113.0 (C-4); 114.9 (C-3); 120.1 (C-5); 123.8 (Pth-aromC3); 131.3 (Pth-aromC3a); 134.5 (Pth-aromC4); 136.1 (C-2); 167.5 (Pth-CO); 169.4 (CO); FTIR (neat) 3477.2, 1775.1, 1716.5cm^{-1}; UV (MeOH) 279.6, 242.8nm; *m/e* (EI, 70eV) 340 (M, 30.8%); 244 (M-$C_5H_6NO^+$, 16.7%); 216 (244-CO, 89.9%); 174 (216-$C_3H_6^+$, 50.6%); 160 (B, Ph-$(CO)_2$-NH-CH_2^+, 100%); HRMS (M)

Found 340.14230 (Calcd. for $C_{19}H_{20}N_2O_4$ 340.14229).

6.4.2.2.3 Hydroxymethyl Pyrroles **3.53**, **3.55** and **3.57**, described in Section 3.3.2

1-(Undecanoyl)-2-hydroxymethylpyrrole 3.53, gave 60mg (58%) as a deep brown oil; R_f 0.55; ^{1}H NMR δ 0.88 (3H, t, *J*=6.5Hz, CH_3); 1.03, 1.08, 1.16 (16H, m, $(CH_2)_8CH_3$); 1.78 (2H, sept, *J*=7.5Hz, $COCH_2CH_2$); 2.86 (2H, t, *J*=7.5Hz, $COCH_2$); 3.75 (1H, vbs, CH_2OH); 4.62 (2H, bs, CH_2OH); 6.19 (1H, t, *J*=3.0Hz, H-4); 6.22 (1H, m, H-3); 7.12 (1H, dd, *J*=3.0 & 1.0Hz, H-5); ^{13}C NMR δ 14.0 (CH_3); 22.6, 29.0, 29.2, 29.3, 29.4, 29.5 x2, 31.8 ($(CH_2)_8CH_3$); 24.5 ($COCH_2CH_2$); 35.6 ($COCH_2$); 57.9 (CH_2OH); 111.9 (C-4); 114.4 (C-3); 120.9 (C-5); 135.5 (C-2); 173.3 (CO); FTIR (nujol) 3340.4, 2852.2, 1716.0, 1497.7cm^{-1}; UV ($CHCl_3$) 268.0, 258.4nm; *m/e* (EI, 70eV) 279 (M, 25.4%); 248 (M-CH_2OH, 1.8%); 183 (M-$C_5H_6N_1O_1$, 1.9%); 97 (B, M-$C_{12}H_{22}O_1^+$, 100%); 80 (B-OH, 74.2%); HRMS (M) Found 279.21982 (Calcd. for $C_{17}H_{29}N_1O_2$ 279.21981).

1-((5-Methoxycarbonyl)hexanoyl)-2-hydroxymethylpyrrole 3.55, gave 25mg (45%) as a brown oil; R_f 0.36; ^{1}H NMR δ 1.77 (2H, m, $CH_2CH_2CO_2CH_3$); 1.81 (2H, m, $COCH_2CH_2$); 2.40 (2H, t, *J*=7.0Hz, $CH_2CO_2CH_3$); 2.91 (2H, t, *J*=7.3Hz, $COCH_2$); 3.68 (3H, s, CO_2CH_3); 4.63 (2H, s, CH_2OH); 6.21 (1H, t, *J*=3.5Hz, H-4); 6.23 (1H, m, H-3); 7.11 (1H, dd, *J*=3.5 & 2.0Hz, H-5); irradiation at 4.63ppm collapses m at 6.23ppm to dd (*J*=3.4 & 2.0Hz); ^{13}C NMR δ 23.8 ($CH_2CH_2CO_2CH_3$); 24.3 ($COCH_2CH_2$); 33.6 ($CH_2CO_2CH_3$); 35.2 ($COCH_2$); 51.6 (CO_2CH_3); 57.9 (CH_2OH); 112.2 (C-4); 114.6 (C-3); 120.8 (C-5); 135.5 (C-2); 172.7 (CO); 173.6 (CO_2CH_3); FTIR (nujol) 3319.1, 2854.9, 1737.0, 1712.9, 1461.2cm^{-1}; UV ($CHCl_3$) 273.6, 259.2nm; *m/e* (EI, 70eV) 239 (M, 11.8%); 153 (M-$C_4H_6O_2^+$, 2.1%); 143 (M-$C_5H_6N_1O_1$, 5.8%); 97 (B, M-$C_7H_{16}O_3^+$, 100%); 80 (B-OH, 54.1%); HRMS (M) Found 239.11575 (Calcd. for $C_{12}H_{17}N_1O_4$ 239.11575).

1-(3-Methylbutanoyl)-2-hydroxymethylpyrrole 3.57, gave 150mg (90%) as a deep mauve oil; R_f 0.42; ^{1}H NMR δ 1.05 (6H, d, *J*=7.0Hz, $CH(CH_3)_2$); 2.30 (1H, sept, *J*=7.0Hz, CH); 2.74 (2H, d, *J*=7.0Hz, CH_2); 4.63 (2H, bs, CH_2OH); 6.19 (1H, t, *J*=3.5Hz, H-4); 6.22 (1H, m, H-3); 7.11 (1H, dd, *J*=3.5 & 2.0Hz, H-5); irradiation at 4.63ppm collapses m at 6.22ppm to dd (*J*=3.5 & 2.0Hz); ^{13}C NMR δ 22.5 ($CH(CH_3)_2$); 25.5 (CH); 44.4 (CH_2); 57.9 (CH_2OH); 111.9 (C-4); 114.5 (C-3); 121.0 (C-5); 135.4 (C-2); 172.7 (CO); FTIR (neat) 3430.1, 2960.3, 1702.8, 1619.9cm^{-1}; UV ($CHCl_3$) 283.6nm; *m/e*

(EI, 70eV) 181 (M, 27.5%); 97 (B, M-$C_5H_8O^+$, 100%); 80 (B-OH, 70.8%); HRMS (M) Found 181.11027 (Calcd. for $C_{10}H_{15}N_1O_2$ 181.11027).

6.4.3 Determination of Enantiomeric Excess of the Hydroxymethyl Pyrrole 2.52 and 2.55 via the Camphanates 2.53 and 2.56, described in Section 2.4.6

6.4.3.1 *Mitsunobu Esterification of* **2.52** and **2.55** *to give the Camphanates* **2.53** and **2.56**

The hydroxymethyl pyrrole under investigation **2.52** and **2.55** were esterified under the Mitsunobu conditions[10].

General Procedure:

A solution of hydroxymethyl pyrrole (10mg, 0.03mmol), triphenylphosphine (15mg, 0.056mmol, 2.1equiv.) and (-)-camphanic acid (12mg, 0.059mmol, 2.2equiv.) in dry THF (1mL) was stirred for 5 min. Diethylazodicarboxylate (DEAD, 9μL, 0.056mmol, 2.1equiv.) was added and the reaction was stirred for a further 3 h at rt under N_2. The solvent was evaporated (H_2O pump, followed by oil pump). The resultant crude product was then dissolved in CH_2Cl_2 (0.5mL) and passed through silica gel column (2cm, EtOAc/Pet. ether=1:2 elutent), to remove all non-pyrrole material. The product camphanate was then purified by radial chromatography (EtOAc/Pet. Ether=1:2) as below.

(1S)-(-)-1-(*N*-Phthaloyl-L-phenylalanoyl)pyrrol-2-ylmethyl Camphanate 2.53, gave 13mg (90%) as a mauve oil; R_f 0.32 and R_f 0.88 on Diol $F_{254}S$; $[\alpha]^D_{26}$ -90° (c1, MeOH); ^1H NMR δ 0.89 (3H, s, camph-CH_3); 0.99 (3H, s, camph-CH_3); 1.03 (3H, s, camph-CH_3); 1.65 (1H, m, camph-CH_2); 1.95 (2H, m, camph-CH_2); 2.40 (1H, m, camph-CH_2); 3.50 (2H, m, Phe-CH_2); 5.35 (1H, dd, *J*=13.2 & 0.8, C*H*$_2$O-camph); 5.49 (1H, dd, *J*=13.2 & 0.9Hz, C*H*$_2$O-camph); 5.57 (1H, dd, *J*=9.3 & 6.2Hz, Phe-CH); 6.09 (1H, t, *J*=3.4Hz, H-4); 6.28 (1H, ddd, *J*=3.5 & 0.9 & 0.8Hz, H-3); 7.07 (1H, dd, *J*=3.5 & 2.0Hz, H-5); 7.09-7.12 (5H, m, Phe-arom); 7.68 (2H, dd, *J*=5.5 & 3.0Hz, Pth-aromH4); 7.75 (2H, dd, *J*=5.6 & 3.0Hz, Pth-aromH3); FTIR (neat) 2970.9, 1783.4, 1732.4, 1716.2, 1698.9cm^{-1}; UV ($CHCl_3$) 284.4nm; HRMS (FAB, M+K^+) Found 593.16899 (Calcd. for $C_{32}H_{30}N_2O_7K$ 593.16899).

(1S)-(-)-1-(*N*-Phthalyl-D-phenylalanyl)pyrrol-2-ylmethyl Camphanate 2.56, gave 12mg (84%) as a mauve oil; R_f 0.32 and R_f 0.74 on Diol $F_{254}S$; $[\alpha]^D_{26}$ +114° (c1, MeOH); ^1H NMR δ 0.92 (3H, s, camph-CH_3); 0.96 (3H, s, camph-CH_3); 1.03 (3H, s, camph-CH_3); 1.65 (1H, m, camph-CH_2); 1.90 (2H,

m, camph-CH_2); 2.40 (1H, m, camph-CH_2); 3.50 (2H, m, Phe-CH_2); 5.34 (1H, dd, *J*=13.2 & 0.9, CH_2O-camph); 5.50 (1H, dd, *J*=13.2 & 1.0Hz, CH_2O-camph); 5.57 (1H, dd, *J*=9.3 & 6.2Hz, Phe-CH); 6.09 (1H, t, *J*=3.4Hz, H-4); 6.27 (1H, ddd, *J*=3.4 & 1.1 & 1.0Hz, H-3); 7.02 (1H, dd, *J*=3.3 & 1.6Hz, H-5); 7.09-7.12 (5H, m, Phe-arom); 7.68 (2H, dd, *J*=5.5 & 3.0Hz, Pth-aromH4); 7.75 (2H, dd, *J*=5.6 & 3.0Hz, Pth-aromH3); HRMS (FAB, $M+K^+$) Found 593.16899 (Calcd. for $C_{32}H_{30}N_2O_7K$ 593.16899).

6.5 Work Discussed in Section 2.5

6.5.1 Attempted Acylation of P-2-Acetal 2.67

P-2-acetal **2.67**, was prepared via the Loader method[12].

Acetyl chloride (7.8μL, 0.11mmol, 1equiv.) was added to p-2-acetal (20mg, 0.11mmol), DMAP (1.2mg, 0.01mmol, 0.1equiv.) and Hünigs base (19.2μL, 0.11mmol, 1equiv.) in CH_2Cl_2 (5mL). After 24 h a non-acidic work up was used. The reaction was diluted with EtOAc (10mL), the organic layer was washed with $NaHCO_3$ (3x5mL, 5% solution in H_2O), dried and evaporated. ^1H NMR spectral analysis of the resulting crude product showed negligable decomposition of the p-2-acetal **2.67** to p-2-c. There was no desired *N*-acylated pyrrole **2.68** detected.

6.6 Work Discussed in Section 2.6

6.6.1 Attempted Formylation of the *N*-Acylated Pyrroles 2.28 and 2.30

Vilsmeier-Haack formylation conditions[13] were employed to attempt the formylation of *N*-acylated pyrroles **2.28** and **2.30.**

General Procedure:

The Vilsmeier-Haack reagent ($POCl_3$/DMF, 1.1equiv.) was prepared. Either *N*-(*N*-Cbz-Phe)-pyrrole **2.30** (30mg, 0.09mmol) or *N*-cinnamoyl-pyrrole **2.28** (50mg, 0.22mmol) was added portionwise to the formylating reagent. After 1 h the solution was heated at reflux for 15 min. $NaOAc.3H_2O$ (5mL, 20% solution in H_2O) was added and the mixture was heated at reflux for a further 15 min.

The *N*-acylated p-2-c **2.33** or **2.31**, respectively, were not evident by ^1H NMR spectroscopy.

6.7 Work Discussed in Section 3.2

6.7.1 Amino Acid Extension in the Peptide "Sense" Direction - Imine 3.12 and 3.15, and Amine 3.27

6.7.1.1 *Formation of the Imines* **3.12** *and* **3.15**, *described in Section 3.2.1*

P-2-c (100mg, 1.05mmol), TEA (146μL, 1.05mmol, 1equiv.) and HCl.NH_2-Ala-OEt **3.11** (161mg, 1.05mmol, 1equiv.) were dissolved in dry pentane (15mL) and the solution was heated at reflux in a modified Dean-Stark apparatus for 18 h. The solvent was evaporated, purification of the crude product by silica chromatography resulted in decomposition to polymer. The crude product was sufficiently clean to obtain the following data.

***N*-(2-Pyrrolylmethylene)-L-alanine Ethyl Ester 3.12**, gave 184mg (90%) as a deep mauve oil; ^{1}H NMR δ 1.28 (3H, t, *J*=7.0Hz, $CO_2CH_2CH_3$); 1.49 (3H, d, *J*=7.0Hz, Ala-CH_3); 4.07 (1H, q, *J*=7.0Hz, Ala-CH); 4.20 (2H, q, *J*=7.1Hz, $CO_2CH_2CH_3$); 6.26 (1H, dd, *J*=6.5 & 3.1Hz, H-4); 6.56 (1H, dd, *J*=6.5 & 3.7Hz, H-3); 6.96 (1H, dd, *J*=3.7 & 3.1Hz, H-5); 8.05 (1H, s, pyr-CH=N); ^{13}C NMR δ 14.2 ($CO_2CH_2CH_3$); 19.7 (Ala-CH_3); 61.1 ($CO_2CH_2CH_3$); 66.6 (Ala-CH); 110.2 (C-4); 116.3 (C-3); 123.2 (C-5); 142.7 (C-2); 152.7 (pyr-CH=N); 172.8 ($CO_2CH_2CH_3$); IR (nujol) 2185, 1655, 1414cm^{-1}; UV ($CHCl_3$) 237.6nm; *m/e* (EI, 50eV) 194 (M); 151 (M-$COCH_3$); 137 (M-$COCH_2CH_3$); 121 (B, M-$CO_2CH_2CH_3$); 106 (B-CH_3); 94 (B-HCN); HRMS (M) Found: 194.1056 (Calcd. for $C_{10}H_{14}N_2O_2$ 194.1055).

P-2-c (100mg, 1.05mmol) and i$BuNH_2$ (104mg, 1.05mmol, 1equiv.) were dissolved in dry pentane (15mL) and the solution was heated at reflux in a modified Dean-Stark apparatus for 14 h. The solvent was evaporated, purification of the crude product by silica chromatography resulted in decomposition to polymer. The crude product was sufficiently clean to obtain the following data.

2-Methyl-*N*-(pyrrol-2-ylmethylene)propanamine 3.15, gave 158mg (100%) as a red/mauve oil; ^{1}H NMR δ 0.92 (6H, d, *J*=6.7Hz, $CH(CH_3)_2$); 1.91 (1H, sept, *J*=6.7Hz, $CH(CH_3)_2$); 3.34 (1H, d, *J*=6.7Hz, $CH_2CH(CH_3)_2$); 6.22 (1H, t, *J*=2.8Hz, H-4); 6.46 (1H, dd, *J*=2.8 & 1.7Hz, H-3); 6.86 (1H, m, H-5); 8.01 (1H, s, pyr-CH=N); ^{13}C NMR δ 20.6 ($CH(CH_3)_2$); 29.8 ($CH(CH_3)_2$); 69.1 ($CH_2CH(CH_3)_2$); 109.6 (C-4); 114.0 (C-3); 121.6 (C-5); 130.3 (C-2); 151.7 (pyr-CH=N); *m/e* (EI, 70eV) 150 (M, 45.3%); 107 (B, M-C_3H_7, 100%); 123 (M-HCN, 3.1%); 80 (B-HCN, 37.6%); HRMS (M) Found 150.1159 (Calcd. for

$C_9H_{14}N_2$ 150.1157).

6.7.1.2 *Further Attempts at Imine Formation using P-2-C, described in Section 3.2.1.1*

H_2N-Ala-OEt **3.11** was freshly generated by dissolving HCl.H_2N-Ala-OEt in CH_2Cl_2 (2mL) followed by TEA (1.1equiv.) and water (2x2mL). The organic layer was dried and evaported and used immediately.

Modifications:

1) P-2-c (10mg, 0.11mmol, 1equiv.) and freshley generated H_2N-Ala-OEt (13mg, 0.11mmol, 1equiv.) were stirred in benzene (5mL). The desired imine **3.12** was not evident by ^1H NMR spectroscopy after 24 h reaction.

2) P-2-c (10mg, 0.11mmol, 1equiv.), freshley generated H_2N-Ala-OEt (13mg, 0.11mmol, 1equiv.) and activated 4Å molecular sieves (500mg) were heated at reflux for 3 h in benzene (5mL), then left to stir at rt for 18 h. The desired imine **3.12** was not evident by ^1H NMR spectroscopy after 24 h reaction.

3) P-2-c (10mg, 0.11mmol, 1equiv.), freshley generated H_2N-Ala-OEt (13mg, 0.11mmol, 1equiv.) and $MgSO_4$ (100mg) were stirred for 3 h in CH_2Cl_2 (5mL). The desired imine **3.12** was not evident by ^1H NMR spectroscopy after 24 h reaction.

4) A solution of p-2-c (10mg, 0.11mmol, 1equiv.) and H_2N-Ala-OEt (9.9mg, 0.11mmol, 1equiv.) in MeOH (2.5mL) and EtOH (5mL) were stirred for 5 d. The solution was evaporated to dryness and Et_2O was added. Unreacted amino acid was removed by filtration. The desired imine **3.12** was evident by ^1H NMR spectroscopy in <1%.

5) P-2-c (10mg, 0.11mmol, 1equiv.), freshley generated H_2N-Ala-OEt (13mg, 0.11mmol, 1equiv.) TsOH (2mg, 0.01mmol) were stirred in CH_2Cl_2. The desired imine **3.12** was not evident by ^1H NMR spectroscopy after 24 h reaction.

6) P-2-c (10mg, 0.11mmol, 1equiv.) HCl.H_2N-Ala-OEt (17mg, 0.11mmol, 1equiv.) and TEA (18μL, 0.13mmol, 1.2equiv.) were dissolved in benzene (5mL) and MeOH (2.5mL) and stirred for 24 h. A ^1H NMR spectral analysis showed imine **3.12** (50%), the remaining material was starting material.

7) P-2-c (10mg, 0.11mmol, 1equiv.), HCl.H_2N-Ala-OEt (17mg, 0.11mmol, 1equiv.) and TEA (18μL, 0.13mmol, 1.2equiv.) were dissolved in benzene (5mL). The solution was heated at reflux using a Dean-Stark apparatus. The desired imine **3.12** was not evident by ^1H NMR spectroscopy after 10 h reaction.

8) P-2-c (10mg, 0.11mmol, 1equiv.), HCl.H_2N-Ala-OEt (17mg, 0.11mmol, 1equiv.) and TEA (18μL, 0.13mmol, 1.2equiv.) were dissolved in CH_2Cl_2 (5mL). The solution was heated at reflux using a modified Dean-Stark apparatus. The desired imine **3.12** was not evident by ^{1}H NMR spectroscopy after 10 h reaction.

9) P-2-c (10mg, 0.11mmol, 1equiv.), HCl.H_2N-Ala-OEt (17mg, 0.11mmol, 1equiv.) and TEA (18μL, 0.13mmol, 1.2equiv.) were dissolved in $CHCl_3$ (5mL). The solution was heated at reflux using a modified Dean-Stark apparatus. The desired imine **3.12** was not evident by ^{1}H NMR spectroscopy after 10 h reaction.

6.7.1.3 *Further Attempts at Imine Formation using N-Acyl-P-2-C, described in Section 3.2.1.4*

Modifications:

1) *N*-Acetyl-p-2-c **2.24** (10mg, 0.07mmol) and H_2N-Ala-OEt **3.11** (8.2mg, 0.07mmol, 1equiv.) were dissolved in benzene (5mL) and MeOH (2.5mL). ^{1}H NMR spectroscopy indicated p-2-imine **3.12** (77%) and p-2-c (23%) after 24 h stirring.

2) *N*-Acetyl-p-2-c **2.24** (10mg, 0.07mmol) and H_2N-Ala-OEt **3.11** (8.2mg, 0.07mmol, 1equiv.) were dissolved in THF (10mL). ^{1}H NMR spectroscopy indicated p-2-imine **3.12** (7%), p-2-c (35%) and starting material (58%) after 24 h stirring.

3) *N*-Acetyl-p-2-c **2.24** (10mg, 0.07mmol), HCl.H_2N-Ala-OEt **3.11** (11mg, 0.07mmol, 1equiv.) and TEA (10μL, 0.07mmol, 1equiv.) were dissolved in pentane (10mL) and heated at reflux in a modified Dean-Stark apparatus. The ^{1}H NMR spectrum of an aliquot after 24 h showed no reaction had occurred. ^{1}H NMR spectroscopy indicated p-2-imine **3.12** (50%) and p-2-c (50%) after 3 d further refluxing.

4) *N*-Acetyl-p-2-c **2.24** (10mg, 0.07mmol), HCl.H_2N-Ala-OEt **3.11** (11mg, 0.07mmol, 1equiv.), TEA (10μL, 0.07mmol, 1equiv.) and titanium(IV) isopropoxide (20.8μL, 0.07mmol, 1equiv.) were dissolved in pentane (10mL). ^{1}H NMR spectroscopy indicated p-2-imine **3.12** (65%) and p-2-c (35%) after 2 h of azeotropic removal of water.

6.7.1.4 *Attempted Amine* **3.27** *Formation from N-Acetyl-P-2-C* **2.24**, *described in Section 3.2.3*

Modifications:

1) *N*-Acetyl-p-2-c **2.24** (10mg, 0.07mmol) and freshly generated H_2N-

Ala-OEt **3.11** (62mg, 0.53mmol, 7.5equiv.) were dissolved in dry MeOH (5mL). After 5 min $NaCNBH_3$ (1equiv., 0.07mmol, 4.5mg) was added and stirring continued. H_2O (5mL) was added and the mixture was washed with saturated $NaHCO_3$ solution (5mL) followed by immediate extraction with CH_2Cl_2 (10mL). ^1H NMR spectroscopy indicated p-2-c (89%) and starting material (11%) after 24 h reaction.

2) *N*-Acetyl-p-2-c **2.24** (10mg, 0.07mmol), freshly generated H_2N-Ala-OEt (62mg, 0.53mmol, 7.5equiv.) and activated 4Å molecular sieves (100mg) were stirred in dry MeOH (5mL). After 5 min $NaCNBH_3$ (1equiv., 0.07mmol, 4.5mg) was added and stirring continued. ^1H NMR spectroscopy indicated p-2-c as the only pyrrole after 24 h reaction, polymer was evident in the reaction vessel.

3) *N*-Acetyl-p-2-c **2.24** (10mg, 0.07mmol), HCl.H_2N-Ala-OEt (11mg, 0.07mmol, 1equiv.) and TEA (10µL, 0.07mmol, 1equiv.) were dissolved in dry DMF (5mL). After 5 min $NaCNBH_3$ (4.5mg, 0.07mmol, 1equiv.) was added and stirring continued. ^1H NMR spectroscopy indicated p-2-c as the only pyrrole after 3 d reaction.

4) *N*-Acetyl-p-2-c **2.24** (10mg, 0.07mmol), HCl.H_2N-Ala-OEt (11mg, 0.07mmol, 1equiv.) and TEA (10µL, 0.07mmol, 1equiv.) were dissolved in dry THF (5mL). After 5 min $NaCNBH_3$ (1equiv., 0.07mmol, 4.5mg) was added and stirring continued. ^1H NMR spectroscopy indicated p-2-c as the only pyrrole after 3 d reaction, polymer was evident in the reaction vessel.

6.7.1.5 *Attempted Amine* **3.27** *Formation from P-2-C, described in Section 3.2.3*

Modifications:

1) A mixture of p-2-c (10mg, 0.11mmol), HCl.H_2N-Ala-OEt **3.11** (17mg, 0.11mmol, 1equiv.) and TEA (1equiv., 0.11mmol, 15µL) were stirred for 1 h at rt. EtOH (2mL) and $NaCNBH_3$ (6.9mg, 0.11mmol, 1eqiuv.) were added and stirring continued. A ^1H NMR spectral analysis of the crude product gave no evidence of the desired amine **3.27**.

2) A mixture of p-2-c (10mg, 0.11mmol), HCl.H_2N-Ala-OEt **3.11** (17mg, 0.11mmol, 1equiv.), TEA (1equiv., 0.11mmol, 15µL) and titanium(IV) isopropoxide (33µL, 0.11mmol, 1equiv.) were stirred for 1 h at rt. EtOH (2mL) and $NaCNBH_3$ (6.9mg, 0.11mmol, 1eqiuv.) were added and stirring continued. A ^1H NMR spectral analysis of the crude product gave evidence of the desired amine **3.27** (5%), but this decomposed on standing in solution.

6.7.2 Amino Acid Extension in the Peptide "Sense" Direction - Amides 3.28 and 3.34, described in Section 3.2.4 -

P-2-COOH **3.29** (20mg, 0.18mmol), DCC (37mg, 0.18mmol, 1equiv.), TEA (25μL, 0.18mmol, 1equiv.) and $HCl.NH_2$-Gly-OEt **3.11** (25mg, 0.18mmol, 1equiv.) were dissolved in CH_2Cl_2 (10mL) under N_2. After 15 h stirring the solvent was removed to give the crude amide **3.28** which crystallised from EtOAC/Pet. Ether.

Ethyl 2-(Pyrrol-2-ylcarbonylamino) Ethanoate 3.28, 168mg (95%); mp 113.5-115°C (EtOAC/Pet. Ether, very pale yellow crystals); R_f 0.14; ^1H NMR δ 1.34 (3H, t, *J*=7.0Hz, $CO_2CH_2CH_3$); 4.19 (2H, d, *J*=5.4Hz, $CH_2CO_2CH_2CH_3$); 4.26 (2H, q, *J*=7.1Hz, $CO_2CH_2CH_3$); 6.25 (1H, m, H-4); 6.32 (1H, bm, CONH); 6.65 (1H, m, H-3); 6.94 (1H, m, H-5); 9.33 (1H, bm, pyr-NH); Irradiation of CONH collapses $NHCH_2CO$ to s; ^{13}C NMR δ 14.1 ($CO_2CH_2CH_3$); 41.3 ($CH_2CO_2CH_2CH_3$); 61.6 ($CO_2CH_2CH_3$); 109.7 (C-3); 110.0 (C-4); 121.9 (C-5); 125.2 (C-2); 161.1 (pyr-$COCH_2$); 170.1 ($CH_2CO_2CH_2CH_3$); IR (KBr) 3205, 3135, 1755, 1655, 1575, 1535cm^{-1}; UV ($CHCl_3$) 295.4, 265.0nm; *m/e* (EI, 70eV) 196 (M, 46.2%); 150 (B-CH_2CH_3OH, 6.9%); 123 (B-$CO_2C_2H_5^+$, 32.1%); 110 (B-$C_4H_9CH{=}NH_2^+$, 2.5%); HRMS Found 196.0847 (Calcd. for $C_9H_{12}N_2O_3$ 196.0848); Anal. Calcd. C 55.08; H 6.17; N 14.28 Found C 55.19; H 6.01; N 14.39.

The pyrrole amide **3.34**

P-2-COOH, DCC and $iBuNH_2$ (18μL, 0.18mmol, 1equiv.) in CH_2Cl_2 (10mL) were stirred for 15 h gave the desired amide **3.34** (22%) by ^1H NMR spectral analysis. ^1H NMR δ 0.86 (6H, d, *J*=4.5Hz, $(CH_3)_2$); 2.05 (1H, m, $CH(CH_3)_2$); 2.36 (2H, m, CH_2); 5.98 (1H, bs, NH); 6.44 (1H, m, H-4); 6.62 (1H, m, H-3); 7.19 (1H, m, H-5).

6.7.2.1 *Attempted Formylation of the P-2-Gly-OEt Amide* **3.28**, *described in Section 3.2.4.1*

DMF (13μL, 0.17mmol) was added dropwise to $POCl_3$ (16μL, 0.17mmol) in 1,2-dichloroethane under the Vilsmeir-Haack formylation conditions (187). P-2-Gly-OEt amide **3.28** (30mg, 0.15mmol) was added portionwise and the soultion stirred for 1 h followed by 15 min reflux. $NaOAc.3H_2O$ (5mL, 20% solution in H_2O) was added to the cooled solution. After reflux for a further 15 min a ^1H NMR spectrum of an aliquot showed evidence of the desired formylated pyrrole (<2%) [^1H NMR δ 9.82 (1H, s,

CHO)]. Further stirring and refluxing before addition of the NaOAc solution did not increase the yield.

6.7.3 Extention of Amino Acids in the Peptide "Anti-Sense" Direction to give 3.36, 3.37, 3.38 and 3.39

6.7.3.1 *Preparation of* **3.36** *and* **3.37** *via the Acid Chloride/DMAP Methodology, described in Section 3.2.5*

1) *N*-Cinnamoyl-p-2-OH **2.32** (20mg, 0.09mmol), DMAP (11mg, 0.09mmol, 1equiv.) and Hünigs base (19μL, 0.11mmol, 1.2equiv.) were dissolved in CH_2Cl_2 (10mL) at rt. Acetyl chloride (8μL, 0.11mmol, 1.2equiv.) was added and the resultant solution was stirred for 24 h. EtOAc (10mL) was added and the organic phase was washed with citric acid (10mL, 10% solution in H_2O), water (2x10mL), dried and evaporated to dryness. The resultant pyrrolic ester was purified by silica chromatography (EtOAc/Pet. Ether=1:2).

1-(3-Phenylpropinoyl)-2-acetoxymethylpyrrole 3.36, gave 21mg (87%) as a brown oil; Rf 0.63; ^{1}H NMR δ 2.08 (3H, s, CH_3); 3.14 (2H, m, CH_2Ph); 3.19 (2H, m, $COCH_2$); 5.35 (2H, bs, pyr-CH_2); 6.21 (1H, t, *J*=3.4Hz, H-4); 6.31 (1H, m, H-3); 7.12 (1H, dd, *J*=3.4 & 1.7Hz, H-5); 7.23 (2H, m, Ph-aromH2); 7.29 (2H, m, Ph-aromH3); 7.31 (1H, m, Ph-aromH4); Irradiation at pyr-CH_2 and H-3 collapsed to dd (*J*=1.7 & 0.9 Hz); ^{13}C NMR δ 20.9 ($OCOCH_3$); 30.3 (CH_2Ph); 37.4 ($COCH_2$); 60.0 (CH_2OCOCH_3); 111.8 (C-4); 115.4 (C-3); 121.0 (C-5); 126.5 (Ph-aromC4); 128.4 (Ph-aromC2); 128.6 (Ph-aromC3); 130.3 (C-2); 140.1 (Ph-aromC1); 170.5 (CH_2OCOCH_3); 170.7 (CO); FTIR (nujol) 3159.0, 2725.0, 1603.1cm^{-1}; UV ($CHCl_3$) 340.0, 267.2nm; *m/e* (EI, 50eV) 271 (M, 17.6%); 228 (M-CH_3CO, 16.2%); 198 (M-CH_2OCOCH_3, 10.2%); 133 (B, M-$PhCH_2CH_2CO$, 100%); HRMS (M) Found 271.1211 (Calcd. for $C_{16}H_{17}N_1O_3$ 271.1208).

2) *N*-Fmoc-Phe-Cl (45mg, 0.11mmol, 1.2equiv.) was added to *N*-cinnamoyl-p-2-OH **2.32**, DMAP and Hünigs base as described above. The resultant pyrrolic dipeptide **3.37** was purified by silica chromatography (EtOAc/Pet. Ether=1:2), after the polymer was removed by filtration.

1-(3-Phenylpropinoyl)-2-[[(9-fluorenylmethyl)oxy)carbonyl-L-phenylalaninoxy]methylpyrrole 3.37, gave 13mg (20%) as a brown oil; R_f 0.36; $[\alpha]^D_{25}$ -23° (c1, MeOH); ^{1}H NMR δ 3.07 (2H, m, Fmoc-CH_2); 3.09 (2H, m,

CH_2CH_2Ph); 3.14 (2H, m, $COCH_2CH_2Ph$); 4.20 (1H, t, *J*=7.0Hz, Fmoc-CH); 4.34 (1H, B part ABX, *J*=7.5 & 3.5Hz, Phe-CH_2); 4.40 (1H, A part ABX, *J*=7.5 & 3.5Hz, Phe-CH_2); 4.70 (1H, X part ABX & d, *J*=8.0 & 3.6Hz, Phe-CH); 5.27 (1H, d, *J*=8.0Hz, NH); 5.40& 5.45 (2H, bABq, *J*=13.0Hz, pyr-CH_2); 6.21 (1H, t, *J*=3.5Hz, H-4); 6.23 (1H, m, H-3); 7.10 (2H, m, Phe-aromH3); 7.13 (1H, dd, *J*=3.5 & 2.0Hz, H-5); 7.21-7.32 (8H, m, Phe-aromH4 & Fmoc-aromH3 & Ph); 7.40 (2H, t, *J*=7.5Hz, Fmoc-aromH3); 7.54-7.58 (4H, m, Phe-aromH2, Fmoc-aromH4); 7.76 (2H, d, *J*=7.5Hz, Fmoc-H5); irradiation at 6.23ppm, the bABq at 5.40ppm & 5.45ppm collapses to sharp ABq; ^{13}C NMR δ 30.2 ($COCH_2CH_2Ph$); 37.5 ($COCH_2CH_2Ph$); 38.1 (Phe-CH_2); 47.1 (Fmoc-CH); 54.6 (Phe-CH); 60.9 (pyr-CH_2); 67.0 (Fmoc-CH_2); 111.8 (C-4); 116.2 (C-3); 120.0 (Fmoc-C5); 121.2 (C-5); 125.0 (Fmoc-aromC4); 125.1 (Phe-aromC2); 126.5 (Ph-aromC4); 127.0 (Fmoc-aromC3); 127.7 (Fmoc-aromC2); 128.4 (Ph-aromC2); 128.5 (Ph-aromC3); 128.6 (Phe-aromC4); 129.3 (C-2); 129.4 (Phe-aromC3); 135.7 (Phe-aromC1); 140.0 (Ph-aromC1); 143.7 (Fmoc-aromC2a); 143.9 (Fmoc-aromC5a); 155.5 (OCO-Fmoc); 170.5 (pyr-CH_2OCO); 171.1 (CO); FTIR (neat) 3338.0, 3028.3, 2855.1, 1736.8, 1713.7, 1689.8, 1650.4, 1514.1cm^{-1}; UV (MeOH) 302.8, 291.6, 281.2nm; *m/e* (FAB) 599 (M+1, 65.1%); HRMS (M+1, FAB) Found 599.2551 (Calcd. for $C_{38}H_{35}N_2O_5$ 599.2546).

6.7.3.2 *Preparation of* **3.37**, **3.38** *and* **3.39** *via the Mitsunobu Reaction*[14], *described in Section 3.2.5*

The methodology is identical to that described for the camphanate formation given in Section 6.4.3.1.

1) *N*-(*N*-Pth-Phe)-p-2-OH **2.52** (30mg, 0.08mmol), triphenyl phosphine (45mg, 0.17mmol, 2.1equiv.) and *N*-Cbz-Val-Val-OH (62mg, 0.18mmol, 2.2equiv.) were dissolved in dry THF (10mL). After stirring for 5 min followed DEAD (27μL, 0.17mmol, 2.1equiv.) was added. The reaction was stirred for 3 h at rt under N_2. The solvents were evaporated, and the residue then dissolved in a minimal amount CH_2Cl_2. The solution was passed through a silica column (2cm, EtOAc/Pet. ether=1:2 elutent). Chromatography (EtOAc/Pet. Ether=1:2) of the resultant oil then yielded **3.39**.

1-(*N*-Phthalyl-L-phenylalinyl)-2-(*N*-benzyloxycarbonyl-L-valinyl-L-valinoxy)methylpyrrole 3.39, gave 11mg (20%) as a brown oil; R_f 0.54; $[\alpha]^D_{23}$ -15° (c1, MeOH); ^1H NMR δ 0.77 (3H, d, *J*=7.0Hz, Val-$(CH_3)_A$-Cbz); 0.89 (3H, d, *J*=7.0Hz, Val-$(CH_3)_B$-Cbz); 0.96 (3H, d, *J*=7.0Hz, pyr-Val-$(CH_3)_A$); 1.04 (3H, d, *J*=6.5Hz, pyr-Val-$(CH_3)_B$); 2.19 (1H, m, pyr-Val-$CH(CH_3)_2$); 2.22 (1H,

m, Val-C*H*$(CH_3)_2$-Cbz); 3.54 (2H, m, Phe-CH_2); 4.24 (1H, dd, *J*=6.5 & 2.5Hz, pyr-Val-CH); 4.67 (1H, dd, *J*=5.0 & 4.5Hz, Val-CH-Cbz); 5.12 (2H, s, Cbz-CH_2); 5.45 (1H, bABq, *J*=14.0Hz, pyr-CH_2); 5.48 (1H, bABq, *J*=14.0Hz, pyr-CH_2); 5.60 (1H, dd, *J*=9.5 & 5.5Hz, Phe-CH); 6.09 (1H, t, *J*=3.5Hz, H-4); 6.24 (1H, d, *J*=6.3Hz, Val-NH-Val); 6.29 (1H, m, H-3); 6.67 (1H, bd, *J*=5.3, NH-Cbz); 7.00 (1H, dd, *J*=3.5 & 1.5Hz, H-5); 7.19 (2H, m, Phe-aromH3); 7.20-7.24 (3H, m, Ph-aromH2 & aromH4); 7.32-7.36 (5H, m, Cbz-arom); 7.70 (2H, dd, *J*=5.5 & 3.0Hz, Pth-aromH3); 7.80 (2H, dd, *J*=5.4 & 3.0Hz, Pth-aromH4); ^{13}C NMR δ 17.3 (Val-$(CH_3)_A$-Cbz); 17.7 (Val-$(CH_3)_B$-Cbz); 19.0 (pyr-Val-$(CH_3)_A$); 19.4 (pyr-Val-$(CH_3)_B$); 31.3 (Val-C*H*$(CH_3)_2$-Cbz); 31.4 (pyr-Val-C*H*$(CH_3)_2$); 35.0 (Phe-CH_2); 53.8 (Val-CH-Cbz); 57.3 (pyr-Val-CH); 59.6 (Phe-CH); 60.2 (pyr-CH_2); 66.8 (Cbz-CH_2); 112.4 (C-4); 116.9 (C-3); 120.9 (C-5); 123.9 (Cbz-aromC4); 127.2 (Phe-aromC4); 127.9 (Cbz-aromC1); 128.0 (Cbz-aromC3); 128.5 (Cbz-aromC2); 128.7 (Phe-aromC2); 129.2 (Phe-aromC3); 131.0 (Pth-aromC3a); 134.5 (Phe-aromC1); 134.6 (Pth-aromC4); 135.8 (C-2); 135.9 (Cbz-aromC1); 156.4 (CO-Cbz); 166.6 (Pth-CO); 167.1 (Val-CO-Val); 170.7 (pyr-OCO-Val); 171.4 (CO); FTIR (neat) 3147.9, 1777.2, 1736.9, 1714.65, 1666.9, 1530.8cm^{-1}; UV (MeOH) 264.8, 216.0nm; *m/e* (FAB) 707 (M+1, 19.7%); 507 (M-$C_{13}H_{11}N_1O_3^+$, Pth-Phe, 23.4%); 357 (507-NHCbz, 53.0%); HRMS (M+1, FAB) Found 707.30807 (Calcd. for $C_{40}H_{43}N_4O_8$ 707.30806).

2) *N*-Cinnamoyl-p-2-OH **2.32** (18mg, 0.08mmol), triphenyl phosphine (45mg, 0.17mmol, 2.1equiv.) and *N*-Fmoc-Phe-OH (69mg, 0.18mmol, 2.2equiv.) were dissolved in dry THF (10mL). After stirring for 5 min followed DEAD (27μL, 0.17mmol, 2.1equiv.) was added. The reaction was stirred for 3 h at rt under N_2. The solvents were evaporated, and the residue then dissolved in a minimal amount CH_2Cl_2. The solution was passed through a silica column (2cm, EtOAc/Pet. ether=1:2 elutent). Chromatography (EtOAc/Pet. Ether=1:2) of the resultant oil then yielded **3.37** 19mg (73%) as a brown oil described in Section 6.7.3.1.

3) *N*-Cinnamoyl-p-2-OH **2.32** (18mg, 0.08mmol), triphenyl phosphine (45mg, 0.17mmol, 2.1equiv.) and *N*-Cbz-Ala-Phe-OH (67mg, 0.18mmol, 2.2equiv.) were dissolved in dry THF (10mL). After stirring for 5 min followed DEAD (27μL, 0.17mmol, 2.1equiv.) was added. The reaction was stirred for 3 h at rt under N_2. The solvents were evaporated, and the residue then dissolved in a minimal amount CH_2Cl_2. The solution was passed through a silica column (2cm, EtOAc/Pet. ether=1:2 elutent). The resultant oil was chromatographed (EtOAc/Pet. Ether=1:2).

1-(3-Phenylpropinoyl)-2-(*N*-benzyloxycarbonyl-L-alanyl-L-phenylalaninoxy)methylpyrrole 3.38, gave 52mg (69%) as a brown oil; R_f 0.20; $[\alpha]^{D}_{25}$ -21° (*c*1, MeOH); ^{1}H NMR δ 1.25 (3H, d, *J*=7.0Hz, Ala-CH_3); 3.00 (2H, m, CH_2CH_2Ph); 3.03 (2H, m, CH_2CH_2Ph); 3.12 (2H, m, Phe-CH_2); 4.13 (1H, m, Ala-CH); 4.80 (1H, m, Phe-CH); 4.98 (1H, ABq, *J*=12.1Hz, Cbz-CH_2); 5.06 (1H, ABq, *J*=12.1Hz, Cbz-CH_2); 5.16 (1H, bd, *J*=7.9Hz, NH-Cbz); 5.30 (1H, bABq, *J*=13.1Hz, pyr-CH_2); 5.38 (1H, bABq, *J*=13.1Hz, pyr-CH_2); 6.15 (1H, t, *J*=3.3Hz, H-4); 6.23 (1H, dbb, *J*=3.3 & 1.5Hz, H-3); 6.29 (1H, bd, *J*=6.9Hz, Phe-NH-Ala); 6.99 (2H, m, Phe-aromH3); 7.08 (1H, dd, *J*=3.3 & 1.5Hz, H-5); 7.15-7.28 (13H, m, Phe-aromH2, aromH4 & Cbz-arom & Ph); Irradiation at 5.34ppm and bdd at 6.23 collapses to dd; ^{13}C NMR δ 18.5 (Ala-CH_3); 30.2 (CH_2CH_2Ph); 37.3 (CH_2CH_2Ph); 37.6 (Phe-CH_2); 50.4 (Ala-CH); 53.0 (Phe-CH); 60.9 (pyr-CH_2); 67.0 (Cbz-CH_2); 111.9 (C-4); 116.3 (C-3); 121.3 (C-5); 126.5 (Ph-aromC4); 127.0 (Cbz-aromC2); 128.2 (Cbz-aromC4); 128.3 (Cbz-aromC3); 128.4 (Ph-aromC2); 128.5 (Phe-aromC2); 128.5 (Ph-aromC3); 128.7 (Phe-aromC4); 129.2 (C-2); 129.4 (Phe-aromC3); 135.6 (Phe-aromC1); 135.8 (Cbz-aromC1); 140.0 (Ph-aromC1); 155.8 (CO-Cbz); 170.5 (Phe-CO-Ala); 170.8 (pyr-CH_2OCO); 171.6 (CO); FTIR (neat) 3319.9, 2962.0, 1722.6, 1720.1, 1701.6, 1666.4, 1531.2, 1492.8cm^{-1}; UV (MeOH) 259.6, 236.8, 204.5nm; HRMS (M+1, FAB) Found 582.26245 (Calcd. for $C_{34}H_{35}N_3O_6$ 582.26039).

6.8 Work Described in Section 4.2 to Section 4.5

6.8.1 Hydrolysis of 2.32 with KOH in d_4-MeOH, described in Section 4.2

1) *N*-Cinnamoyl-p-2-OH **2.32** (1mg, 4μmol) was dissolved in d_4-MeOH (0.6mL). KOH (5mg, 0.089mmol, 22equiv.) was added. ^{1}H NMR spectroscopy indicated immediate deacylation to give two non-*N*-acylated pyrroles **4.1** and **4.2**. The final ^{1}H NMR spectra yield was **4.1** (60%) and **4.2** (40%).

The final yields varyied depending on the concentration of KOH and solvent used in the reaction, these are described in Section 4.2.

hydroxymethyl pyrrole **4.1**[15]: ^{1}H NMR (d_4-MeOH) δ4.50 (2H, s, CH_2OH); 5.99 (1H, t, *J*=2.6Hz, H-4); 6.07 (1H, m, H-3); 6.67 (1H, m, H-5)

methoxymethyl pyrrole **4.2**: ^{1}H (d_4-MeOH) δ3.59 (3H, s, OMe); 4.36 (2H, s, CH_2OMe); 6.00 (1H, t, *J*=3.1Hz, H-4); 6.04 (1H, m, H-3); 6.70 (1H, m, H-5).

2) *N*-Cinnamoyl-p-2-OH **2.32** (1mg, 4μmol) was dissolved in d_4-MeOH (0.6mL). KOH (10μL, 0.44mmole solution of KOH in D_2O, 1equiv.). ^{1}H NMR spectroscopy indicated deacylation to produce the two pyrrole non-*N*-acylated pyrroles **4.1** and **4.2**. The final ^{1}H NMR spectra yield was **4.1** (10%) and **4.2** (30%).

3) A larger scale reaction using pyrrole **2.32** (10mg, 40μmol) was carried out to ensure the reproducability of the small scale method described above.

N-Cinnamoyl-p-2-OH **2.32** (10mg, 40μmol) was dissolved in d_4-MeOH (0.6mL). KOH (10μL, 4.4mmole solution of KOH in D_2O, 1equiv.) was added. ^{1}H NMR spectroscopy indicated deacylation to produce the two pyrrole non-*N*-acylated pyrroles **4.1** and **4.2**. The final ^{1}H NMR spectra yield was **4.1** (10%) and **4.2** (30%), the same as for the smaller scale reaction, 2) above.

6.8.2 Hydrolysis of 2.32 with KOH in d_3-Acetonitrile, described in Section 4.3

1) *N*-Cinnamoyl-p-2-OH **2.32** (1mg, 4μmol) was dissolved in d_3-CD_3CN (0.6mL). KOH (10μL, 0.44mmole KOH solution in d_4-MeOH, 1equiv.) was added. ^{1}H NMR spectroscopy indicated deacylation to produce the two pyrrole non-*N*-acylated pyrroles **4.1** and **4.2**. The final ^{1}H NMR spectra yield was **4.1** (30%) and **4.2** (70%).

2) *N*-Cinnamoyl-p-2-OH **2.32** (1mg, 4μmol) dissolved in d_3-CD_3CN

(0.6mL). KOH (10μL, 0.44mmol solution KOH in D_2O, 1equiv.) was added. ^1H NMR spectroscopy indicated deacylation to produce the pyrrole **4.5** (80%) and starting material **2.32** (20%). The yield of **4.5** dropped (to 71%) as **4.1** (12%) formed, with starting material present (18%) over 4 d. Recovery of the material from the NMR tube found approximately 60% as polymer.

4.5 was found to be unstable in solution, but was characterised by NMR spectroscopy at -20°C.

2-Methylpyrrol-2-yl-3-phenylpropanoate 4.5, ^1H NMR (CD_3CN) δ 2.66 (2H, t, *J*=7.5Hz, CH_2Ph); 2.95 (2H, t, *J*=7.5Hz, $COCH_2$); 5.07 (2H, s, pyr-CH_2); 6.10 (1H, t, *J*=2.2Hz, H-4); 6.18 (1H, dd, *J*=2.5 & 1.5Hz, H-3); 6.80 (1H, dd, *J*=2.3 & 1.5Hz, H-5); 7.25 (1H, m, Ph-aromH4); 7.30 (1H, m, Ph-aromH2); 7.33 (1H, m, Ph-aromH3); ^{13}C NMR (CD_3CN) δ 29.7 (CH_2Ph); 34.7 ($COCH_2$); 58.0 (pyr-CH_2); 106.9 (C-4); 108.9 (C-3); 118.2 (C-5); 125.2 (C-2); 125.4 (Ph-aromC4); 127.6 (Ph-aromC2); 127.7 (Ph-aromC3); 140.1 (Ph-aromC1); 172.3 (CO).

3) *N*-Cinnamoyl-p-2-OH **2.32** (1mg, 4μmol) was dissolved in d_3-CD_3CN (0.6mL). KOH (20μL, 0.44mmol solution KOH in D_2O, 2equiv.) was added. ^1H NMR spectroscopy indicated deacylation to produce the pyrrole **4.5** (95%) and starting material **2.32** (5%) in 1 min. The yield of **4.5** dropped (to 40%) as **4.1** (60%) formed over 3 d. None of the material recovered from the NMR tube was polymeric.

4) *N*-Cinnamoyl-p-2-OH **2.32** (1mg, 4μmol) dissolved in d_3-CD_3CN (0.6mL) and n-$BuNH_2$ (0.45μL, 4μmol, 1equiv.) was added. A ^1H NMR spectrum prior to deacylation was run for analysis purposes. KOH (10μL, 0.44mmol solution KOH in D_2O, 1equiv.) was added. ^1H NMR spectroscopy indicated deacylation to produce the pyrrole **4.5** (70%), starting material **2.32** (20%) and the pyrrole amine **4.6** (10%), described below, in 1 min. The yield of **2.32** (to 10%) and **4.5** (to 10%) dropped as **4.6** (80%) formed over 1 d. None of the material recovered from the NMR tube was polymeric.

5) *N*-Cinnamoyl-p-2-OH **2.32** (1mg, 4μmol) dissolved in d_3-CD_3CN (0.6mL). n-$BuNH_2$ (0.45μL, 4μmol, 1equiv.) was added a preliminary ^1H NMR spectrum was run. KOH (20μL, 0.44mmol solution KOH in D_2O, 2equiv.) was added. ^1H NMR spectroscopy indicated deacylation to produce the pyrrole **4.5** (95%) and the pyrrole amine **4.6** (5%), described below, in 1 min. The yield of **4.5** dropped (to 0%) as **4.6** (100%) formed over 1 h. None of the material recovered from the NMR tube was polymeric.

2-Butylaminomethylpyrrole 4.6, an isolated but unstable oil; ^{1}H NMR (CD_3CN) δ 0.87 (3H, t, *J*=7.3Hz, CH_3); 1.26-1.42 (4H, m, $NHCH_2CH_2CH_2CH_3$); 2.90 (2H, bt, *J*=7.4Hz, $NHCH_2$); 3.62 (2H, s, pyr-CH_2NH); 6.03 (1H, m, H-3); 6.06 (1H, t, *J*=2.9Hz, H-4); 6.67 (1H, m, H-5); ^{13}C NMR δ 13.6 (CH_3); 20.5 (CH_2CH_3); 35.8 ($CH_2CH_2CH_3$); 50.5 ($NHCH_2$); 59.1 (pyr-CH_2NH); 109.8 (C-4); 119.2 (C-3); 121.8 (C-5); 125.9 (C-2); *m/e* (EI, 50eV) 152 (M, 12.5%); 80 (B, M-NHBu, 100%; HRMS (M) Found 152.1314 (Calcd. for $C_9H_{16}N_2$ 152.1313).

6.8.3 Stability of Hydroxymethyl Pyrrole 2.32 in Solution in the Absence of HO^-, described in Section 4.3.5

1) *N*-Cinnamoyl-p-2-OH **2.32** (1mg, 4μmol) was dissolved in d$_3$-CD_3CN (0.6mL) and D_2O (5μL, 5μmol, 1.25equiv.) was added. There was no change in the ^{1}H NMR spectral observed over 5 d.

2) *N*-Cinnamoyl-p-2-OH **2.32** (1mg, 4μmol) was dissolved in d$_3$-CD_3CN (0.6mL), D_2O (5μL, 5μmol, 1.25equiv.) and n-$BuNH_2$ (0.45μL, 4μmol, 1equiv.) were added. There was no change in the ^{1}H NMR spectral observed over 2 months.

6.8.4 Kinetic Analysis: Hydrolysis of 4.5 with KOH in d$_3$-Acetonitrile, described in Section 4.4

N-Cinnamoyl-p-2-OH **2.32** (1mg, 4μmol) was dissolved in d$_3$-CD_3CN (0.6mL) and n-$BuNH_2$ (0.45μL, 4μmol, 1equiv.) was added. KOH (either 10μL, 1equiv., 0.44mmol solution KOH in D_2O, or 15μL, 1.5equiv., 0.44mmol, solution KOH in D_2O, or 20μL, 2equiv., 0.44mmol, solution KOH in D_2O, or 30μL, 3equiv., 0.44mmol, solution KOH in D_2O) was added and vigourously shaken. A ^{1}H NMR spectrum was obtained after 30 s of KOH addition. The rate of change of the pyrrolic species **4.5** was monitored via the ^{1}H NMR spectra pyr-$CH_2OCOCH_2CH_2Ph$ (5.07ppm) signal.

Raw Data for Kinetic Analysis of Hydrolysis of 4.5†

Data from One Experiment at Each Concentration Shown

Time t (min)	1 Equiv. HO^-	1.5 Equiv. HO^-	2 Equiv. HO^-	3 Equiv. HO^-
0	112.0	165.1	135.4	155.7
1	98.6	154.8	116.4	106.7
1.5				83.8
2	89.6	156.0	100.5	74.2
2.5				72.4
3	77.3	147.0	91.9	60.9
4			88.4	54.1
5	76.4	147.7	83.5	45.0
6				43.5
7		146.4	79.3	27.4
8			67.5	23.0
10	75.2	145.6	64.5	21.1
13		138.9	63.8	17.6
15	73.9	136.3	59.7	4.5
30	68.3	135.1	56.4	0•
45	64.9	132.9		
60	59.4	132.0	55.4	
90	56.0	129.8	54.1•	
120	54.7	118.9•		
1 (day)	21.4•			
Abs_∞	21	130	56	0

† Data Collected at 23.1°C; • End of Data Collection

Table 6.1

The absorbance at infinity (Abs_∞) was determined by observation of the data extrapolated to the value $t=\infty$.

The observed rate, k, was obtained is presented below.

Observed Rate of Hydrolysis of 4.5 with respect to HO^- Concentration

Concentration HO^- (M)	Equivalents HO^-	Observed Rate k
$0.66x10^{-3}$	1	$1.34x10^{-3}$
	1	$1.33x10^{-3}$
	1	$1.30x10^{-3}$
$0.95x10^{-3}$	1.5	$1.98x10^{-3}$
$1.29x10^{-3}$	2	$2.79x10^{-3}$
	2	$2.81x10^{-3}$
$1.90x10^{-3}$	3	$3.96x10^{-3}$

Table 6.2

The plot of k_{obs} versus HO^- concentration gave a straight line, representing $k_{OH}[HO^-]$ or the k_{obs} with respect to decomposition of **4.5**.

The deacylation of **4.5** was found to be first order with respect to HO^- at zero to three equivalents of added HO^- and has a rate constant of $k=0.458 Lmol^{-1}s^{-1}$.

6.9 Work Described in Section 4.6, Eludidation of Mechanism of Hydroxide Attack on 2.32 to give 4.5

6.9.1 Formation of Optically Active Hydroxymethyl Pyrrole *N*-(*N*-Pth-L-Leu)-p-2-CHDOH 4.14

6.9.1.1 *DMAP Promoted Acylation of 6-D_1-p-2-c with N-Pth-L-Leu-Cl to give 6-D_1-Labelled Formyl Pyrrole* **4.14**

Dry hexane (10mL) was added to crude *N*-Pth-L-Leu-Cl **2.36** (prepared as in Section 6.1.2). After shaking, the hexane was removed and more hexane (10mL) was added, mixed and decanted. The combined hexane extracts were evaporated to dryness to give the purified acid chloride used in the following reaction.

6-D_1-Pyrrole-2-carboxaldehyde **4.15** (20mg, 0.21mmol), Hünigs Base (41μL, 0.21mmol) and DMAP (2.6mg, 0.021mmol) were dissolved in CH_2Cl_2 (2mL) and the solution was added dropwise to a stirred, ice cooled solution of the purified *N*-Pth-L-Leu-Cl **2.36** (0.31mmol, 87mg) in CH_2Cl_2 (5mL) under N_2. The resultant yellow oil was found to be pure by ^1H NMR spectroscopy for the desired *N*-(*N*-Pth-Leu)-p-2-CDO **4.16**.

All of the data with the exception of the ^1H NMR spectrum were identical to the previously described non-labelled *N*-(*N*-Pth-Leu)-p-2-c **3.44**, Section 6.4.1.2.

1-(*N*-Phthalyl-L-leucyl)-2-formylpyrrole 4.16, ^1H NMR δ 0.98 (3H, d, *J*=6.5Hz, (Leu-CH_3)$_A$); 1.04 (3H, d, *J*=6.5Hz, (Leu-CH_3)$_B$); 2.00 (2H, m, Leu-CH_2); 2.42 (1H, m, C*H*(CH$_3$)$_2$); 5.67 (1H, X part ABX, *J*=10.5 & 4.5Hz, Leu-CH); 6.31 (1H, t, *J*=3.5Hz, H-4); 7.16 (1H, dd, *J*=3.5 & 1.5Hz, H-3); 7.29 (1H, dd, *J*=3.4 & 1.6Hz, H-5); 7.77 (2H, dd, *J*=5.5 & 3.0Hz, Pth-H14); 7.85 (2H, dd, *J*=5.8 & 3.1Hz, Pth-H15); ^{13}C NMR δ 21.4 (CH_3)$_B$); 23.0 (CH_3)$_A$); 24.9 (CH(CH_3)$_2$); 37.5 (Leu-CH$_2$); 51.5 (Leu-CH); 113.2 (C-4); 122.6 (C-3); 123.8 (Pth-C14); 125.5 (C-5); 131.5 (Pth-C13); 134.6 (Pth-C15); 135.3 (C-2); 167.3 (Pth-CO); 168.7 (CO); 181.6 (CHO).

6.9.1.2 *Chiral Reduction of 6-D_1-Labelled Formyl Pyrrole* **4.16** *to give* **4.14**

Freshly prepared R-alpine borane[16] (1.1equiv.) was added to a stirred solution of D_1-labelled formyl pyrrole **4.16** (1equiv.) in THF (10mL). The solution was stirred for 4 h then evaporated to dryness. Excess (+)-α-pinene was removed under high vacuum (oil pump) to yield the optically active hydroxymethyl pyrrole **4.14**.

All the data, with the exception of the ^{1}H NMR, ^{13}C NMR spectra and mass spectrum were identical to the previously described non-labelled non-labelled *N*-(*N*-Pth-Leu)-p-2-OH **3.45**, Section 6.4.2.2.

[6-D$_1$]-1-(*N*-Phthaloyl-L-leucyl)-2-hydroxymethylpyrrole 4.14 ^{1}H NMR δ 0.98 (3H, d, *J*=6.5Hz, CH(C*H*$_3$)$_A$); 1.05 (3H, d, *J*=6.5Hz, CH(C*H*$_3$)$_B$); 2.00 (2H, m, Leu-CH$_2$); 2.46 (1H, m, C*H*(CH$_3$)$_2$); 4.63 (1H, s, C*H*DOH); 5.54 (1H, X part ABX, *J*=10.5 & 4.5Hz, Leu-CH); 6.17 (1H, t, *J*=3.5Hz, H-4); 6.22 (1H, m, H-3); 7.06 (1H, dd, *J*=3.4 & 1.5Hz, H-5); 7.76 (2H, dd, *J*=5.5 & 3.4Hz, Pth-aromH3); 7.86 (2H, dd, *J*=5.6 & 3.4Hz, Pth-aromH4); ^{13}C NMR δ 21.4 (CH(C*H*$_3$)$_B$); 23.0 (CH(C*H*$_3$)$_A$); 25.0 (CH(C*H*$_3$)$_2$); 37.7 (Leu-CH$_2$); 51.3 (Leu-CH); 57.6 (CHDOH, t, J_{C-D}=22.1Hz); 113.0 (C-4); 114.9 (C-3); 120.1 (C-5); 123.8 (Pth-aromC3); 131.3 (Pth-aromC3a); 134.5 (Pth-aromC4); 136.1 (C-2); 167.5 (Pth-CO); 169.4 (CO); HRMS (EI, 50eV) Found 341.14856 (Calcd. for $C_{19}H_{19}D_1N_2O_4$ 341.14857); Isotopic incorporation 93.6% D.

6.9.2 Hydrolysis of Chiral, Labelled 4.14 with HO$^-$

6.9.2.1 *Trial Hydrolysis of Unlabelled N-(N-Pth-Leu)-p-2-OH* **3.45** *with HO$^-$*

N-(*N*-Pth-Leu)-p-2-OH **3.45** (5mg, 0.01mmol) was dissolved in d$_3$-CD$_3$CN (0.6mL). Addition of KOH (10μL, 0.44mmol, KOH solution in D$_2$O, 1equiv.) caused rapid hydrolysis of **3.45** to the unstable *O*-acyl pyrrole derivative **4.13**.

4.13, ^{1}H NMR δ (d$_3$-CD$_3$CN) 0.99 (3H, t, *J*=6.4Hz, (Leu-CH$_3$)$_A$); 1.04 (3H, t, *J*=6.3Hz, (Leu-CH$_3$)$_B$); 1.99 (2H, m, Leu-CH$_2$); 2.44 (1H, m, CH(CH$_3$)$_2$); 4.96 (1H, m, Leu-CH); 5.09 (1H, A part ABq, *J*=12.6Hz, pyr-CH$_2$); 5.13 (1H, B part ABq, *J*=12.6Hz, pyr-CH$_2$); 6.06 (1H, m, H-4); 6.09 (1H, m, H-3); 6.78 (1H, t, *J*=3.1Hz, H-5); 7.87-7.89 (4H, m, Pth-aromH).

6.9.2.2 *Hydrolysis of Labelled N-(N-Pth-Leu)-p-2-OH* **4.14** *with HO$^-$*

N-(*N*-Pth-Leu)-p-2-CHDOH **4.14** (5mg, 0.01mmol) was dissolved in d$_3$-CD$_3$CN (0.6mL). Addition of KOH (10μL, 0.44mmol, KOH solution in D$_2$O, 1equiv.) caused rapid conversion to the D$_1$-labelled pyrrolic ester **4.19**.

4.19, ^{1}H NMR δ (d$_3$-CD$_3$CN) 0.99 (3H, t, *J*=6.4Hz, (Leu-CH$_3$)$_A$); 1.04 (3H, t, *J*=6.3Hz, (Leu-CH$_3$)$_B$); 1.99 (2H, m, Leu-CH$_2$); 2.44 (1H, m, CH(CH$_3$)$_2$); 4.96 (1H, m, Leu-CH); 5.09 (1H, s, pyr-CHD); 6.06 (1H, m, H-4); 6.09 (1H, m, H-3); 6.78 (1H, t, *J*=3.1Hz, H-5); 7.87-7.89 (4H, m, Pth-aromH).

The one upfield signal was attributted to the 'S' configuration and therefore retention of configuration.

6.9.3 Formation of the 6-D_1-Labelled Hydroxymethyl Pyrroles *N*-Cinnamoyl-p-2-CHDOH 4.10 and 4.24, described in Section 4.6.4

6.9.3.1 *Preparation of N-Cinnamoyl-p-2-CDO* 4.23

Hydrocinnamoyl chloride (0.31mmol, 46μL) was added to a solution of 6-D_1-pyrrole-2-carboxaldehyde **4.15** (20mg, 0.21mmol), Hünigs Base (41μL, 0.21mmol) and DMAP (2.6mg, 0.021mmol) dissolved in CH_2Cl_2 (2mL) under N_2. The resultant brown oil was found to be ^1H NMR pure for the *N*-cinnamoyl-p-2-CDO **4.23**.

All the data with the exception of the ^1H NMR spectrum and mass spectrum were identical to the non-labelled *N*-cinnamoyl-p-2-c **2.31**.

[6-D_1]-1-(3-Phenylpropanoyl)-2-formylpyrrole 4.23, ^1H NMR δ 3.16 (2H, t, *J*=7.2Hz, $COCH_2$); 3.27 (2H, t, *J*=7.2Hz, CH_2Ph); 6.33 (1H, t, *J*=3.1Hz, H-4); 7.21 (1H, dd, *J*=3.1 & 1.6Hz, H-3); 7.24 (2H, m, Ph-aromH2); 7.24 (1H, m, Ph-aromH4); 7.31 (2H, m, Ph-aromH3); 7.32 (1H, dd, *J*=3.1 & 1.6Hz, H-5); FTIR (KBr) 3114.0, 1654.2, 1540.2cm^{-1}; HRMS (M) Found 228.10090 (Calcd. for $C_{14}H_{12}D_1N_1O_2$ 228.10091); Isotopic incorporation 99.07% D.

6.9.3.2 *Reduction of 6-D_1-Formyl Pyrrole* 4.23 *to give* 4.10 and 4.24, *described in Section 4.6.4*

The D_1-labelled formyl pyrrole **4.23** was reduced under each of the following conditions.

1) Achirally, under the $Zn(BH_4)_2$ conditions to give racemic hydroxylmethyl pyrrole **4.24**, as described in Section 6.4.2.2. The D_1-labelled formyl pyrrole **4.23** (20mg, 0.21mmol) was dissolved in dry Et_2O under N_2. $Zn(BH_4)_2$ (0.25mmol, 2.3mL of 0.11M solution in dry Et_2O, 1.2equiv.) was added and the resultant solution was stirred at rt for 30 min. The Et_2O solution was decanted from the organic insoluble zinc salts. Further Et_2O (2x5mL) was added, decanted and combined with the previous washings. H_2O (2mL) and acetic acid (2mL, 10% solution in water) were carefully added to the Et_2O extracts. The separated aqueous phase was re-extracted with CH_2Cl_2 (2x5mL) and the combined organic solvents were washed with H_2O (2x10mL). The organic phase was dried and evaporated. The resultant

racemic, labelled hydroxymethyl pyrrole **4.24** was purified by silica chromatography (EtOAc/Pet. Ether=1:2). All the data with the exception of the ^1H NMR spectra were identical to the unlabelled hydroxymethyl pyrrole **2.32** described in Section 6.4.2.2.3.

[6-D_1]-1-(3-Phenylpropanoyl)-2-hydroxymethylpyrrole 4.24, ^1H NMR δ 3.08 (2H, dt, *J*=7.8 & 1.5Hz, CH_2Ph); 3.17 (2H, dt, *J*=7.8 & 1.5Hz, $COCH_2$); 3.71 (1H, bs, CH_2OH); 4.62 (1H, bs, CHDOH); 6.17 (1H, t, *J*=3.3Hz, H-4); 6.21 (1H, m, H-3); 7.06 (1H, dd, *J*=3.3 & 1.6Hz, H-5); 7.22 (1H, m, Ph-aromH3); 7.28 (2H, m, Ph-aromH2); 7.30 (1H, m, Ph-aromH4).

2) Chirally, under the R-alpine borane reduction conditions, Section 6.9.3.1.1, to give the optically active hydroxymethyl pyrrole **4.10**. Freshly prepared R-alpine borane[12] (1.1equiv.) was added to a stirred solution of D_1-labelled formyl pyrrole **4.23** (20mg, 1equiv.) in THF (10mL). The solution was stirred for 4 h, then evaporated to dryness. Excess (+)-α-pinene was removed under high vacuum (oil pump) to yield the optically active D_1-labelled hydroxymethyl pyrrole **4.10**. The chirality of the -CDH- group was described as 'S' by analogy with known chiral hydroxymethyl pyrroles, see Section 4.7. All the data, with the exception of the mass spectra, was identical to the racemic, labelled hydroxymethyl pyrrole **4.24** described 1) above.

[6-D_1]-(6S)-1-(3-Phenylpropanoyl)-2-hydroxymethylpyrrole 4.10, HRMS (M) Found 228.10090 (Calcd. for $C_{14}H_{12}D_1N_1O_2$ 228.10091); Isotopic incorporation 99.07% D.

6.9.4 Formation of the 6-D_1-Labelled *N*-Cinnamoyl-p-2-CHDO-camphanates 4.25 and 4.26, described in Section 4.6.4

6.9.4.1 *N-Cinnamoyl-p-2-CHDO-camphanate* **4.25**

N-Cinnamoyl-p-2-CHDOH **4.24** was treated under the acid chloride/DMAP conditions, described in Section 6.7.3.1.

N-Cinnamoyl-p-2-CHDOH **4.24** (20mg, 0.09mmol), DMAP (11mg, 0.09mmol, 1equiv.) and Hünigs base (19μL, 0.11mmol, 1.2equiv.) were dissolved in CH_2Cl_2 (5mL) at rt. (-)-Camphanic chloride (19mg, 0.09mmol, 1equiv.) was added and the resultant solution was stirred for 24 h under N_2. EtOAc (10mL) was added and the organic solvents were washed with citric acid (10mL, 10% solution in H_2O), water (2x10mL), dried and evaporated to dryness. The resultant pyrrolic ester was purified by silica chromatography (EtOAc/Pet. Ether=1:2) to yield the labelled camphanate **4.25**.

(1S)-(-)-1-(3-Phenylpropinoyl)pyrrol-2-ylmethyl Camphanate 4.25, gave 38mg (99%) as a brown solid; R_f 0.30; $[\alpha]^D_{18}$ -86° (*c*1, MeOH); ^1H NMR δ 0.89 (3H, s, camph-CH_3); 0.95 (3H, s, camph-CH_3); 1.03 (3H, s, camph-CH_3); 1.59 (2H, m, camph-CH_2); 1.83 (1H, m, camph-CH_2); 1.94 (1H, m, camph-CH_2); 2.34 (2H, m, camph-CH_2); 2.99 (2H, dt, *J*=6.8 & 2.0Hz, CH_2Ph); 3.10 (2H, dt, *J*=7.0 & 1.8Hz, $COCH_2$); 5.39 (1H, ABq, *J*=12.4Hz, CH_2O-camph); 5.43 (1H, ABq, *J*=12.4Hz, CH_2O-camph); 6.14 (1H, t, *J*=3.5Hz, H-4); 6.29 (1H, m, H-3); 7.07 (1H, dd, *J*=3.5 & 1.5Hz, H-5); 7.15 (2H, m, Ph-aromH3); 7.19 (2H, m, Ph-aromH2); 7.24 (1H, m, Ph-aromH4); ^{13}C NMR δ 9.7 (camph-CH_3); 16.6 (camph-CH_3); 16.6 (camph-CH_3); 29.0 (camph-CH_2); 30.2 (CH_2Ph); 30.7 (camph-CH_2); 37.2 ($COCH_2$); 54.2 (camph-C); 54.8 (camph-C); 60.9 (CH_2O-camph); 91.2 (OCO-camph-C); 111.8 (C-4); 116.3 (C-3); 121.4 (C-5); 126.5 (Ph-aromC4); 128.4 (Ph-aromC2); 128.6 (Ph-aromC3); 129.1 (C-2); 140.0 (Ph-aromC1); 167.1 (CH_2O-CO); 170.5 (CO); 178.3 (camph-CO); FTIR (neat) 2966.1, 1789.3, 1748.6, 1731.2, 1495.4cm^{-1}; UV ($CHCl_3$) 286.4, 266.4nm; *m/e* (EI, 70eV) 409 (M, 2.7%); 277 (B, M-$C_7H_8^+$, 100%); 80 ($C_5H_6N^+$, 67.6%); HRMS (M) Found 409.18891 (Calcd. for $C_{24}H_{27}N_1O_5$ 409.18891).

6.9.4.2 *N-Cinnamoyl-p-2-CHDO-camphanate* **4.26**

The D_1-labelled camphanate **4.26** was prepared under the same conditions as in Section 6.9.4.1 from the D_1-labelled hydroxymethyl pyrrole **4.10**.

N-Cinnamoyl-p-2-CHDOH **4.10** (20mg, 0.09mmol) was treated under the acid chloride/DMAP conditions, as described above.

The resultant pyrrolic ester was purified by silica chromatography (EtOAc/Pet. Ether=1:2). All the data with the exception of the ^{1}H NMR, ^{13}C NMR spectra and the mass spectrum were identical to the racemic, labelled camphanate **4.25**.

[6-D_1]-(6S,1S)-(-)-1-(3-Phenylpropinoyl)pyrrol-2-ylmethyl Camphanate 4.26. ^{1}H NMR δ 0.89 (3H, s, camph-CH_3); 0.95 (3H, s, camph-CH_3); 1.03 (3H, s, camph-CH_3); 1.59 (2H, m, camph-CH_2); 1.83 (1H, m, camph-CH_2); 1.94 (1H, m, camph-CH_2); 2.34 (2H, m, camph-CH_2); 2.99 (2H, dt, *J*=6.8 & 2.0Hz, CH_2Ph); 3.10 (2H, dt, *J*=7.0 & 1.8Hz, COCH_2); 5.38 (1H, s, C*H*DO-camph); 6.14 (1H, t, *J*=3.5Hz, H-4); 6.29 (1H, m, H-3); 7.07 (1H, dd, *J*=3.5 & 1.5Hz, H-5); 7.15 (2H, m, Ph-aromH3); 7.19 (2H, m, Ph-aromH2); 7.24 (1H, m, Ph-aromH4); ^{13}C NMR δ 9.7 (camph-CH_3); 16.6 (camph-CH_3); 16.6 (camph-CH_3); 29.0 (camph-CH_2); 30.2 (*C*H_2Ph); 30.7 (camph-CH_2); 37.2 (CO*C*H_2); 54.2 (camph-C); 54.8 (camph-C); 60.9 (CHDO-camph, t, J_{C-D}=23.6Hz); 91.2 (OCO-camph-*C*); 111.8 (C-4); 116.3 (C-3); 121.4 (C-5); 126.5 (Ph-aromC4); 128.4 (Ph-aromC2); 128.6 (Ph-aromC3); 129.1 (C-2); 140.0 (Ph-aromC1); 167.1 (CH_2O-*C*O); 170.5 (CO); 178.3 (camph-*C*O); HRMS (M) Found: 410.19521 (Calcd. for $C_{24}H_{26}D_1N_1O_5$ 410.19519); Isotopic incorporation 90.01% D.

The D_1-labelled camphanate **4.26** was found to be the same configuration at pyr-CHD-R as the starting material **4.10** on the basis of ^{1}H NMR spectral analysis of the known configuration of similar pyrrolic camphanates[17]. The configuration was therefore assigned as 'S'.

6.9.5 Hydrolysis of *N*-Cinnamoyl-p-2-OAc 3.36 for Elucidation of Mechanism of Hydroxide Attack on 2.32, described in Section 4.6.5

N-Cinnamoyl-p-2-OAc **3.36** (1mg, 3μmol) was dissolved in d_3-CD_3CN (0.6mL) and n-$BuNH_2$ (0.35μL, 3μmol, 1equiv.) was added. KOH (7.5μL, 0.44mmol, solution KOH in D_2O, 1equiv.) was added and the ^{1}H NMR spectra obtained at t=30 s. The rate of reaction was monitored via the pyr-CH_2X ^{1}H NMR signals, X=$OCOCH_3$ 5.35ppm, X=$OCOCH_2CH_2Ph$ 5.07ppm, X=NHn-Bu 3.62ppm the rate of deacylation is discussed in Section 4.6.2.

Raw Data for Hydrolysis of 3.36†

Time t (min)	2 Equiv. HO^-
0.0	164.3
1.5	163.9
2.5	162.8
4.0	161.4
5.5	159.9
7.5	158.9
10.0	159.0
12.0	159.4
14.0	155.2
20.0	154.2
25.0	152.2
30.0	154.3
40.0	153.7
50.0	152.9
70.0	151.2
85.0	151.2•

† Data Collected at 23.1°C; • End of Data Collection

Table 6.3

6.10 Azafulvene Chemistry: Experimental Evidence, described in Section 4.7

6.10.1 Decompostion of 2-Hydroxymethyl Pyrrole 4.1

P-2-c (10mg, 0.11mmol) was dissolved in dry ether, followed by the addition of $Zn(BH_4)_2$ (0.13mmol, 1.0mL of 0.11M solution in dry Et_2O, 1.2equiv.) was added and the resultant solution was stirred at rt for 30 min. The Et_2O solution was decanted from the organic insoluble zinc salts. Further Et_2O (2x5mL) was added, decanted and combined with the previous washings. H_2O (2mL) and acetic acid (2mL, 10% solution in water) were carefully added to the Et_2O extracts. The separated aqueous phase was re-extracted with CH_2Cl_2 (2x5mL) and the combined organic solvents were washed with H_2O (2x10mL). The organic phase was dried and evaporated. The ^1H NMR spectra was consistent with authentic 2-hydroxymethyl pyrrole **4.1**[11].

4.1 (5mg, 5μmol) was dissolved in d_3-CD_3CN (0.6mL) and the ^1H NMR spectra were recorded. After 2 h the ^1H NMR spectra of **4.1** had broadened into the baseline, suggesting polymer formation. The NMR tube had also become stained.

6.10.2 Azafulvene Formation Suppressed by *N*-Acylation: Evidence Gained from Camphanates 4.25, 4.26 and 4.28, discussed in Section 4.7.1

The preparation of the camphanates **4.25** and **4.26** used in this Section is discussed in Section 6.9.4.

The camphanate **4.28** was prepared via the Mitsunobu reaction on the chiral, labelled hydroxymethyl pyrrole **4.10**. *N*-Cinnamoyl-p-2-CHDOH was treated under the Mitsunobu reaction conditions, described in Section 6.7.3.2.

N-Cinnamoyl-p-2-CHDOH **4.10** (30mg, 0.08mmol), triphenyl phosphine (45mg, 0.17mmol, 2.1equiv.) and (-)-camphanic acid (35mg, 0.18mmol, 2.2equiv.) were dissolved in dry THF (10mL). Stirring for 5 min followed, then DEAD (27μL, 0.17mmol, 2.1equiv.) was added. The reaction was stirred for 3 h at rt under N_2. The solvents were evaporated, and the residue then dissolved in CH_2Cl_2 (0.5mL). The solution was passed through a silica column (2cm, EtOAc/Pet. ether=1:2 elutent). Chromatography (EtOAc/Pet. Ether=1:2) of the resultant oil then yielded **4.28**. All the data, with the exception of the ^1H NMR spectra were identical to the D_1-labelled

camphanate **4.25**, described in Section 6.9.4.2.

(6S,1S)-(-)-1-(3-Phenylpropinoyl)pyrrol-2-ylmethyl Camphanate 4.28, ^{1}H NMR δ 0.89 (3H, s, camph-CH_3); 0.95 (3H, s, camph-CH_3); 1.03 (3H, s, camph-CH_3); 1.59 (2H, m, camph-CH_2); 1.83 (1H, m, camph-CH_2); 1.94 (1H, m, camph-CH_2); 2.34 (2H, m, camph-CH_2); 2.99 (2H, dt, *J*=6.8 & 2.0Hz, CH_2Ph); 3.10 (2H, dt, *J*=7.0 & 1.8Hz, COCH_2); 5.39 (1H, s, *CH*DO-camp); 6.14 (1H, t, *J*=3.5Hz, H-4); 6.29 (1H, m, H-3); 7.07 (1H, dd, *J*=3.5 & 1.5Hz, H-5); 7.15 (2H, m, Ph-aromH3); 7.19 (2H, m, Ph-aromH2); 7.24 (1H, m, Ph-aromH4);

The camphanate **4.28** was found to have a major component as the opposite configuration, ie: 'R' at pyr-CHD-R to that of the starting material **4.26**, ie: 'S', this is discussed in Section 4.7.1.

Derivation of Camphanate		NMR Signal δ	Configuration %'S'	Configuration %'R'
Achiral Reduction	**4.25**	5.38:5.39	49	51
Acid Chloride/DMAP	**4.26**	5.38	99	1
Mitsunobu	**4.28**	5.39†	39	61

† Major Signal

A discussion of the ^{1}H NMR spectral results is found in Section 4.7.1.

6.10.3 Pyrrole Amines 4.6, 4.35 and 4.36: Evidence for Azafulvene Formation, described in Section 4.7.2

The hydrolysis of non-labelled *N*-(*N*-Pth-Leu)-p-2-OH **3.45** and 6-D_1-labelled *N*-(*N*-Pth-Leu)-p-2-CHDOH **4.14** were carried out in the presence of *sec*-BuNH_2.

6.10.3.1 *Trial Hydrolysis of the Hydroxymethyl Pyrrole* **3.45**

N-(*N*-Pth-Leu)-p-2-OH **3.45** (5mg, 0.01mmol) was dissolved in d_3-CD_3CN (0.6mL) and racemic *sec*-BuNH_2 (1.2μL, 0.01mmol, 1equiv.) was added. Addition of KOH (10μL, 0.44mmol, KOH solution in D_2O, 1equiv.) caused rapid hydrolysis of to the pyrrolic ester **4.13**, described in Section 6.9.4.2, and the pyrrole amine **4.35**.

2-(1-Methylpropanoylamino)methylpyrrole 4.35, an unstable, isolated oil; ^{1}H NMR δ 0.92 (3H, t, *J*=7.2Hz, CH_2CH_3); 1.11 (3H, d, *J*=6.3Hz,

$CH(CH_3)$); 1.43 (2H, m, CH_2CH_3); 2.89 (1H, m, CH); 3.54 (1H, A part ABq, J=14.2Hz, pyr-CH_2); 3.56 (1H, B part ABq, J=14.1Hz, pyr-CH_2); 5.98 (1H, m, H-3); 6.03 (1H, t, J=2.9Hz, H-4); 6.72 (1H, m, H-5); ^{13}C NMR δ 12.5 (CH_2CH_3); 25.6 ((CH)CH_3); 39.6 (CH_2CH_3); 45.8 (CH); 54.9 (pyr-CH_2); 106.7 (C-4); 107.2 (C-3); 116.9 (C-5); 128.4 (C-2); *m/e* (EI, 70eV) 152 (M, 12.6%); 123 (M-CH_2CH_3, 18.1%); 80 (B, M-NHBu, 100%); HRMS (M) Found 152.13134 (Calcd. for $C_9H_{16}N_2$ 152.13134).

6.10.3.2 *Hydrolysis of the Chiral, Labelled Hydroxymethyl Pyrrole* **4.14**

N-(*N*-Pth-Leu)-p-2-CHDOH **4.14** (5mg, 0.01mmol) was dissolved in d_3-CD_3CN (0.6mL) and chiral (S)-(+)-*sec*-$BuNH_2$ (1.2μL, 0.01mmol, 1equiv.) was added. Addition of KOH (10μL, 0.44mmol, KOH solution in D_2O, 1equiv.) caused rapid conversion to the D_1-labelled pyrrolic ester **4.19**, described in Section 6.9.4.3, and the D_1-labelled pyrrole amine **4.36**.

The data for **4.36** was identical to that described for the unlabelled amine **4.35**, except for the ^1H NMR spectrum.

[6-D_1]-(8S)-(+)-2-(1-Methylpropanoylamino)methylpyrrole 4.36, an unstable, isolated oil; ^1H NMR δ 0.92 (3H, t, J=7.2Hz, CH_2CH_3); 1.11 (3H, d, J=6.3Hz, $CH(CH_3)$); 1.43 (2H, m, CH_2CH_3); 2.89 (1H, m, CH); 3.54 (1H, s, pyr-CHD); 3.56 (1H, s, pyr-CDH); 5.98 (1H, m, H-3); 6.03 (1H, t, J=2.9Hz, H-4); 6.72 (1H, m, H-5).

This is consistent with azafulvene chemistry to give the racemic product **4.36**.

6.11 Work Described in Chapter Five

6.11.1 α-Chymotrypsin Assay of 2.52, 2.55, 3.45, 3.53 and 3.55, described in Section 5.1

6.11.1.1 *General Assay Conditions*

The assay was based on a colourimetric technique and carried out in microtitre plates (NUNC flat bottomed plates, GIBCO). The enzyme and test solution were preincubated to ensure maximum inhibition before addition of substrate. After the addition of substrate the optical density was measured over approximately 2 h. The lack of colour development, caused by enzymic release of 4-nitroanilide derivatives, indicated inhibition. Control samples were included in all cases. Each sample had a duplicate that was tested in conjunction with each other. MeOH was used to dissolve the proposed inhibitor and for sample dilution, as it is H_2O soluble and directly compatible with the assay system.

6.11.1.2 *α-Chymotrypsin Assay*[18,19]

Solutions of the pyrroles **2.52**, **2.55**, **3.45**, **3.53** and **3.55** were made to 12.5μg mL^{-1} and 125μg mL^{-1} in dry MeOH. Tris-HCl (50μL of 0.4M solution in H_2O, pH 7.6), test solution (100μL) and α-chymotrypsin solution (50μL, Sigma ex-Porcine pancreas, 9units mL^{-1} in 50mM Tris-HCl buffer pH 7.6) were added to each well of the microtitre plate. Incubated at 37°C for 30 min was followed by the addition of *N*-succinyl-phenylalanine-4-nitroanilide (100μL, 1mgmL^{-1} solution in 50mM Tris-HCl buffer, pH 7.6). The absorbance was read at 410nm at t=0, and after incubation at 37°C when significant colour change had taken place (approximately 0.4 absorbance units per h at 37°C).

The inhibitor results are given in Section 5.1.

6.11.2 HIV-1 Protease Assay[20] of 2.32, 2.52, 3.39, 3.53 and 3.55, described in Section 5.2

The method described by Dreyer was used for the HIV-1 protease assay[21]. The samples were preincubated for 1 h with the enzyme in the MENDT buffer at pH 6.0, at 37°C. Addition of the substrate to the system started the peptidolytic reaction. After 20 min the amount of inhibition was determined.

The inhibition results are detailed in Section 5.2.

6.11.3 Pyrrole Derivatives Stability Test, described in Section 5.2

Hydroxymethyl pyrrole **2.52** (10mg, 0.04mmol) was dissolved in DMSO (2mL) and placed in an acidic buffer (10mL, potassium phthalate/phthalic acid pH 5.9) at 37°C for one hour. After fifteen minutes a precipitate had formed indicating decomposition. The precipitate was insoluble in water, and chloroform, and was attributed to pyrrolic polymer formation.

6.12 References to the Experimental

[1] Aue, W. P.; Bartholdi, E.; Ernst, R. R. *J. Chem. Phys.* **1976**, *64*, 2229.

[2] Sorensen, O. W.; Ernst, R. R. *J Magn. Res.* **1983**, *51*, 477.

[3] Bax, A.; Morris, G. *J. Magn. Res.* **1981**, *42*, 501.

[4] Neuhaus, D. *J. Magn. Res.* **1983**, *53*, 109.

[5] Perrin, D. D.; Armarego, W. L. F.; Perrin, D. R. *Purification of Laboratory Chemicals*; Pergamon Press: Oxford, 1980.

[6] Carpino, L. A.; Cohen, B. J.; Stephens Jr, K. E.; Sadat-Aalaee, S. Y.; Tein, J-H.; Landridge, D. C. *J. Org. Chem.* **1986**, *51*, 3732-3734.

[7] Nickisch, K.; Klose, W.; Bohlmann, F. *Chem. Ber.* **1980**, *113*, 2036-2037.

[8] Meek, T. D.; Lambert, D. M.; Metcalf, B. W.; Petteway Jr., S. R.; Dreyer, G. B. *HIV-1 Protease as a Target for Potential anti-AIDS Drugs*; Elsevier Science Publishers: Amsterdam, 1990; Vol. 14, pp. 225-256.

[9] Kipping, F. S. *J. Chem. Soc. (Lond).* **1894**, *65*, 480-503.

[10] Kisfaludy, L.; Löw, M.; Nyéki, O.; Szirtes, T.; Schön, I. *Liebigs Ann. Chem.* **1973**, 1421-1429.

[11] Schauder, J-R.; Jendrezejewski, S.; Abell, A.; Hart, G. J.; Battersby, A. R. *J. Chem. Soc., Chem. Commun.* **1987**, 436-438.

[12] Loader, C. E.; Barnett, G. H.; Anderson, H. J. *Can. J. Chem.* **1982**, *60*, 383-389.

[13] *Organic Syntheses*, Col. Vol. 4; John Wiley & Sons: New York, 1963; pp. 831-833.

[14] Mitsunobu, O. *Synthesis* **1981**, 1-28.

[15] Silverstein, R. M.; Ryskiewicz, E. E.; Chaikin, S. W. *J. Am. Chem. Soc.* **1954**, *76*, 4485-4486.

[16] Midland, M. M.; Tramonato, A.; Zderic, S. A. *J. Am. Chem. Soc.* **1977**, *99*, 5211-5212.

[17] Abell, A. D. Post-Doctoral Thesis, Cambridge, England, 1986.

[18] Cannell, R. J. P.; Kellam, S. J.; Owsianka, A. M.; Walker, J. M. *Planta Med.* **1988**, *54*, 10-14.

[19] Cannell, R. J. P.; Kellam, S. J.; Owsianka, A. M.; Walker, J. M. *J. Gen. Microbiol.* **1987**, *133*, 1701-1705.

[20] SmithKline Beecham Pharmaceuticals, King of Prussia, Pennsylvania

[21] Dreyer, G. B.; Strickler, J. E.; Tomaszek, T. A.; Hyland, L.; Metcalf, B. W.; Meek, T. D.; Moore, M. L.; Magaard, V. W.; Chandler, A. C.; Carr, T. J.; Debouck, C.; Fakhoury, S. A. *Proc. Natl. Acad. Sci. USA* **1989**, *86*, 9752-9756.

APPENDICES

7.1 Abbreviations

Ac	acetyl
AIDS	acquired immunodeficiency syndrome
Boc	*N-tert*-butoxycarbonyl
bs	broad singlet (NMR)
Bu	butyl
Cbz	benzyloxycarbonyl
COSY	correlation spectroscopy
dd	doublet of doublets (NMR)
DCC	1,3-dicyclohexylcarbodiimide
DEAD	diethyl azodicarboxylate
DEPT	distortionless enhancement by population transfer
DMAP	4-dimethylaminopyridine
DMF	*N,N*-dimethylformamide
DMSO	dimethylsulfoxide
Et	ethyl
Fmoc	((9-fluorenylmethyl)oxy)carbonyl
HETCOR	heteronuclear correlation
HIV	human immunodeficiency virus
Hünigs Base	*N,N*-diisopropylethylamine
IR	infrared
m	multiplet (NMR)
MS	mass spectra
m/e	mass to charge ratio (MS)
NMR	nuclear magnetic resonance
NOE	nuclear Overhauser enhancement
ORD	optical rotary dispersion
p-2-c	pyrrole-2-carboxaldehyde
Pth	phthalyl
q	quartet (NMR)
s	singlet (NMR)
t	triplet (NMR)
TLC	thin layer chromatography
TEA	triethylamine
THF	tetrahydrofuran
Ts	tosyl (*p*-toluenesulfonyl)
UV	ultraviolet

7.2 Amino Acid Glossary

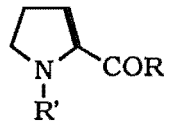

Pro
proline

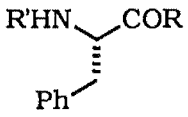

Phe
phenylalanine

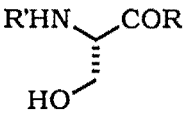

Ser
serine

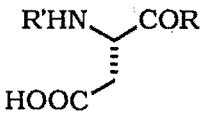

Asp
aspartic acid

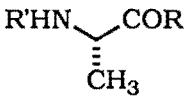

Ala
alanine

Gly
glycine

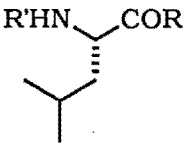

Leu
leucine

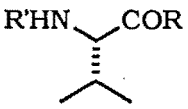

Val
valine

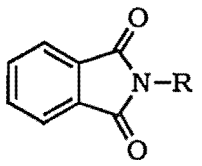

Pth

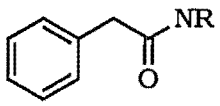

Cbz

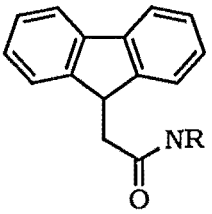

Fmoc

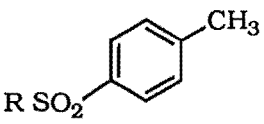

Ts

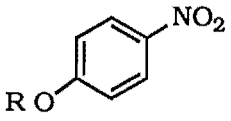

*p*nitrophenyl ester

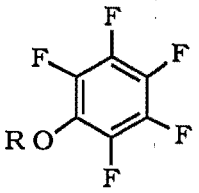

penta-fluorophenyl
ester

7.3 Pyrrole Glossary

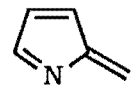

1.3
azafulvene

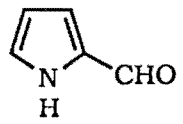

p-2-c
pyrrole-2-carboxaldehyde

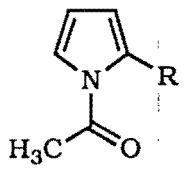

2.24 R=CHO
2.47 R=CH_2OH

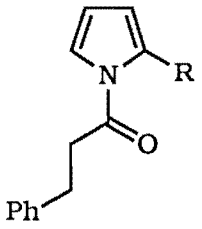

2.31 R=CHO
2.32 R=CH_2OH

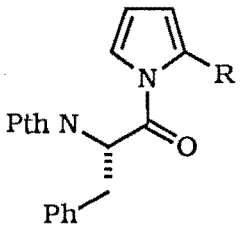

2.37 R=CHO
2.52 R=CH_2OH

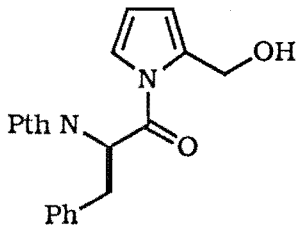

2.55

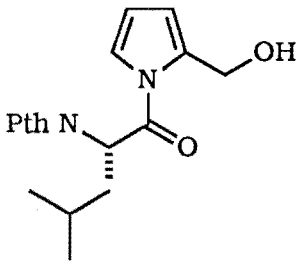

3.45

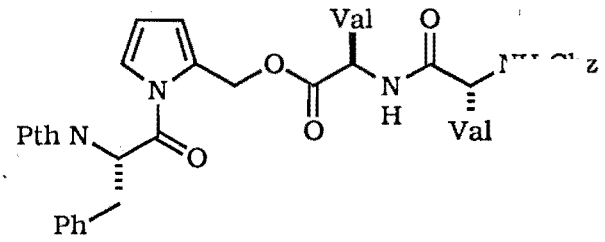

3.39

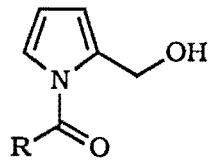

3.53 R=$(CH_2)_{10}CH_3$
3.55 R=$(CH_2)_4CO_2Me$

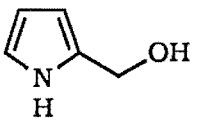

4.1

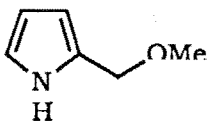

4.2

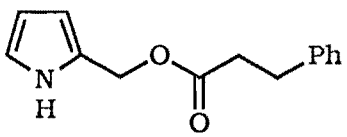

4.5

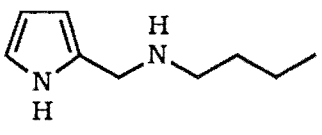

4.6

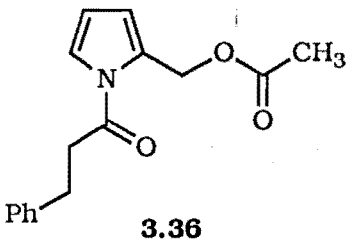

3.36